Green ammonia as a vector for intercontinental energy transport

Nicholas Salmon

Supervisor: Professor René Bañares-Alcántara

Doctor of Philosophy

Department of Engineering Science
Oxford University
June 2023

Abstract

Green ammonia is an essential key in the decarbonisation toolkit. For energy systems, it can play a myriad of roles: it is a zero-carbon fertiliser, shipping fuel, hydrogen vector, and dispatchable, portable energy source. Ammonia is already the second-most produced industrial chemical in the world, and yet its production may need to increase five-fold to meet these emerging, green demands.

This thesis provides the first global optimisation of the supply chains that will be needed to deliver green ammonia at such large scales. It considers first the production of ammonia, advancing our understanding of the tools needed to design green ammonia plants, and providing for the first time a viable strategy for operating green ammonia plants without a grid connection. It then explores the constraints on ammonia production, with a focus on land restrictions, which may create a business case for ammonia production on the ocean. Finally, it integrates the results for production and land availability into a supply chain model that incorporates the cost of ammonia transport, and applies the model to two case studies: one focussing on ammonia's use as a shipping fuel, and one on its application for back-up energy production.

The most significant contribution of this thesis is the global supply chain model, which is a blueprint for an emerging sector of the energy system. In the journey to reaching that blueprint, other interesting outcomes emerge. Of particular interest: (i) connecting to the electricity grid can meaningfully reduce the cost of green ammonia compared to an 'islanded' system; (ii) Haber-Bosch flexibility is important for producing affordable green ammonia, but may not be as significant as portrayed in some literature; (iii) in land-constrained regions, there is good reason to believe there is a techno-economic case for offshore green ammonia production; (iv) ammonia supply chains optimised on the basis of cost will involve less energy transport than today's fossil-fuel derived systems.

Publications

Refereed Journal Papers

- N. Salmon, R. Bañares-Alcántara. *A global, spatially granular techno-economic analysis of offshore green ammonia production*. Journal of Cleaner Production, 2022, **367**, 133045

- N. Salmon and R. Bañares-Alcántara. *Impact of grid connectivity on cost and location of green ammonia production: Australia as a case study*. Energy Environmental Science, 2021, **14**, 6655–6671

- N. Salmon, R. Bañares-Alcántara and R. Nayak-Luke. *Optimisation of green ammonia distribution systems for intercontinental energy transport.* iScience, 2021, **8**, 102903.

- N. Salmon and R. Bañares-Alcántara. *Green ammonia as a spatial energy vector: a review*. Sustainable Energy Fuels, 2021, **5**, 2814-2839

- S. Wu, N. Salmon, M. Li, R. Bañares-Alcántara, E. Tsang. *Energy Decarbonization via Green H2 or NH3?* ACS Energy Letters. 2022, **7**, 1021

- N. Salmon, R. Bañares-Alcántara. *Offshore Green Ammonia Synthesis*. Nature Synthesis, 2023, **2**, 604-611

- N. Salmon, R. Bañares-Alcántara. *Impact of process flexibility and imperfect forecasting on the operation and design of Haber-Bosch green ammonia*. RSC Sustainability, 2023, **1**, 923

- J. Verschuur, N. Salmon, J. Hall, R. Bañares-Alcántara. *Optimal fuel supply of green ammonia to decarbonise global shipping*. Under Review.

- B. David et al. *Ammonia as a carbon-free fuel*. Under Review.

Refereed Conference Papers

- N. Salmon and R. Bañares-Alcántara. *Importance of interannual renewable energy variation in the design of green ammonia plants*. PSE, 2022, **1**, 757-763, Kyoto.

- N. Salmon and R. Bañares-Alcántara. *Sector coupling of green ammonia production to Australia's electricity grid*. PSE, 2022, **3**, 1903-1909, Kyoto.

- N. Salmon and R. Bañares-Alcántara. *The relationship between plant flexibility and optimum operating cost for green ammonia production*. Ammonia Energy Symposium, 2022, Cardiff.

- H. Driscoll, N. Salmon and R. Bañares-Alcántara. *Technoeconomic Evaluation of Offshore Green Ammonia Production using Tidal and Wind Energy in the Pentland Firth*. Ammonia Energy Symposium, 2022, Cardiff.

- N. Salmon and R. Bañares-Alcántara. *Incorporation of non-linear efficiency constraints in green ammonia production optimisation for cost minimisation*. European Symposium for Computer Aided Process Engineering, 2023, Athens.

Non-Refereed Conference Submissions

- N. Salmon. *Is Bigger Better? The optimum scale for green ammonia plants*. Australian Ammonia Energy Association Conference, 2021, Melbourne.
- N. Salmon., J. Verschuur, R. Bañares-Alcántara. *Forecasting the global demand, investment costs and spatial distribution of green ammonia for maritime decarbonisation*. Ammonia Energy Association conference, 2023, Rotterdam.

Acknowledgements

I am greatly thankful for the support of my supervisor, Dr. René Bañares-Alcántara, who is a reliable, dedicated and useful source of guidance. He is always available, and that availability made it possible to construct a (hopefully defensible) thesis despite starting smack-bang in the middle of a pandemic. Since starting the thesis, he has facilitated, with great patience, a wide range of opportunities that has made my time at Oxford enriching and edifying, for which I am deeply grateful.

Help with my research came from a range of sources, and I am indebted to all of them: Zac Cesaro provided assistance with many things - in particular, converting weather data into solar panel and wind turbine energy output; Natasha Lutz helped me navigate the MODIS6 dataset without which Chapter 5 would not exist; and collaboration with Jasper Verschuur enabled a far more detailed case-study of the decarbonisation of the maritime sector than would otherwise have been possible. To exploit a well-worn phrase: that maritime sector model is still wrong, but thanks to Jasper, it is now useful. The whole of the Mini-TESA building provided an environment that I was happy to return to each and every day.

Funding the thesis was also quite important, and I am very appreciative of the generous support offered by the Rhodes Trust, which has fed me, wined me, paid me, paid the university, and paid Dom at The Oxford Physiotherapy Service, much to the gratitude of my left knee and ankle. I wouldn't have had the scholarship at all if not for the support of my brilliant referees during my application, and at the conclusion of my time in Oxford, I am more grateful than ever to each of them: Abigail Twyman, Greg Birkett, Bev Coulter, Ian Cameron, and Lesley Ironside, who is much missed.

A thesis is, of course, a marathon, not a sprint, and I ran my race surrounded constantly by emotional support sign-holders who pushed me toward the finish. I compiled a list of particular favourites, randomised the order of that list for fairness, and then unrandomised the order of that list slightly, for comedy. Thanks to Bec, for being the most entertaining companion I've ever had in the kitchen; thanks to Beth, for filling the hole left by Bec's untimely departure for London, and for bringing oats into my life; thanks to everyone in 9 Canal St (Julia, Grace, Annie, Manpreet, Kiwi Ollie, Nina and Anja, and I disclaim that your order was also randomised) for the best year of my life (Tassie Ollie was around the corner and also a constant source of joy); thanks to Christina (and Fini, obviously), for teaching me everything I know that's worth knowing; thanks to Katie, for being a brilliant life-drawing partner; thanks to Josechu, for being a brilliant cycling partner; thanks to Pat, for gossiping to keep his heart rate up when I was an inadequate cycling partner; thanks to Sara, for gossiping to keep *my* heart rate up always; thanks to Laura, for keeping me in check; thanks to Ash and Henry, for making me feel welcome in Oxford, on mountains, and on Barnes family holidays; thanks to Emma, for letting me move 15,000 km away; thanks to Antonia, Catherine and Georgie, for letting me move 16,000 km away; thanks to James, for also ignoring the allure of Antonia, Catherine and Georgie, and bringing a slice of home with him; thanks to Lana, for being eminently practical even before

moving to Germany; and thanks to Lizzie, for being a source of sunshine more important than all the solar power in this thesis. And I reserve a special mention for Alli, who gets a bonus because she is both friend and colleague, but who will remain a friend long after this thesis is submitted and we cease to be colleagues.

Family is most important, and so they get to come last: thanks to Hugo, for enthusiasm, humour, practicality, kindness, and for having the wits to marry Muirgen; thanks to Muirgen, for enthusiasm, humour, practicality, kindness, and for agreeing to marry Hugo; thanks to Mum and Dad for more than I could ever express in the 250 page limit applied to this thesis; and thanks to David, for everything.

List of acronyms

AC	Alternating current	LHV	Lower Heating Value
AEMO	Australian Energy Market Operator	LNG	Liquid Natural Gas
AIS	Automatic identification systems	LOHC	Liquid Organic Hydrogen Carrier
AREH	Australian Renewable Energy Hub	LP	Linear program
ASU	Air separation unit	LPG	Liquid propane gas
AUD	Australian dollars	LV	Low voltage
CAPEX	Capital expenditures	MILP	Mixed integer linear program
CCS	Carbon Capture and Storage	MMTPA	Million metric tonnes per annum
CER	Chlorine Evolution Reaction	MOR	Minimum operating rate
DAC	Direct Air Capture	MPC	Model predictive control
DC	Direct current	NPV	Net present value
DUOS	Distribution use of system	O&M	Operating and maintenance costs
HB	Haber-Bosch	OPEX	Operating expenditures
HFO	Heavy Fuel Oil	PEM	Proton Exchange Membrane
HHV	Higher Heating Value	PPA	Power Purchasing Agreement
HV	High voltage	RCP	Representative concentration pathway
IEA	International Energy Agency	SSP	Shared-socioeconomic pathway
IRENA	International Renewable Energy Agency	TEA	Techno-economic analysis
LCOE	Levelised cost of electricity	TRL	Technology Readiness Level
LCOA	Levelised cost of ammonia	TUOS	Transmission use of system
LCOA-P	Levelised cost of ammonia produced	USD	US dollars
LCOA-D	Levelised cost of ammonia delivered	VRE	Variable renewable energy

List of symbols

Symbol	Definition
$LCOAP$	Levelised cost of ammonia production (USD/t)
CRF	Capital Recovery Factor
F	Annual production of ammonia (t)
i	Discount Rate
PL	Project Lifetime
π	Power flow from renewable generators (LP)
β	Power flow to and from batteries (LP)
γ	Power flow from fuel cell (LP)
κ	State of charge of battery/hydrogen storage (LP)
η	Power flow from grid (LP)
P	Power equipment size (LP)
V	Energy storage equipment size (LP)
$T_w(t)$	Weighting applied to a time step
t	Time step
CF	Conversion factor between units and energy flows
Z	Hourly energy generated from renewables (LP)
$Cost_x$	Unit CAPEX of equipment x
ζ	Curtailed energy from renewables (LP)
x_H	Amount of hydrogen in storage (MPC)
x_B	Amount of energy stored in battery (MPC)
x_A	Amount of ammonia produced at time t
π_x	Energy flowing to unit x (MPC)
α	Energy produced by renewables (MPC)
P	MPC Objective Function
n	MPC time horizon
k	MPC tuning factor

Contents

List of Figures

List of Tables

Chapter 1

Introduction

Decarbonising electricity production is (mostly) easy. In the words of the International Renewable Energy Agency, there has been a "seismic decline" in the cost of renewables in the last decade [1]; electricity from solar photovoltaics, in particular, has become almost an order of magnitude cheaper in that time[2].

The challenge of net-zero therefore lies not in electricity production, but in three new hurdles: energy storage, energy transport, and the decarbonisation of hard-to-abate sectors. Energy storage is needed to balance the inherent variability of renewable energy sources[3, 4]; long-distance energy transport is a fundamental component of our existing system, and is likely to continue in some form as we decarbonise [5, 6]; and hard-to-abate sectors (e.g. steel, shipping, and aviation) will struggle to directly use the electricity produced from renewables [7–9]. Energy for those sectors will therefore be needed in a different medium.

Ammonia is a simple molecule, but it holds the solution to all three of these challenges. It has a plethora of applications in energy systems: as a zero-carbon fertiliser[10], as a marine fuel [11], as a hydrogen vector, or as long-term energy storage[12]. It can be produced from just water, air and renewable power (meaning its emissions footprint can be very low [13]). Compared to hydrogen, it is liquid under mild conditions and it has a higher volumetric energy density. Because of these properties, green ammonia is a good candidate for the "spatio-temporal" arbitrage of renewable electricity: it enables renewable energy to be stored, and moved to the place, time and end-use where it is needed.

Despite the sizable role it could play in energy systems of the future, our understanding of where and how green ammonia will be produced and consumed remains limited. The production of green ammonia is complex - historically, ammonia production has occurred at a constant rate, whereas green production will need to vary with renewable resources. Once it has been produced, the ammonia needs to be transported to demand centres - but quantifying the scale of ammonia demand depends on the rate of decarbonisation, and the unknown rate of technology uptake. The uncertainty on both supply and demand sides hinders the ability for the private sector to invest in production with certainty, and for governments to make policies which can support nascent industry.

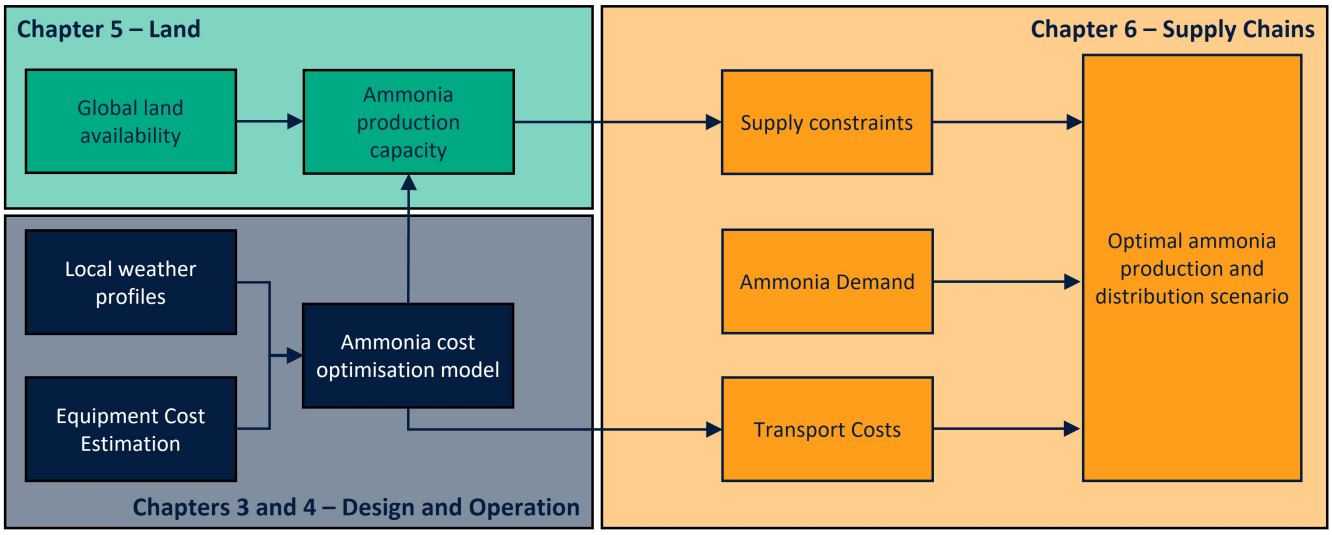

Fig. 1.1 A high-level representation of the ammonia optimisation model which is the goal of this thesis. The model takes information relating to ammonia supply, demand, and transport cost (which is itself informed to some-extent by production cost). Chapters 3 to 5 enable a robust prediction of ammonia supply constraints: chapters 3 and 4 provide and validate a method for determining production cost, while chapter 5 incorporates the impact of land constraints on production capacity. Chapter 6 integrates this prediction into the supply chain model, explaining the model itself, as well as the estimation of transport costs, and two demand scenarios.

Trying to predict the specifics of an 'ammonia economy' therefore requires an optimisation approach which identifies locations which enable low-cost production without excessive supply-chain costs. In brief, this thesis aims to describe and solve this optimisation problem. It provides a pathway to a future where the decarbonisation of energy storage, energy transport, and hard-to-abate sectors is - like electricity production - easy.

1.1 Research goals and chapter outline

The research goal is to use optimisation models to determine the least-cost scenarios for green ammonia supply chains. Figure 1.1 shows a high level construction of the optimisation problem. The core inputs to the model are determined in chapters 3 to 5; the model itself is then described and solved in chapter 6.

The optimisation model solves for the minimum levelised cost of delivered ammonia, or the LCOA-D; this is the cost at which ammonia would need to be sold at the destination port in order for the net present value of the entire supply chain to be 0 at the nominated discount rate. For the avoidance of confusion, the levelised cost of ammonia *delivery* (LCOA-D), which is the focus of chapter 6, includes transport, storage and production costs, and is therefore different from the levelised cost of ammonia *production* (LCOA-P) which is the focus of chapters 3 and 4. Energy systems do not always reach least-cost solutions, as identified in the introduction; however, the purpose of this research is to identify the least-cost solution as a baseline for supply-chain development.

Table 1.1 summarises the research questions posed by the thesis, and identifies which chapters will answer them.

Chapter 2 describes the state of the literature into ammonia, demonstrating the need for the research described in this thesis.

Table 1.1 Summary of research questions

	Research Question	Chapter
Main	What are the core features of a global system for the production and distribution of green ammonia?	All
1	How can green ammonia production plants be designed to minimise production costs?	3
2	Are the designs proposed by the model from chapter 3 robust to imperfect weather forecasting, and to what extent do they rely on plant flexibility?	4
3	To what extent do land limitations impact the supply of green ammonia?	5
4	How should supply and demand locations for green ammonia be paired in order to minimise delivered costs?	6

Chapter 3 is shown by the blue area on Figure 1.1, and explains the modelling taken to estimate green ammonia production costs. The most significant and substantial contribution to the academic literature in this chapter is a demonstration that connecting otherwise islanded green ammonia plants to national electricity grids can reduce costs by approximately 10%. This finding was reported in Energy and Environmental Science (*Impact of grid connectivity on cost and location of green ammonia production: Australia as a case study*); a deeper dive into the implications of grid connection were presented at the Process Systems Engineering conference in Kyoto (*Importance of interannual renewable energy variation in the design of green ammonia plants* and *Sector coupling of green ammonia production to Australia's electricity grid*). These three publications have been adapted to formulate this single chapter.

Chapter 4 introduces a model predictive control (MPC) approach which is used to optimise the operation of a green ammonia plant subject to imperfect forecasting information. Although this MPC model is not a direct input into the overarching optimisation model of the thesis, it is included in the blue area on Figure 1.1 because it shows that the designs calculated using the perfect forecasting approach from Chapter 3 can be operated with imperfect forecasting (subject to some adjustment). There are two core research outcomes: firstly, this MPC model shows that the plants sized using the design model can mostly be operated as designed, given appropriate oversizing; and secondly, the consideration of both models shows that the benefits of improved HB flexibility on the LCOA are limited. This chapter is strongly based on an article published in RSC Sustainability, *Impact of process flexibility and imperfect forecasting on the operation and design of green ammonia plants*.

From the high-level view of the thesis, the purpose of **Chapter 5** is to calculate the impact of land availability as a major supply constraint for green ammonia production. While doing so, it provides a deep analysis of whether land constraints may drive green ammonia production offshore. The results are reported in the Journal of Cleaner Production (*A global, spatially granular techno-economic analysis of offshore green ammonia production*), and the

discussion of technical factors which may lead to offshore production is described in Nature Synthesis (*Offshore green ammonia synthesis*).

Chapter 6 integrates these results together into a single focus on supply chains for green ammonia. It uses the production cost results reported in Chapter 3, the land constraints described in Chapter 5, and an estimate of transport costs for green ammonia in different contexts to optimise distribution networks. The broad outline of the method is reported in iScience (*Optimisation of green ammonia distribution systems for intercontinental energy transport*), although it was updated significantly for an article currently under review at Joule (*Optimal fuel supply of green ammonia to decarbonise global shipping*). This chapter considers two demand cases; one for the maritime industry, and one for long-term grid storage.

Chapter 7 summarises the key findings of the thesis, and proposes further research.

1.2 Scope of Thesis

Green hydrogen is more widely discussed than ammonia by academia, industry and governments. Although green hydrogen has a high gravimetric energy density, its volumetric energy density is very poor; even in the liquid state under cryogenic conditions it carries only 2.4 kWh/L [14] (compared to gasoline, whose liquid energy density is 9 kWh/L [15]). 'Upgrading' hydrogen into a chemical derivative could make it more easily portable; derivatives can enable transport cost reductions of at least a factor of three [16, 17].

Green ammonia is a particularly promising derivative. Its liquid energy density of 3.5 kWh/L [15] is achieved under far milder conditions than its parent molecule: –33°C at atmospheric pressure, or room temperature at $\sim$10 bar [15] (liquid hydrogen boils at –253°C[15]). Global systems for ammonia transport are well established and understood because of its existing wide-scale use in the fertilizer industry - it is the second most widely produced chemical in the world [18]. Although the comparison between hydrogen, ammonia, and other derivatives is discussed in more detail in the Literature Review (Chapter 2), it is these properties that have led ammonia to be the primary focus of this thesis.

The focus of this thesis is on techno-economic analysis - it does not attempt to improve technologies for green hydrogen or ammonia production themselves; rather, it aims to demonstrate how existing technologies can be put to their most effective use.

1.2.1 Ammonia production methods

Hydrogen is often ascribed a label, or colour, which refers to the feedstock used and emissions released in its production. When hydrogen is reacted with nitrogen in a Haber-Bosch (HB) loop to produce ammonia, that ammonia is referred to with the same label as the hydrogen from which it was synthesised. At present, ammonia is produced mostly from fossil fuels: it is labelled as brown if hydrogen is made using coal gasification, or grey if hydrogen is made using natural gas reforming. These fossil fuel processes are also referred to as conventional ammonia production. Blue ammonia uses the same feedstock as brown and grey ammonia, but includes a carbon capture and storage

(CCS) unit. To be truly 'blue', this CCS unit must capture the CO_2 in both flue gas streams: the concentrated stream leftover from the water-gas-shift reactor after hydrogen is removed, and the comparatively dilute stream released from the furnace. Green ammonia is not widely produced at present and is made entirely from electricity, water and air: the hydrogen for its synthesis is generated from the electrolysis of water. The term 'green' ammonia implies that the electricity is renewably sourced, although much of the literature at present includes a grid connection, and some considers nuclear power; the suitability of this approach is discussed in Chapter 3. Future technologies which produce ammonia directly from raw feed materials without an interim hydrogen generation step could also be considered green if they use only renewable electricity for energy input and have no other associated carbon emissions.

This thesis focusses on green ammonia. Brown and grey ammonia are unsustainable, and while blue ammonia has comparatively low emissions, its production cost will always be higher than conventional technologies because it requires additional processing. Since green ammonia has no emissions, and its cost expected to fall below that of brown and grey ammonia at some point before 2050, it will be the most affordable and merits further investigation for its use as a sustainable energy vector in the long term[18]. Unless otherwise specified, all "ammonia" referred to in this thesis is green.

Downstream of hydrogen production, the HB loop used to produce ammonia remains broadly unchanged regardless of the 'colour' of ammonia produced, but there are three minor differences. Firstly, all currently commercially available electrolysers operate at low temperature, so cannot recycle heat as useful energy. Conventional and blue ammonia plants normally recycle heat from the exothermic Haber-Bosch reactor into the endothermic hydrogen reformer; green ammonia plants remove this heat using cooling air or water. Secondly, removal of oxygen from air to obtain the nitrogen required for Haber-Bosch synthesis is integrated into the hydrogen production in conventional ammonia production, usually in an autothermal reformer. Green ammonia plants require a dedicated air separation unit to produce this nitrogen. Thirdly, green ammonia plants drive compressors using electricity, rather than steam [19].

This thesis focusses only on ammonia synthesised using a HB loop, although it does (particularly in Chapter 4) describe the conditions that may enable novel technologies to become the most profitable means of ammonia production in the future. The focus on HB synthesis will therefore provide conservative estimates for ammonia costs and production constraints; in case of a major technological breakthrough, these costs are expected to fall.

Chapter 2

Literature review

The purpose of this literature review is (i) to demonstrate that ammonia is a suitable candidate as a green energy vector and therefore for further research; (ii) to determine the current status of the techno-economic literature investigating ammonia; (iii) to establish a need for more detailed modelling of green ammonia supply chains that will be described in this thesis, and (iv) survey the data used in literature in order to identify an informed set of inputs for the modelling work done in subsequent chapters.

It is divided into three parts that broadly match these goals. The first part briefly explores alternatives to green ammonia and justifies the need to, at the very least, research ammonia in more detail. The second part explores methodologies for estimating the levelised cost of ammonia production (LCOA-P). The third part explores supply chains considering first supply and then demand.

2.1 Energy Carriers

Ammonia is one of many possible green energy carriers. The introduction identified a need for these green energy carriers during periods of low renewable energy generation. This section of the review compares different carriers throughout their life cycle, from production to consumption in an energy-importing region. It begins with a description of each of the options, before comparing the cost estimates available for each in the literature. In doing so, it will identify both the competitors to ammonia as an energy transport vector, and the approximate cost of energy transport.

2.1.1 Production and Storage

A range of options are available for long-distance energy transport and are surveyed in detail in the literature. These are summarised in Table 2.1.

Of the five technologies discussed in the literature (summarised in Table 2.2, four are chemical storage technologies. The exception is HVDC, which is included for completeness. Although HVDC is suitable in a number of cases for energy transport, it is not efficient across very large distances (i.e. >5,000 km) due to the energy losses

Table 2.1 Summary of main energy carriers described in the literature

Carrier	Abbreviation/ Chemical formula	Volumetric Energy Density (kWh/L)[15]	Hydrogen wt. %	Synthesis energy losses (kWh/kg H_2)[(i)]	Storage Conditions[15]	Renewable production technologies [(ii)]
Ammonia	NH_3	3.50	17.6	12.2 [15] [(iv)]	–33°C, 1 bar	Electrolysis + Haber-Bosch
Liquid hydrogen	LH_2	2.36	100	6-12 [(v)]	–253°C, 1 bar	Electrolysis + Liquefaction
Liquid organic hydrogen carriers	LOHC	1.57 [14]	5-6 [20]	0 [(vi)]	Ambient	Electrolysis + Hydrogenation
Synthetic Hydrocarbons (e.g. MeOH, syn-LNG)	MeOH [(iii)]	4.94	12.5	31 [(vii)]	Ambient	Electrolysis + CO2 capture + Methanol synthesis [(viii)]
High Voltage Direct Current Electricity	HVDC	N/A	N/A	4.9%/1000 km [21]	N/A	Solar PV, Wind

[(i)] Synthesis energy losses do not include energy losses during hydrogen production, which are considered equivalent in all cases, except for HVDC.
[(ii)] Some novel technologies are emerging for hydrogen generation, and for carrier synthesis. These are not considered here. The scope of this analysis is limited to processes with a high technology readiness level (TRL).
[(iii)] A range of synthetic hydrocarbons is considered in the literature; data is provided for renewable methanol, the most frequently considered option.
[(iv)] Includes 1.5 kWh/kg NH_3 energy loss from exothermic reaction, and a production energy demand of 0.642 kWh/kg NH_3 [18] for compression and air separation. Energy loss is substantially reduced to 5 kWh/kg H_2 if steam can be raised and used from the heat of reaction.
[(v)] 6 kWh/kg H_2 may be possible in future applications; at present 10-12 kWh/kg H_2 is required[22].
[(vi)] Hydrogenation of LOHCs is exothermic and self-sustaining; the majority of energy consumption (between 8-10 kWh/kg)[22] occurs during the endothermic dehydrogenation process (which is not included in this table).
[(vii)] Based on analysis in Hank et al.[22]: includes 8 kWh/kg H_2 to supply the endothermic heat of reaction, 2.6 kWh/kg H_2 for compression, and the balance of energy for direct air capture (DAC) of carbon dioxide.
[(viii)] CO_2 can be obtained using direct air capture (DAC), or from a point emissions source from industry, such as flue-gas from a coal fired power plant. Biomass as a CO_2 source is excluded as the land-use efficiency of DAC is 100 times higher than that of biomass, and production capacity is finite [5].

associated with cable resistance and high capital costs [5]. In addition, it cannot provide all the benefits associated with chemical fuels, including energy storage or the provision of high-grade heat.

The major economic costs of the remaining four technologies occur at different points of production and use. Liquid hydrogen requires significant energy input for liquefaction. Because it is a cryogenic liquid, the storage equipment required has very high CAPEX. Additionally, some daily boil-off is inevitable regardless of the quality of storage equipment. The rate of boil off is a function of tank design, but is typically reported to be between 0.2-

0.3%/day [23], meaning storage delays in shipping or receiving ports are costly. Very large costs are also forecast for the unloading and loading equipment required to transfer LH_2 [24]. Salt caverns for gaseous hydrogen are often discussed as a storage alternative to liquid hydrogen [25]; although these may offer storage cost reductions, they are not advantageous for energy transport because the hydrogen remains at low density.

Liquid organic hydrogen carriers use molecules that are typically liquid at ambient conditions which can be loaded with hydrogen by the energy supplier, and unloaded by the importer, processes referred to as hydrogenation and dehydrogenation respectively. A range of liquid organic carriers have been considered, including toluene, di-benzyltoluene, methanol and naphthalene [14]. Shipping and storage of LOHCs can be done under ambient conditions using existing systems for hydrocarbons. However, the volumetric hydrogen density is poor[14], the most efficient carriers themselves can have very high capital costs [22], and additional shipping costs are accrued as the unloaded molecule must be returned to the energy supplier for hydrogenation.

Synthetic hydrocarbons are produced by reacting electrolytic hydrogen with a carbon source. The affordability of this technology depends strongly on the availability of carbon; if a concentrated stream of CO_2 is not available, then the energy costs of obtaining carbon via direct air capture are very high[22]. Decarbonised energy systems will not have concentrated streams of CO_2 available; even if they were available, chemicals produced using CO_2 captured from fossil sources face regulatory barriers to being considered carbon neutral [26]. Once synthetic hydrocarbons are produced, shipping and transport is straightforward, and can be performed using existing technologies.

The main inefficiency in producing ammonia (compared to other hydrogen carriers) is the exothermic synthesis reaction. Although some energy is recovered to pre-heat reactants, most of the excess energy is removed as waste heat from the electrified Haber-Bosch process using cooling water. However, ammonia synthesis is much more energy efficient than synthetic hydrocarbon synthesis, and, like synthetic hydrocarbons, its transport is straightforward given its comparatively high energy density and mild storage conditions.

2.1.2 Distribution and Consumption

2.1.2.1 Distribution

On arrival in the importing nation, further domestic transportation or distribution is likely to be required, unless a specific application is available at the port. Cracking of ammonia, if required, and dehydrogenation of LOHCs could be more economic if completed in a (semi-)centralised location before distribution [22]. This is particularly true for LOHCs, for which the return of the unloaded carrier through the distribution network would likely add significant costs.

Having extracted the hydrogen, pipeline distribution is likely to be the norm (as trucking of compressed gas is highly inefficient due to hydrogen's low density). Pipeline distribution of hydrogen is expected to be cheap relative to hydrogen production for very large systems. Existing natural gas grids can tolerate a small percentage of hydrogen (typically 4-6% depending on national regulation[24]), but for large scale hydrogen economies, new pipeline

Table 2.2 Summary of hydrogen carrier end uses

Carrier	Additional Processing Steps	Additional Energy Consumption (kWh/kg H2)	Distribution Method	End-use	End-use efficiency (%)
NH_3	None	0	Trucking/Pipeline	Fertilizer	N/A
	None	0	Trucking/Pipeline	SOFC/CCGT/ Shipping Fuel	60[27]
	Ammonia cracking	8.52	Trucking/Pipeline	CCGT/ Hydrogen Fuel Cell	50-60[28]
LH_2	Evaporation	0[(i)]	Trucking (Liquid) OR Pipeline (Compressed Gas)	CCGT/ Hydrogen fuel cell	50-60[28]
LOHC	Dehydrogenation	8.25 [22]	Pipeline (After Dehydrogenation)	CCGT/ Hydrogen fuel cell	50-60 [28]
MeOH/ Syn-LNG	None	0	Trucking/ Pipeline	CCGT/ Shipping Fuel	60 [27]

[(i)] In some cases, it may be possible to generate some power from the evaporation of liquid hydrogen, by using the hydrogen as a cold sink. It is assumed that this is negligible in comparison to the power which can be generated by using hydrogen in a fuel cell or combustion turbine.

and compressor systems, or significant retrofitting, will be required given the potential for hydrogen embrittlement of steel in existing pipelines [29]. Ammonia pipelines are forecast to be cheaper than hydrogen pipelines due to increased carrier density and reduced costs of pumping compared to compression [30].

Trucking may be a useful option for distribution over short distances; this option is better for fuels which can be used directly (i.e. liquid hydrogen, synthetic hydrocarbons, and ammonia if combustion/SOFCs are available). For trucking most carriers, existing infrastructure can be used, although liquid hydrogen will require specially designed trucks. Focussing specifically on distribution of hydrogen, Yang and Ogden[31] identified trucking of liquids as the best option for moderate distances at small hydrogen distribution rates; for larger distribution rates, pipelines were preferable at all distances.

2.1.2.2 Consumption

Despite having high costs during the production and transport phases, both liquid hydrogen and synthetic hydrocarbons are useful molecules once they have been delivered, because they can be used directly without substantial further processing. High efficiencies are achievable using liquid hydrogen in a fuel cell, which may also be possible for synthetic hydrocarbons in solid oxide fuel cells (SOFCs).

In some applications, ammonia may also be used directly without further processing. The clearest example is in the fertiliser industry. While ammonia can be directly used as fertiliser [32], it is typically upgraded into urea, ammonium nitrate or calcium ammonium nitrate [33]. While this may be helpful to create early supply chains for green ammonia, its scope of use in other sectors is potentially much larger. Current fertilizer consumption is in the

order of 180 MMTPA ammonia per year, whereas shipping demands could be double or even triple that amount [34]; its only substantial competitor in that sector is methanol [35].

Alternatively, ammonia can be used directly in a fuel cell; solid oxide fuel cells (SOFCs) offer the highest efficiencies [33, 36]. When ammonia is used in an SOFC, it can be fed directly to the anode, because the high temperature of these cells effectively cracks the ammonia into its constituent elements before the hydrogen is oxidised into water [10]. Recent developments have substantially increased cell durability and efficiency, which is comparable to a hydrogen fuel cell [37]; further growth of this market is expected [17].

Traditionally, combustion of ammonia has been challenging due to its low burning velocity and high minimum ignition energy. However, because of renewed interest in the field, ammonia turbines are likely be commercialised in the medium term and are currently being used at a pilot scale of 50 kWe [38]. To the extent that pure ammonia combustion is difficult, partial cracking of ammonia and the combustion of a hydrogen/ammonia blend can overcome the challenges of ammonia combustion with comparatively small energy losses in the endothermic cracking process; a 70/30 mixture of ammonia and hydrogen by volume has been identified as a viable operating point [27, 39].

If ammonia cannot be directly combusted, then it requires substantial energy input to crack it back into hydrogen. Similar requirements also exist for LOHCs (although the size of the energy demand for this technology varies between carrier molecules). The process for ammonia cracking occurs at high temperatures (>550°C), and resembles steam methane reforming [27]; the typical dehydrogenation temperature for an LOHC is comparatively low (300°C) [40]. While some estimates assume that the energy for these cracking reactions can be supplied using waste heat [41], it is unlikely that a large number of applications will have waste heat available at such high temperatures. In certain applications, therefore, significant energy loss may be observed for ammonia or LOHC consumption in the energy-importing nation. The approximate cost of ammonia cracking is estimated to add 1 €/kg to the cost of produced hydrogen [42], assuming that no waste heat is available. The cost of cracking is likely to fall over time as novel membrane technologies allow for the single-step ammonia cracking and its subsequent purification; this will enable simpler conversion of ammonia to high-purity hydrogen for use in proton exchange membrane (PEM) fuel cells. [43, 44].

2.1.3 Carbon Neutrality

Each of the carriers described can be carbon neutral if appropriate technologies are used. In general, true carbon neutrality requires no greenhouse emissions at any point in the supply chain: i.e. hydrogen production, carrier synthesis, fuel for transporting and distrbuting the carrier, and cracking/dehydrogenation must all emit no carbon. In the case of synthetic hydrocarbons, the carbon source must be direct air capture; if CCS is used when these synthetic fuels are combusted, then the fraction of CO_2 captured from the combustion gases may be considered carbon negative.

Some regulatory schemes are emerging to certify hydrogen as "carbon neutral". One example is the EU program CertifyHy [45]. Its 2019 specifications required that CO_2 equivalent emissions of hydrogen production be less than 36 g CO_2-e/MJ, based on lower heating value (LHV), which amounts to a 60% reduction compared to production by steam methane reforming. Under this scheme, producers can exclude emissions caused during transport. It would therefore be possible under this scheme to use some non-green grid electricity in production, and to use transport technologies which emit CO_2; however, in the long term, this scheme is likely to tighten its requirements, and the true carbon neutrality described above will become the industry standard. The development of more wide-reaching schemes is a prerequisite for exporting chemicals as energy vectors in order to guarantee their origin[26].

One challenge for ammonia if it is directly combusted or used in a fuel cell is its comparatively high NOx emissions. Beyond the harms of NOx as a local and regional pollutant, it is also a potent greenhouse gas[17]. Bicer and Dincer[46], for instance, identified that an ammonia powered car could be responsible for almost twice the emissions of acid gases as one powered by diesel, mainly due to NOx. Emissions of NOx from ammonia based energy generation can be controlled by using unburned ammonia for catalytic reduction of exhaust gasses [47, 48], or with novel burner designs [39]. Similarly, use of the SOFC-H type fuel cell (in which a hydrogen proton is transported through the electrolyte, rather than an oxygen ion in an SOFC-O fuel cell) will enable efficient electricity generation without NOx formation [36, 49].

2.1.4 Economic Comparison of Carriers

2.1.4.1 Methodology for compiling energy transport cost estimations

Although having an understanding of how the supply chains for each carrier work, of more significance is the ultimate cost of delivered energy. This section reviews literature which estimates the cost of that energy.

As an initial step in the search for research which estimates the cost of ammonia energy transport, a keyword search was performed on Scopus for literature which contained in their title, abstract or keywords one of the trigger words listed for each of the categories shown in Table 2.3.

Table 2.3 List of keywords used to identify supply chain literature

Category	Trigger Words
Ammonia	Ammonia, Haber-Bosch
Renewable	Renewable, Green
Transport	Transport, Shipping, Inter-continental, Export, Import
Cost	Cost, Techno-economic, LCOA, Levelised Cost

Further literature was identified in the citations of the papers located using the Scopus search. Papers were eliminated from this search if they did not provide an estimate of transport costs over a large distance (>300 km). The results of the literature search are summarised in Table 2.4.

Despite its high hydrogen density and comparatively straightforward storage requirements, ammonia has received limited attention as an energy vector. In the literature surveyed, only 9 authors provided an economic assessment of the cost of international ammonia transport (compared to at least 17 who analysed liquid hydrogen).

All studies considered were at industrial scale, with either pipeline or shipping as the main mode of transport. The shipping volume ranged from 30,000 m^3 to 160,000 m^3. Authors using 160,000 m^3 ships are forecasting significant growth in the industry; at present ammonia is shipped in the same vessels used for LPG, only a small fraction of which are greater than 90,000 m^3[50].

2.1.5 Ammonia transport costs

Seven authors directly compared ammonia to another medium for international transport purposes. In four of these cases[14, 22, 24, 51], ammonia was identified as the cheapest option for international energy transport. Of the remaining authors, Ishimoto et al.[52] and Hijikata[23] preferred LH2, and DNV GL [20] preferred LOHCs. Hijikata observed only very small differences between various energy carriers and used data from 2002 which no longer provides an accurate measure of production costs. Ishimoto et al. only preferred liquid hydrogen over very short distances, used ambitious forecasts for hydrogen liquefaction costs, and used transport costs that were inconsistent with other literature: approximately 6 USD/GJ of ammonia over 10,000 km, compared to 2-3 USD/GJ from most other sources over comparable distances. DNV GL estimates the cracking energy demand for ammonia to be much higher than the dehydrogenation energy for an LOHC; they also do not clearly factor the capital costs of the LOHC itself, which Hank et al.[22] and the Hydrogen Import Coalition [51] report to be very large. The shipping distance considered by DNV GL is only 1,000 km; over intercontinental distances ($\sim$10,000 km) the lower volumetric and gravimetric energy density of LOHCs will substantially increase their relative transport costs compared to ammonia. In both the cases of DNV GL and Ishimoto et al., if the energy associated with cracking were not considered, because ammonia could be directly combusted or used in a fuel cell, then ammonia would be the preferred option.

Authors tended to consider hydrogen export from one energy exporting nation/region to an energy importing nation/region. The energy exporters included: Algeria, Argentina, Australia, Chile, Iceland, Morocco, Norway, Oman, Saudi Arabia and the US. The only specific energy importers considered were Germany, Belgium, and Japan, although Europe as a general region was considered by Wietschel and Hasenauer [53]. In some cases [24, 52, 53], multiple importer-exporter pairs were considered, and Kawakami et al. [54] performed a simple optimisation to select shipping size, and to determine which of the Middle East and the US would be more suitable energy exporters to Japan. The Hydrogen Import Coalition [51] estimate the costs of shipping various hydrogen derivatives to Belgium from five locations; their results showed it was cheaper to import ammonia from Morocco than Chile, even though production was cheaper in Chile, because of the impact of transport costs. No paper considered the general optimisation problem of which nations would be best placed to export, and to which regions they could most economically ship their product.

Table 2.4 Summary of chemical energy vector supply chain literature

Author	Year	Dis-count rate	Hydrogen Production Method	H_2 carrier	Produced in	Delivered to	Ocean transport distance (km)	Transport mechanism	Produc-tion Cost (USD/GJ)	Terrestrial Transport cost [i] (USD/GJ)	Ocean Transport cost(i) (USD/GJ)	Delivered costs of carrier (USD/GJ) [ii]	Delivered costs of carrier[ii] (USD/t)
Funez Guerra et al. [55]	2020	14.67	Solar (7,000 h/year)	NH_3	Chile	Japan	17,300	Ship	14.67[iii]	-	2.44	16.89	380[iii]
Hydrogen Import Coalition[51]	2020	4.3	Wind/Solar; weather profile details not specified	NH_3	Morocco	Belgium	3,000	Ship	17.42	-	1.53	18.94	426
				LH_2					16.81		10.69	27.5	3,905
				MeOH					22		1.53	23.53	541
				CH_4					23.22		2.44	25.67	1,425
				LOHC					15.58		11.31	26.89	3,818
Hank et al.[22]	2020	5	Wind/Solar; salt cavern for H2 storage	NH_3	Morocco	Germany	4,000	Ship	35.75	-	2.14	37.89	853
				LH_2					36.36		2.14	38.5	5,467
				MeOH					39.11		0.92	40.03	921
				CH_4					39.11		5.19	44.31	2,459
				LOHC					27.5		20.17	47.67	6,769
IEA [56]	2020	5	Not specified	LH_2	Australia	Japan	9,000	Ship	38.73	-	10.56	49.3	7000
				NH_3					32.16		1.57	33.73	759
				LOHC					29.58		11.97	41.55	5,900
Ishimoto et al.[52]	2020	7.5	NG & CCS + Wind	LH_2	Norway	Japan	23,000	Ship	24.63	-	29.59	54.23	7,700
				NH_3					37.01	-	11.56	48.57	1,093
Heuser et al.[57]	2019	8	Wind	LH_2	Patagonia	Japan	21,400	Pipeline/Ship	128.28	4.29	10.4	35.02	4,972
Kawakami et al.[54]	2019	10	NG+CCS	NH_3	Middle East	Japan	12,000	Ship	15.94	-	2.96	18.91	425
Wijayanta et al.[14]	2019	-	-	NH_3	Australia	Japan	9,000	Ship	14.6	1.22	4.06	19.87	447
				LH_2					12.6	1.09	12.38	26.07	3,702
				LOHC					11.65	1.09	4.01	22.94	3,257
Babarit et al. [58]	2018	-	Wind	LH_2	Offshore	Land	1,000	Truck/Ship	27.1	4.56	3.74	35.4	5,027
DNV GL[20]	2018	7	Greened Grid Electricity	LH_2	-	-	1,000	Ship	52.40 [iii]	-	27.32	79.71	11,319
				NH_3					63.95 [iii]		0.42	64.38	1,486
				LOHC					49.25 [iii]		3.15	52.4	4,755
Kamiya et al.[59]	2015	-	Coal + CCS	LH_2	Australia	Japan	9,000	Pipeline/Ship	18.67	0.24	4.73	23.63	3,356
Teichman et al.[41]	2012	6	Solar	LOHC	Africa	Germany	5,050	Ship/Truck	31.48[iii]	1.51	2.08	35.06	4,979
				LH_2					34.99[iii]	1.27	9.2	45.46	6,456
Watanabe et al.[60]	2010	-	Wind	LH_2	Patagonia	Japan	21,400	Pipeline/Ship	23.47	0	13.87	37.34	5,302
Stiller et al.[21]	2008	8	Onshore Wind	LH_2	Norway	Germany	2,300	Ship	35.30[iii]	-	5.75	41.06	5,830
				HVDC			2,300	HVDC	15.2		24.66	39.86	-
Wietschel et al.[53]	2007	-	Hydro/ Geothermal	LH_2	Iceland	UK	1,300	Ship	22.02	-	0.96	22.98	3,262
			Solar	LH_2	Algeria	Italy	1,000	Ship	40.21		0.96	41.16	5,845
Hijikata et al.[23]	2002	-	Hydro	LH_2	-	-	5,000	Ship	-	-	-	99.43	14,119
				NH_3								102.94	2,316
				MeOH								100.21	2,305
Gretz et al. [61]	1993	8	Hydro	LH_2	Quebec	Hamburg	6,000	Ship	54.81[iii]	-	34.16	88.98	12,635

Notes on Table 2.4:

[i] Transport costs include special storage/load out equipment required at the shipping and receiving ports. They do not include costs of carrier synthesis, hydrogen liquefaction or LOHC hydrogenation. Fuel energies are reported on a higher heating value (HHV) basis.

[ii] The delivered costs are a full life-cycle cost estimate, including renewable electricity, hydrogen production, any carrier synthesis costs and transport. Dehydrogenation costs are included for LOHCs, since they are a prerequisite for usage; cracking costs are not included for ammonia, except in the case of DNV GL[20].

[iii] Values are best estimates from other data reported in the paper.

There is a wide disparity between transport costs themselves. For instance, most authors estimate the cost of ammonia shipping to be ∼2 USD/GJ; however, Wijayanta et al.[14] estimates almost double that value, although they do not provide a clear basis for their estimate. Additionally, the data relating the cost of transport to the transport distance is scattered between different authors. Ishimoto et al.[52] estimate that increasing the transport distance by a factor of 10 only doubles the transport cost, because in their analysis, the capital costs of port infrastructure and ships dominate the shipping costs.

The cost of transport will depend on the financial arrangements of exporters and importers. The most likely export model is comparable to those currently used in the oil and gas industries, where it is rare for energy producers to own gas carrier ships. Instead they charter ships as required. Figure 2.1 summarises the costs from literature, including a comparison with the estimates used in this research.

The high-level estimate in Figure 2.1 is not a precise representation of shipping costs, due to the significant uncertainty surrounding the charter rate and fuel price. Berthing fees could also be substantially higher if an ammonia plant cannot take advantage of an existing nearby port. At an intercontinental scale, the model estimates a price of 1.5-3 USD/GJ; as a benchmark, a typical cost for shipping LNG on this scale is 1 USD/GJ [62]. Ammonia's energy density is 50% lower than LNG, and it is assumed that the ship itself is powered by green ammonia. These two factors collectively account for the increased shipping costs of ammonia compared to LNG. If a conventional fuel were to be used to power the ship, the transport cost would be significantly reduced as per the lower bound on the estimate in the Figure.

This estimate demonstrates a trend which is not clear in the literature, and contrary to the perspective of Ishimoto et al.[52]: it appears the price of shipping is a strong function of shipping distance, because of the impact of daily charter costs, and the significant contribution of shipping fuel to transport costs. Only 4 of the 8 authors which provided ammonia shipping costs fall within the plausible range identified by this estimate. This is caused predominantly by oversimplified or vague assumptions [14, 51, 55], or because authors price shipping as a capital investment, rather than using the cheaper charter model that is the norm in the existing energy transport industry [26, 52, 54].

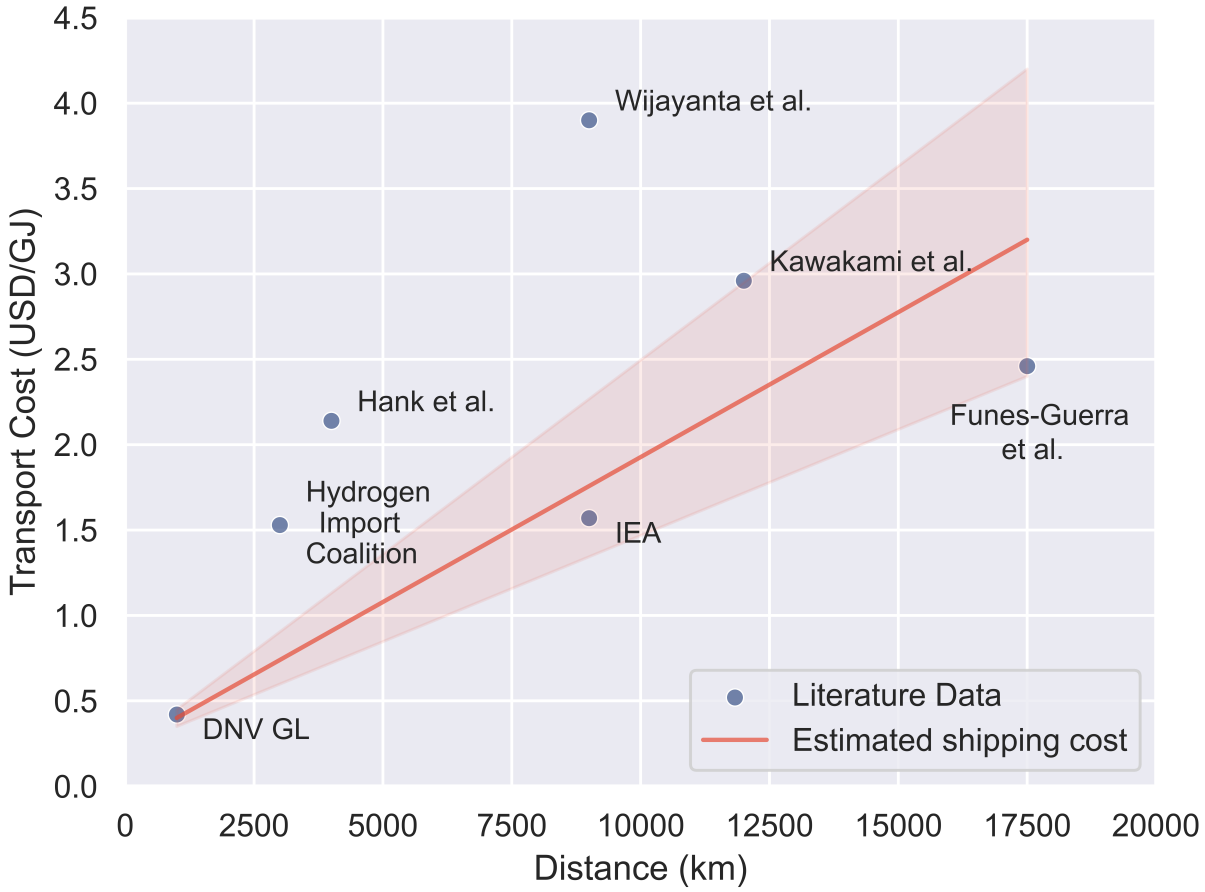

Fig. 2.1 Estimated green ammonia shipping cost (See Chapter 6 for discussion of shipping cost estimation) compared to literature values. The solid line is estimated assuming ammonia as the shipping fuel, and a cost of 500 USD/t; the shaded region shows a low (300 USD/t) and high (700 USD/t) case. The data from Ishimoto et al.[52] are not displayed; they estimate a cost of 11 USD/GJ over 21,000 km.

Beyond the cost of transport, authors also used a range of approaches to estimate the cost of production. As described later in this chapter, estimating ammonia production costs is a complex process which requires consideration of the specific nature of the available renewable resource; simply estimating a number of annual operating hours is overly simplistic. Failing to make this consideration can underestimate ammonia production cost by ∼40% [18]. Even if ammonia synthesis is substituted with any other carrier synthesis process such as liquefaction, similar complexities are expected to increase the production cost. Some works greatly simplified this complexity [21, 31, 55, 60], either ignoring the variability of the resource altogether, or failing to make specific provision for intermediate hydrogen storage. Other authors relied on grid electricity [20], or on conditions very specific to certain locations, such as excellent hydroelectric or geothermal resources [23, 53], or salt caverns [22]. Kawakami et al.[54] and Ishimoto et al.[52] assume that hydrogen is produced using natural gas and CCS. No author who considered transport costs provided as robust an estimate of production costs as is available in other literature (although that literature

typically excludes consideration of transport [18, 63, 64]).

2.1.6 Future Developments

Fair comparison of hydrogen carriers also requires a consideration of how their relative price may change in response to future developments. The only transport carriers whose synthesis or transport costs are likely to reduce significantly in the future are liquid hydrogen (mainly due to technology improvements in liquefaction, storage, loading and unloading) and synthetic hydrocarbons (if direct air capture of carbon dioxide becomes more viable). Most literature that considered these technologies already factored in an improvement in these technologies; for instance, liquefaction energy demand was typically between 6 and 8 kWh/kg; current technologies can only achieve 12-15 kWh/kg [57]. Similarly, the Hydrogen Import Coalition [51] assumes direct air capture is available at 80€/t CO2, which they observe is an ambitious estimate.

By contrast, Haber-Bosch synthesis and LOHC hydrogenation are already well understood and their costs are not expected to fall substantially. It is possible for the green ammonia cost to fall if new synthesis technologies are designed which are superior to Haber-Bosch synthesis, but these receive little attention in the literature due to their low technology readiness level [18, 65, 66].

One key development which may significantly reduce the cost of green ammonia, LOHCs and synthetic hydrocarbons is the technical readiness of solid oxide electrolyser cells (SOECs). Many papers consider SOECs to have a low technology readiness level and to be unable to handle dynamic load variations; however, Hauch et al.[67] and Posdziech et al. [68] both report substantial technological growth in the area in the past two years and indicate that dynamic load flexibility may be possible. These cells have higher efficiencies, to some extent because they able to use heat as an energy supply to the hydrogen production process (as opposed to low temperature cells, which can only use electricity). Therefore, useful work can be performed using the heat released from the exothermic reactions which occur when hydrogen is synthesised into a carrier; in low temperature cells that energy is wasted. Integration of the solid oxide electrolyser cell and ammonia synthesis loop also removes the requirement for a dedicated air separation unit (in the HaldorTopsoe design concept, some hydrogen is combusted in air inside the unit to produce steam, the energy from which is recaptured by the SOEC, leaving a stream of nitrogen[67]). This may reduce capital investment and increasing air separation energy efficiency.

2.1.7 Developments since 2021

There has been relatively little focus on comparing different hydrogen carriers in the literature since 2020; this reflects a growing consensus of which fuels are best suited to fulfill which duties, reducing the need for specific comparative literature. Franz et al.[8] considered several different fuels that may be used for decarbonising shipping (although they considered only changing production costs over time, and not the impacts of supply chains); they found that ammonia would be dominant for decarbonisation of that industry by 2050.

Wang et al.[69] also considered a multi-lateral trading system of ammonia specifically to fulfill maritime demand; however, their production model was fairly simple, and their demand modelling was based on a small subset of publicly available shipping information.

2.1.8 Energy Carriers Summary

There are a range of transport carriers available for energy transport, each with different strengths and weaknesses that will make them more or less economic based on specific circumstances.

The literature has not achieved a unanimous consensus on a single best chemical energy vector. Although liquid hydrogen is often discussed, there is limited evidence that it will be the most affordable carrier. It is more likely that LOHCs, ammonia or methanol will be preferable depending on the intended use case. However, there is clear evidence that ammonia is the best option if it is being used as fertilizer, or if it can be used directly without cracking, (i.e. in a fuel cell, as a shipping fuel, or in a direct combustion engine). Even if none of those conditions are met, many authors still consider it to be the best available hydrogen carrier. For that reason, the focus of this thesis on ammonia is appropriate: at the very least, it will be an important vector for a significant group of sectors, and at it is possible that it will become the dominant chemical for intercontinental energy transport in a future decarbonised economy.

There are clearly gaps in the literature: predictions of production costs neglect important details, transport cost estimations are vague, and there has been very little consideration of multilateral trade.

2.2 Ammonia Production

As is clear from Table 2.6, it is expected that the most substantial contributor to the cost of delivered green ammonia in an energy-importing nation will be the cost of production. Because of significant interest in chemical energy storage, a slew of recent techno-economic analyses (TEAs) have attempted to provide a clear description of the costs of green ammonia production, yielding a range of cost estimates.

These TEAs tended to consider both current and future production costs, due to the expected fall in renewable and electrolyser costs in the next decade. For those papers which reported LCOA-Ps using technology currently available, the minimum reported values of the LCOA-P are 480 USD/t [18, 63]. Other literature, however, reports far higher prices in the order of 1,000 USD/t [70–72]

Looking to the future, most of the literature is in agreement that the cost of green ammonia will trend downwards, but there are inconsistencies between the date at which it is expected to reach parity with conventional ammonia. More ambitious estimates believe parity will be possible in some locations in 2030 [18]; others do not expect this point will be reached until 2040 or even 2050 [70].

This section analyses the cause of the difference between LCOA-Ps in order to identify which works have produced the most reliable assessments of green ammonia cost, and to identify the key factors which impact the LCOA-P. The wide range of LCOA-Ps reported in the literature can be attributed to variance in (i) technical approach, (ii)

project financial considerations, (iii) renewable energy resource, and (iv) technological inputs; this section deals with each in turn.

While parity with the cost of conventional ammonia is a useful benchmark for the cost of green ammonia, reductions below this cost are expected and necessary to drive uptake of green ammonia as a clean energy vector in the long term. This is because, as observed in Wijayanta et al. [14], ammonia's chemical role as a fertiliser increases its market price well above its value as an energy vector. Prior to the inflationary post-covid environment, the price of ammonia fluctuated between 350 and 550 USD/t[34, 73]. Even at the minimum value, 350 USD/t, the value of energy provided by ammonia on a HHV basis is 15.55 USD/GJ, which compares unfavourably to natural gas in the US, whose price ranged between 3 and 8 USD/GJ in the 2010s, depending on the specific location and market conditions [33, 74]. For that reason, green ammonia needs to be significantly cheaper than conventional ammonia to provide very cheap energy (although this direct comparison does not factor in efficiency of usage, which may be marginally higher for ammonia using SOFCs than for natural gas).

2.2.1 Ammonia Production Routes

Historically, synthetic ammonia has been produced from hydrogen and nitrogen almost exclusively using the Haber-Bosch (HB) process. This is a high temperature (>500°C), high pressure (150-400 bar) reaction driven by catalysts. It was remarkable at the time of its development for being one of the first chemical processes to operate continuously using a recycle loop [10].

Because of the prospects offered by green ammonia, a wide range of alternative technologies to HB have been considered. MacFarlane et al. [10] lay these out in a far-reaching review which classifies ammonia production into three phases: Phase 1 is the current phase, reliant on conventional ammonia; Phase 2 refers to ammonia made using the Haber-Bosch process but using green hydrogen produced from renewable electricity; Phase 3 refers to novel ammonia production processes. That study focussed in particular on direct electrochemical nitrogen reduction (eNRR) as the most likely Phase 3 technology. eNRR reduces the production process to a single electrolysis step which takes renewable power, water, and either nitrogen or air as inputs. The authors also make reference to indirect reduction technologies in which lithium is used to reduce the nitrogen into Li_3N in an aqueous environment, after which it is more chemically straightforward to substitute the metal atoms for hydrogen, producing ammonia and releasing the lithium metal back into solution. There are a wide number of other approaches which are also discussed as possibilities in the literature - photochemical synthesis [75], which uses light as the energy source for nitrogen fixation, and bioelectrocatalysis, which may enable enzymes which produce ammonia in nature (e.g. nitrogenase) to operate at industrial scales [76].

Although there is promise to these alternative technologies, they have not yet been demonstrated beyond the lab scale. Because of the urgency of introducing green ammonia into supply chains, this thesis focusses on Haber-Bosch technology since it is available immediately. In that sense, modelling performed in this thesis is conservative;

if a superior technology came to the fore, its only impact would be reducing the cost of green ammonia below the predictions made here. Chapter 4 discusses the potential benefits of alternative technologies on ammonia production cost.

2.2.2 Methodology for analysing ammonia production research

In order to obtain an initial short-list of publications in this field, a keyword search was performed on Scopus for literature containing the trigger words shown in Table 2.5.

Table 2.5 Trigger words for LCOA-P literature search. Literature needed to include at least one word from each of the categories listed to be included in the search.

Category	Trigger Words
Ammonia	Ammonia, Haber-Bosch
Renewable	Renewable, Green
Price	Price, Techno-economic, LCOA, Levelised

Literature was excluded if it relied upon a technology that was not yet commercially available (e.g. photocatalytic ammonia production), if the ammonia production technology was brown, grey or blue, or if the author did not provide a detailed cost assessment of hydrogen or ammonia production. After reviewing the list generated by Scopus, 22 of these papers were found to contain a detailed assessment of the LCOA-P. A further 8 papers were identified in the citations of the shortlisted literature, leading to a total of 30 papers considered. All papers considered are summarised in Table 2.6. As in Section 2.1.4, the LCOA-P was adjusted to 2020 prices using an inflation rate of 2.5%.

2.2.3 Technical Approach

Managing flexibility is a prerequisite in the production of green ammonia powered by variable renewable energy (VRE). Hydrogen electrolysers are highly flexible [77]; proton exchange membrane (PEM) type electrolysers, in particular, can reduce their operation to 5% of rated capacity [3], increasing efficiency as they do so [78]. However, the ammonia synthesis plant presents the major complexity to flexible operation, because it operates at high temperatures and pressures[17, 79], which means frequent cycling of production rate may damage catalysts and equipment [78]. Managing the ammonia plant when renewable energy is not available is therefore a major challenge.

In some literature, it is assumed that the Haber-Bosch loop is entirely inflexible, and can only operate at its maximum rate of 100% [64, 70]; other research has forecast a theoretical minimum operating rate of 20% [79], with remaining authors falling between these values [47, 63].

Table 2.6 Summary of ammonia energy production costs

Author	Category	Year	Location	Electrolyser Energy Efficiency (kWh/kg)	Dis-count Rate	Electrolyser Size (MW)	Electrolyser CAPEX (USD/kW)	Energy Cost (USD/ MWh)	LCOA-P[(i)] (USD/t)
Fasihi et al.[80]	Relevant	2030-2050	Global	53.6	7	N/A	726	N/A	> 440
Armijo et al.[63]	Relevant	2020	Argentina/Chile	47.6	8.5	1	600	30	-
Gomez et al.[81]	Did not use HB ammonia	2020	-	-	-	-	-	-	-
Fúnez Guerra et al.[55]	Lack of clarity for handling VRE	2020	Chile	47.6	8	150	495	20	-
Lin et al.[42]	Relies heavily on grid electricity	2020	Minnesota, USA	50	7	20.1	995	41	955
Nayak-Luke, R et al.[18]	Relevant	2020	Multiple	49	3.3-18	100	700	19	470
Osman et al.[64]	Relevant	2020	UAE	47.6	4	1300	652	25	617
Palys et al.[82]	LCOA-P subsidized by selling electricity	2020	USA	-	10	1	800	-	527
Wang et al.[83]	Relies heavily on grid electricity	2020	Germany	35.1	5	-	100	71	580
Zhang et al.[84]	Relies heavily on grid electricity	2020	-	-	10	43	-	73	544
Allman et al.[85]	Wind farm also sells to grid; subsidises NH3	2019	Minnesota, USA	60	8.3	0.25	2347	-	-
Rivarolo et al.[73]	Relies heavily on grid electricity	2019	Paraguay	52.7	-	200	784	17	374
Tso et al.[86]	Lack of clarity for handling VRE	2019	Texas, USA	-	-		607	45	2110
Zhao et al.[25]	Relies heavily on salt cavern	2019	USA Gulf Coast	-	6	-	433	51	361
Demirhan et al.[87]	Lack of clarity for handling VRE	2018	USA (Various states)	-	-	-	622	46	826
Eichhammer [88]	Lack of clarity for handling VRE	2018	Morocco	49	6.12	700	708	38	708
Ikäheimo et al.[89]	Wind farm also sells to grid; subsidises NH3	2018	Northern Europe	53	7	-	462	-	498
Nayak-Luke, R et al. [90]	Out of date inputs/assumptions	2018	Scotland, UK	53	Not used	196	1202	92	1366
Palys et al. [91]	Relies heavily on grid electricity	2018	USA Midwest	66.1	7	-	1313	32	641
ISPT [92]	Out of date inputs/assumptions	2017	Netherlands	53	7	40	1421	-	-
Morgan et al.[70]	Relies heavily on grid electricity	2017	USA	53.8	7	135	-	-	1318
Pfromm[93]	Lack of clarity for handling VRE	2017	-	54	-	-	-	25	275
Sánchez et al.[94]	Lack of clarity for handling VRE	2017	Southern Europe	53.2	-	-	-	-	-
Wang et al.[77]	Lack of clarity for handling VRE	2017	-	-	7.5	100	275	32	1023
Bañares-Alcántara et al. [95]	Out of date inputs/assumptions	2015	Victoria, Australia	47	8	12	1353	57	1474
Beerbühl et al.[78]	Out of date inputs/assumptions	2015	Germany	49.3	-	34.5	-	45	647
Matzen et al.[96]	Lack of clarity for handling VRE	2015	-	54.8	-	-	735	51	749
Trop et al. [97]	Relies heavily on hydro electricity	2015	Iceland	63.5	90	600	162	34	495
Morgan et al.[72]	Lack of clarity for handling VRE	2014	Maine, USA	53.6	7	-	-	-	1488
Tunå et al.[71]	Out of date inputs/assumptions	2014	General	47.6	8.5	10	669	46	1177

[(i)] Where literature reported multiple LCOA-Ps, the lowest value reported was selected. Where multiple time horizons were considered, data for the shortest time horizon was selected (i.e. 2020 estimates were preferred to 2030 estimates).

Lower operating rates may be facilitated by technology developments, such as the use of advanced catalysts and ammonia separation using absorbents, which enable ammonia synthesis to be conducted at low temperatures and pressures (∼275°C and 8 bar [98, 99]). Chapter 4 explores how these modifications could be useful in order to mitigate hydrogen storage costs; however, these modifications alone cannot entirely smooth out the variability of wind and solar farms.

There are a range of approaches taken in the literature to manage the challenge of operating the Haber-Bosch loop in periods without enough available renewable energy. However, in much of the literature [55, 72, 84, 88, 93, 94, 96], this challenge is not discussed in enough detail to confirm if the proposed design is operable. In other cases [77, 89] flexibility is neglected in order to simplify process modelling; because of this simplification, these cases provide limited insight into specific process design.

Some authors manage variable operation using the grid [42, 70, 71, 83, 84] or dispatchable hydro electricity [73, 97] to entirely supply the electrolyser and ammonia plant at almost all times, or whenever renewables are not available. Although this approach enables maximum value to be extracted from the installed capital equipment, and no costs to be allocated to hydrogen storage, it demands the use of either of hydroelectricity, whose global potential is far less than global demand [100], or of prohibitively expensive grid electricity, which is not generally decarbonized. In addition, relying on highly renewable-dependent grids is not likely to be possible for green ammonia plants when wind or solar farms are not operating, because those times will be correlated with periods when grid demand exceeds supply. At best, drawing on the grid at these times will be expensive; at worst it will be prohibited by regulators.

In the remaining papers limited to islanded VREs (i.e. without grid connection), several authors [18, 63, 64, 80, 82] include a hydrogen buffer which can store excess hydrogen produced during periods of high electricity generation and therefore maintain the required supply of raw material to the ammonia plant. The size of the buffer required depends on the renewable energy profile, and the expected flexibility of the ammonia plant. An additional energy source (e.g. non-variable renewables, batteries, or cannibalisation of some hydrogen) may be used to provide continuous electricity to the ammonia compressor and air separation unit. The authors who included hydrogen buffers used some form of optimisation model to select the size of the equipment in the ammonia plant, including the hydrogen storage; these approaches are discussed in more detail in Chapter 3.

Interestingly, although flexibility is a major complicating factor in plant design, plants which fail to give due consideration to flexibility do not always have the lowest calculated LCOA-P. This is typically because those papers use more conservative financial estimates and do not optimise plant design for the weather profile.

2.2.4 Discount Rate

The literature proposes a range of financial parameters to amortise the large capital costs of green ammonia plants caused by the significant investment required in the electrolysis unit. This range of finance options can distort the

LCOA-P and therefore conceal underlying project strengths or weaknesses.

The simplest financial approach to reducing the LCOA-P within a model is to reduce the discount rate, which can be achieved with more favourable loan conditions (e.g. high debt/equity ratios, long loan terms, and low interest rates on debt). In contrast to traditional engineering applications, changing these financial parameters can have a major impact on LCOA-P because green ammonia production is highly capital intensive [101].

Excluding Nayak-Luke et al. [90], in which the discount rate was set to 0 to specifically exclude it from consideration, then the range of discount rates considered in the literature surveyed spanned from 4% [64] to 12%[71]. Nayak-Luke and Bañares-Alcántara [18] varied the discount rate based on location, sector, and the nature of the investor (domestic or multinational); that study used a minimum discount rate of 3.3% for a multinational corporation investing in a renewably powered utility, and a maximum of 18.74% for a Venezuelan domestic company investing in an ammonia plant. This range of discount rates may be reflective of actual difference in the cost of capital available to projects in different regions. For instance, Steffen [101] estimated the discount rate considered for a large number of renewable projects using different techniques, finding values as low as 2.5% in Germany, and in excess of 10% in India for both solar and wind installations.

With the exception of Nayak-Luke and Bañares-Alcántara [18] and Fúnez Guerra et al. [55], few papers provided clear detail as to the selection of the discount rate, despite its significant impact on the LCOA-P. This thesis in general uses a discount rate of 7% (unless otherwise specified), which is comfortably within the range of forecast LCOA-Ps

2.2.5 Technology cost curves

The most substantial contributors to the cost of green ammonia are renewable electricity and electrolyser CAPEX. These two contributions also represent the components of the cost which are most likely to fall in the future; their gradual fall in price is generally referred to as the technology's "cost curve". Although the capital cost of ammonia synthesis is substantial, it is small compared to electrolyser costs, and is a mature technology that is unlikely to see significant cost reduction. For that reason, accurate estimates of electricity prices and electrolyser CAPEX are critical to accurate LCOA-P forecasting, but the selection of suitable cost curves often receives limited attention in the literature.

Comparison of renewable energy price in the literature is complicated by the varied approaches taken by different authors. In some instances, electricity was purchased by a power purchasing agreement (PPA) [64, 93, 96]; in others, it was supplied by onsite energy farms [18, 63, 95]. In some cases, renewable power was also sold directly onto the grid, cross-subsidizing its costs [82], or was supplied from an existing windfarm which was being curtailed [85]. Some authors did not specify a renewable energy cost [78] The total amount of energy available from wind and solar farms was also not typically reported, making it impossible to convert between the capital and amortized costs of renewable energy. For those reasons, a comparison of renewable energy inputs to the model used across the literature was not possible. This speaks to a broader problem in the literature that the consideration of how and

when renewable energy is available has not been present in most cases.

It is easier to compare the electrolyser capital cost used in the model. Using an excessively low electrolyser CAPEX will not only underestimate project costs, but will also lead to a non-optimal design, favouring lower load factor renewable sources if they provide cheaper power. International energy bodies are divided over the expected costs of electrolysers for both today and in 2030. Bloomberg NEF [102], for instance, predicted a price of just 200 USD/kW for a Chinese electrolyser purchased in 2020, falling to 135 USD/kW by 2030. Both IRENA[3] and the IEA [24] disagree with this forecast, reporting prices of 840 USD/kW and 900 USD/kW for electrolysers purchased today. IRENA suggests that a price of 200 USD/kW will not be possible until 2050; the IEA's forecast ends in 2030 at a minimum price of 450 USD/kW.

The green ammonia literature is similarly divided over the price of electrolysers, with minimum prices of 143 USD/kW [97] compared with maximum prices in excess of 1,000 USD/kW, which tend to be found in papers published in 2015 or earlier [71, 95]. However, the papers identified as most robust in earlier sections [18, 63, 64, 80], with rigorously optimised designs, tended to use prices between 600 and 1,000 USD/kW, which are plausible estimates given the data available.

Forecasting of electrolyser price is complicated by variations in the electrolyser scope. For instance, Wang et al.[83] specifies a very low price of 100 USD/kW for a solid oxide cell (typically the most capital intensive cell type [67]); however, this only includes the stack and excludes all balance of plant, as well as installation costs, which they do not specify. Lin et al.[42] and Palys et al.[91] both use a bare module cost (327 USD/kW and 637 USD/kW respectively) alongside published installation factors to estimate a project CAPEX (994 USD/kW and 1,248 USD/kW). IRENA [3] and Nayak-Luke et al. [18] specify that their electrolyser costs include installation and balance of plant costs. In general, though, authors are not specific as to the scope of what is included within their electrolyser cost.

Equating the bare material cost of electrolysers to their installed cost is risky and is likely to result in a large underestimation of total project costs. Electrolyser vendors typically provide the stack and some electrical equipment; they do not provide installation or the entire balance of plant, which may include additional electrical work, pipework, and civil/structural engineering. Those costs must be borne separately by the project owner. The US National Renewable Energy Laboratory provides a complete cost breakdown of the installation of electrolysis units, concluding that the electrolyser stack alone may represent only 1/6th of the total project CAPEX; installation costs may be as high as 1/3rd of total costs [103]. All electrolyser costs in this thesis include the entire installation scope (i.e. transformers, membranes, stacks, balance of plant and installation).

2.2.6 Ammonia Production Summary

There are a large number of inputs into ammonia plant design, which have not always been handled consistently or sensibly in the literature. As a consequence, there remains a significant gap in our understanding of how ammonia

is produced affordably which merits further investigation.

However, almost all literature is in agreement that the location of a green ammonia plant is central to the LCOA-P. This drives the opportunity for 'spatial arbitrage' in the ammonia market, which is to say that it is possible to profit by producing energy in one country and exporting it to another. The arbitrage is justified economically if the costs of energy conversion to ammonia and transport are less than the energy cost difference between the two locations at which energy is produced and consumed.

2.3 Ammonia supply and demand

The purpose of this section is to summarise literature on production and demand capacities. It first assesses the limits on ammonia supply at large scales, and then compares those limits to various estimates of ammonia demand, to identify potential hurdles to very large-scale ammonia economies.

2.3.1 Ammonia supply

Green ammonia supply capacity depends on both the number and size of ammonia facilities. While smaller ammonia systems are often touted as a solution which can decentralise energy grids, for intercontinental energy transport it is more likely that a comparatively small number of large ammonia facilities will be used given the economies of scale associated with HB production of ammonia [80] as well as port and shipping infrastructure [104]. Two projects have been announced whose scale is very large (i.e. more than 10 MMTPA of ammonia, and more than 25 GW of renewable capacity)[105, 106] in Australia (the Australian Renewable Energy Hub) and Oman (the Green Energy Oman project); both of these are several times larger than the biggest ammonia plants in existence today[107].

This section therefore aims to identify constraints on both individual project size and domestic production capacity. Four major factors are identified which may constrain the production of ammonia, both at the level of individual projects and global markets: material availability, land availability, capital availability, and public support.

2.3.1.1 Material Availability

There are five major components required for green ammonia export facilities: renewable energy supply, hydrogen electrolysis, water supply, ammonia synthesis, and ammonia storage and transport. This section focusses on the first three components, as the remainder (ammonia synthesis, storage and transport) are already operated on a global scale of millions to hundreds of millions of tons per year and are constructed mostly from structural materials (e.g. concrete and steel) which are expected to be available in adequate quantities.

2.3.1.1.1 Renewable energy supply Renewable energy supply on a very large scale requires either wind or solar electricity generation. Both wind and solar farms require substantial investment in structural materials and electrical equipment. Beyond these basic components, both technologies also require more specialised materials. Wind turbines use rare earth metals – typically neodymium, praseodymium, dysprosium and terbium – in order to

create the permanent magnet generators in which power is produced. The metals used in solar panels depend on the type; the most commonly occurring type uses silver and silicon, but other varieties require a range of different rare earth elements. [108]

An investigation into the availability of these materials in the EU[108] found that in a complete decarbonisation scenario, significant pressure was expected on the supply chains of dysprosium and terbium for wind, and germanium, tellurium, indium and selenium for Solar PV. Weng et al.[109] agreed with the assessment that supply chains of rare earth metals required for renewable energy technology are likely to be strained. They performed an assessment of all rare earth metals globally, and concluded that supply chain limitations were not caused by a lack of geological availability, rather by China's monopoly of the current rare earth metal market. China is historically responsible for >95% of global production of rare earth metals, which can create distortive effects on global trade. For instance, in 2006, China placed export limits on three rare earth metals in order to build domestic industry, causing a spike in prices globally.

In the context of materials shortages, it will not be justifiable to use limited renewable energy for chemical energy storage; instead, widespread societal change will be required to substantially reduce both average and peak energy consumption. However, to avoid this constraint, it may be possible to expand access to rare earth metals: Weng et al.[109] found that a number of large, non-exploited resources exist outside of China, with deposits in Australia, Russia, Canada and Brazil. The size of the deposits outside of China is likely an underestimate caused by a lack of geological exploration for these metals. Therefore, it is very likely that there is an adequate amount of to produce very large-scale wind and solar farms; obtaining those materials will require geopolitical stability, and diversification of rare earth metal mining efforts in a range of countries.

2.3.1.1.2 Electrolyser Type There are three types of hydrogen electrolyser: alkaline (AEC), proton exchange membrane (PEM) and solid oxide (SOEC). AECs are already used on an industrial scale in the chlor-alkali process, producing sodium hydroxide and chlorine gas. The technology circulates potassium hydroxide and uses nickel-based catalysts[110]. It is unlikely that materials shortages will limit the use of this cell; however, they are unlikely to be as efficient as other electrolyser cell types in the future [3]. PEM cells are not yet widely used at industrial scale, and rely more heavily on precious metals, including platinum and iridium. Hauch et al. [67] argue that shortages of these materials could prevent widespread use of PEM cells. For instance, only 5 t/year of iridium are produced globally; a 1 GW installation would require 0.5 t of this element, although these quantities may reduce with technological advancement. Like AECs, SOECs typically use common materials, the scarcest of which is yttrium; a 1 GW installation would require only about half a day's global production of this material[111].

Overall, availability of materials may inform technology selection of renewable electricity generators and electrolysis cell types; however, it should not significantly limit the size of large-scale green ammonia plant installations. It may encourage the production of ammonia in nations which have access to certain materials, or who have stable relationships with countries that produce those materials.

2.3.1.1.3 Water availability Once power has been supplied, water is the only raw material required in significant amounts for ongoing operation of an electrolysis plant; each kilogram of hydrogen produced requires approximately 9 kg of deioinised water, the production of which may require in the order of 25 kg of sea water [112].

The availability of water is often raised as a concern for hydrogen electrolysers which are heavily reliant on solar energy; these are often in arid regions with limited rainfall and may therefore be challenged by water scarcity. In these circumstances, desalination is the only viable technology for water production [64]. However, even the energy demands of desalination are relatively low compared to the power input required by the electrolyser, and desalination would contribute at most 0.02 USD/kg to the cost of hydrogen [112] In theory, therefore, water supply should not be a major problem to the establishment of a global ammonia industry; however, it may constrain production away from areas with significant water stress, or encourage operation near coastal areas to reduce the costs of desalinated water. Solutions for managing desalination, and its integration into the green ammonia production process, are discussed in greater detail in Chapter 5.

2.3.1.2 Land availability

In general, land availability should not meaningfully limit total global production of renewable energy. For instance, Moriarty and Honnery [113] found that the solar insolation on the Sahara desert alone would be adequate to supply the global population in 2050, even assuming limited energy efficiency innovations. Similarly, Babarit et al. [58] found the offshore wind potential at shallow and intermediate depths alone could theoretically supply 75% of global energy demand in 2050, and that the capacity of floating windfarms in deep water could meet energy demand almost 10-fold.

In practice, land limitations can be substantial; collecting all of the solar irradiation on the Sahara, for instance, is not practical due to the difficulty of installing panels on sloping dunes. This can be particularly problematic in specific regions: in Japan and Korea, which have low levels of agricultural self-sufficiency, installation of significant solar infrastructure would displace land usually used for food production [114, 115]. Moreover, the land-use change associated with conversion of land from crops to energy generation can impact atmospheric CO_2 levels. In Japan and Korea, the emissions intensity of electricity from solar panels which have displaced agriculture could be as high as 10% of emissions intensity of electricity from natural gas[114].

By contrast, other countries are not land-limited. The aforementioned Australian Renewable Energy Hub has a land area of 6,500 km^2; factoring a 60% conversion efficiency to ammonia, this facility would generate 3.5% of Australia's annual energy consumption on just 0.08% of its land [105]. In other words, renewable energy harvested at this rate on less than 2.5% of Australia's land mass could produce its entire energy consumption. In practice, as panel and end-use energy efficiency improve, this forecast area may be even smaller. Because the land in question is not agricultural land, and because of the higher solar insolation in Australia compared to Japan and Korea, the

land-use change effects are not likely to be significant [114]. In other contexts, though, they may have a significant impact: 6,500 km^2 is about four times the area of greater London.

Fasihi et al. [80] considered land consumption in the context of green ammonia specifically, and found that the global potential for green ammonia production far exceeded all potential estimates of demand; however, they did not consider any constraints on using land in possible production locations.

In summary, it is possible to produce enough renewable energy to supply global demand in 2050; however, the distribution of energy production will not enable all nations to be self-sufficient. Countries with low land-availability (either because of population density, highly sloping terrains, or substantial agricultural demands) will need to import energy from countries with comparatively high land availability. This is discussed in significantly more detail in Chapters 5 and 6.

2.3.1.3 Capital Availability

Green ammonia production is highly capital intensive; this is particularly true if a facility includes capital investment on a wind or solar farm, rather than purchasing electricity through a PPA. The presence of significant capital investment is therefore a prerequisite for large-scale ammonia production at the global level, and at the level of individual projects.

The IEA [56] reports that investment in clean energy technology has largely been stable over the past 5 years, at approximately 600 billion USD/annum (including investment in power, nuclear, energy efficiency and energy storage technologies). For reference, the AREH has an expected CAPEX of 36 billion USD [105], or 6% of the current global annual investment in clean energy. Using the same assumptions for its conversion efficiency described in the previous section, it will produce only $\sim$1% of Japan's annual primary energy demand [28]; in other words, converting energy systems to make substantial use of ammonia will require capital investment on a very large scale over a sustained period of time.

Although investment in renewables comes predominantly from the private sector, it can be stimulated by government incentives, or sold at a premium to state-owned utilities [56, 116]. For instance, governments can create supply chains (e.g. by supporting pilot projects, building capacity, and facilitating international trade), and by provide risk mitigation to projects in difficult sectors (e.g. providing innovative financing instruments, guarantees, and promoting a green bond market) [116]. Meanwhile, energy importing governments can create demand for hydrogen that enables offtake agreements with large projects, de-risking major capital investments. In doing so, they can create virtuous cycles that enable an adequate injection of capital to create these ammonia supply chains [4]

2.3.1.4 Public Perception

In democratic nations, the public, voting either directly or with their feet, can shape the success or otherwise of major projects. The capacity of a country to export energy on a very large scale therefore depends on a supportive

public that is comfortable to allocate large areas of land to produce energy for a different country. Similarly, importing chemical fuels relies on a public that is willing and able to use those fuels safely.

2.3.1.4.1 Public attitudes towards renewable energy Despite perceptions which may be gleaned from the media, several comprehensive studies have found the public to be supportive of large scale energy projects in general; this support is even more significant for renewable energy projects, particularly solar [117]. Most of the literature and analysis has been performed in the UK and the US, where opposition is perceived to be most significant; there is limited data from the rest of the world.

Because of perceived opposition, the literature on public resistance to energy projects focusses particularly on wind, although here too, both local communities and the public at large are broadly supportive[118] The perception of opposition is created by highly vocal minorities who receive disproportionate media air time [119]. Although support is generally high, there are some grounds upon which local communities have objected to windfarms, such as aesthetic and noise complaints. Rand and Hoen[118] find that these concerns are all manageable by taking small tangible steps in a project which alleviate community angst, by providing the public with detailed information about projects, and by taking the public's concerns seriously.

Some objections reported in the literature are unlikely to materialise if a project intends to export chemically stored energy (e.g. concerns that a project will increase local electricity prices [118], or that renewable energy is unreliable [120]). On the other hand, other objections may become more severe (e.g. fear that profits from a project are being delivered to multi-national companies rather than local communities [118]).

2.3.1.4.2 Public attitudes towards hydrogen and ammonia Because the production of hydrogen and ammonia is currently limited to industrial settings, there is limited project-specific research quantifying the public's views on a proposed or existing green hydrogen/ammonia facility.

To the extent that research has been conducted, Ono and Tsunemi [121] identified that 66% of the Japanese public was supportive of implementing hydrogen fuel stations. Schmidt and Donsbach [122] found that attitudes towards hydrogen were broadly positive, and could be improved by reframing arguments in favour of hydrogen to focus on energy independence and decentralisation of energy grids. Lambert and Ashworth [123] specifically asked Australian respondents about their support for hydrogen export, with 78% in support, although only 38% were supportive of a hydrogen port if it were located close to their home. The main concern identified in all surveys was safety.

Even where there is some public opposition to green hydrogen, localised energy projects are rarely a source of objection from the public; they are more often opposed to transmission and distribution of electrical power, usually for aesthetic reasons [117]. Therefore, to the extent that the public may object to elements of chemical energy storage projects, it is a relatively favourable method of energy transport.

It was consistently observed that the public's knowledge of hydrogen was relatively poor. Ashworth and Lambert[123] asked five simple questions pertaining to hydrogen; only 7% of survey respondents answered all questions

correctly; these respondents were almost three times as likely to be supportive or very supportive of a hydrogen industry in Australia. Itoaka et al. [124] asked similar questions; less than 30% correctly answered all of them, and there was only a marginal improvement in public knowledge observed between 2008 and 2015.

The majority of research focusses on public attitudes to hydrogen, and there may be unique concerns associated with ammonia that are not yet examined in the literature. Given the public's lack of understanding of hydrogen as an energy vector, Guati-Rojo et al. [125] find that it is unlikely that the public has yet formed opinions of hydrogen derivatives such as ammonia. In their small study in Mexico, focus groups were generally supportive of ammonia as an energy vector once the concept had been explained to them, although they raised concerns about NOx emissions and water consumption. In the same way that these challenges can be managed technically, concerns about NOx emissions and water consumption should be manageable with quality public education and consultation on the benefits and risks of ammonia. In another focus-group study focussing on expert perspectives, the most substantial concern for green ammonia use pertained to its toxicity [125].

Ammonia has been used as an industrial chemical since the 1920s; therefore, while safe handling of ammonia is a critical engineering challenge, it is not a novel one. Although it is toxic to humans above 25 ppm, it has a strong odour at lower concentrations (5 ppm) which can provide warning of its presence. Several studies have found it to be as safe or safer than similar hydrocarbons, because it is less flammable [10].

Overall, it appears that there is a reasonable level of public support for the hydrogen industry, and a shortage of research into support for the ammonia industry. If the public's concerns are taken seriously, and an effort is made to educate the public about green fuels, then social acceptance should not be a constraint to a hydrogen or ammonia export economy. High levels of public support may stimulate the government action described earlier, which in turn incentivises the capital investment required for ammonia plants.

2.3.1.5 Supply Summary

There are a number of challenges across different sectors of the supply chain that may limit the scope and growth of a green ammonia plant; however, none of these challenges are insurmountable. This thesis will therefore focus on the technical challenge of optimising supply chains given land-constraints, as these supply chains are feasible within reasonable limitations on production.

2.3.2 Ammonia Demand

Forecasting ammonia demand is challenging, because of the range of possible use-cases, and the significant changes that will occur in energy systems over the next three decades. In chapter 6, this thesis explores two strategies for estimating ammonia demand in the maritime and grid electricity sectors.

As a basis for demand estimation, it is unlikely that existing uses of ammonia will significantly decline, although there may be some pressure to reduce nitrogenous fertiliser usage for environmental reasons. Existing demand is in the order of 200 MMTPA [126].

Demand estimation in the maritime sector is most straightforward because it is very likely to continue to rely upon chemical fuels, and because ammonia is the most promising of those fuels. IRENA estimates the maritime sector consumed 2,472 TWh of bunker fuel in 2017 [127]; if it were a country, it would be the world's sixth largest emitter of carbon dioxide [128]. In 2018, the International Maritime Organisation (IMO) set a target of reducing total shipping emissions by 50% by 2050, which will require an emissions intensity reduction of more than 70%[129] If the entirety of the IMO's target emissions reduction were achieved by fuel substitution, approximately 500 MMTPA of green ammonia would be required. The IEA, however, argues it will be possible to achieve some emissions reductions through operational modification (e.g. reducing speed limits), and by electrification (for very short routes only), meaning a more realistic estimate of may be as low as half that value [129]. However, to meet even this demand, 27 projects of equivalent size to the Asian Renewable Energy Hub would be required; constructing them would more than double current global ammonia production [130].

Beyond the maritime sector, ammonia may also play a role in the electricity sector [131], and from use as a hydrogen vector (to subsequently supply the metallurgy industry [7]) and transport industries[124], for instance). Estimating consumption in these sectors is complex, but may also be significant; approximately 1,800 MMTPA of crude steel are produced each year [132], which would demand around 90 MMTPA of hydrogen [7] - if that were to be supplied with ammonia, it would amount to 500 MMTPA.

Although demand for green ammonia is challenging to estimate, it could be very large, and dwarf existing consumption of ammonia for fertiliser only. The scale of demand will require an international network of ammonia trade that is not at present well described. There is a need for (i) more rigorous demand forecasting, and (ii) for a consideration of how systems will be designed to enable that demand.

2.4 Literature Review Summary

There is a growing body of literature recommending ammonia as an important contributor to global decarbonisation. It will become more significant over the next three decades as its price falls.

Most authors concur that it outperforms other chemical energy vectors because of its promising hydrogen density and ease of distribution and storage. The largest constraints on ammonia supply are land availability and finance, although these will tend to encourage production in certain countries, rather than limiting the overall size of an ammonia economy. There is growing demand for ammonia specifically, and for ammonia as a carrier of hydrogen.

Despite these promising findings, more rigorous consideration of ammonia as a spatial energy vector is still merited. There is a lack of detailed consideration of the relationship between ammonia production and ammonia transport. Typically, the papers which provide a detailed solution to the complexities of production neglect to consider how they may interact with the complexities of transport, and vice versa. Additionally, research to date has focussed on the bilateral exchange of energy. This contrasts with the multilateral nature of fossil-fuel transport and is therefore likely to be an oversimplification of future energy systems.

This thesis sets out to more comprehensively optimise a system for ammonia delivery, including all aspects of production, transport, and consumption. These include:

1. Selection of ammonia production location for the purpose of energy export, considering both the quality of the local resource and the transport costs to the intended destination or destinations
2. Management of process flexibility on a short-term basis to ensure continuous and safe operation of the Haber-Bosch process
3. Understanding of the constraints on ammonia supply and demand, including physical limits (e.g. land, materials), project-specific factors (e.g. availability of capital, public support) and maximum consumption rates in energy-importing nations
4. Consideration of possible synergies between production and transport requirements

Collectively, these gaps in the literature represent a risk to the optimisation of what is likely to be a major energy supply chain of the future. By optimising this supply chain, this thesis will:

1. Enable efficient allocation of finite capital [133]
2. Enable investors to identify lowest-cost options for large scale ammonia development, which is necessary in the short term to stimulate demand [3] and demonstrate feasibility
3. Prevent wasteful allocation of large capital subsidies offered by governments (renewable subsidies were greater than 60 billion USD in 2016 in the EU alone [134])
4. Enable energy importers to identify appropriate export partners, and to facilitate international relationships
5. Enable energy exporters to identify possible future markets, and tailor policy and regulation to encourage investment and growth of new renewable export industries.

Chapter 3

Optimisation of green ammonia plant design

Green ammonia plants could be conceptualised as a machine for converting variable renewable power into a continuously available energy supply. Green ammonia production therefore differs from conventional ammonia plants, which could be conceptualised as machines for converting one form of energy (natural gas) into a valuable commercial product (ammonia for fertilisers). This means green ammonia plants will ooperate very differently to conventional ammonia plants, which have historically operated continuously at a load factor as close to their design rate as possible in order to maximise the value of the capital investment.

In those conventional plants, each piece of equipment would typically be sized to process approximately the same total plant flow, with storage buffers or oversized equipment only used in specific instances (e.g. where the mode of operation is semi-batch, or a unit has unusually large maintenance requirements). In contrast, because operation in green ammonia plants necessarily occurs at a variable rate, the optimal plant design will use different sizing for different equipment to avoid the under-utilisation of downstream components. Equipment sizing is further complicated by two other factors: firstly, selecting the appropriate balance of solar PV and wind-turbines to power the plant depends specifically on the local renewable profile; and secondly, managing the limited flexibility of the the Haber-Bosch process, which prevents it from being ramped at the same rate as the renewable power profile changes.

Therefore, sizing equipment on a green ammonia plant is a much more complex problem than that faced by conventional ammonia plants, and optimisation models need to be developed in order to estimate suitable plant size. This chapter describes the development of such a model, and then uses the model for a case-study into green ammonia plant operation with a grid connection. The selected model needs to provide an optimal solution which considers the inherent variability of renewable power production; it must also solve rapidly enough that a large

number of locations can be modelled.

3.1 Methodology

3.1.1 Historical Approaches

Many authors have estimated the cost of green ammonia or hydrogen production, although the optimisation approach used is not always rigorous. For instance, the Hydrogen Economic Fairways Tool developed by Geoscience Australia[135, 136] estimates the NPV of producing green hydrogen at all locations in Australia, and considers the role of other infrastructure in the cost estimation. However, it simplifies the renewable energy profile down to a simple estimation of load factor, rather than optimising the size of all equipment based on the time-varying profile of the renewable source.

For authors who had a more robust approach, techniques have included brute-force optimisation[63] and genetic algorithms[18]. In both of these approaches, the model essentially guesses a plant design, and then determines (i) if the plant design is feasible, and (ii) the cost associated with the plant design. The genetic algorithm is superior to the brute-force approach, since it uses a searching technique to gradually improve the quality of its guess, meaning it does not need to trial every option in the search space in order to locate the optimum. These techniques are sufficiently sophisticated to factor in the inherent variability in plant operation; however, they are both designed for non-linear problems, and a fairly small number of variables. As discussed below, this optimisation problem can be linearised, and exploiting this feature enables far more rapid solution. Additionally, to limit the number of variables which need to be modelled, both of these authors used a power allocation algorithm, which apportioned the available electricity at a given time step according to a simple set of rules. This introduces two limitations: firstly, it may not achieve the 'true' optimum, and secondly, it reduces the capacity to introduce additional complexity into plant design.

On the first limitation: consider a location with a highly seasonal renewable energy availability. It will generally be logical in the months before the low season to ensure the hydrogen storage unit is full in order to prevent ammonia plant shutdowns during the low season, even if doing so requires operating the ammonia plant at a slightly lower rate. In the months after the low season, the opposite will be true, and it will generally be preferable to prioritise ammonia production over filling hydrogen storage. Allocating energy using a simple algorithm that depends only on the current power produced by the renewable energy supplies does not enable different approaches to be adopted in different seasons, and therefore the solution reached may not be the optimum. Section 3.2.2 demonstrates this point, showing that allocating power according to the power profile on a 'representative day' is not a reliable approach to predicting ammonia costs.

On the second limitation: because of the need for a power allocation algorithm to solve the model in a sensible period of time, the plant cannot be made more complex without introducing arbitrary power allocation rules. For instance, the plants modelled in Nayak-Luke and Bañares-Alcántara [18] use hydrogen fuel cells as a source of

back-up power, cannibalising some of the stored hydrogen. If a second source of energy storage - for instance, a battery - were introduced, then some allocation decision must be made as to whether excess energy should be stored in the battery or the hydrogen storage unit. While an allocation hierarchy may be possible, or even necessary, on a constructed plant that has a fixed design and a well-understood local weather profile, it is non-trivial to design general rules which optimally allocate power between these two storage units given the slightly different roles hydrogen and battery storage play onsite. Even if less complicated modifications are made to the model, such as the inclusion of both fixed and single-axis tracking solar PV, the number of unknowns increases. This in turn vastly increase the size of the search space and the number of iterations the model will require to identify an optimal solution using these non-linear approaches.

For these reasons, several other authors have adopted Mixed Integer Linear Programs (MILPs) as an alternative method, which has been adopted in a number of other publications [64, 80, 137]. The model presented here is similar to that presented by Fasihi et al.[80], although a large number of modifications are discussed to determine the impact of specific changes to green ammonia plant design. After the research in this chapter was published, Campion et al. [137] constructed a similar model that also considered the possibility of a grid connection; however, their study was more focussed on technology selection, and they therefore considered only three locations in very different contexts - it is not useful for specifically examining the role of the grid connection itself, and the conditions that make it useful.

The benefit of the MILP approach is that the allocation of power is achieved using variables that are selected by the optimisation solver, rather than by a pre-specified algorithm, which resolves the two limitations identified in the last paragraph. The solver is able to exploit the predictable gradient of linear problems in order to find the solution very rapidly; further, the large number of MILPs in a range of contexts has led to development of commercial solvers which can quickly solve problems with many variables.

Green ammonia production is well-suited to analysis using MILPs because each component in the design is modular, and the modules are much smaller than the typical size of a industrial scale plant. The exception to this point is the Haber-Bosch synthesis unit, which is a conventional chemical unit, and will tend to benefit from economies of scale in order to reduce material demands during construction [94, 138, 139]. Because the per-unit cost is a function of the equipment size, the cost cannot be modelled as a simple linear constraint. In theory, this is resolvable by linearising the constraint, either by decomposing it into a series of linear inequality constraints, or by using integer variables which switch on and off in different capacity ranges and select a per-unit cost of ammonia plant suitable to that capacity range. In practice, this is undesirable since the greater the number of linear inequality constraints/integer variables, the greater the complexity of the model, and the slower the solution time. However, at very large scales, the non-linearity in this specific problem breaks down, since the largest single-train Haber-Bosch plant which exists at present has a capacity of around 1 MMTPA[107]. Plants larger than this use duplicate trains, at which point economies of scale cease to benefit production cost, and the scale factor tends to a value of

1. Therefore even the cost of this unit can be modelled as having a linear dependence on its size, meaning that a MILP approach is valid.

Because of the logic described above, the MILP was selected to model green ammonia production. This section describes the development of a 'generic' model implemented in Python using the pyomo module. It then describes testing done to the model which enables it to solve rapidly, and presents a case-study on grid connection.

3.1.2 Model Framework

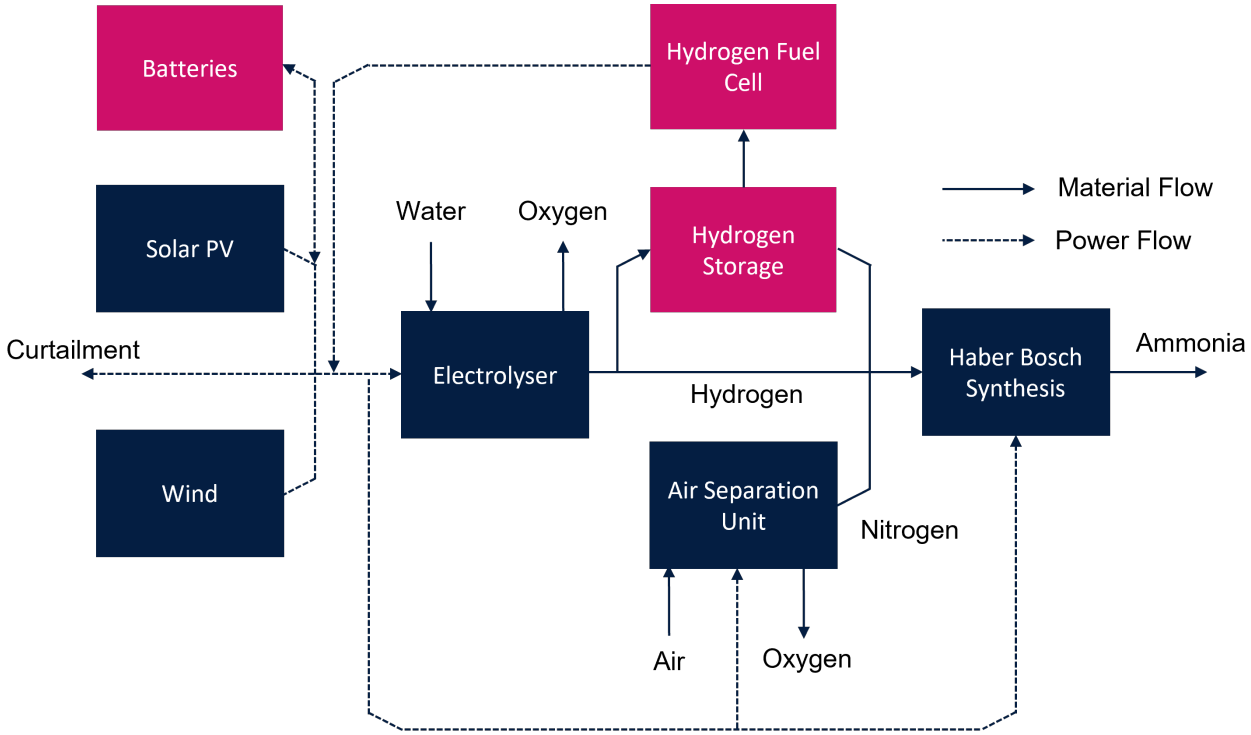

Fig. 3.1 Schematic demonstrating operation of ammonia production, as it is interpreted by the MILP model in this section: power is produced from renewables, and fed to electrolysers, the Haber-Bosch plant and the Air Separation Unit; the Haber-Bosch plant also receives hydrogen and nitrogen. Back up storage of hydrogen and power are also included to enable operation from intermittent renewable energy. Boxes in dark blue represent equipment which must be included for the plant to operate (although only one of wind or solar is strictly required); pink boxes represent equipment whose inclusion is optional, and are included as required to manage the inflexibility of the Haber-Bosch plant.

The goal of the optimisation model is to minimise the levelised cost of ammonia produced according to the process shown in Figure 3.1. The plant considered here uses electricity from any of the three power sources to (i) run a water electrolyser which produces hydrogen, (ii) charge a battery, and/or (iii) operate the Haber-Bosch (HB) loop and air separation unit (ASU). The HB & ASU together produce nitrogen and then react it with the hydrogen from the electrolyser to produce ammonia - these units are modelled as a single unit here for simplicity. In order to maintain stable operation of the Haber-Bosch loop, the model includes hydrogen storage (as a compressed gas) and back-up power, which can be supplied by discharging the battery, or from a hydrogen fuel cell. The optimised solution at a given location will sometimes exclude one or more of these components depending on the input data

[10, 79, 140].

Plant components can be categorised based on if they are sized according to their rated power capacity in MW (the electrolyser, the HB+ASU, the battery power capacity and the fuel cell), or if they are sized according to their energy storage capacity in MWh or tons of hydrogen (the battery and the hydrogen storage unit). In the formalism of the model, the former set is denoted as S_C, and the latter is denoted as S_{SC}. Two other sets are also included: a set of all times, S_t, and a set of renewable energy generators, S_R, which for the example plant shown in Figure 3.1 would include wind and solar PV.

The levelised cost of ammonia is the price at which ammonia must be sold in order to achieve a net present value of zero for a given plant lifetime and discount rate. It is calculated from:

$$LCOAP = \frac{CRF \cdot CAPEX + OPEX}{F} \tag{3.1}$$

where F is the annual production of ammonia in tonnes. This formula is suitable because a constant value is assumed for the OPEX and the annual production in each year, making equation (3.1) equivalent to taking the ratio of the project NPV to the (discounted) total flow over the project lifetime. For the general case of this model, F is set to 1 MMTPA, which as discussed is required for linearisation, and is a plausible scale for industrial ammonia plants. CRF is the capital recovery factor, calculated from:

$$CRF = \frac{i(1+i)^{PL}}{(1+i)^{PL}-1} \tag{3.2}$$

where i is the discount rate and PL is the plant lifetime. A default value of 7% is used for the discount rate in this work; this may vary considerably in different contexts, but the purpose of this analysis is to focus on the role of technical rather than financial factors in determining project costs. A plant lifetime of 30 years is assumed.

The model inputs and operation are summarised in Figure 3.2. Wind and solar data is sourced from the ERA5 database, which estimates a range of parameters relating to historical weather data at hourly frequency on a 30 km grid,[141] although for analysis in this thesis a general spatial resolution of 1 degree was applied. Using the Python PVLib and the curve for a Vestas 3 MW wind turbine, these weather data were transformed into hourly energy production in MWh per installed MW of renewable energy capacity. This method typically returns reasonable results that are consistent with recorded data [142].

Because hydrogen electrolysers typically use DC power, the DC power output from solar cells was used, which is more efficient. This is fed into the optimisation model alongside the cost and efficiency of each piece of equipment, and technical and physical constraints on that equipment. The model can then be solved with any MILP solver; for this application, Gurobi was used because it is freely available under an academic license, and has superior performance compared to open source solvers.

The model variables are shown in Table 3.1, and can be divided into two classes: time-variant and time-invariant.

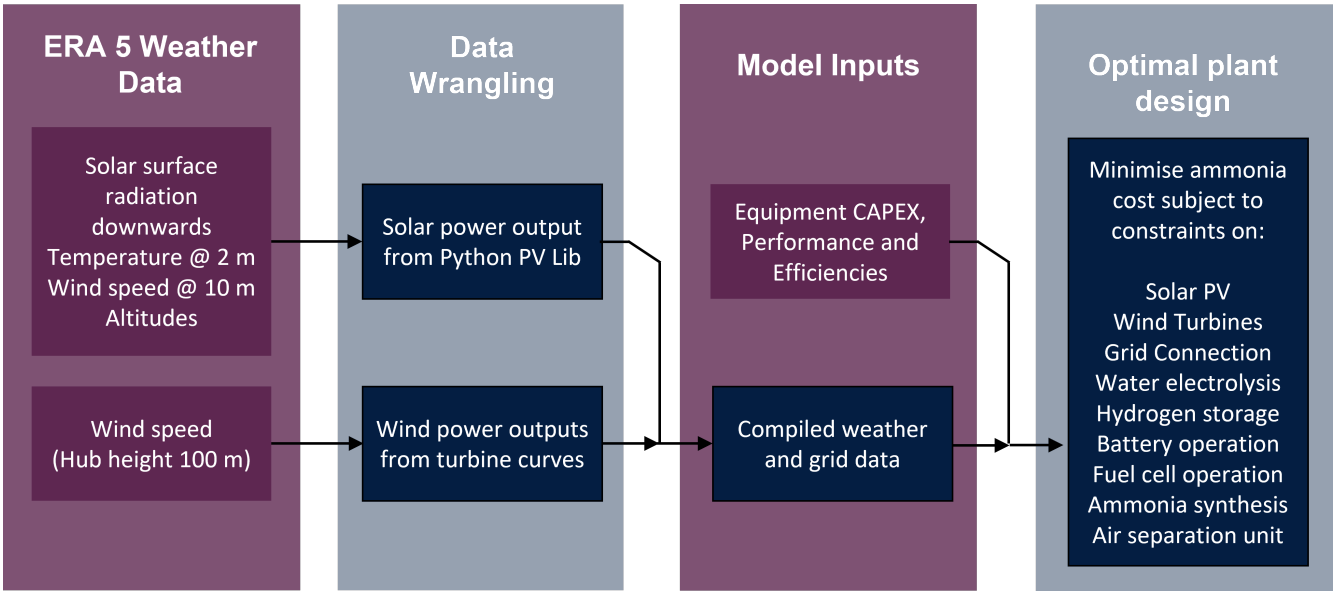

Fig. 3.2 Schematic demonstrating operation of ammonia production model. Boxes in purple represent input data to the model. Boxes in dark blue represent processes carried out by the model. Weather data is sourced from ERA5, and processed using PVLib (solar) and a Vestas turbine curve (wind) to produce the input weather data. Equipment information is also fed to the model, which then can optimise plant design.

The time variant variables are here represented using Greek letters, and are defined at each time-step in the model. These represent how power is allocated around the plant (which determines the rate of equipment operation), and the state of charge of the two storage units (the battery and the hydrogen stores). The time invariant variables are represented using Latin letters, and indicate the size of equipment; it is these parameters that determine the plant cost.

The remaining parameters in the model are summarised in Appendix Table A.2. Most are represented using G, with the exception of (i) the capacity factors (see below); (ii) the hourly energy production from a renewable source given by $Z(R,t)$, where R is the renewable source; and (iii) the weighting applied to a specific time step, shown by $T_w(t)$ (see Section 3.2).

Material flows of ammonia and hydrogen are represented in tons, and energy flows are represented in MWh. Suitable conversion factors CF are used to convert units between flows as appropriate. In the case of power to material flows, the conversion factor represents the amount of product produced from 1 MWh of electricity (or vice-versa for material to power flows). For material to material flows, the conversion factor is the stoichiometric ratio (e.g. 17/3 for H_2 to NH_3). For power to power flows, the conversion factor represents efficiency losses. In the case of the battery, a self-discharge factor, $G_{Discharge}$ is also included to represent losses which occur from the battery over time.

Although solar panels and wind turbines are typically modular, which could in theory constrain the installation capacity of renewable equipment to integer multiples of standard equipment sizes, we consider the size of renewable energy production units to be continuous. Since the whole plant capacity (in the order of GW) is much larger than

Table 3.1 Variables used in the model.
*Note that power can only flow to the (i) electrolyser, (ii) battery and (ii) HB+ASU, and not the fuel cell, so there are only three variables associated with each of π, β and γ.

Symbol	Description	Associated Set	Number of variables
$P_R(R)$	The installed capacity of the renewable energy source (in MW)	S_R	2
$P_C(C)$	The installed capacity of the plant component (in MW)	S_C	4
$V(SC)$	The installed capacity of the storage component (battery in MWh; hydrogen in t)	S_{SC}	2
$\pi(C,t)$	The energy flow directly from input power to the specified component (in MWh) at each time	S_C	$3max(S_t)$
$\beta(C,t)$	The power flow from the battery to the specified component (in MWh) at each time	S_C	$3max(S_t)$
$\gamma(C,t)$	The power flow from the fuel cell to the specified component (in MWh) at each time	S_C	$3max(S_t)$
$\kappa(SC,time)$	The amount of electrical energy or hydrogen stored in the storage component (in MWh for batteries, tons for hydrogen) at each time	S_{SC}	$2max(S_t)$

a single turbine/panel (in the order of MW), this approximation does not introduce significant error, and prevents the inclusion of a large number of integer variables that would significantly increase solution time.

3.1.3 Model Formulation

There are ten constraints imposed on the optimisation problem. These fall into two groups: capacity constraints and balance constraints. Capacity constraints ensure that equipment is sufficiently large to handle the power and material flows they receive. Balance constraints enforce energy and mass conservation around various units in the model.

There are six capacity constraints:

$$\pi(C,t)+\beta(C,t)+\gamma(C,t) \leq P_C(C)\cdot T_w(t) \qquad \forall C \in S_C, t \in S_t \tag{3.3}$$

$$\kappa(SC,t) \leq V(SC) \qquad \forall SC \in S_{SC}, t \in S_t \tag{3.4}$$

$$\sum_{C \in S_C} \beta(C,t) \leq P_C(Battery)\cdot T_w(t) \qquad \forall t \in S_t \tag{3.5}$$

$$\sum_{C} \gamma(C,t) \leq P_C(FC)\cdot T_w(t) \qquad \forall t \in S_t \tag{3.6}$$

$$\pi(HB+ASU,t)+\beta(HB+ASU,t)+\gamma(HB+ASU,t) \geq G_{HB_{Min}}\cdot P_C(HB+ASU)\cdot T_w(t) \qquad \forall t \in S_t \tag{3.7}$$

$$
\begin{aligned}
-G_{HB_{\text{Ramp down}}} \cdot P_C(HB+ASU) \cdot T_w(t) \leq \\
&\big(\pi(HB+ASU,t) - \pi(HB+ASU,t-1)\big) + \\
&\big(\beta(HB+ASU,t) - \beta(HB+ASU,t-1)\big) + \\
&\big(\gamma(HB+ASU,t) - \gamma(HB+ASU,t-1)\big) \\
&\leq G_{HB_{\text{Ramp up}}} \cdot P_C(HB+ASU) \cdot T_w(t) \qquad \forall t \in S_t \quad (3.8)
\end{aligned}
$$

Equation (3.3) requires that the installed capacity of each component be larger than the total power provided to it at all times. Equation (3.4) requires that, for each storage component, the capacity available for storage be large enough to contain the capacity demanded by the model at that time. Equations (3.5) and (3.6) ensure that the total power provided by the battery and fuel cell respectively is less than their capacity. Equation (3.5) is rarely constraining to the model, as due to inefficiencies the power flowing into the battery is typically larger than that leaving it (already constrained by Equation (3.3)). However, it is possible that at some times the demand on the battery will exceed what it has the capacity to supply, and the constraint is therefore necessary.

Equations (3.7) and (3.8) account for the limited flexibility of the Haber-Bosch plant. Equation (3.7) ensures that at least a fraction of the total power is provided at all times; enforcing a minimum power requirement also imposes a minimum hydrogen supply through the hydrogen balance constraint (Equation (3.12) below). Equation (3.8) prevents very rapid ramping of the ammonia plant; different maximum rates are imposed on the ramp-down and the ramp-up, since ammonia plants can typically ramp down more quickly than they ramp up (as per Fasihi et al.[80]). Note that in Equation (3.8), $t-1$ is used to indicate the previous time step; if $t = 1$, then the previous time step is actually given by $t = max(S_t)$, which the model will use to define the constraint; this eliminates the need to provide an arbitrary initial condition.

There are four balance equations; this is one fewer than the total number of elements in the set of flows, as the power from the fuel cell is incorporated into the hydrogen balance. The balance equations are shown below:

$$CF(\pi, NH_3)\frac{G_{Hours}}{24 G_{Days}} \sum_{t \in S_t} \Big(\pi(HB+ASU,t) + \beta(HB+ASU,t) + \gamma(HB+ASU,t) \Big) = F \quad (3.9)$$

$$\sum_{R \in S_R} \Big(Z(R,t) P_R(R) \Big) \geq \sum_{C \in S_C} \pi(C,t) \qquad \forall t \in S_t \quad (3.10)$$

$$\kappa(Battery,t) = G_{Discharge}\kappa(Battery,t-1) + CF(\pi,\beta)\pi(Battery,t) - \sum_{C \in S_C} \beta(C,t) \qquad \forall t \in S_t \quad (3.11)$$

$$\kappa(Hydrogen,t) = \kappa(Hydrogen,t-1) + CF(\pi,H_2)\left[\pi(Electrolyser,t) + \beta(Electrolyser,t)\right] - \frac{1}{CF(H_2,\gamma)}\sum_{C\in S_C}\gamma(C,t) -$$

$$\frac{CF(\pi,NH_3)}{CF(H_2,NH_3)}\left[\pi(HB+ASU,t) + \beta(HB+ASU,t) + \gamma(HB+ASU,t)\right] \qquad \forall t \in S_t \quad (3.12)$$

Equation (3.9) is a simple sum of all ammonia produced; it must equal the target production. It includes a factor of $\frac{G_{Hours}}{24G_{Days}}$; this is equal to the fraction of uptime available to the plant, accounting for some time off due to maintenance. This is a conservative estimate; actual plants will typically schedule downtime based on poor outlook for renewable production, whereas this model discounts all production evenly.

Equation (3.10) is the power balancing equation; it requires that the total input energy is greater than the energy directly consumed by the plant. The difference between the two sides of the inequality is equal to amount of electricity curtailed. Equations (3.11) and (3.12) are the balances for the battery and the hydrogen storage unit respectively. In both cases, the current storage at time t is given by the storage in the previous time step, plus any flows in minus any flows out. As in the case of the Haber-Bosch ramping constraint - Equation (3.8) - the previous time step is represented by $t-1$ in these equations, but at $t = 1$, the model will use the storage level at $t = max(S_t)$ to avoid the need to introduce arbitrary initial conditions.

Having sized the plant equipment, the model estimates the CAPEX and OPEX according to:

$$CAPEX = \sum_{R\in S_R}\left(P_R Cost_R\right) + \sum_{C\in S_C}\left(P_C Cost_C\right) + \sum_{SC\in S_S C}\left(P_{SC} Cost_{SC}\right) \quad (3.13)$$

$$OPEX = \frac{CF(H_2O,H_2)}{CF(H_2,NH_3)} Cost_W F + Cost_{OM} CAPEX \quad (3.14)$$

The first term in the OPEX expression relates to the cost of water, which is estimated on a per tonne basis assuming desalinated water is required for such large productions. The final term is an operating and maintenance cost that is estimated as a fraction of the CAPEX.

3.2 Increasing model speed

The optimisation strategy described above has a large number of variables, given by $11max(S_t)+8$; for a single year of data using an hourly time step (the maximum granularity available in weather data), this corresponds to 96,368 variables. Some solutions to mediate this problem are available: Gurobi can very rapidly remove some of these variables using its presolve formulation (for instance, the fuel cell will never sensibly be used to power the electrolyser, which the algorithm can detect and simplify), and the MultiProcessing module in python was used to solve the model in multiple locations in parallel, although the impact of this solution is limited by computer RAM. Despite these simplifications, the number of variables remains in the order of 10^5, and solution times are non-trivial. While it is possible to solve MILPs with much higher number of variables, the time taken to do so increases quickly as the problem becomes more complex.

Historically, this has forced researchers to either consider a comparatively small number of locations [18], or to use only one year of weather data for plant design [80]. Doing so either prevents high quality locations from being identified, or may fail to capture interannual variation that may be significant for plant design. In the UK, for instance, the energy shortage at the start of autumn 2021 was exacerbated by a long-term wind-drought, the scale of which had not been observed since the early 1960s [143]. The frequency of such wind droughts is forecast to increase with climate change [144]. Given the intended use of ammonia to store energy between years, factoring this interannual variation is important, and larger volumes of weather data need to be processed to develop a robust ammonia economy.

This section explores three data clustering approaches which can be used to simplify the optimisation model, demonstrating that it is possible to significantly accelerate calculation without sacrificing accuracy. Several applications of accelerated calculation are then discussed.

3.2.1 Data clustering methods

Rigorous existing models for ammonia plant design typically use hourly weather data. However, in other energy optimisation analyses, some data clustering techniques have been attempted.

The Balmorel energy systems model, a popular open-source application, uses time aggregation, whereby larger time steps are used to reduce the data size [145]. Palys and Daoutidis [82] modelled a grid-based energy system which included ammonia that used a hierarchical approach, in which the most similar input data points are iteratively clustered until the data is reduced in size by a pre-specified factor. Not all time steps are the same size using this approach, so the model affords them different weights to determine the impact of a time-step on ammonia production, and the levels in energy and mass storage equipment. Figure 3.3 shows the difference between these two techniques. The former is simpler for both the coder and the computer to implement; the latter can capture more dynamic variation in weather with the same number of time steps used.

A third approach in the literature simplifies the data using representative days [146]; one such technique used by Gabrielli et al.[147] for selecting these representative days is K-means clustering, which uses a principal component analysis to classify days into groups (clusters), and then represents each day in the group by its centroid. This approach is complex to implement, but corresponds well to our inherent understanding of weather and energy systems, which is often based around a 'typical' day.

The implementation of K-means clustering is more complex than time or hierarchical aggregation. Firstly, the clusters themselves must be selected. The number of principle components used was determined such that they explained 99% of the variance in the dataset (this differed between sites), and the number of clusters was changed depending on the desired degree of data simplification. Figure 3.4 shows an example of the clusters.

Secondly, the model itself needs to be updated. An additional set, of days, S_D is introduced, and S_t is redefined as a list of integers between 0 and 24 (i.e. the nominated hour of the day). All time dependent variables and

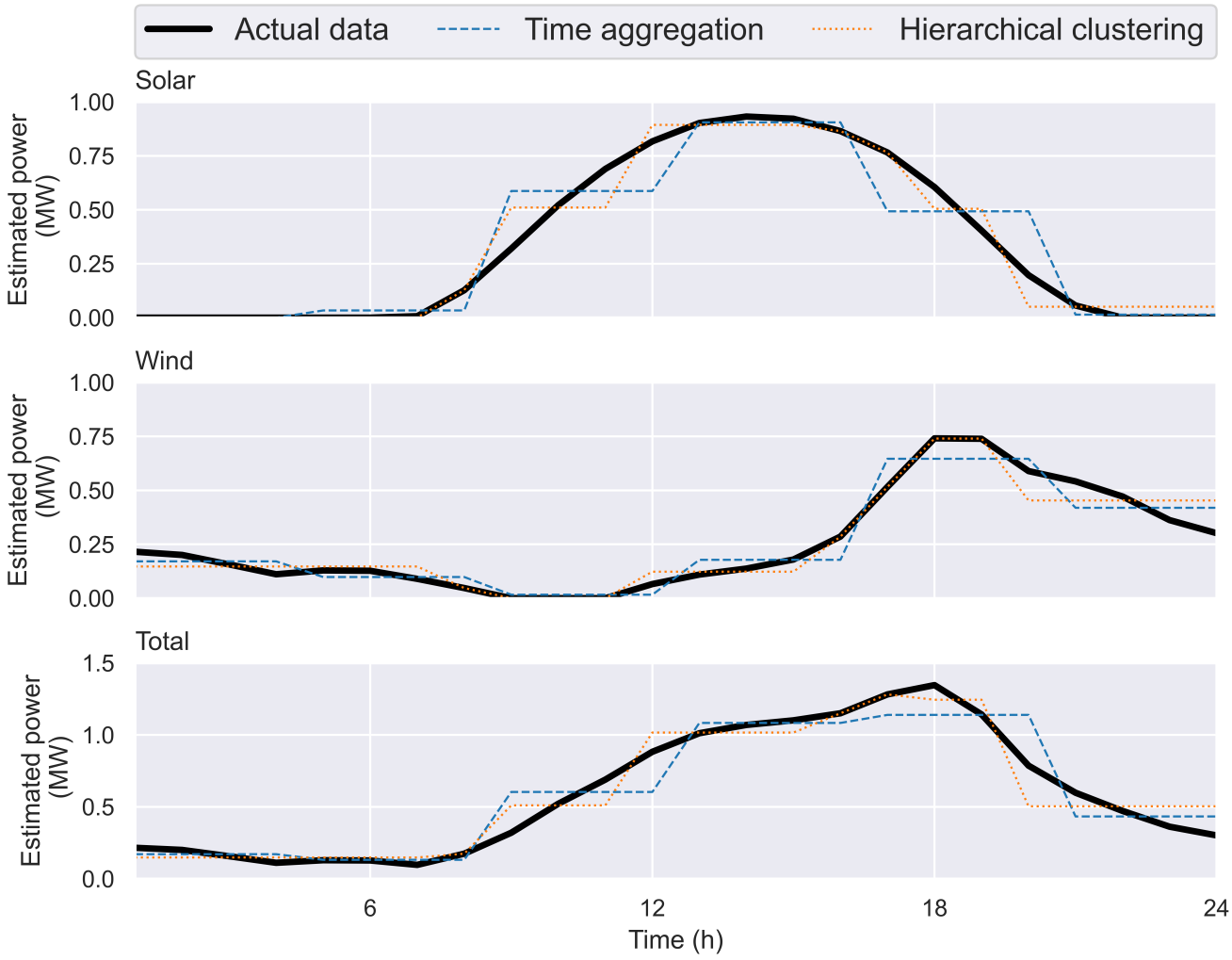

Fig. 3.3 Comparison of two methods for data clustering for a single representative weather day, for solar (**top**), wind (**middle**) and the combined output (**bottom**). **Black, solid**: raw data; **Blue, dashed**: data averaged across four hours (time aggregation); **Orange, dotted**: closest time values iteratively aggregated until the number of data points is equal to the blue data series (hierarchical clustering).

parameters take both the day and the hour as inputs. The selection of the date determines which cluster is being considered, and the inputs draw data from the centroid of that cluster, rather than the data specific to that day. The output variable values also match within clusters (if this were not enforced then the number of variables would not be reduced); the exception is κ, the state of charge of the storage components. If these values are fixed within clusters, there will be discontinuities between days, which is unphysical, and therefore the state of charge was allowed to vary within clusters.

To compare the performance of these clustering approaches, we define the simplification factor (SF), which is the ratio of the number datapoints in the raw hourly data to the number of datapoints in the clustered data; for instance, data using a two-hourly time-step would have SF $= 2$, and $T_w = 2$ for all values of t. An 8-core desktop computer with an i7 processor and 16 GB of RAM was used to solve the model for 701 locations in Australia (spread in a grid pattern across the country). The process was repeated using a range of simplification factors to

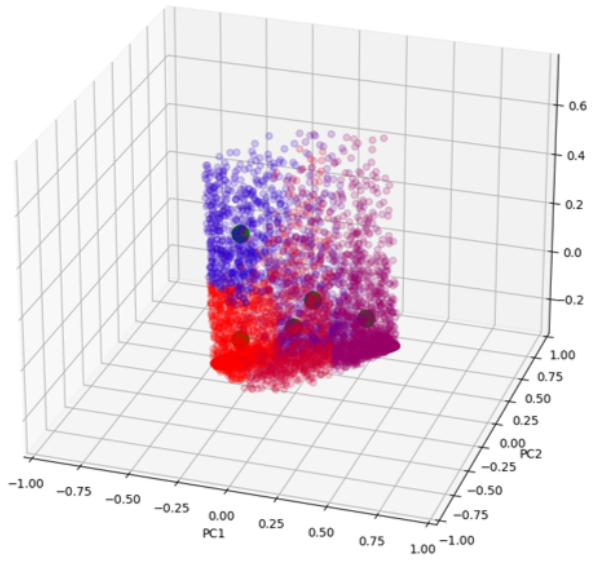

Fig. 3.4 Visual representation of K-means clustered data at one Australian location. For this location, PC1 and PC2 are most strongly correlated to the wind profile, and PC3 is correlated to the solar profile. The centroids of each cluster are shown in green, and data points are coloured according to the cluster to which they belong.

measure performance. The equipment CAPEX and efficiencies are the same as described for the case study on grid connectivity in Section 3.3.

3.2.2 Clustering Results

3.2.2.1 Comparison of performance

Figure 3.5 compares the techniques at different simplification factors to results at a simplification factor of 1 (i.e. the raw, unclustered data). Each point represents results at one location; if the points form 45° lines, this indicates good agreement between the simplified model and actual results.

Time aggregation and hierarchical clustering perform well at low simplification factors. Performance starts to degrade around a simplification factor of 12, because the diurnal variation of solar panels begins to be smoothed into a near constant supply of electricity, which will underestimate the amount of energy storage required. As expected, the performance of time aggregation degrades more quickly than hierarchical clustering, since the aggregation captures less dynamic variation. In general, both techniques tend to slightly underestimate the LCOA-P; this is because the smoothing inherent to reducing the size of the time data provides more reliable electricity and therefore reduces the need for batteries, hydrogen storage, or back-up grid power.

The performance of K-means clustering is very poor at all simplification factors. While other techniques exist by which representative days can be selected, it is unlikely that a different selection of centroids would radically change the poor performance of this approach. To some extent, the poor performance is caused by the long-term nature of ammonia plant design, and the representative day is too short a time frame over which to base plant

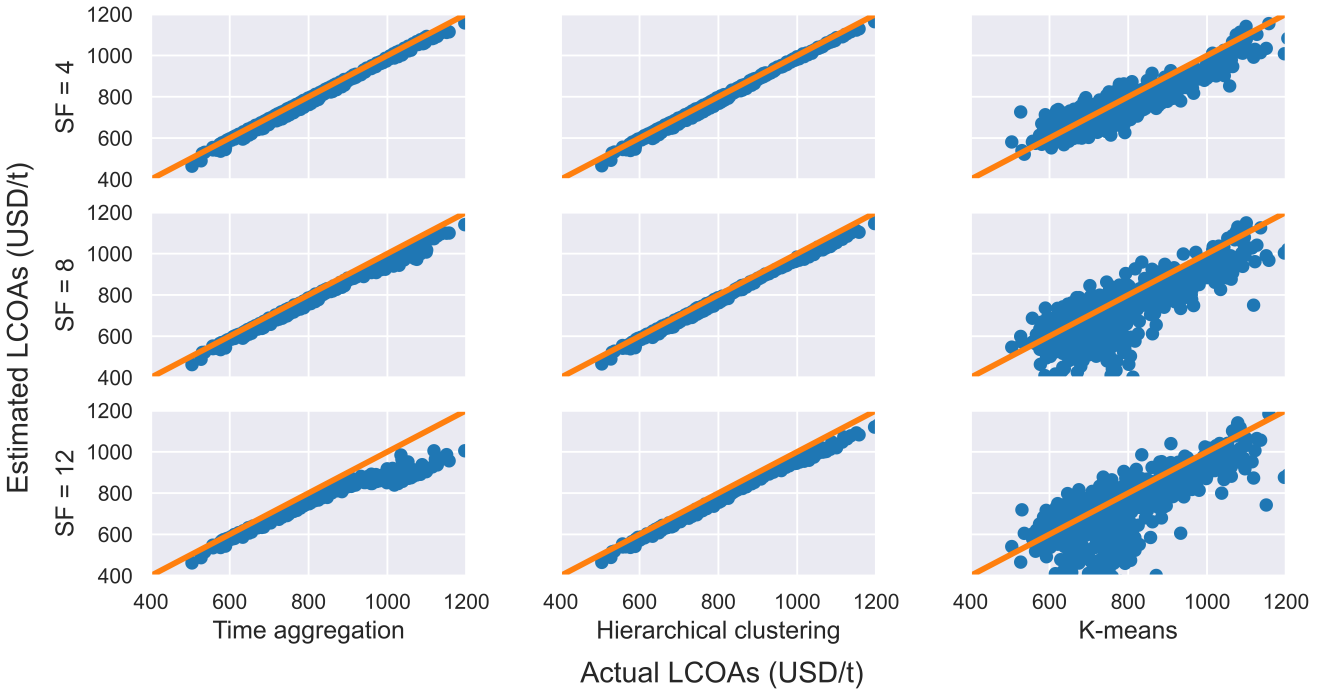

Fig. 3.5 x-y plots for comparing the LCOA-P estimated from simplified approaches against the LCOA-P estimated using a rigorous one-hour time-step. Each of the points (blue) represents a single site; the orange line is an x-y line included for reference. Left to right shows the different methods (**Left**: Time aggregation; **Centre**: Hierarchical clustering; **Right**: K-means clustering). Top to bottom shows increasing simplification factors (SFs), which are the number of data points in the original unclustered dataset for each point in the clustered dataset (**Top**: SF = 4; **Middle**: SF = 8; **Bottom**: SF = 12). Greater deviation of the blue points from the orange x-y line indicates worse performance of the clustering method.

design. For instance, as described in Section 3.1.1, plant operation may need to be different on two days with identical weather based on the inventories of the hydrogen storage and battery, or the upcoming weather patterns. K-means clustering using individual days does not enable that time-scale to be incorporated.

3.2.2.2 Comparison of speed

Figure 3.6 shows the relationship between the time taken for the model to converge in all of the 701 locations considered, and both the average and maximum error observed in the results compared to the result obtained using a one-hour time step. The speed comparison is more useful than the simple performance comparison from the previous section, as it allows a more direct trade-off between model speed and precision.

Predictably, because of the results shown in Figure 3.5, the results for K-means clustering generate very high errors; additionally, they also take a long time to converge. This is because (i) the principal component analysis and clustering algorithm take a substantial amount of time, and (ii) the dimensionality of the hydrogen and battery storage variables is not reduced by representative day clustering (since the model still needs to build a continuous storage profile).

For the other two clustering techniques, higher simplification factors tend to result in shorter solution times and higher errors. In all cases, the error observed using the hierarchical clustering was lower than that observed using

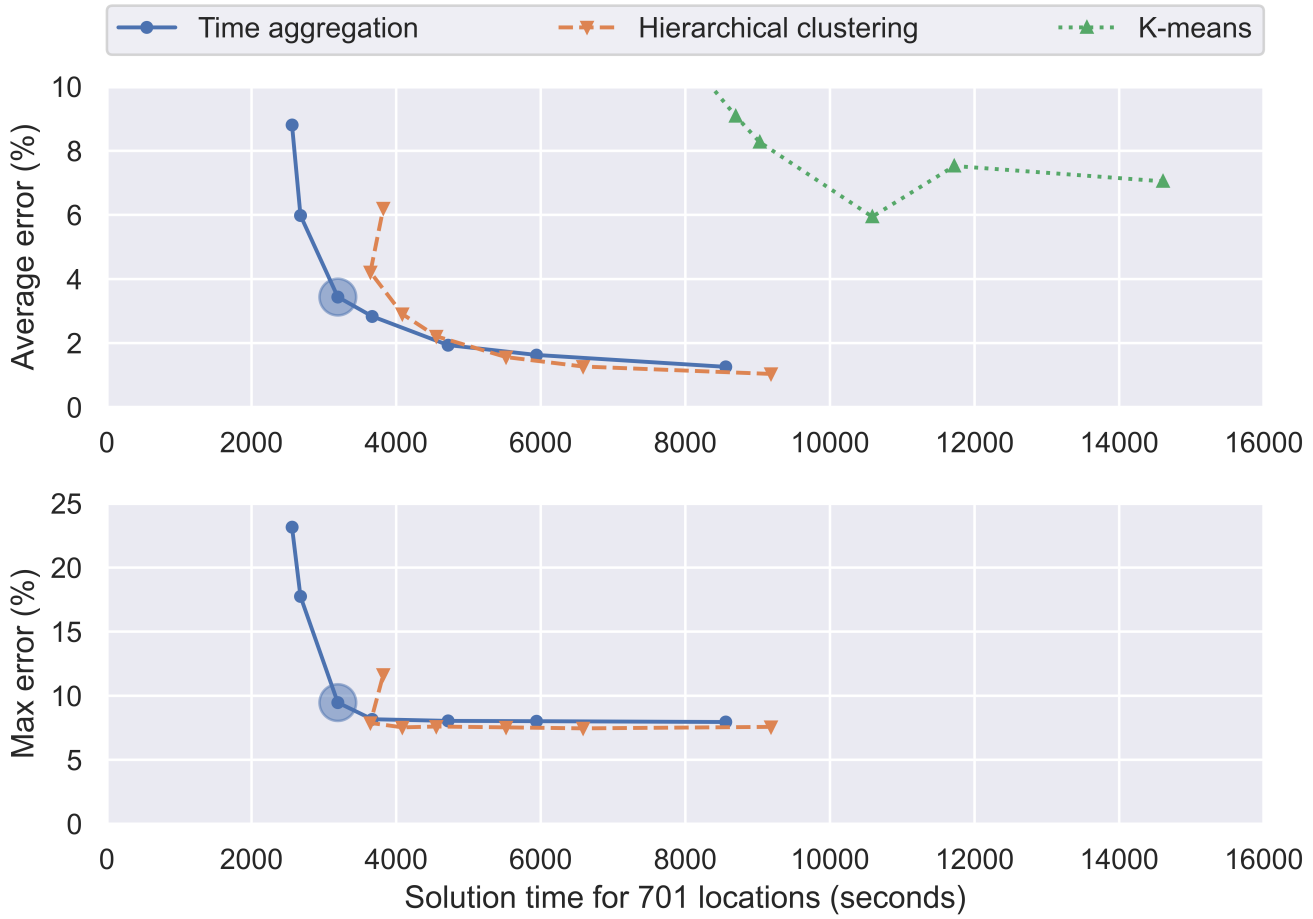

Fig. 3.6 Relationship between error and solution time for the three data clustering methods. Each data point represents a different simplification factor. The highlighted marker is the option selected as optimal for further analysis. **Top**: Average error across all locations. **Bottom**: Maximum error across all locations; the errors from K-means clustering are too large to be visible on this axis.

time aggregation at the same simplification factor, but the time required for convergence was greater.

At low simplification factors, the majority of time taken for the model to converge is taken by the optimisation solver. However, as the simplification factor increases, the computational time required to simplify the data itself begins to increase, and the time required for the optimisation solver decreases. This limits the time taken for the model to converge to the time taken to perform the data clustering itself. Because the hierarchical clustering approach is more computationally challenging than time aggregation, this minimum limit on convergence time is higher; indeed, at the highest simplification used here (24), the model begins to take longer to converge than at the next-lowest factor (12).

The best option for further analysis will deliver a fast solution with an acceptably small error. In this thesis, a suitable point is selected for different analysis which balances the needs of accuracy and solution time. The point selected for the following subsection on historical data analysis is highlighted on Figure 3.6; it combines acceptable errors (∼3.5% on average, 9.5% at most) with quick solution times (∼3,500 s). Increasing the time required for

modelling by ∼20% could have yielded more accurate results, but the improvement is not large, particularly given the error implicit in the model due to input parameter estimation.

Note that since the case considered in the grid data section of this chapter is relatively small (only 700 locations), no clustering was required. However, Chapters 5 and 6 discuss a granular global heat map for ammonia costs, the production of which relied on time aggregation as discussed here.

3.2.3 Historical Data Analysis

Green ammonia plants for energy storage need to operate under different conditions over a large time period (∼30 years). Using time aggregation with a simplification factor of 8, the model was converged repeatedly using different starting years, and considering time periods of 1, 3, 5 and 10 years.

The LCOA-P results for a single representative location are plotted in Figure 3.7. They demonstrate that as more years of data are considered, the optimum value for the LCOA-P tends to converge around a single value; if only one year of data is used, there is a wide spread in the LCOA-P estimates.

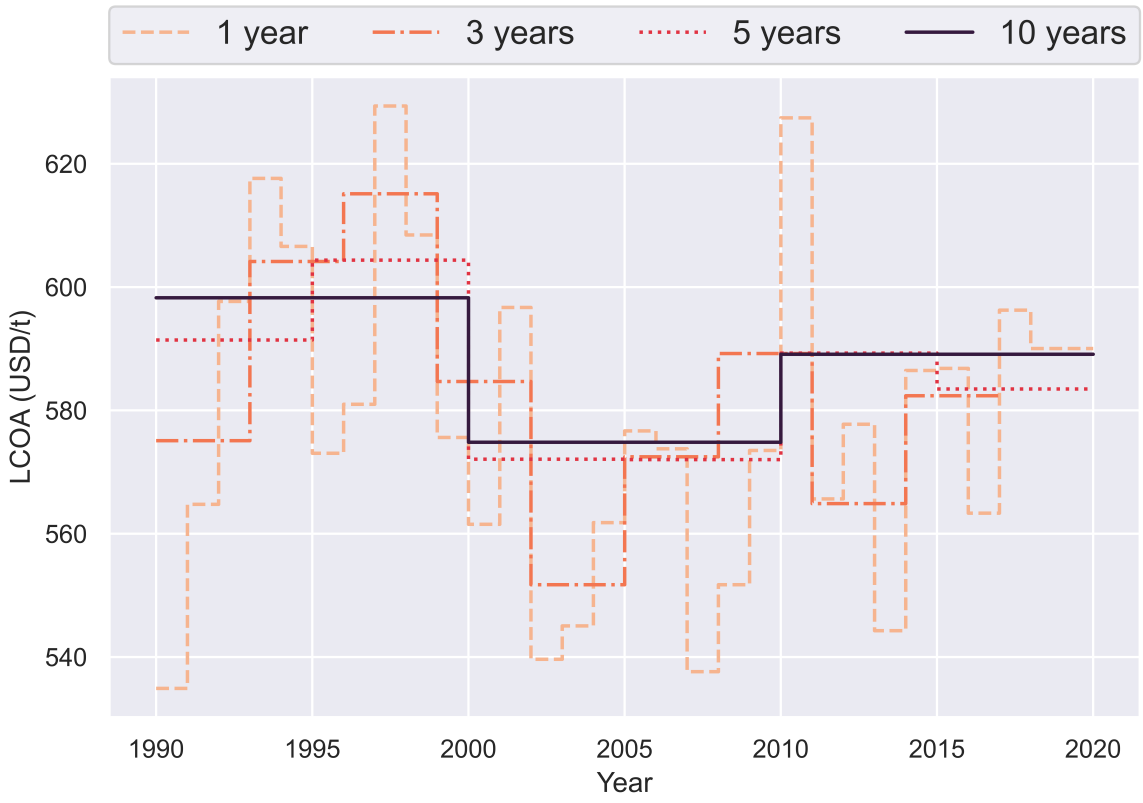

Fig. 3.7 Optimum LCOA-P for a location in South Australia, calculated using different years of weather data, using temporal aggregation with a simplification factor of 6 (i.e. 6-hourly time steps). Different data series represent the different number of years of data included in the cost estimate; variability for using only one year of data is much higher compared to using 10 years of data.

Considering all locations for the cases where only one year of data was analysed, the average range between the

minimum and maximum LCOA-Ps estimated was 15% (substantially higher than the error introduced by clustering); in the worst case, it was more than a third of the total ammonia cost. When a larger number of years of data are considered, the results are much more stable over different time periods. Using ten years of input data, the average range between the minimum and maximum cases across all locations was only 2%, and the largest error observed was only 6% (across all sites).

If the long term average LCOA-P is taken from the cases where a single year of data is used, the cheapest location for ammonia production is located near the Pilbara in Western Australia. However, this site only has the cheapest production cost in ten of thirty years of individual data; in one poorly performing year, it was the 50th ranked site of the 701 considered.

There is a weak relationship between the number of years of data used for the optimization and its outcome. In 677 of the 701 cases considered, there was a positive correlation between the number of years of data considered and the LCOA-P; i.e. considering more years of data slightly increases the LCOA-P. Although this relationship is small (on average, the LCOA-P estimated increases by 10 USD/t when comparing average results from ten individual years to the results from one ten-year period), it does suggest that an engineering plant designed over a single year alone will be underdesigned.

3.2.4 Model speed conclusions

This research has demonstrated that the length of the time step used to design an ammonia plant does not meaningfully affect the outputs until those time steps exceed about 8 hours. This allows for significant acceleration of solution times, which is an important result for ammonia plants that may be extendable to other components of the energy system.

Alongside their utility in this thesis, the accelerated solution techniques described here could facilitate significant further research. Two options would include (a) Monte-Carlo simulation of green ammonia plant design given the uncertainty in equipment cost and performance, and (b) consideration of climate forecasting (which returns a large array of possible outcomes) in future-proofing ammonia plant designs against various possible scenarios. The inability of K-means clustering to provide sensible results in energy systems modelling over long-time scales is also a relevant conclusion.

3.3 Case study: Grid connectivity

Until this point, the literature and this thesis have focussed on islanded production, which is to say, green ammonia plants which are isolated from the energy systems of the countries in which they operate.

However, future applications of green hydrogen and ammonia are likely to see significant integration of production into electricity networks [131] as 'prosumers' (producers and consumers) of renewable electricity. In the 'prosumer' model, green hydrogen and ammonia production can absorb excess grid capacity during periods of curtailment that are likely in highly renewable electricity networks; conversely, during periods of low renewable

availability (so-called "dunkelflaute"), they can modulate down production and export energy to the grid to ensure demand can be met.

Current applications of green ammonia production may also benefit from grid connection, even in energy systems that are still reliant on fossil fuels. As the next chapter shows, the requirement to keep the ammonia plant operating above very low rates requires energy storage equipment that increases costs by around 30-40% for plants designed in 2022. It may be possible to reduce the size of that energy storage if a grid connection can be exploited to supply back-up power when needed. This 'semi-islanded' approach therefore has the capacity to reduce both costs and operating risks posed by relying on batteries or hydrogen fuel cells for back-up supply (although the majority of power must still be sourced from on-site renewables due to the carbon intensity of the grid). By contrast, islanded production must rely on only local resources for power supply, which may pose challenges during extended dunkelflaute.

Several authors have considered the interaction between green ammonia and the grid. Palys and Daoutidis[82] used an MILP model to optimise the design of energy systems in 15 US cities; however, the model was designed to use ammonia and other technologies to supply demand for electricity grids, as opposed to understanding how variable grid electricity prices could minimise the production costs of ammonia. Similarly, Beerbühl et al.[78] used the electricity grid to power ammonia production, but used only grid electricity, and did not also consider the role of on-site renewables or power storage. Pan et al.[148] also consider the use of the grid for green hydrogen production in China; however, their model does not include wind energy, ammonia generation, variance in renewable energy potential at different locations within the provinces they model, or an option for the plant to both buy and sell grid electricity.

The contribution of this research is an assessment of how grid connection can directly reduce ammonia production costs; this may prove an important stepping-stone to establishing a green energy export industry. It extends on previous work by including consideration of (i) the capital costs of grid connection at a large number of locations in Australia; and (ii) the variable retail price of electricity which can be used to supplement onsite power generation.

Australia is used as a case study for this section. It is well positioned to produce green ammonia: it has (i) a reliable wind and solar resource; (ii) an abundance of available land; and (iii) is strategically located close to Japan and Korea, who have flagged their intention to import green fuels like ammonia. The nascent Australian industry faces competition from other global green ammonia producers such as Morocco, which may be able to produce at a lower cost because of a superior resource[80], and lower project costs [18]. However, by global standards Australia has a highly reliable electricity network, which may offer it a competitive advantage; it is therefore a relevant location upon which to focus. Unless otherwise specified, all costs in this analysis are reported in USD; where data is provided in AUD, a conversion rate of 0.7 AUD/USD is assumed, which is the approximate long-term average value[149].

3.3.1 Grid connection methodology

3.3.1.1 Model Updates

In order to model the connection of the grid to the electricity network, four extra variables are required. x_{Grid} is included as a binary variable that determines whether the grid connection should be included; the term $x_{Grid}Cost_{Grid}$ is added to the CAPEX Equation (3.13) (the estimation of $Cost_{Grid}$ is discussed in Section 3.3.1.3). $\eta_{in}(t)$ and $\eta_{out}(t)$ represent the amount of electricity bought and sold from the grid respectively; the product of these variables with the electricity price at the relevant time, $Y(t)$, are added to the OPEX estimate (Equation 3.14).

$\zeta(t)$ represents the electricity curtailed (which now must be treated as a separate variable as outlined below). To account for this change, the power balance constraint (Equation (3.10)) is modified to be a strict equality constraint, with ζ taking the place of the slack variable:

$$\sum_{R\in S_R}\left(Z(R,t)P_R(R)\right)+\eta_{in}(t)-\zeta(t)=\sum_{C\in S_C}\pi(C,t)+\eta_{out}(t)\qquad\forall t\in S_t \tag{3.15}$$

Two additional constraints are required to enforce sensible behaviour of the grid connection:

$$\sum_{R\in S_R}Z(R,t)\cdot P_R(R)\geq\zeta(t)\qquad\forall t\in S_t \tag{3.16}$$

$$\frac{\sum_{t\in S_t}\left(\eta_{in}(t)+\eta_{out}(t)\right)}{24G_{days}\left(\eta_{in}(UB)+\eta_{out}(UB)\right)}\leq x_{Grid} \tag{3.17}$$

Equation (3.16) requires that the maximum electricity curtailed at any given time be less than the total energy produced from renewable electricity; without this limit, the model will import very large amounts of electricity from the grid on the rare occasions when the cost of grid electricity is negative. While some electricity import during this time is likely, it is non-physical to import more than the plant can consume. The model therefore needs to be constrained so it can only curtail electricity produced onsite.

Equation 3.17 switches on the grid connection variable x_{Grid} if any electricity is imported from or exported to the grid; the denominator in the fraction is used to scale the total electricity import to between 0 and 1, where $\eta_{in}(UB)$ and $\eta_{out}(UB)$ are the upper bounds on the values of those variables, which are common to all time steps. Since switching x_{Grid} on increases the plant CAPEX, the model will only switch this variable on if the benefits from electricity purchase or sale outweigh the grid connection costs.

The model is run over a single year of operation at a time. The majority of analysis in this report uses 2019 as a base consideration, as it represents average grid behaviour; the sensitivity analysis considers other years.

3.3.1.2 Electricity Data

Australia has six major electricity markets. The East Coast markets - which include South Australia (SA), Victoria (Vic), Tasmania (Tas), New South Wales (NSW) and Queensland (Qld) - are correlated by virtue of interconnectors between these markets. The West Coast market - which includes only Western Australia (WA) - is entirely independent. The Australian Energy Market Operator (AEMO) provides historical data describing the demand and retail price of grid electricity in each of these markets on a half hourly basis[150]; these prices and demands were averaged in order to convert the data to an hourly frequency, so that it would match the weather data.

In order to select the most suitable grid connection point, the minimum distance between a nominated location for ammonia production and Australia's existing transmission network was calculated. GeoPandas data listing all major Australian electricity transmission lines was obtained from the Australian Government[151, 152]. Transmission lines that are not part of major electricity grids were excluded (e.g. microgrids which supply power to rural mines, and the Darwin-Katherine interconnection); it was assumed they would not have the capacity to supply an adequate amount of energy to green ammonia plants. The minimum distance between the plant and the grid is always used in the model, even if it causes a location to connect to a grid which is in a different state; if that occurs, the model uses the electricity price from the state in which there is a connection to the grid, rather than the state in which the plant is located. While it is possible that the optimum price may sometimes be obtained by connecting to a more distant electricity grid in a state with a more complementary power profile, it is expected that this will be a very rare occurrence given the cost and inefficiencies of long-distance electricity transport. Allowing the model the flexibility to select the optimal electricity grid would have significantly increased solving time, and thus this option was discarded.

In addition to the retail price, electricity consumers will typically need to pay Transmission Use of System (TUOS) and Distribution Use of System (DUOS) charges. DUOS charges are neglected in this analysis; because the proposed designs connect directly to the transmission system they do not rely on power distribution systems. TUOS charges are set each year by state grid operators based on the costs required to maintain the electricity grid. Different users are charged in different ways depending on the nature of the grid connection. On an energy basis, charges are typically in the order of 10 AUD/MWh[153–155]; however, site specific costs can be negotiated with state grid operators. The cost allocation is driven both by average supply and peak demand. Green ammonia plants face two advantages in negotating low TUOS costs: firstly, they will typically only draw power from the system during periods of low demand (when it is affordable to do so), and they do not therefore contribute to peak demand. Secondly, new green ammonia plants represent an emerging Australian industry and therefore may merit government support. It is therefore reasonable to expect that lower TUOS prices may be negotiable. A conservative estimate of 10 AUD/MWh is therefore used in this analysis, but sensitivity testing is performed in which it is as low as 5 AUD/MWh. It is because of the TUOS charge that electricity bought and sold must be modelled as two separate variables ($\eta_{in}(UB)$ and $\eta_{out}(UB)$) which are constrained to be greater than 0, rather than a single variable which

can be negative, because the costs associated with imported and exported electricity differ by the TUOS.

Electricity can be transmitted at low or high voltage (LV or HV), and as a DC or an AC current. In general, power losses in wires are lesser for high voltages and DC currents; however, these also have increased capital costs due to the additional transformers required. In the context of green ammonia production, there are also advantages to DC transmission, since electrolysers use DC power. In the model, efficiency losses in the line manifest themselves as an increase in the price of delivered electricity. That is, if the losses in transmission reduce the power to the site by a factor of ε, then additional power needs to be purchased to make up for those losses, and the cost of power increases by a factor of ε^{-1}.

3.3.1.3 CAPEX estimates

For reasonable outputs, sensible and regionally specific CAPEX estimates are required as model inputs. These are summarised in Appendix A.1. This poses a challenge, since much of the equipment included in green ammonia plants is relatively new technology. Solar and wind costs, for instance, are falling rapidly as technologies improve and economies of mass production develop. The exception is the HB loop and ASU, which are comparatively well established - their cost is estimated at 7.444 million USD/installed MW, taken from Nayak-Luke and Bañares-Alcántara [18].

A further challenge is that there are different technologies available to perform the same function: the best example is for hydrogen electrolysis, where alkaline and PEM electrolysers are both considered good options for systems which require flexible hydrogen generation. Because both have strengths and weaknesses, the model developed here is 'technology neutral' - it adopts reasonable parameter values from the literature for efficiency and cost, but is agnostic as to the precise nature of the technology adopted. This is consistent with the cost curve forecasting of Way et al. [2], whose research is central to the findings of later chapters.

Solar PV and Wind costs were sourced from the IRENA database[156], which takes historical data from a large number of projects in order to form estimates. Solar costs are provided explicitly for Australia; wind costs are provided for the region of Oceania. The sensitivity modifications applied in subsequent sections to solar are larger than those applied to wind ($\pm$30% as opposed to $\pm$10%), because (i) the price of solar panels is falling more rapidly than the price of wind turbines, and (ii) the removal of the inverter from the solar plant may enable savings that have not otherwise been considered here.

Previous techno-economic analyses of green ammonia production have used a wide range in costs of electrolyser modules, as described in Chapter 2. However, the majority of authors use estimates between 600 and 1,000 USD/kW of installed capacity [13]. Here, we use an estimate of 700 USD/kW [18], and a large sensitivity range of $\pm$30%. Similar uncertainties surround hydrogen storage and fuel cells; again, a large sensitivity range is used to understand the impact of these parameters, whose average costs are set at 500 USD/t and 960 USD/kW respectively[18].

Cost estimation for batteries is complicated by the need to estimate both the costs of energy storage in MWh

and power output in MW. Most authors specify costs independently for both equipment types [80, 157]. In some applications, the power to energy ratio may constrain design (since very fast discharge is not possible); however, because this model is on an hourly time scale, the maximum value of the power-energy ratio allowable in the model is 1 W/Wh (i.e. the fastest a battery can discharge completely is one hour). Smaller power-to-energy ratios tend to be easier to achieve in battery design (generally < 4W/Wh is considered achievable), so it is not expected that the batteries in this design will be constrained by their power-to-energy ratio[158], and it is therefore reasonable to size the power and energy components separately. The cost of the power component (here referred to as the interface) is estimated from Cesaro et al[27].

The cost of the energy storage component was then back-estimated from the actual cost of a recent very large battery installation in South Australia [159]. The two phases of this South Australian battery project had very different costs; the first phase cost only 300 USD/kWh, whereas the second required 700 USD/kWh (at the same power-to-energy ratio). The first phase was the subject of significant media attention - at the time it was the largest battery ever built - which may explain its unusually low price. For this model, a cost of 500 USD/kWh is used as the base cost, but the range observed by the actual installed battery (i.e. 300-700 USD/kWh) is used for sensitivities.

The costs of transformers and wires were provided by CSIRO [160], and their efficiency of transmission is estimated from EU[161] and IEA[162] resources. In general, the CSIRO estimates that LV AC is the cheapest form of transmission for short distances, HV AC is cheapest for medium distances, and HV DC is best over longer ranges. The disadvantage of HV DC is that rectification and inversion are required at the supply and demand sites respectively, in order to take AC power from the grid and return AC power to users. However, since the demand site uses mainly DC power, this disadvantage is comparatively small, as inversion is not required at the terminus of the transmission line, and a rectifier is required at some point in the electricity transmission, regardless of the technology used (note that, particularly if the plant makes dominant use of solar, a small inverter may be required to supply AC power to the Haber-Bosch synthesis loop and ASU, regardless of whether the grid connection is used; however, since these represent around 3% of installed plant power capacity, the associated costs are likely to be negligible). When the costs of inversion are excluded, there is very little difference in the costs of HV DC compared to HV AC in the medium distance, as shown in Figure 3.8, which assumes that 7.5% of power used to produce ammonia comes from the grid at an average price of 50 USD/MWh (this usage and price are averages from the base case). For that reason, the model will use a LV AC connection for distances of 30 km or less, and a HV DC connection at long ranges; HV AC lines are not used.

One possible benefit of HV DC which is not utilised in this model is that HV DC lines tend to have higher capacities than LV AC. The LV AC lines considered here have a maximum capacity of 175 MW, which is fairly small compared to most HV DC lines [160]. Larger capacities can also be used for LV AC lines, but at increased cost. In this model, imported power is capped at 175 MW, which could theoretically supply around 12% of a plant's power if utilised at all times. Higher capacities are not allowed for two reasons. Firstly, supplying more than 12% of a plant's

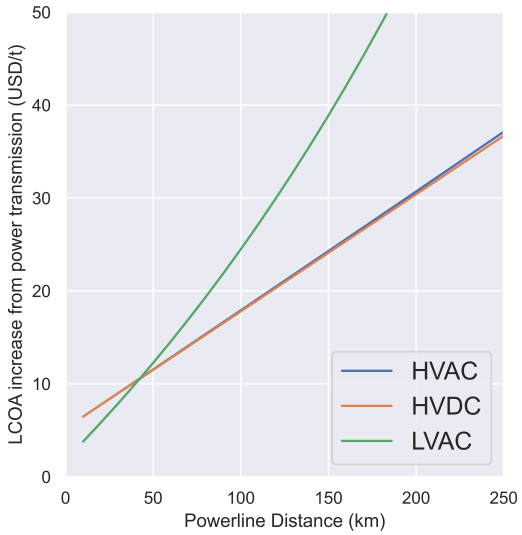

Fig. 3.8 Schematic showing the increase to the LCOA-P as a function of the electricity transmission distance in high voltage alternating current (HVAC), high voltage direct current (HVDC) and low voltage alternating current (LVAC) wires, for an electricity price of 50 USD/MWh. Although LVAC is cheaper over short distances, HVDC is preferable above ~40 km. HVAC is not competitive in this context because rectification is always required.

power from the electricity grid, which is not entirely decarbonised, may increase the emissions associated during production beyond the minimum threshold at which ammonia can be considered green. Secondly, at demands greater than 175 MW, ammonia plants would begin to become very significant consumers of grid electricity. In Tasmania, the smallest electricity grid, average demand on the entire grid is only around 1125 MW (this does not include electricity exported to Victoria). This 175 MW limit on the grid is discussed further in Section 3.3.2.3.

3.3.2 Grid connection results

The model was run in three regimes: without any grid connection (i.e. where $\eta_{in} = \eta_{out} = 0$ for all times); with a grid connection that could only draw from the grid (the consumer-only case, where $\eta_{out} = 0$ for all times); and with a grid connection that could both buy and sell electricity from the grid (the consumer-supplier case, where the maximum constraint on η_{in} and η_{out} is dictated by constraints on the transmission lines).

3.3.2.1 Consumer-only case

A heat map showing the LCOA-P at each location, as well as the fractions of grid electricity and wind electricity used in each location, is shown in Figure 3.9. The results are shown for the base case year, which is 2019.

An electricity grid connection is included in slightly more than 40% of cases. Whether a site includes a grid connection is a strong function of its distance from a major transmission line. At distances less than 150 km, all sites included a grid connection, while above 400 km, no sites included a grid connection; between 150 and 400 km is a transition region. Compared to the average site, grid-connected locations use more solar PV, because the majority of Australia's electricity grid is concentrated on the east coast, which has a solar-dominated renewable energy profile. However, a considerable number of sites with wind-dominated profiles (in Western Australia, South

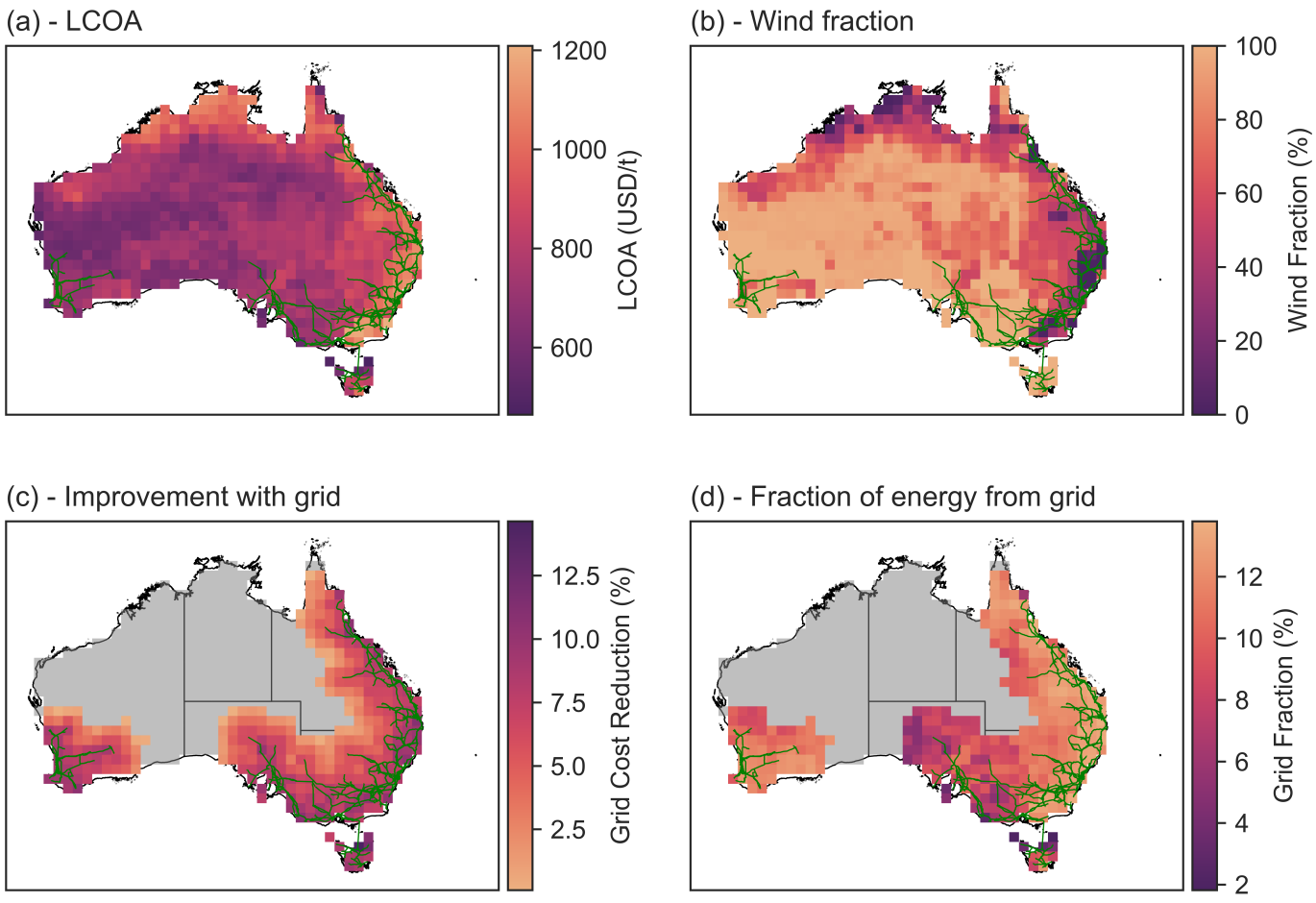

Fig. 3.9 Heatmaps showing LCOA-P at all locations within Australia. Transmission lines are shown in green. **(a) - Top left**: LCOA-P in USD/t; although the centre of the country - which largely does not connect to the grid - produces cheap ammonia, there are also sites near the grid in South Australia, the southern island of Tasmania, and in Western Australia which connect to the grid and have a favourable renewable profile. **(b) - Top right**: Fraction of renewable energy provided by wind as a percentage; the majority of sites rely more on wind than on solar. **(c) - Bottom left**: Reduction in LCOA-P compared to a no-grid case. **(d) - Bottom right**: Fraction of total power provided to the ammonia plant from grid. Note for (c) and (d), sites shown in grey do not benefit from connecting to the grid, and that only sites close to the grid make a connection.

Australia and Tasmania) also connect to the grid.

The main role of the grid in the ammonia plant is energy supply when not enough wind and solar power are available. Because of the maximum capacity constraint on the imported electricity discussed in Section 3.3.1.3, the grid cannot be the main supplier of electricity to the plant. Therefore, the grid predominantly causes a reduction in the size of energy storage equipment. Figure 3.10 demonstrates this point - comparing the cases with no grid to the cases with a grid connection, the majority of the equipment in the plant is unchanged, or changes only by a small proportion; however, the cases with a grid connection eliminate batteries entirely, and require about 25% less hydrogen storage.

The best site in Australia for ammonia production (both with and without a grid connection) is in Tasmania - the grid connection enables a 3.3% reduction in its LCOA-P. On average, the sites which included a grid connection in the consumer-only mode reduced their LCOA-P by 4.7%. There is an inverse relationship between the distance

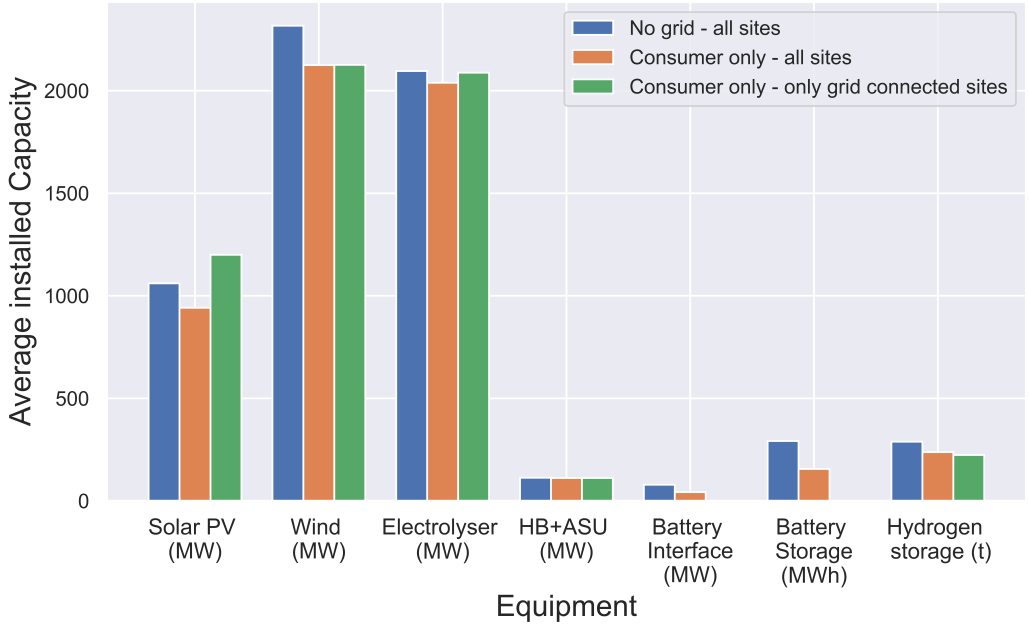

Fig. 3.10 Comparison of equipment size in grid and non-grid cases, for a model in which electricity is only consumed by the ammonia plant and not sold back to the grid. The change in size of the power generation and electrolyser is proportionally small; however, the proportional change in size of the storage equipment - in particular batteries - is substantial.

of the site from the grid and the size of the cost reduction - for sites which are less than 50 km from the grid, the cost reduction jumps to more than 8%. A summary of the results by state is included in Table 3.2.

Table 3.2 Summary of results by state for 2019.
* All data is grouped according to the state in which the grid connection is made (or would be made, if the site does not have a connection), not the state in which the site is actually located.

State	Average LCOA-P without grid (USD/t)	Average LCOA-P with grid (USD/t)	Average absolute reduction in LCOA-P (USD/t)[i]	Average relative reduction in LCOA-P (%)[i]	Average grid power price (AUD/MWh)	Number of hours $Y(t) < 40$ AUD/MWh	Average distance to transmission line (km)[i]
NSW	921	880	50	4.9	85	378	61
QLD	864	845	46	4.6	72	828	97
SA	726	718	27	3.4	99	1098	78
TAS	801	750	51	6.0	94	1047	37
VIC	913	860	53	5.6	109	680	24
WA	712	701	40	5.3	46	3638	98

[i] Only grid connected sites included.

Somewhat counter-intuitively, the impact of the grid in Western Australia is the second smallest, even though the power price in Western Australia is around half that of other states. By contrast, Victoria, which has the highest power price, sees the largest fall in its absolute LCOA-P from connecting to the grid. There are two reasons for this behaviour. Firstly, Victoria's electricity grid is much denser than Western Australia's; while locations in Western Australia reach around 100 km to connect to the grid, the average distance required by a site in Victoria is around

one quarter that distance. As per Figure 3.8, increasing the transmission distance from 24 km to 98 km increases the LCOA-P by around 10 USD/t. Secondly, Victoria is one of the worst performing states without the grid, meaning that even its comparatively expensive grid may be better than its wind and solar electricity.

This unexpected impact of the grid may also be caused by the relationship between periods of good renewable energy generation and low grid demand. In general, a grid connection will be more profitable if these two parameters are anti-correlated, because the ammonia plant can use the grid cheaply when its on-site production is low. On the flipside, it does not need to pay for expensive electricity when the grid is congested, as on-site production is good at those times. Evidence of this behaviour is seen in the difference between Tasmania and South Australia's grid connections. Although (i) the ammonia plants in both states are wind-dominated, (ii) they have similar average electricity prices, and (iii) they have a similar number of hours per year in which the electricity is cheap (see Table 3.2), the price reduction achievable with the grid in South Australia is much less than that achievable in Tasmania. Even if only sites within 50 km of the grid are considered (in order to prevent sites far from the grid in South Australia affecting the result), the cost reduction in Tasmania is about 40% more than the reduction in South Australia. This indicates that the synergies between the Tasmanian grid and its local renewable energy profile are better than those in South Australia.

To some extent, those synergies depend on the demand electricity profile, but they also depend on the supply mix in the electricity grid. Tasmania's electricity network is predominantly (>80%) supplied by hydropower, which is dispatchable as required. In contrast, South Australia's network is transitioning towards a wind-battery mix, with some solar plants. All coal plants in that state have been retired, and gas is used for dispatchable power to meet demand[163]. This suggests that (i) as decarbonisation continues, and grids themselves become more renewable, the benefits of ammonia plants connecting to the grid may reduce, and (ii) the largest benefit from grid connection will come from sites whose renewable profile is distinct from that which dictates the local electricity grid. However, if significant grid energy storage is available, and the cost of grid electricity is dictated by demand, rather than supply, the grid connection may continue to be useful even if the renewable profile onsite is similar to the renewable profile which drives the local grid.

Figure 3.11 provides a more detailed picture of the relationship between the grid and the ammonia plant. Panel (b) shows that the role of the grid is different in different states based on their local energy profiles. However, in general, for each state, higher grid consumption means higher electricity costs, and hence higher LCOA-Ps, because the marginal costs of operation mean it should be used as little as possible. In Western Australia, if a grid connection is made, relatively large amounts of grid electricity (10-12%) can be used without significantly increasing the LCOA-P, because the local electricity cost is so low. Therefore, if a site makes the expensive decision to construct a transmission line in that large state, it will have high utilisation. Queensland and NSW also have high grid electricity consumption at their sites; because these states are solar dominated as per Figure 3.11 (a), they require more back-up power than the wind-dominated states. In Tasmania, even though the grid meaningfully

reduces the LCOA-P, the fraction of electricity used from the grid is comparatively small. For the sites in those states, the wind energy is reliable, meaning the utilisation of installed back-up power will be low. Given those conditions, it is better to use a low-CAPEX, high-OPEX grid solution than a high-CAPEX, low-OPEX battery that will have a low load factor.

However, even though more grid electricity use tends to indicate that the LCOA-P will be higher, once a connection has been made, there is almost no relationship between how much grid electricity is used and how much the LCOA-P falls compared to a non-grid case, as shown by Figure 3.11 (c). If anything, higher grid use correlates to a bigger reduction in the ammonia cost (this is most obvious in the data for QLD and NSW), most likely because those sites would otherwise have required very large amounts of energy storage. Panel (d) of that Figure indicates the relationship depends much more strongly on distance between a site and the grid.

In general, wind-dominated sites have lower LCOA-Ps than solar-dominated sites, which is observable for both sites which are grid-connected and sites which are not grid connected. Consequently, the majority of locations use mostly wind turbines rather than solar PV for power generation. This is contrary to the forecast of Fasihi et al. [80], whose estimation using 2020 data predicted that Australia's optimal ammonia production sites would be dominated by solar PV, not wind. There are several points of difference between the analyses. Firstly, that work considered a global analysis, and did not differentiate costs of equipment in different countries. Their CAPEX/kW for wind was almost double that used for solar. In contrast, the costs used in this analysis are specific to Australia, based off information in the IRENA database; they forecast a comparatively small difference per kW in the installed price of those two technologies. Secondly, that work used a very low price for battery storage - around 280 USD/kWh; as discussed in Section 3.3.1.3, this is significantly cheaper than has been observed in Australia. Cheap batteries are an enabler of solar PV dominated ammonia production, since they enable continued operation through the night. Thirdly, that work used weather data from NASA; it may make different predictions to the ERA5 data considered in this analysis. Comparison between the results from these data sources would be a useful area of further work. The significant use of wind in this analysis is not unexpected, for two reasons: not only does wind electricity based on this input data have a lower LCOE (levelised cost of electricity) in most locations compared to solar, but it tends to be more evenly distributed (i.e. it is available during the day and night), meaning higher utilisation of the electrolyser is possible.

3.3.2.2 Consumer-supplier case

Allowing the model to sell electricity back to the grid, as well as importing electricity, enables further cost reductions since electricity which might otherwise have been curtailed can instead be sold. In general, this makes grid connection more favourable: an extra 42 sites achieve their minimum LCOA-P by connecting to the grid compared to a case in which electricity can only be purchased from the grid. At the best site for ammonia production, the cost of production fell by 11% compared to a no-grid case, or 8% compared to a consumer-only model. In total this reduces the LCOA-P from around 520 USD/t to 460 USD/t, at which value the ammonia would have been

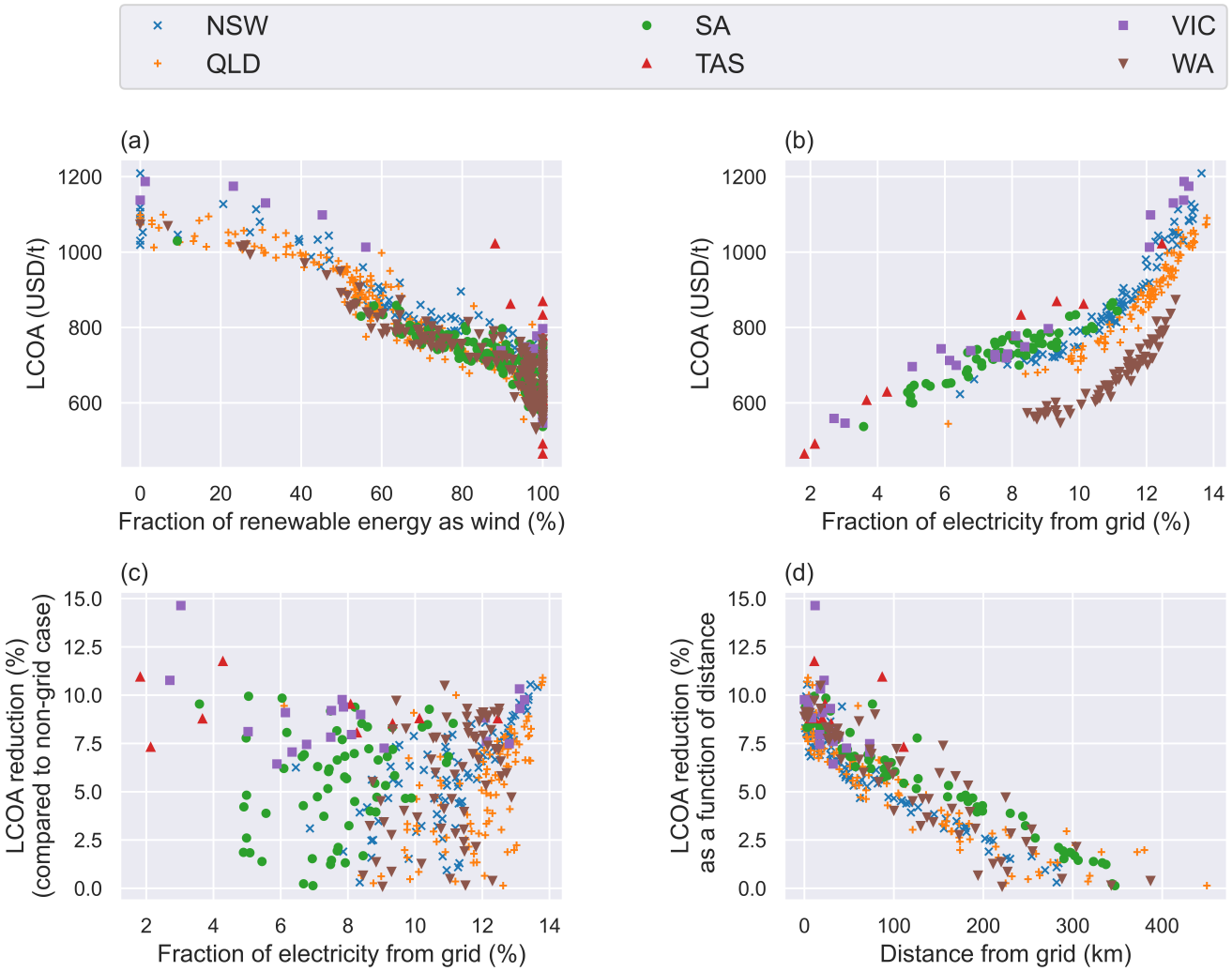

Fig. 3.11 Relationship between energy source and LCOA-P for different states in 2019, for sites which choose to connect to the electricity grid. Top panels show the direct impact on LCOA-P in USD/t; bottom panels show how much the LCOA-P falls because of connection to the grid (as a percentage). **(a) - Top left**: LCOA-P against fraction of wind energy installed, by state; in general, wind-dominated sites outperform solar sites. **(b) - Top right**: LCOA-P against fraction of grid electricity used, by state; in general, sites which need to buy less energy from the grid are cheaper. **(c) - Bottom left**: LCOA-P reduction compared to a non-grid connection case, as a fraction of grid demand. Perhaps counter-intuitively, there is no visible relationship between what fraction of electricity is sourced from the grid and how much the LCOA-P improves. **(d) - Bottom right**: LCOA-P reduction as a function of distance from the grid; closer sites benefit much more from the grid connection.

competitive on a global spot market for about 3 years in the decade from 2010 to 2020, compared to for about 1 year at the LCOA-P achievable without the grid [80].

This mode of operation changes the sites which are best for ammonia production. 15 of the best 20 sites for ammonia production use a grid connection; only 6 of these sites are in the top 20 if they do not use a grid connection at all. The site in northern Tasmania which sees the largest reduction in its LCOA-P becomes the sixth best site in the country when it can sell electricity; it is 104$^{\text{th}}$ with no grid connection. A number of the new best sites are better suited for ammonia export than their competitors, because their location is close to the coast (where the grid is concentrated), meaning costs for ammonia pipelines and desalinated water will not accrue. Of the top 20 sites, 8

are coastal without a grid connection, and 12 are coastal with a grid connection. The average distance to the coast for sites in the top 20 drops from 300 km to around 150 km.

There are two changes to plant operation and design in the consumer-supplier mode: curtailment reduction and renewable capacity increase.

Firstly, the curtailment of renewable plants falls by 40%, from an average of 5% (of the total energy produced by the plant) to an average of 3% at the sites which have a grid connection. Even though the plant can sell electricity to the grid, there are several occasions on which it may still need to curtail: (i) if the total energy produced from the renewables exceeds the total capacity of the plant plus the capacity of the electricity wires, which is set here to 175 MW - this is particularly common in hybrid plants with both wind and solar installations; (ii) if the total energy produced from the renewables exceeds the total capacity of the plant, and the electricity price is negative; or (iii) if the renewables are exporting to the grid at capacity, but the hydrogen storage is full, and the ammonia plant is below its operating limit (because of its slow ramp-up rate), meaning limited power can be redirected to the plant.

Secondly, the size of the renewable equipment tends to increase slightly for grid connected sites compared to the consumer-only model, as shown in Figure 3.12; there is an increase of 23 MW on average for solar, and 68 MW on average for wind. Noting that the maximum rate at which electricity can be exported is 175 MW, this represents slightly over 50% of the plant's total capacity to export.

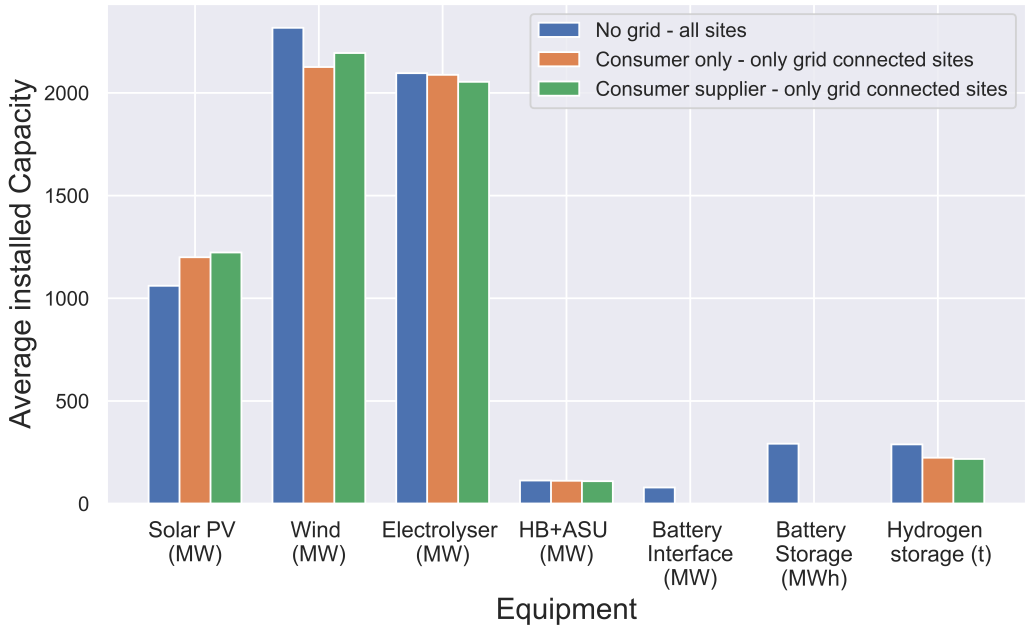

Fig. 3.12 Comparison of equipment capacities for no grid, consumer-only, and consumer-supplier cases. In the consumer supplier case, relative to the consumer only case, there is still a much lower storage requirement compared to the no-grid case. However, renewable energy generating capacity - that is, installed solar and wind - increases in consumer-supplier compared to consumer-only. Note that consumer-only and consumer-supplier data are provided for the sites at which there is a grid connection in the *consumer-only case* - i.e. sites which only connect to the grid in the consumer-supplier case are excluded from the averaging to avoid skewing the data.

There is a relationship between how a plant produces the electricity which it sells and the size of the reduction in the LCOA-P, which is shown in Figure 3.13. In general, sites which install more wind capacity see a larger reduction in their LCOA-P than sites which simply curtail less electricity (see panels (a) and (c)). This trend is particularly observable in Tasmania and Victoria, where some sites install significantly more wind in the consumer-supplier case compared to the consumer-only case - in two cases, more than 200 MW of additional capacity is installed, even though only 175 MW can be sold along the transmission wires (although wind turbines rarely produce at their maximum capacity). In those sites, sale of green electricity is a profitable venture, independent of the presence of an ammonia plant; they could be considered to be two separate sites where the sale of wind electricity subsidises the green ammonia (although there are still some synergies - the consumer-supplier model allows a smaller electrolyser that operates with a higher load factor).

At other sites in Tasmania and Victoria, and in other states like Western Australia, the potential for profit from a wind farm is smaller (either because the times at which the wind farm generates power at those sites do not correlate with high grid prices, or because the grid is generally low cost). In those cases, there is little benefit to increasing the size of a wind farm - instead the electricity which is sold is simply electricity which would otherwise have been curtailed in a consumer-only design. This approach still reduces the LCOA-P compared to the consumer-only case, but the benefits realised are comparatively small. Most sites will therefore adopt a balance of the curtailment reduction approach and the increased wind capacity approach, with every site increasing its total capacity to some extent (as per panel (d) of Figure 3.13).

The relationship between increasing the capacity of a solar farm and the LCOA-P reduction is not clear (see panel (b) of Figure 3.13). In some sites in Queensland and New South Wales, solar capacity is removed and replaced by wind power; in others, additional solar capacity is profitable. South Australia's behaviour is unique - the consumer-supplier case almost always installs additional solar capacity, which in some locations even replaces wind. This behaviour is related to the nature of the South Australian grid - as discussed in Section 3.3.2.1, that grid relies heavily on wind power and has comparatively little solar electricity, causing high daytime prices which can be exploited by a solar farm.

3.3.2.3 Grid power constraints

The model in this report is strongly constrained by the limit applied to power imported from the grid, which is 175 MW. As described in Section 3.3.2.1, this constraint forces the grid to adopt the role of energy storage, replacing the battery. However, based on the trend in Figure 3.11 (b), an increasing fraction of grid electricity consumption will tend to drive up costs, suggesting that few sites in the consumer-only model would change their behaviour if more electricity import from the grid were available.

For the consumer-supplier model, the impact of this constraint depends on the site. For sites which tend to reduce curtailment (rather than building extra equipment), the constraint on power export is not as significant, as these sites are less likely to hit this limit (since they are constrained by the power available at a given time).

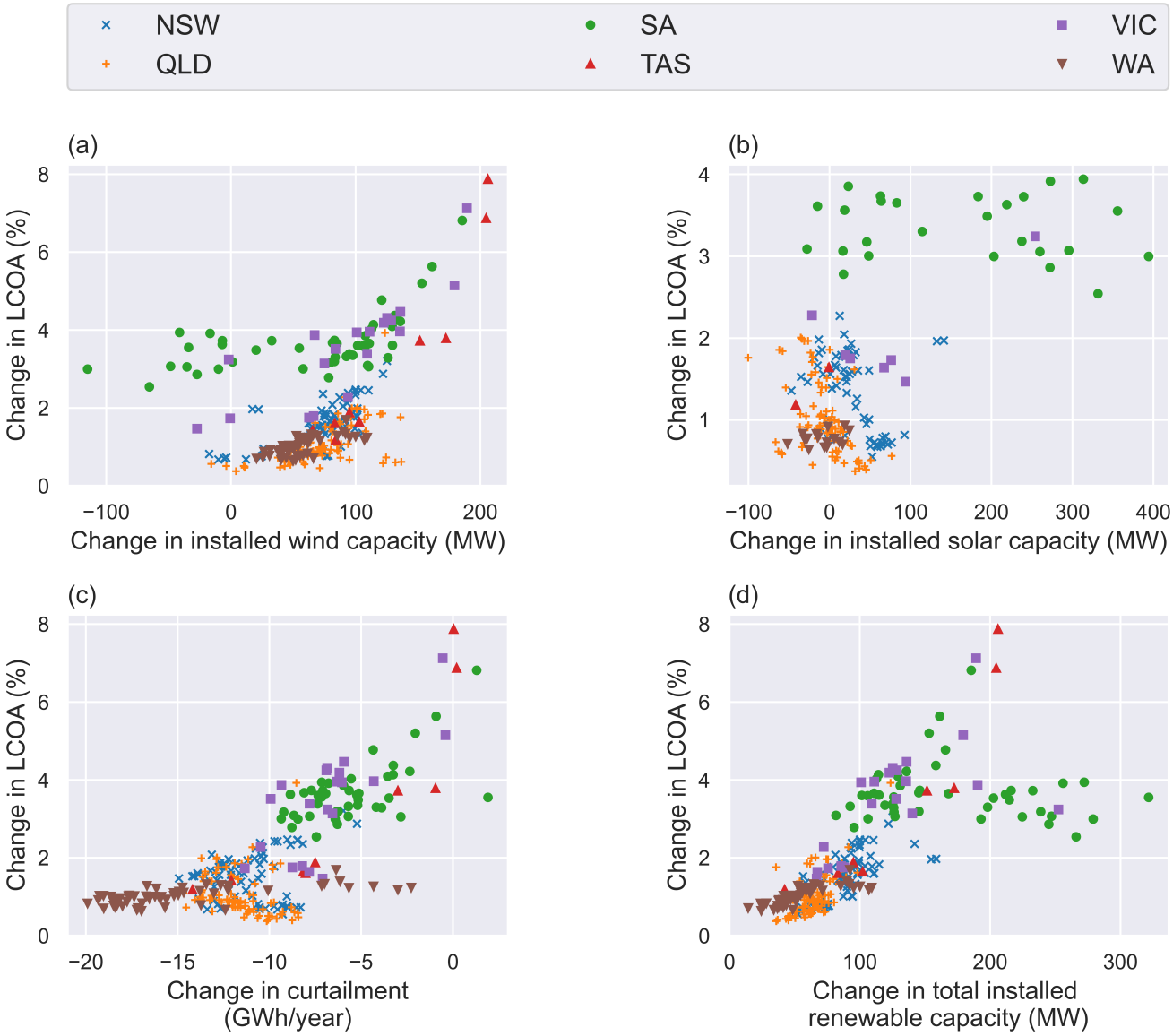

Fig. 3.13 Relationship between the change in plant design and LCOA-P reduction when the model changes from consumer-only to consumer-supplier mode. The change from consumer-only to consumer-supplier is always a reduction. **(a) - Top left**: Change in wind capacity (only for sites with wind installed in the consumer-only case). In general, there is an increase in the amount of wind installed, whose size is between 0 and the maximum capacity of the grid export (175 MW). **(b) - Top right**: Change in solar capacity (only for sites with solar installed in the consumer-only case). With the exception of South Australia, there is not significant installation of additional solar; in South Australia, the grid is mostly powered by wind and natural gas, so additional solar may be able to sell into the grid at a higher price. **(c) - Bottom left**: Change in curtailment (absolute difference between the amount of electricity curtailed at all grid-connected sites). In general, curtailment tends to be lower when more electricity is sold into the grid. **(d) - Bottom right**: Change in total installed renewable capacity at all grid-connected sites. All sites install some additional renewable capacity.

On the other hand, for sites which install additional renewable capacity, the constraint on power export is very limiting; at those sites, the construction of wind and solar farms is independently profitable, and if grid export is unconstrained then the model will construct very large renewable energy facilities which mostly sell electricity to the grid (effectively creating a second business which subsidises the green ammonia plant). In practice, there are many limitations which would prohibit such operation: land may not be available in very large quantities; very

large upfront capital expenditures would be required; and there are market risks associated with being a very large contributor to Australia's electricity grid, which is finite in size.

In general, the ammonia plant in consumer-supplier mode will stabilise the operation of the national grid, by buying electricity when the price is low, and selling it while the price is high. In 90% of cases, the cost of electricity sold to the grid is greater than the cost purchased on a per MWh basis; assuming that the price is reflective of the grid demand, this will have a stabilising effect. Most of the remaining 10% of cases were in Western Australia, whose grid is already far more stable than the other states. Even in those locations, if the TUOS costs and efficiency losses are factored in, the levelised cost of electricity sold exceeds the levelised cost of electricity purchased. However, the ammonia plants do represent a large additional load on electricity grids; only in about 5% of locations did the system sell more electricity back to the grid than in purchased, meaning the remaining cases represent new loads.

3.3.2.4 Emissions constraints

The suitability of using the grid as a back-up power supply is limited by the Scope 2 emissions associated with the consumption of grid electricity[164], which may impact the accreditation of ammonia as 'green'. In the very short term, some consumers may be willing to accept ammonia with a moderate carbon intensity in order to establish supply chains; however, the demand for green ammonia will soon require low or zero carbon emissions intensity. As described in Chapter 2, there are few agreed-upon standards for what constitutes 'low-carbon' ammonia; the best which is available comes from CertifHy [45], who require that the emissions associated with green hydrogen be less than 36 g of CO_2-eq per MJ of fuel (which is equivalent to approximately one third of the emissions associated with conventional hydrogen production). The same limit is applied here to ammonia.

Figure 3.14 shows the LCOA-P as a function of the carbon intensity at each site with a grid connection, calculated for the consumer-supplier case. The carbon intensity calculation neglects emissions associated with plant construction, and considers solar and wind electricity to be entirely carbon neutral. The carbon intensity from the grid on a given day is obtained from AEMO [150]; daily data is not available for Western Australia, so an average annual rate is used instead, although that state is almost entirely reliant on natural gas for electricity, so emissions factors will not change much during the year. In fact, the only state in which the emissions factor changes significantly during the year is Tasmania, which relies mostly on hydro power, but which turns to dispatchable hydrocarbons during dry seasons.

There are clear differences between different states evident in Figure 3.14 (a). Tasmania, South Australia, and, to a lesser extent, Western Australia, have relatively low grid carbon intensities, meaning the vast majority of sites in those states fall below the CertifHy limit, independent of grid energy consumption. On the other hand, nearly every site in Queensland and New South Wales will produce ammonia with a carbon intensity which cannot be considered green; those sites also tend to be significantly more expensive because of their substantial reliance on the grid, and were therefore poor candidates for ammonia sites regardless of their emissions.

Panel (b) of Figure 3.14 assumes that sites are able to claim a carbon credit for the green electricity which

they export to the grid. This carbon accounting may be considered acceptable by potential consumers, particularly if it can be shown that the green input to the grid has displaced a fossil-fuel electricity producer. In that mode, 75% of sites produce ammonia with an acceptable carbon intensity; in some cases, the avoided emissions may even exceed the emissions associated with consuming grid electricity. In two sites, the avoided emissions are much larger than the emissions from the grid; both sell into the Victorian electricity grid, which is carbon intensive, and anti-correlated in price with the wind resources used at those two sites.

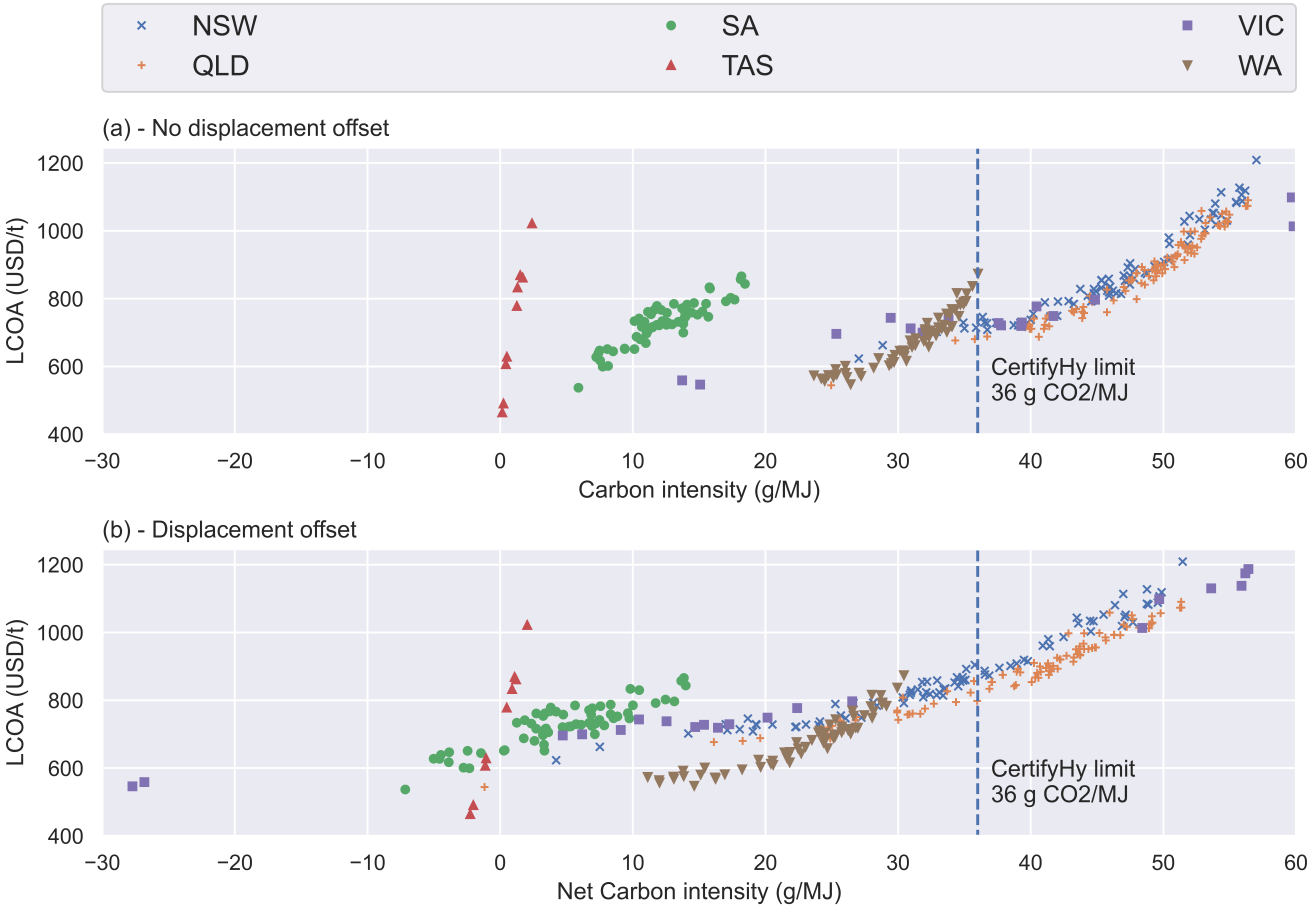

Fig. 3.14 LCOA-P at consumer-supplier sites as a function of fuel carbon intensity. **(a) - Top**: Carbon intensity considering only electricity imported. Whether ammonia produced with a grid connection is sufficiently low carbon to be considered 'green' is determined almost entirely based on state. In general, cheaper sites are less likely to have high carbon emissions. **(b) - Bottom**: Carbon intensity assuming carbon credits are available for electricity sold. This reduces emissions intensity at most sites; some sites could be considered to have strongly negative emissions.

3.3.3 Sensitivities

3.3.3.1 Annual sensitivities

The analysis so far has focussed on data from 2019. In different years, both the renewable power available and the cost of grid electricity fluctuates significantly. The difference caused by annual variation in electricity market behaviour is much more substantial than the difference caused by annual variation in renewable power; using

nationwide average costs for electricity, the difference between the cheapest and most expensive year is around 75% of the median price between 2013 and 2020; even larger fluctuations are observable in individual states.

Because of this significant cost variation, it is important that ammonia plants which are designed to rely on semi-islanded operation are robust to different grid behaviour. For that reason, a sensitivity analysis was performed by re-solving the model using data from both 2016 and 2017 to understand the impact of this variation. In general, the electricity price in 2016 was cheap (averaging 67 AUD/MWh), and 2017 was expensive (averaging 92 AUD/MWh), compared to 2019 (averaging 84 AUD/MWh); however, because each state has a slightly different trajectory in grid electricity costs over time, results are reported on the basis of the local average electricity price, rather than the year for which the analysis was performed.

In order to minimise the impact of interannual variation of in-situ renewable electricity production from this analysis of the electricity grid's impact on green ammonia costs, the basis for the reported results is the improvement enabled by the grid. That is, grid performance is measured by taking the difference at each site between the LCOA-P with the grid and without the grid, rather than the absolute value of the LCOA-P (assuming that in-situ variation in renewable production impacts both grid and non-grid cases equally, and therefore cancels out). Results are displayed in Figure 3.15.

In panel (a), which shows results for the consumer-only case, there is a consistent and unsurprising trend observable in all states: as the electricity price becomes cheaper, connecting to the grid becomes a better proposition. However, in panel (b), which shows the consumer-supplier case, this trend is not observable. Instead, in the three largest states (NSW, QLD and Victoria), as well as in the national average, there is a local minima in the data: although very cheap electricity is still preferable, ammonia producers which sell electricity back to the grid can exploit high prices, which in some cases will offset the increased costs of drawing electricity from a more expensive grid. Although this is not observable in the three smaller states, the trend in WA is much flatter for the consumer-supplier case than the consumer-only case, and Tasmania and South Australia are decarbonising relatively quickly compared to the rest of the country, so there may be other factors at play in those states, as their grids change over time.

While this analysis would be improved by being run over more years of data, there is evidence that across multiple states, adopting a consumer-supplier model will make green ammonia production more robust to variable grid behaviour.

3.3.3.2 Parameter sensitivities

A number of additional sensitivities were also considered in order to understand the impact of a number of key parameters on the conclusions drawn in this analysis: project finance, electricity cost, electrolyser cost, grid connection cost, and the cost of storage. Appendix A.1 summarises which parameters are modified, and the size of the modification, in each case. Results are summarised in Table 3.3.

Reducing the cost of finance can have a substantial impact on the LCOA-P, because such a significant portion of

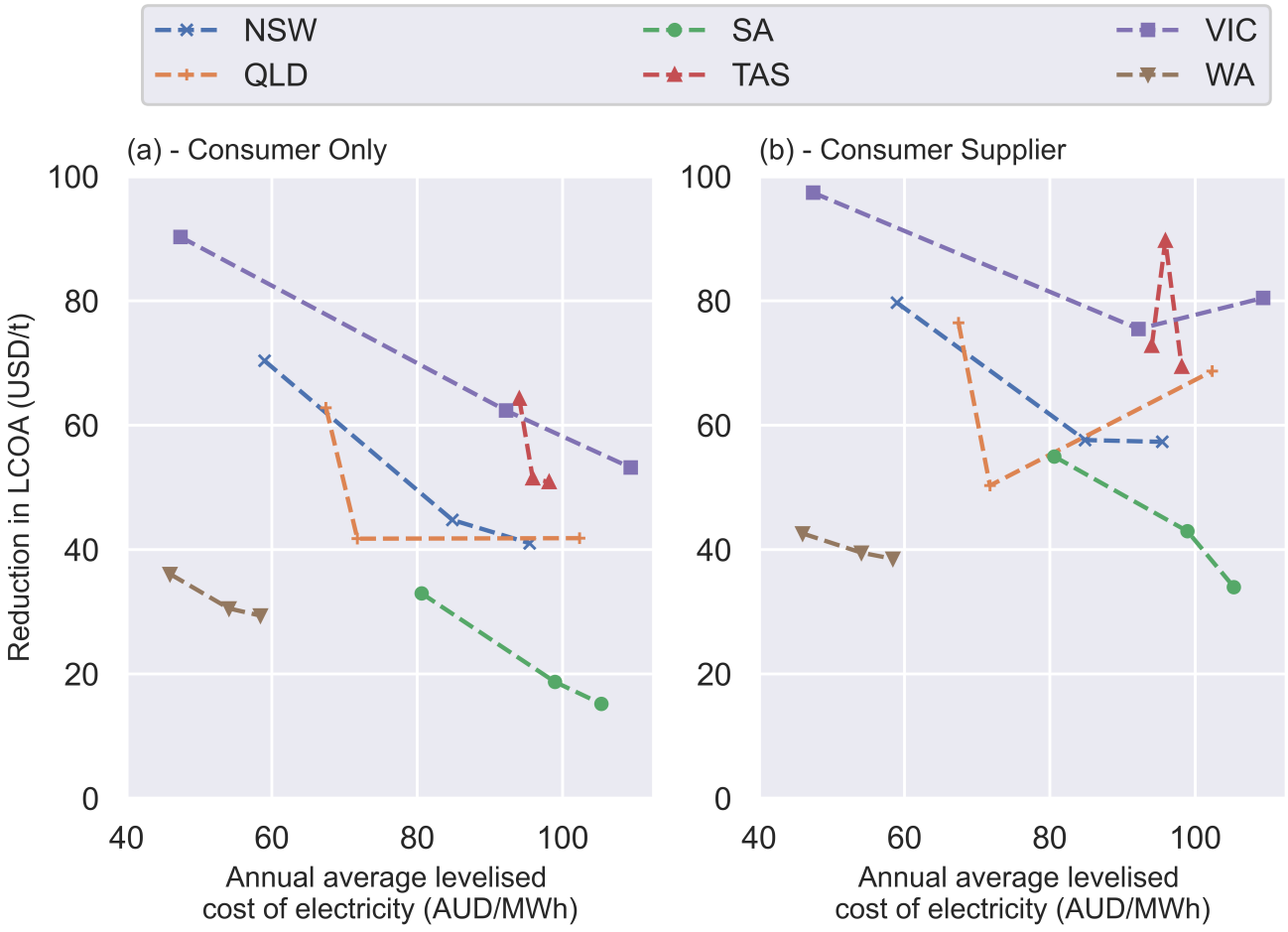

Fig. 3.15 Improvement in LCOA-P as a function of average levelised cost of electricity for each state in that year. Averages are taken only over sites that connected to the grid in the consumer-only case for 2019. **(a) - Left**: Consumer-Only results; **(b) - Right**: Consumer-Supplier results. Where there is always a negative correlation between power costs and the improvement in the LCOA-P associated with increasing power prices in the consumer only case, operating in consumer-supplier mode can improve performance even when costs on the grid are high.

the project costs are CAPEX. However, cheaper project finance will typically make a grid connection less desirable, because the grid connection is a comparatively low CAPEX, high OPEX investment. This effect is only significant in the consumer-only mode; in the consumer-supplier mode, since the grid connection often pays for itself through additional sales, the impact of finance on the number of sites which connect to the grid is relatively small.

Unsurprisingly, cheaper electrical equipment can also have a meaningful impact on the LCOA-P. Like cheap finance, cheap equipment also makes a grid connection less favourable, as onsite electricity can be generated more cheaply compared to grid electricity. However, it should be noted that a significant drop in the price of solar or wind is likely to correlate with a drop in the price of grid electricity which may be powered by those renewables, meaning the grid may still be competitive as prices fall. Even in the cheap electricity scenario, a substantial number (>40%) of sites still use a grid connection in the consumer-supplier mode.

Electrolyser and grid sensitivities were included because of the uncertainties associated with those parameters. Although the electrolyser case had a moderate impact on the LCOA-P, neither case caused a substantial variation

Table 3.3 Sensitivity results for grid connectivity

	Consumer Only		Consumer-Supplier	
	Cheap	Expensive	Cheap	Expensive
LCOA-P (USD/t)	(Base = 775)		(Base = 769)	
Finance	634	928	627	922
Electricity	692	846	683	835
Electrolyser	733	822	723	815
Grid	773	780	767	774
Storage	769	781	763	774
Average fraction of renewable electricity from wind (%)	(Base = 77)		(Base = 77)	
Finance	77	77	77	77
Electricity	54	87	56	87
Electrolyser	78	74	80	74
Grid	77	76	77	76
Storage	78	76	78	76
Fraction of sites with grid connection (%)	(Base = 42)		(Base = 48)	
Finance	38	45	48	49
Electricity	37	46	44	50
Electrolyser	42	44	46	49
Grid	43	41	49	47
Storage	39	44	45	50

in the fraction of wind used (which is indicative of the optimum plant design), or in the number of sites which connected to the grid; this suggests that the results of this analysis are robust to the uncertainties in those parameters. The impact of energy storage costs on both the LCOA-P and the fraction of wind energy used is fairly small. However, there remains a moderate impact on the number of sites which connect to the grid (comparable in size to the impact from cheaper project finance). This is further evidence for the behaviour described in Section 3.3.2.1, which indicated that the role of the grid is to substitute energy storage equipment; if there is a significant fall in the price of that energy storage equipment, then the substitution no longer occurs.

3.3.4 Impact of Scale

Without grid connection, the production LCOA-P at industrial scale has limited dependence on production rate; while downstream infrastructure may benefit from economies of scale, most equipment required for ammonia production is modular. However, including a grid connection introduces scale dependency. At small scales (<0.1 MMTPA), the fixed cost of grid connection is not worthwhile; at large scales (i.e. 10 MMTPA), a grid connection will not be sufficient to supply a meaningful amount of electricity to the ammonia plant without impacting the local network (meaning the grid connection is small relative to overall plant size). Between these extremes lies a minimum production cost, at which the plant makes maximum use of its investment in the electricity grid.

The precise value of this minimum production cost depends on the distance of the plant from the electricity grid,

the extent to which the plant makes use of the grid connection, and the size of grid connection available (fixed here at 175 MW, as discussed in Section 3.3.1.2). To factor this effect into the analysis, the ammonia plant was sized at increasingly small scales while keeping the grid connection size constant. The per MW cost of the Haber-Bosch plant was selected by pre-estimating the total cost using a load factor of 80% and a scale factor of 0.7 compared to the base case 1 MMTPA (for sizes less than the base case only).

Figure 3.16 shows the impact of scale on production in two locations. At the first location (in WA), which uses more grid electricity than it exports, the minimum production cost corresponds to a high carbon intensity; to reduce these emissions, a larger plant scale is required at which the grid provides less of the power, slightly increasing costs. On the other hand, at the second location in Tasmania (the cheapest identified for 2019 data), which sells more electricity than it purchases, the ammonia is carbon negative at all scales. At this location, it is profitable to sell electricity from the renewable energy production; that sale effectively subsidises the cost of green ammonia, and therefore benefits from very small scales – the larger the production rate, the smaller the subsidy from electricity export per ton.

The different behaviour at the two locations is caused both by different weather patterns, and different electricity grids. Western Australia has a stable, carbon intensive grid powered dominantly by gas; Tasmania's grid uses mostly hydropower and wind, enabling more opportunity for cost arbitrage and low-carbon grid connection.

3.3.5 Operating Considerations

Because the plant is optimised to minimise the LCOA-P, the plant (grid-connected or not) may not operate as efficiently in different weather conditions than in those under which it was designed. To some extent, grid-connected sites can use back-up power to maintain stable operation, but doing so increases costs, so electricity inputs should be minimised. Islanded (non-grid connected) sites rely on energy and hydrogen storage when they cannot generate power; if storage is too small, there is a risk of system failure (shutdown).

The main operating challenge is the requirement of the HB plant to maintain continuous operation. The key parameter is the minimum operating rate (MOR). If the designed plant cannot maintain its minimum rate for a given weather profile, regardless of how it is operated, the operating model will fail to converge, which occurs for many grid-connected and islanded cases.

In order to examine this challenge, the model was solved in "operating mode", in which the time-independent variables were fixed (i.e. the plant design). The model then takes as inputs a different year of weather data (and associated grid electricity costs), and selects only the values of the time-dependent variables (i.e. the operating conditions) which maximise the cash flow. For simplicity, the costs of water and O&M are neglected, and the cash flow is calculated simply as the ammonia sales minus the net electricity cost. The model is run using data from 2008 to 2018. The sale price of ammonia for estimating the cash flow is estimated as 500 USD/t, which is at the higher end of spot prices from the last decade.

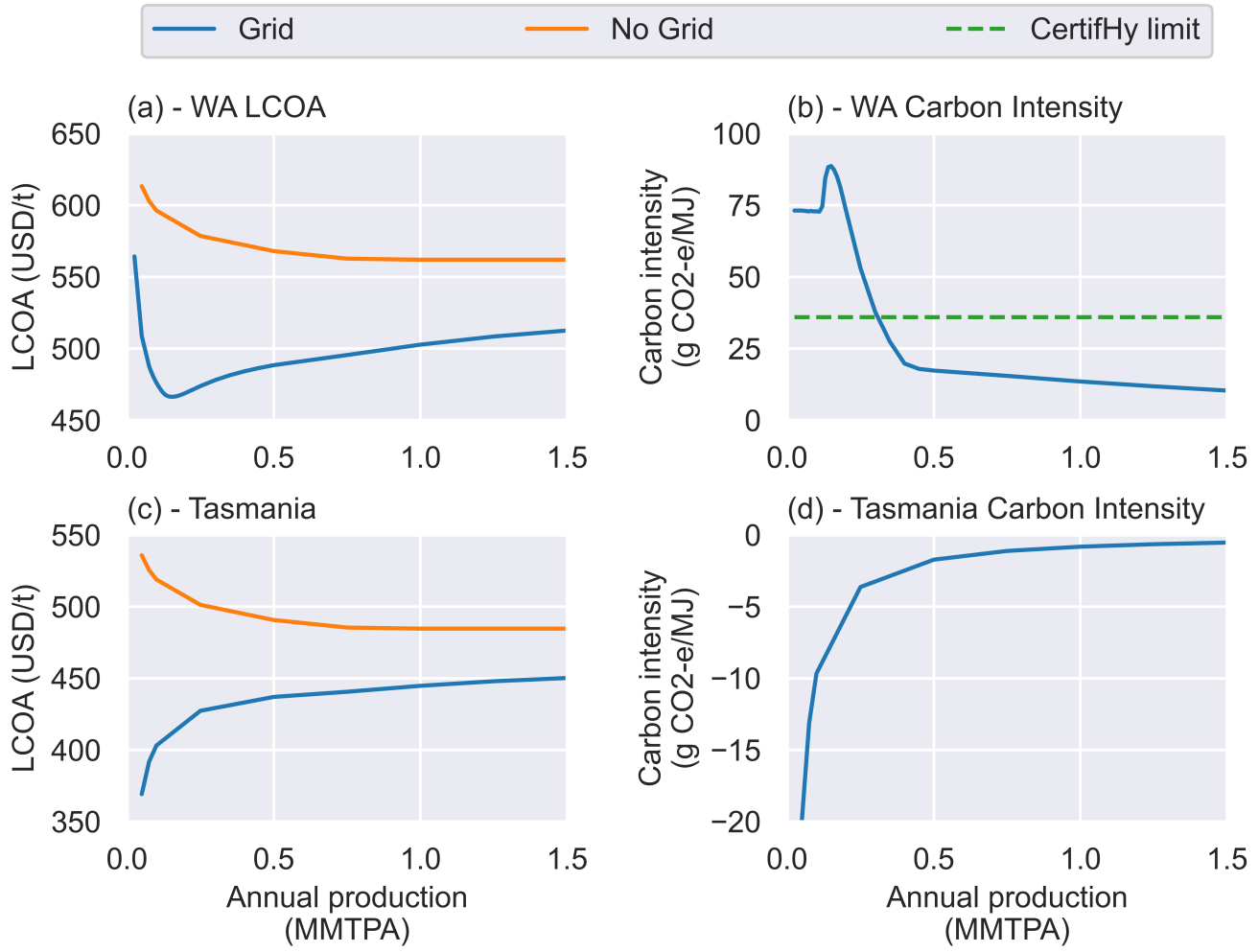

Fig. 3.16 Impact of scale on LCOA-P and carbon intensity at two low-cost sites, one in Western Australia **(top)**, and the other in Tasmania **(bottom)**.

Two sets of islanded sites are compared to grid-connected sites: The Islanded (I) set refers to sites in the same location as grid-connected sites at which the model was re-run without the grid; the Islanded (II) set refers to different sites where grid connection is not optimal, whether or not it is allowed. At all islanded sites, costs are mostly capitalised; at grid-connected sites, electricity costs are operational, and therefore impact cash flow. For fair comparison between sets, we report the "Cash flow delta", which is given by the cash flow in the operating year minus the cash flow that was anticipated in the design year (assuming ammonia is sold at the LCOA-P).

3.3.5.1 Overdesign Approach

Because the MILP design approach minimises the size of the plant, the result is effectively as 'lean' as possible. Since the operating approach does not have total foresight, it will not be able to replicate the perfectly lean behaviour of the optimal design, and therefore will either (i) fail to produce the same amount of ammonia, or (ii) occasionally be unable to sustain operation of the ammonia plant at or above the target rate. Therefore, we also include consideration of overdesigned plants, which will have higher upfront costs, but are less likely to fail.

Conventionally, 'overdesign' of a plant would involve applying some fixed factor to each piece of equipment, with larger factors applied to some, potentially less reliable, units. In this context, oversizing all equipment by the same amount would not improve reliability, since, although power generation grows, so too will the HB plant, necessitating a higher baseline power. Even scaling up all equipment except the HB plant is not sensible, as some equipment is not useful for supporting the plant during periods of low production (solar PV, for instance, should not be scaled up to correct an imbalance that occurs at nighttime or in winter). Instead, the plant is *designed* using increasingly tight limitations on HB MOR but is then *operated* using more a relaxed value for that parameter. This enables the oversizing to be concentrated on the equipment that enables flexible operation.

3.3.5.2 Operating Mode results

Both grid-connected and islanded sites require overdesign to reduce the plant failure risk, but grid-connected sites still outperform islanded sites on two fronts. Firstly, the cost to overdesign is higher at both sets of islanded sites than at grid-connected sites – see Figure 3.17 (a). Secondly, while imposing stricter overdesign requirements reduces the failure rate at all sites, there are fewer failures at grid connected sites than at either set of islanded sites – see Figure 3.17 (b). Figure 3.17 (c) also indicates that sites are more likely to connect to the grid during the design process if the constraints imposed on the HB plant are tighter.

With no overdesign, the average cash flow delta overall is below 0, which indicates that performance is generally worse during operation than was anticipated during system design, because the plant is not optimised for the new weather or grid electricity profile. However, grid-connected sites on average had a cash flow delta slightly greater than 0, even though the operating timeframe included both years in which the grid was cheaper and years in which it was more expensive than the design year. The operating mode is able to achieve a positive cash-flow delta by sacrificing some ammonia production in favour of electricity sale, which it cannot do in the design mode where it is forced to produce a fixed amount of ammonia as cheaply as possible. Perhaps counter-intuitively, the cash-flow delta worsens for islanded sites as the plant is more overdesigned, while for grid-connected sites it stays relatively constant: this is an artefact of cases which recorded failures at low overdesign rates.

3.3.6 Summary of grid connection findings

This case-study explored the benefits of sector coupling for green ammonia production. It demonstrates that significant reductions in the LCOA-P are achievable using a grid connection. The most substantial cost reductions, which are in the order of 10%, occur when the plant is located near the electricity grid. In Australia, these sites are mostly coastal, which will locate them close to other supporting industry and to export ports. Further cost reductions are achievable by optimising the plant scale relative to the maximum allowable size of the grid connection. In some locations, ammonia production can be significantly subsidised by profitable participation in the grid.

When a site connects to the grid, it is less likely to fail during operation, and will generate more cash flow than if a grid connection is not used. Regardless of whether a site is grid-connected, it requires some overdesign, which

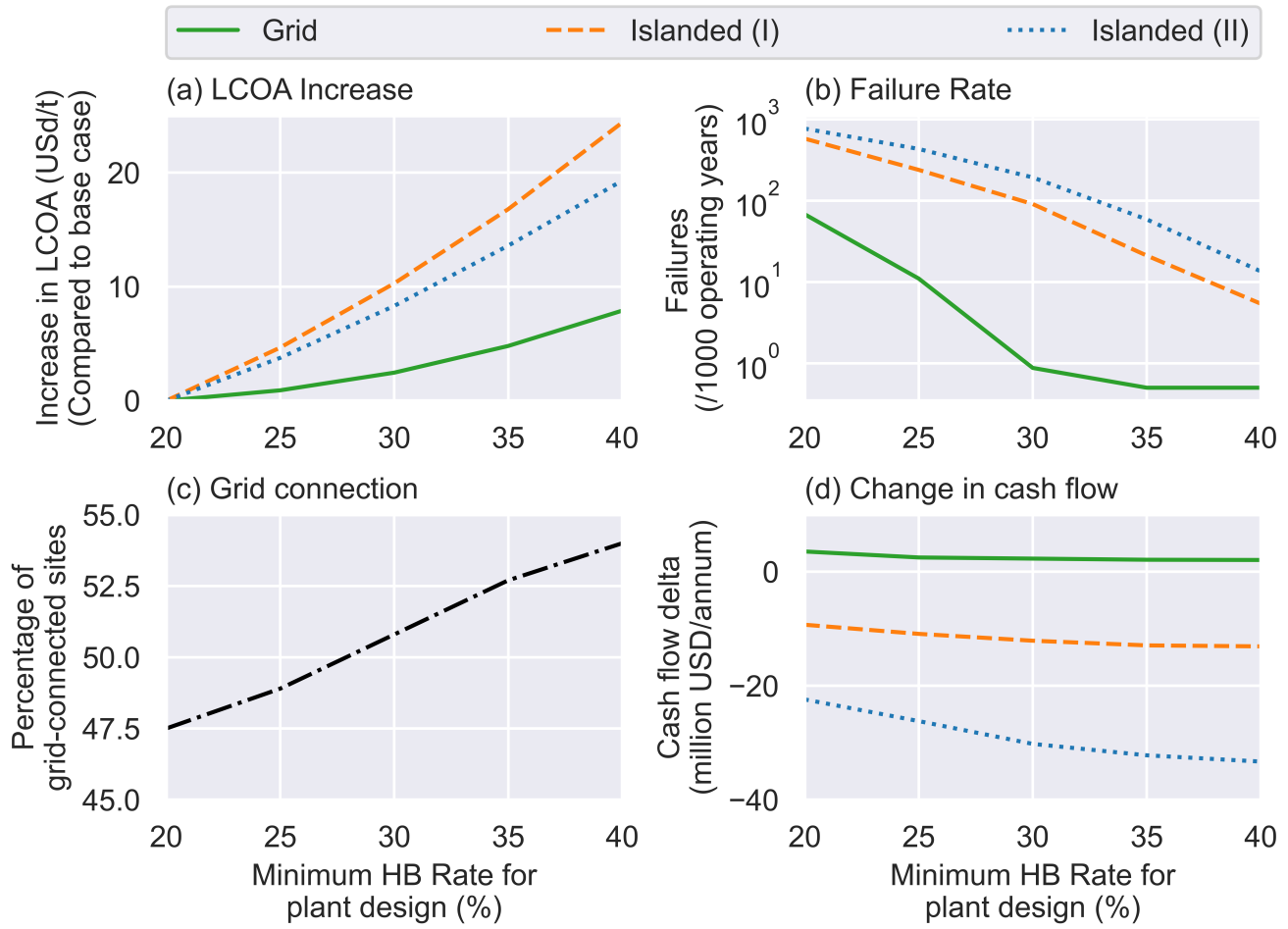

Fig. 3.17 Operating performance as a function of plant overdesign at three sets of sites: grid connected, islanded I (i.e. sites in the same location as grid connected sites, but without a grid connection), and islanded II (sites at which it is not optimal to connect to the grid). The plant is oversized for most of the runs by designing at a minimum HB operating rate greater than that allowed during operation. **(a) - Top left**: Increase in LCOA-P associated with the overdesign - increasing the design margin at grid connected sites costs less than on islanded sites. **(b) - Top right**: Failure frequency when the oversized plant was run with a new weather data profile. The failure rate for grid connected plants is much lower than for non-grid connected plants. Note that no operating failures were recorded for grid-connected sites with minimum operating rates of 35% or greater, which is recorded as a rate of 0.5/thousand years so it can be read on a log scale. **(c) - Bottom left:** Relationship between the number of grid connected sites and how oversized the plant is; the larger the oversize, the more sites benefit from a grid connection. **(d) - Bottom right**: The "cash-flow delta", or the difference between the cash flow predicted in the design case and the cash-flow attained in the operating case. Grid-connected sites are able to achieve the target cash-flow, or even slightly exceed it; the islanded sites make less money than forecast during design.

can be achieved by designing with tighter limitations on the minimum rate of the HB plant than are achievable during operation; the cost of overdesign at grid-connected sites is less than at islanded sites.

The integration of optimised green ammonia production and grid electricity is a first step in understanding how sector-coupling in the energy system can reduce the costs of decarbonisation. Further research should consider other industries which may have synergies with electricity grids, and how electricity grids themselves will transform over time. Additionally, the operating model demonstrated that there is a risk of plant failure caused by a shortage of back-up power or hydrogen that can occur whether connected to the grid or not; further research is required to

understand how ammonia plants will be operated with imperfect weather forecasting information.

The majority of the grid connection research was performed in 2021, before the significant spike in global energy prices of 2022 (which did not leave Australia unaffected). Although the results here indicate that production costs are reasonably robust to high grid prices (with additional renewable capacity potentially benefiting the grid during peak periods), further research should be conducted into how ammonia plants may interact with electricity grids which are under very substantial supply or demand side pressure.

3.4 Green ammonia production summary

This chapter has presented a model that can be used to optimise the cost of green ammonia production using a robust method that accounts for the variation of renewable energy production throughout the year. It has demonstrated that model speed improvements can be achieved using larger time steps without sacrificing accuracy. The model then was applied to a case-study on the Australian grid network, which had a number of significant inclusions: (i) the grid could be responsible for cost reductions in the order of 10% of the LCOA-P, provided a site was located nearby existing grid infrastructure; (ii) cost reductions were more effective when the ammonia plant operated as a 'prosumer'; (iii) grid connection introduced a scale dependency that may improve profitability at smaller sites in the short term; (iv) grid connection improved the response of the green ammonia plant to uncertain weather forecasts.

This final point related to plant operability merits more attention: clearly, the lean design determined by the optimisation method described in this chapter may struggle when operated in unfamiliar weather patterns. Understanding what may cause failure, and the extent to which overdesign is required, are core outcomes of Chapter 4.

Chapter 4

Operating green ammonia plants with imperfect forecasts and partial flexibility

4.1 Rationale

The model described in Chapter 3 provides a useful and rapid method for ammonia plant design. However, as emerged in the operating analysis at the end of the chapter (see Section 3.3.5), this model will not always design a plant which can operate robustly in unfamiliar weather conditions.

This has implications for green ammonia plant design models in the literature, which to the best of the author's knowledge rely on perfect forecasting i.e. the optimisation model is provided with the entirety of the weather data to which the plant it designs will be exposed. This simplifies the challenge of managing the storage inventories of hydrogen and back-up power: if the weather will improve, the model "knows" it can drain the storage without risking having insufficient hydrogen to operate the ammonia plant; otherwise it sets the HB to the minimum operating rate (MOR) [83]. With less forecasting information, making this decision is more difficult.

Although this problem arises during plant operation, it must be considered during plant design. Predictable weather profiles will be easy to operate and thus will perform as designed; others may require redundancy to buffer against long dunkelflaute that may increase capital costs well-beyond the optimum.

At the same time as managing storage inventories, the operator has another important lever at their disposal: ramping down the green ammonia plant. However, their ability to ramp the plant using existing HB technology is not well understood. There is an emerging consensus in the literature than an inability to ramp down the HB plant is responsible for significant increases in the LCOA-P [63, 165–167].

This chapter considers the impact of both plant flexibility and imperfect forecasting at the same time. It does this by first determining the impact of plant flexibility in the design phase, independent of imperfect forecasting; this section is an extended case-study using the model introduced in the previous chapter (referred to in this chapter

as the linear program, or LP). It then introduces a new model which takes a fixed ammonia plant design as well as limited weather forecast information as an input and uses an algorithm to determine an operating approach that balances production and operational stability. This model is based on model predictive control, and is henceforth referred to as the MPC approach.

The MPC approach is novel in its application to islanded green ammonia plants, and places guard rails around the results offered by the LP. The purpose of the MPC is not to design control loops which specifically determine the operating parameters of the ammonia plant (temperatures, pressures, feed ratios, etc.); rather, the MPC's purpose is to function as an algorithm which determines the set-point of the equipment within the ammonia plant. In other words, the MPC presented here is analogous to the primary loop in a cascade-control arrangement, dictating the power allocation and ammonia production.

The previous chapter introduced a clustering methodology for accelerating solution of the LP. Using this methodology would interfere with assessment of the ramp rate; for instance, clustering the data into 4 hour time steps would enable the plant to ramp from a minimum operating rate (20%) to maximum in a single time step under the baseline parameters considered here. Therefore all models solved in this chapter use a time step of one hour.

4.2 LP approach

This section uses the model developed in the last chapter to determine the extent to which ramping and flexibility impact on the ammonia cost in the optimal plant design. The ability of ammonia plants to operate flexibly is not well understood, but is likely to be constrained.

4.2.1 Technical basis for flexibility limitations

Flexibility constraints originate from the elevated temperature at which the HB process occurs. These temperatures are sustained by excess heat from the exothermic reaction; if production slows excessively, heat loss will exceed heat generation and the reaction will be quenched. Thermal expansion on start-up and shut-down has a damaging impact on equipment and catalysts, and therefore frequent cycling between an operating and quenched state is not possible. This requires a minimum rate to be sustained at all times [98]

Even above the minimum rate, HB ramping is also constrained, in order to prevent temperature hot spots inside the adiabatic catalyst bed reactors [166, 168]. Rate limitations are also constrained by the large inventory of material in the recycle loop of the HB process (necessitated by the reactor's low single-pass conversion); this creates some 'inertia' in the reaction system, meaning there is some dead-time between modification of the reactant concentration and a corresponding modification of the reaction rate.

While technical solutions are emerging using innovative reactor designs (which, for instance, are less reliant on large recycle loops[169]), it is not likely that the HB process will be able to match its own operation to that of a variable renewable energy plant. This chapter does not aim to address the technical basis for these flexibility constraints; rather, it seeks to understand how they may impact overall plant design, and the extent to which

removing constraints on flexibility is a justified investment.

4.2.2 LP model input detail

421 onshore sites were selected to analyse ramping and flexibility. The sites have a range of weather profiles and a range of latitudes (from 5°, near the equator, to 59°).

At each location, the model was solved under 13 different conditions: there are four different minimum operating rates (MORs) (20%, 40%, 60% and 80%) and three ramp rate factors (0.1, 1, and 10; these factors are applied to the base upward and downward rates of 5% and 20% respectively). The thirteenth case is an entirely inflexible plant, which operates continuously at 100% (in which instance consideration of ramping rates is obviously meaningless).

The model was solved using costs for 2022 and for 2050; because of the rapidly falling prices of batteries and solar PV, future electrolyser plants will be differently designed and therefore may respond differently to flexibility limitations. Present costs of equipment were taken from IRENA [156] [3] and from Nayak-Luke et al. [90]. Future costs were estimated using Way et al. [2], who use a stochastic approach to determining cost forecasts, historical analysis of which has demonstrated to be highly accurate. These inputs are used for the remainder of this thesis, and are summarised in the appendix (Table D.1).

4.2.3 Cycling constraints

This chapter requires a modification to the LP proposed in the previous chapter by including constraints on the frequency with which storage units can cycle. These constraints are necessary, as real energy storage units (particularly batteries) degrade at increased rates if they are cycled at high frequency. Cycling energy storage equipment in place of ramping the HB plant could mask the potential benefits of a flexible HB plant. Battery degradation can be categorized as calendar aging (which occurs inevitably over time) and cycling aging. Both forms of aging are incorporated in this chapter.

4.2.3.1 Calendar aging

Calendar aging, and cycling aging in normal use, is incorporated in two ways: firstly, by accounting for equipment replacement costs, and secondly, by adjusting equipment efficiencies. Equipment replacement costs are accounted for by applying higher Operating and Maintenance (O&M) costs to units subject to degradation (i.e. assuming the replacement is carried out on a rolling basis, rather than en masse when equipment reaches end of life, although the impacts on NPV are the same). In the previous chapter, the O&M was set at a flat rate of 2% for all equipment; in this version, increased costs are applied to equipment subject to degradation: the electrolysers, fuel cells and batteries.

Because their membranes require replacement approximately every 50,000 operating hours, electrolysers and fuel cells are subject to a 3% O&M fraction, of which 1% would be allocated to annual operating costs (i.e. labour,

insurance, etc.), and the remaining 2% would be allocated to membrane replacement. This has roughly the same impact on the NPV as reinvesting one-third of the electrolyser CAPEX every decade into membrane replacement at the nominated discount rate of 7% (i.e. if a plant were to replace all the membranes at once, rather than on a rolling basis). One-third is an appropriate cost-estimate for membrane replacement at end of life [103].

Similarly, batteries have comparatively short life spans (maximum 10 years) compared to the project as a whole (30 years); their O&M fraction is set at 3.5%. To again compare this annual maintenance cost with a decennial replacement of all the batteries, this is roughly equivalent to reinvesting half the CAPEX every decade (since only the battery itself needs to be re-installed; other components such as balance of plant electrical equipment do not).

Equipment efficiencies are also adjusted to represent some degree of degradation; electrolyser efficiency for 2022 is set to 53 kWh/kg, which is below the best market performance for a new electrolyser [170] but includes a 3.5 % degradation rate [171]. For 2050, superior performance of 46 kWh/kg is assumed, which incorporates both overall improvements and a reduction in degradation rate [172]. Battery charging/discharging efficiency is set at 95% for similar reasons[173].

4.2.3.2 Cycling aging

Having accounted for the costs of calendar aging and a standard amount of cycling aging, the model then imposes constraints which prevent high frequency usage from degrading the batteries faster than anticipated. There are a number of metrics for battery usage that can impact the rate of degradation, although total accumulated charge and depth of discharge are considered the most significant [173]. These parameters are related to each other: batteries which completely discharge on each cycle require replacement after around 6,000 cycles [174]; assuming a ten-year replacement cycle, this allows slightly less than 2 cycles per day. We assume a worst case scenario in which each cycle completely discharges, and limit the number of cycles using three constraints:

$$\lambda(SC,t) \geq \lambda(SC,t-1) + (\kappa(SC,t) - \kappa(SC,t-1)) \qquad \forall t \in S_t \tag{4.1}$$

$$\lambda(SC,t) \geq \lambda(SC,t-1) \qquad \forall t \in S_t \tag{4.2}$$

$$\lambda(SC,t_{final}) \leq G_{CL}(SC) \cdot C_{SC}(SC) \tag{4.3}$$

Equations (4.1) and (4.2) count the total amount of charge which has flowed into the storage component ($\lambda(t)$) as a function of time. If the state of charge of the storage component ($\kappa(t)$) has increased (i.e. it is charging), then $\lambda(t)$ increases by at least that amount. If the equipment is discharging, then the condition in Equation (4.1) is always met, because $\lambda(t)$ is prevented from decreasing by Equation (4.2). $\lambda(0)$ is set to 0. The total number of cycles is constrained by Equation (4.3), in which the charge accumulation in the final time step (t_{final}) must be less

than the total allowable number of cycles (G_{CL}), scaled according to the capacity of the storage component (C_{SC}).

Although battery cycling is far more widely discussed in the literature, hydrogen stores may also degrade under cycling. The extent to which degradation occurs will depend on the mode of storage. Pressure vessels should be robust to cycling within design limits, but the integrity of salt caverns may degrade if they are subject to rapid and frequent pressure fluctuation [175], and hydrogen storage by adsorption onto alloys is known to degrade with cycling [176]. We therefore include hydrogen storage cycling limits in order to understand how much they impact ammonia production costs.

4.2.4 LP model results

4.2.4.1 Impact of minimum operating rate without cycling constraints

The results for the plant design cases are shown in Figure 4.1; note this figure does not include cycling limits, which are incorporated in the subsequent section.

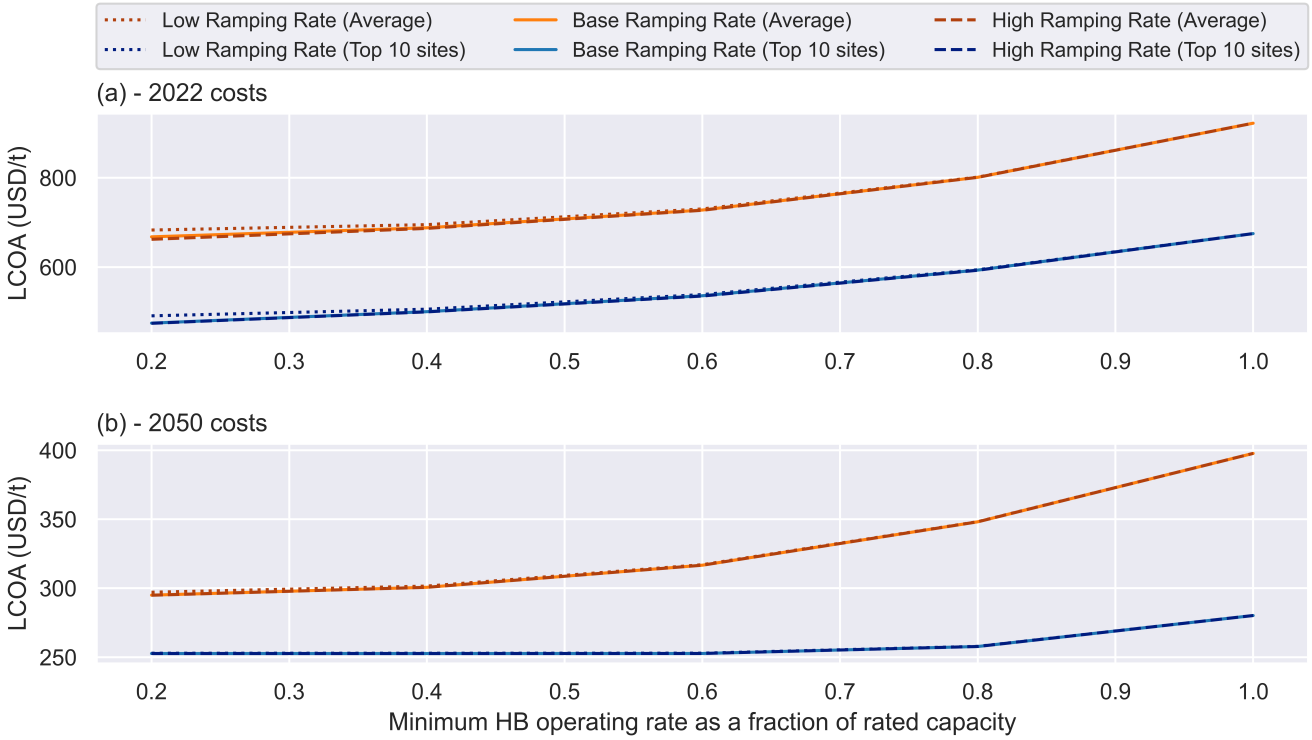

Fig. 4.1 Plot of relationship between Haber Bosch minimum operating rate (HB MOR) and LCOA-P for 2022 (**top**) and 2050 (**bottom**), for the average site (**orange**) and the top ten performing sites (**blue**). In general, a lower HB MOR translates into a lower LCOA-P, although this effect is only pronounced at MORs between 0.6 and 1; the effect is small at MORs less than 0.5. The effect is also smaller in 2050 than in the present day.

The most important observation in the figure is that there are diminishing marginal returns on increasing plant flexibility. In both 2022 and 2050, reducing the HB MOR from 60% to 20% achieves only one quarter of the cost reduction of reducing the HB MOR from 100% to 60% (for the average cases). For the cheapest sites in 2050, the

results are even more stark, with almost no benefit gained whatsoever from reducing the HB MOR below 60% of rated capacity.

This is predominantly because the ammonia plant represents a significant capital expense, but its power draw is comparatively small. That means that the plant, for most of the year, receives relatively little benefit from turning down the ammonia plant to very low operating rates, since it can sustain operation using the battery and hydrogen storage units (and it is preferable to exploit the capital expense of that equipment to the greatest load factor possible). This may cause the state of charge in the batteries and hydrogen storage to cycle more (compared to a case in which the HB operating rate could be turned down further), but does not significantly increase their size. Therefore the increase in costs is fairly small, as there is no limit on cycling imposed in this section. The effect is even more pronounced in 2050, because solar electricity and battery storage are expected to fall in price so significantly, whereas the CAPEX of the ammonia plant is likely to remain fairly steady.

The overall process can operate the HB plant at high rates for most of the year by cycling the battery and hydrogen storage; this only becomes challenging during the deepest dunkelflaute. The model sustains the HB MOR through this period either by: (i) turning down the HB plant, (ii) increasing the size of energy storage equipment, or (iii) increasing the extent to which the renewable power generation is oversized. The results indicate that the benefits which accrue from using the lever of ammonia plant capacity tail off below 60% of the rated capacity, and that the model can adopt other strategies without significantly increasing cost.

Although there is some benefit to increasing plant flexibility, it is not as large as potential other sources of improvement to the plant. Firstly, site selection is evidently of great importance; in both 2022 and 2050, a completely inflexible site in the top 10 locations is roughly equivalent in performance to a highly flexible site in an average location. Secondly, potential improvements in equipment performance are bigger drivers of cost reduction than plant flexibility. In 2022, the site with the largest improvement in ammonia cost with plant flexibility is in the order of 30%, but this falls to around 10% for the high quality sites in 2050. In contrast, equipment improvements unlock price reductions in the order of 50%. This suggests that, as long as Haber-Bosch production is partially flexible (down to a level of say, 60%), additional capital investment in more expensive but more flexible technologies (e.g. electrochemical ammonia synthesis) may not be justified.

A final relevant observation is that the impact of ramping rate on plant costs is small. In the low ramping cases, the plant ramps down at 2%/hour, and up at just 0.5%/hour; despite this quite significant constraint, the impact on plant performance is around 15 USD/t on average in 2022, and less in 2050, and only impacts results meaningfully when the plant has an MOR close to 0.2.

4.2.4.2 Impact of HB minimum operating rate with cycling constraints

Figure 4.2 shows the relationship between the LCOA-P and the plant flexibility when different penalties on cycling are imposed. As for the previous section, costs are shown at both the average sites and the top 10 sites.

The most important observation in Figure 4.2 is that cycling limitations are not likely to have large impacts

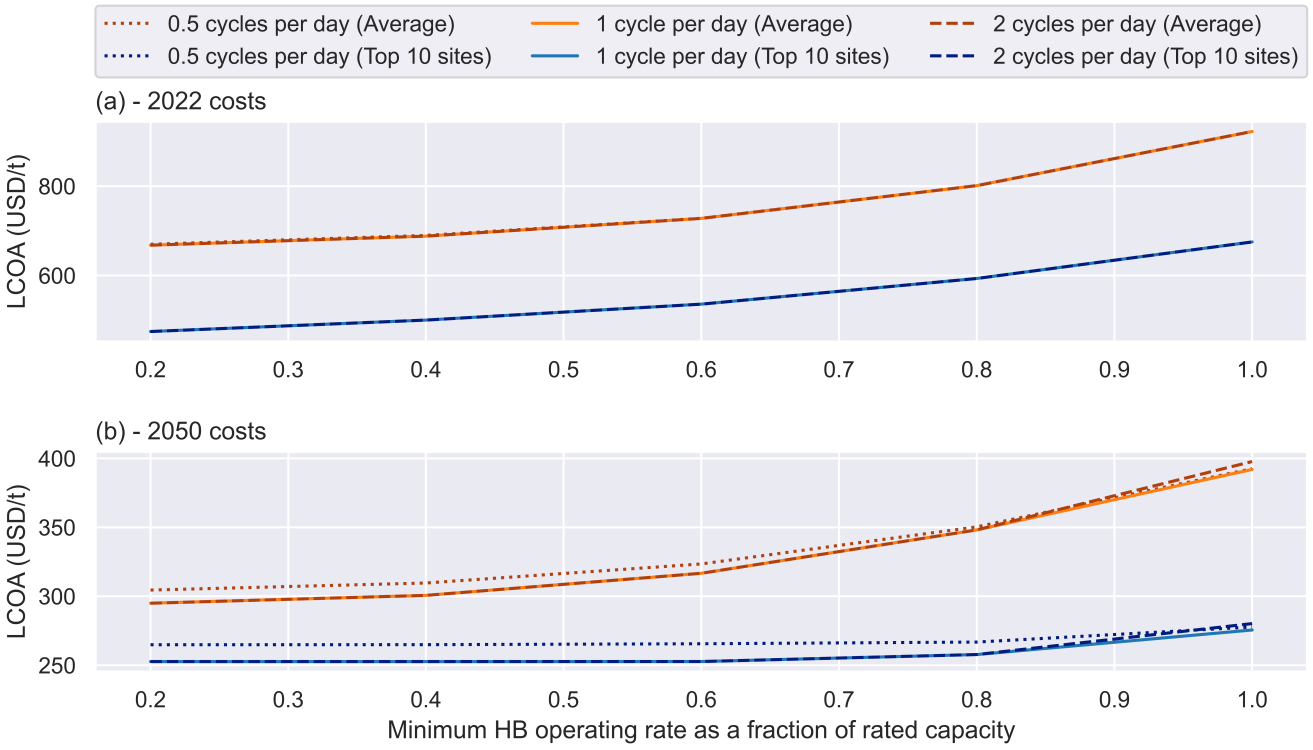

Fig. 4.2 Plot of relationship between Haber-Bosch minimum operating rate and the LCOA-P, including penalties on cycling, for 2022 (**top**) and 2050 (**bottom**). Different line styles show the impact of different battery cycle limits. The impact of battery cycling on LCOA-P is very small; impacts are only meaningful in 2050 for very tight (less than 1/2 a cycle per day) limits on battery utilisation

on the performance of ammonia plants at any degree of flexibility. The constraint has no impact on the LCOA-P when one or more cycles per day is allowed, which is well within the plausible operation of normal energy storage equipment. Even when only half a cycle per day is allowed, the impact on the LCOA-P is fairly minor (i.e. $< 5\%$).

The impacts in 2022 are particularly small because back-up power in 2022 is dominated by fuel cells. The LP model predicts that fuel cells are preferable in the short term because, compared to batteries, fuel cells connected to hydrogen storage have high power costs but relatively low stored energy costs (i.e. each additional MW of back-up power from a fuel-cell costs more than each additional MW from a battery, but each additional MWh of hydrogen storage is cheaper than each additional MWh of battery storage). Note that these results are different from Chapter 3, because the available forecasts for fuel cell costs for Australia in that chapter were very high; most estimates, including those used in this chapter, are significantly lower. Because the power demand of the HB plant at its MOR is a small fraction of the total power supplied around the plant, typically it is more costly to meet the energy storage requirements than the back-up power requirements, so the model opts for a fuel cell. Energy for the cases in 2022 therefore comes from cycling hydrogen storage, rather than batteries; this hydrogen storage typically stores enough energy for several days worth of production at the HB MOR, so it rarely needs to cycle quickly. In 2050, fuel cells are used less widely because the cost forecasting indicates that energy storage in batteries will become substantially cheaper.

The cycling limitations tend to impact the HB plants which are *more* flexible, which is somewhat surprising, since cycling of the ammonia plant should reduce the need to cycle energy storage equipment. There are two factors which are responsible for this result; they are summarised in Figure 4.3.

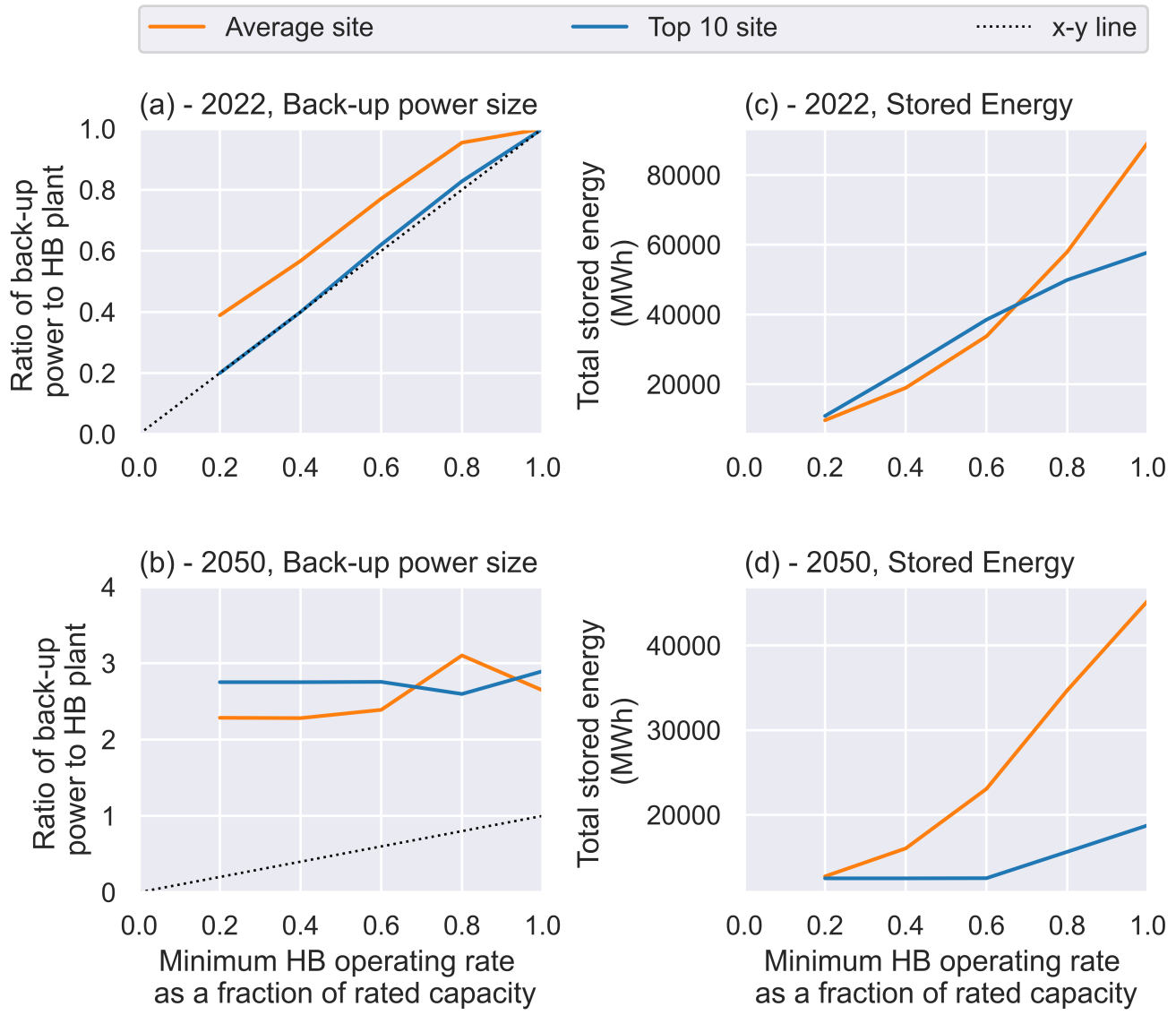

Fig. 4.3 Plot of relationship between HB minimum operating rate and back-up system size. **(a)** and **(b) - Left**: Rated capacity of back-up power in MW, scaled by the size of the HB plant. **(c)** and **(d) - Right**: Total energy storage capacity of the battery and hydrogen plant in MWh (the mass of hydrogen stored is converted to energy using its HHV). Data are shown for 2022 (**Top**) and 2050 (**Bottom**); in 2022, the back-up power is very similar in size to the minimum power requirement of the HB plant, whereas in 2050, the back-up power is much larger than the minimum power requirement of the HB plant, indicating it is used for other purposes (e.g. increasing the load factor of the electrolyser).

The first factor causing increased cycling of the battery in flexible plants in 2050 is a change in operating strategy over time. In 2022, the energy storage equipment is rated only to sustain operation of the HB plant; in the case of the top 10 sites, the back-up power capacity is almost the same as the power draw of the HB plant at its minimum rate (i.e. in panel (a), the top-ten sites sit exactly on the x-y line). At the average sites, the total back-up power

is slightly larger than the MOR. This is caused by the inability of the HB plant to ramp down sufficiently quickly, meaning back-up power needs sometimes to be larger than the MOR.

By contrast, the back-up power in 2050 is significantly larger than the whole HB plant. Clearly, the role of back-up power in these plants is more than solely operating the HB plant during periods of low VRE output (if it were, the back-up power capacity would never exceed the power demand of the HB plant); it is partially to power the electrolyser. When the batteries are powering the electrolyser as well as the HB plant, they will tend to charge and discharge more frequently to maximise the amount of hydrogen produced and are therefore more affected by cycling constraints. This change in behaviour is driven by the rapid fall in the cost of batteries.

Prices of solar panels will also fall, which will drive ammonia production towards solar PV rather than wind. In a solar-driven system, the value of powering the electrolyser from the batteries is higher, since it otherwise sits unused during the night; in high quality wind sites, which will typically have a higher load factor, the electrolyser will be used more consistently. Again, this will drive increased cycling of batteries.

The second factor causing increased cycling of storage equipment in flexible plants in 2050 is simply that the storage equipment is smaller (see panel (d)). The total energy passing through the storage equipment is much higher in inflexible plants, but these plants have installed so much storage that the number of cycles remains relatively low.

4.3 MPC Approach

The final section of Chapter 3 considered the role of changing the design year of weather data input to the LP model at a given location [177, 178], describing how operation changed as plant design was adjusted. This section extends that research by including imperfect forecasting.

There have been relatively few studies into the operation of green ammonia plants with a fixed design and finite forecasting information. Verleysen et al. [179] considered the role of uncertainty in changing design, although this work applied an uncertainty to wind inputs to determine a relationship between plant oversizing and robustness. Kelley et al.[180] examined the role of ammonia plants in providing a demand response service, looking at process chemistry to determine if a grid-connected plant could ramp down quickly in response to high prices, although this was not focussed on using weather forecast information. Allman and Daoutidis [181] adopted a rolling optimisation forecast to determine the operating state of their plant - this is similar to the MPC approach described here. However, they considered a grid-connected plant, which is simpler to operate since the inventories in the batteries and hydrogen storage do not need to be so carefully managed to account for dunkelflaute.

Research into imperfect forecasting is better developed in the power-to-hydrogen space, although the control problem in that context is simpler since the largest complexity in ammonia production is the inflexibility of the HB process. In power-to-hydrogen applications, Model Predictive Controllers (MPCs) have been widely discussed as a possible approach to optimising plant operation given limited forecast information, and the same technique

is adopted here [182]. MPCs have been widely adopted for the operation of chemical processes globally, and are considered a useful tool for handling problems pertaining to variable operability [183].

4.3.1 MPC Method

MPCs rely on an internal model to predict the behaviour of the plant as determined by plant operating decisions over a specified time horizon. At each time step, the MPC optimises the operation of the plant according to an objective function, and subject to constraints on the controlled variables and the state of the plant. The plant takes the first step along the optimum path it has determined, and then re-evaluates a new optimum path as new information becomes available. Here, the external disturbance is the varying weather pattern, and the time horizon in the model is considered to be equivalent to the forecast duration.

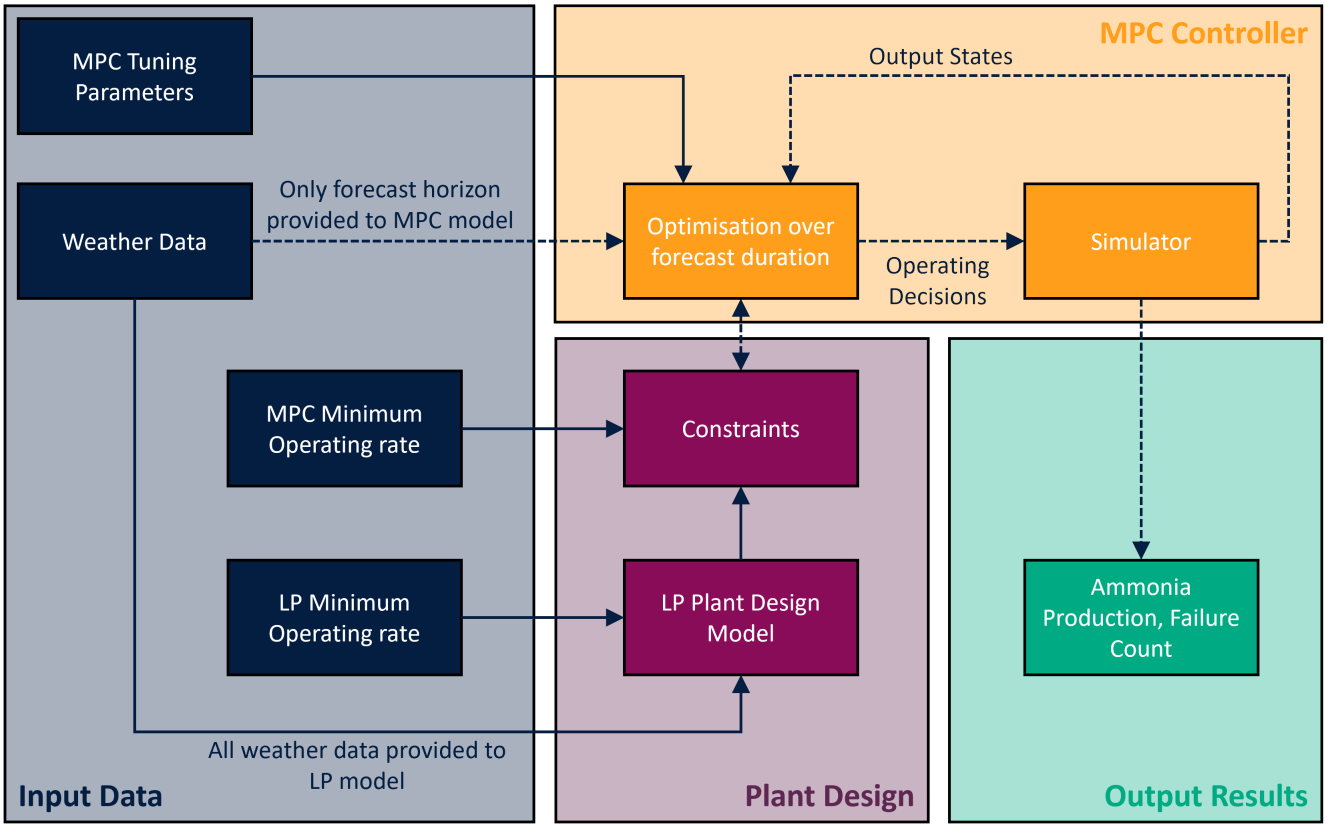

Fig. 4.4 A flowchart showing the relationship of the MPC and LP models, and how they import data. Solid lines represent information that flows before the MPC solution commences. Dotted lines represent information that flows at each time step. Input weather data is used in the LP model to determine a suitable plant design, subject to a design value of the Haber-Bosch Minimum operating rate (HB MOR). The MPC controller then operates the plant. It uses a different value for the HB MOR (which enables more flexible operation); however, it only receives a limited horizon of weather data. MPC tuning parameters determine the relative weight applied to the model maximising ammonia production or managing the inventory of intermediate stored energy.

Figure 4.4 explains the operation of the MPC model in this context. A year of weather data is used to determine an optimum design of the plant at a given location using the LP. The plant design creates the constraints on the

MPC model, by setting the upper and lower bounds on the amount of power which can be sent to the various plant components. Again, the most important constraint is the HB MOR, which is not necessarily the same between the design (LP) and operating (MPC) modes, depending on the extent to which the plant has been overdesigned, for which the approach here is the same as the end of Chapter 3 (see Section 3.3.5.1). Where the LP model is provided with a full year of weather data, the MPC is only provided with the next n hours at each time step, where n is the forecast horizon and takes values of 12, 24 and 48 in this analysis. At each time step, the optimiser determines the best operating rate of each piece of equipment (as defined by the objective function, see Section 4.3.2) which in turn determines the ammonia production. The plant state is then sent back to the optimiser, as it interacts with the constraints and the new weather pattern that emerges in the next time step. In general in this analysis, the same year of weather data is used for the LP and MPC models so the results can be directly compared; however, in Section 4.3.3.4 the impacts of using a weather dataset which spans a much greater time period for the MPC model than was provided to the LP model are considered.

In order to robustly consider the performance of the MPC, three sites were chosen from the >400 considered in the design cases. The three sites selected were chosen to offer a range of renewable profiles - one site is located in Algeria, and has excellent solar insolation; another in the United Kingdom is dominated by wind; a third in Morocco uses a hybrid of both. In general, the results displayed in this section on operation relate to production in 2022, when back-up energy is largely supplied by fuel cells; the appendix section B includes equivalent figures for 2050, which demonstrates the applicability of the MPC method to batteries.

4.3.2 MPC implementation

The MPC is implemented using the python module Do-MPC [184], which modularises the process of building an MPC into a series of simple processes. The first process is constructing a model of plant operation, including state variables, model inputs and rate equations. Four state variables are considered: (i) the amount of hydrogen stored (x_H); (ii) the amount of power stored in the battery (x_B); (iii) the amount of ammonia produced in a given time step (x_A); and (iv) the amount of electricity curtailed in a given time step (x_C). These are dictated by the total renewable energy available to the plant at a given time (α) as well as five decision variables, which are controlled by the MPC: (i) the power to the electrolyser (π_E); (ii) the power to the HB plant (π_{HB}); (iii) the power to the battery (β_{In}); (iv) the power from the battery (β_{Out}); and (v) the power generated by the fuel cell (γ). A list of symbols used for the model is provided in Appendix Section B, and is generally consistent with Chapter 3, although all states of the system here use x.

The inputs and disturbances are related to the states according to:

$$x_H(t) = x_H(t-1) + \pi_E(t) \cdot \eta_E - \gamma \cdot \eta_{FC} - \frac{3}{17}\pi_{HB}(t) \cdot \eta_{HB} \tag{4.4}$$

$$x_B(t) = [1 - \varepsilon_B] \cdot x_B(t-1) + \eta_B \cdot \beta_{In}(t) - \beta_{Out}(t) \tag{4.5}$$

$$x_A(t) = \pi_{HB}(t) \cdot \eta_{HB} \tag{4.6}$$

$$x_C(t) = \alpha(t) + \gamma(t) + \beta_{Out}(t) - \pi_E(t) - \pi_{HB}(t) - \beta_{In}(t) \tag{4.7}$$

Equations (4.4) and (4.5) are simple balance equations over the hydrogen storage and the battery storage respectively (equivalent to Equations (3.12) and (3.11) respectively). η_E and η_B are the efficiencies of the electrolyser and battery, respectively; the same values are used in the MPC case as were used for the LP design model. In the case of the hydrogen, the state of the storage unit is given by the storage from the previous time step, plus any inflows from electrolyser production, minus outflows to the fuel cell or to the HB plant. The outflows to the HB plant are determined from the power consumption (converted into tons of ammonia using the efficiency, and then into tons of hydrogen using the reaction stoichiometry). The battery equation is the same in principle, except a self-discharge factor ε_B is included to represent the gradual reduction in battery charge over time. For the battery, the energy losses are imposed on the charging power as it enters the storage unit. Equations (4.6) and (4.7) are simple instantaneous balances over ammonia production and power respectively.

This model construction provides enough information for the plant to predict future behaviour. The MPC then needs to be provided with direction under an objective function and constraints to determine the operating process.

The objective function is given by:

$$P = \sum_{t=1}^{n-1} \left[x_A(t) - k_R \cdot [x_A(t) - x_A(t-1)]^2 \right] + x_A(n) + k_H \cdot x_H(n) + k_B \cdot x_B(n) \tag{4.8}$$

The goal of the MPC is to maximise P, the objective variable. This broadly corresponds to maximising the total amount of ammonia produced over the time horizon n, which is given by the first term inside the summation, and the first term outside the summation.

Three penalties need then to be imposed upon the optimisation model to ensure it acts as intended. The first is a penalty on ramping the ammonia plant, given by the quadratic term inside the summation, which is scaled by the tuning parameter k_R. Without this term, the HB plant will change its operating rate significantly in each step; as k_R grows, the rate of change of the HB plant is increasingly penalised. Because this penalty is quadratic, the model will prioritise slow ramping over sudden large steps, which is reflective of the slow ramping needed by the HB synloop. The second and third penalties are for depleting the storage inventories, which is represented by the final two terms, scaled by the tuning parameters k_H (for hydrogen storage) and k_B (for battery storage). In the absence of these terms, the model will attempt to maximise the ammonia produced at the expense of the storage

inventories, which it will often plan to drain over the time horizon (since the low production or plant failure in the subsequent time horizon does not impact the optimisation). The parameters k_H and k_B are tuned depending on operator risk tolerance; as they grow, the plant is less likely to fail, because it will prioritise keeping the storage inventories full; however, doing so comes at the cost of ammonia production. To simplify the sensitivity modelling, the value of k_H and k_B are set to be equal for this analysis, but specific tuning should be done on a site-by-site basis.

The MPC is constrained in the same way as the LP model. In general, states and inputs are constrained to be greater than 0, and less than the capacity of the equipment in the plant, as determined by the LP. The additional constraint is on the Haber-Bosch plant, which must maintain its MOR as described in Section 4.2. The explicit constraint on plant ramping from the LP is removed; this is achieved by the ramping parameter k_R described in the previous paragraph.

4.3.3 MPC model results

The MPC was run in several configurations in order to understand how the MPC implementation affects the results, and the extent to which the MPC is effective for operating the plant. There are four sets of results: (i) an hourly comparison of the LP to the MPC; (ii) a sensitivity analysis on the impacts of the tuning parameters; (iii) an assessment of the actual LCOA-P from an operating plant compared to the optimally designed plant; and (iv) a long-term comparison to determine whether it is possible for the MPC to operate the plant in unfamiliar weather conditions without sacrificing excessive production.

4.3.3.1 Hourly result comparison

Figure 4.5 compares plant operation under an LP and an MPC scenario. For this configuration, the plant design was selected by the LP with a HB MOR of 0.4; the MPC model then tested the operation of such a plant using a HB MOR of 0.2. The horizon is 24 hours, and the tuning and ramping parameters are both set to 0.1. The influence of these parameters is discussed in the following section; these specific values were selected because at this location under these design conditions, it causes the LP and MPC models to follow a broadly similar trace (which would be the target for the tuning of the MPC).

The most important result in this figure is that it demonstrates that a green ammonia plant can be operated using limited forecast information without exceeding the limits of the HB plant, provided the plant is adequately overdesigned. It is the first demonstration of this point for a HB plant that is not reliant on electricity grids.

There are a number of key differences between the LP results and the MPC results. Firstly, the MPC controller tends to store more hydrogen than the LP optimiser. This is partially because the overdesigned plant operated by the MPC has more hydrogen storage available than the LP plant; however, it is also encouraged to keep the storage full by the tuning parameter in the MPC optimisation function. The LP is only maximising ammonia production and is unconcerned by the storage inventory; for that reason, it more frequently allows the storage inventory to drop to 0, since it has enough forecast information to be confident that the hydrogen storage can be refilled.

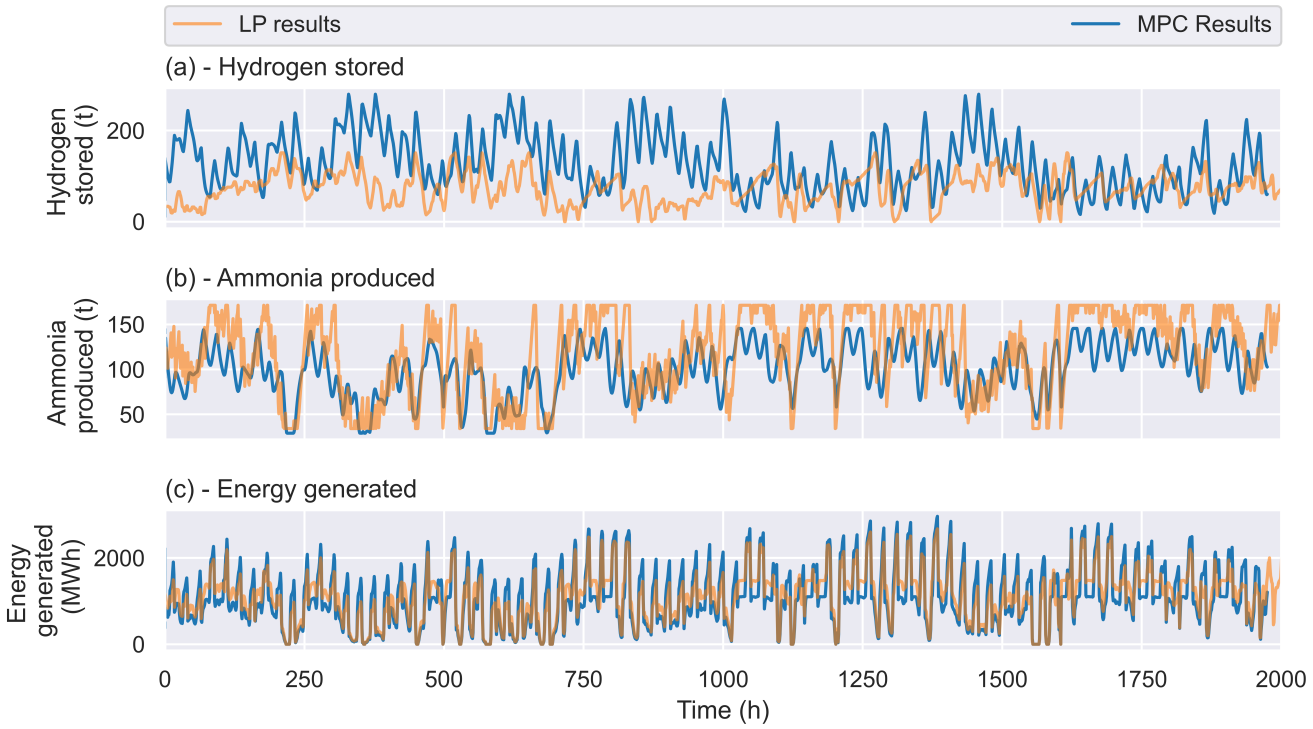

Fig. 4.5 Comparison of hourly plant behaviour in the operating mode, run by the MPC controller (**blue**), and the design mode optimised by the LP (**orange**) for a hybrid site containing both wind and solar in 2022. The MPC time horizon is 24 hours, both tuning parameters are set to a value of 0.1, and the plant has been overdesigned using a Haber-Bosch minimum operating rate of 0.4 (compared to 0.2 for the MPC). **(a) - Top**: compressed hydrogen in storage (A failure would be indicated by the storage level dropping below 0). Typically the tuning parameter which punishes low storage inventories keeps hydrogen stored by the MPC above hydrogen stored by the LP. **(b) - Middle**: ammonia produced in a given hour; note that due to the ramping parameter, the MPC makes fewer adjustments on an hourly basis than the LP. **(c) - Bottom**: total energy generated from all available renewable resources. Examples for the other two sites are provided in Appendix Section B.

Secondly, the LP model shows far more short-term variability in HB operation, which is most visible on panel (b). The LP model is constrained in how quickly it can ramp the operation of the HB plant (up at 5% of rated capacity/hour, down at 20% of rated capacity/hour). However, there are no limitations on how frequently it adjusts the HB rate of operation, so it makes changes almost at every time step. On the other hand, the MPC is not directly constrained to limit how quickly it can ramp the ammonia plant, but there is a general penalty for rapid ramping imposed upon the objective function. It therefore only changes operating rate if strictly necessary, and this results in 'smoother' operation, although it may sometimes surpass the ramping limits imposed on the LP. Less frequent cycling of the HB plant conditions reduces the risk of catalyst damage and is therefore likely to be advantageous, although some production may be sacrificed.

4.3.3.2 MPC Sensitivity

The previous section showed the results of the MPC over a short period of time in order to give an indication of how the MPC operates the plant compared to the LP. This section considers an entire year of data, and investigates the role of the MPC parameters on the annual ammonia production. Figure 4.6 demonstrates the results of changing

the forecast horizon, and the tuning and ramping parameters, on the probability of a plant failure. Parameter values are summarised in Table 4.1.

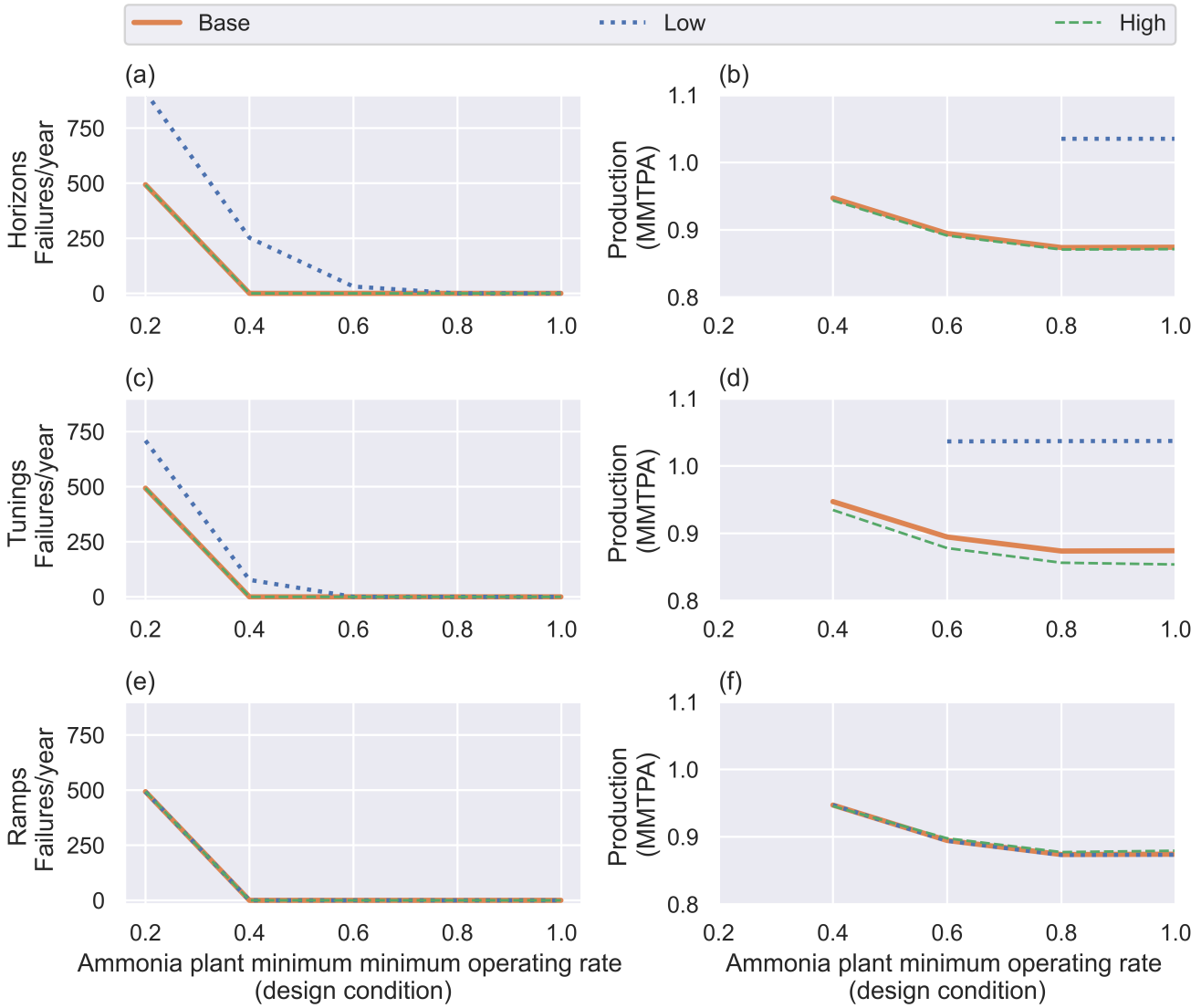

Fig. 4.6 Sensitivity analysis on MPC tuning parameters for a wind dominated site. Plots of the failure frequency (**left**) and ammonia production (**right**) for a wind-dominated site in 2022. Different plots show the impact of varying different MPC parameters: forecast horizon (**top**), tuning parameters (**middle**) and ramping penalty (**bottom**). Each plot shows the impact of changing overdesign - in each case, the plant was operated with a minimum HB rate of 20% of rated capacity, but was designed with tighter constraints. Where the plant failed during operation, the design was considered untenable, and the associated production is excluded from the plots on the right. Examples for the hybrid and solar-only sites are provided in Appendix Section B

Firstly, the figure demonstrates that, at this location, some plant oversizing is required in order to prevent plant failures. A 'failure' occurs when, given the forecast weather conditions, the model cannot keep all the state variables within their target bounds (i.e. a storage inventory falls below 0, the HB plant operates below its allowable MOR, or the plant curtails a negative amount of electricity). Given the relatively short time-frame of the input data used

Table 4.1 Parameters used for sensitivity testing of the MPC.

Parameter	Low	Base	High	Units
Horizon	12	24	48	Hours
Tuning	0.1	0.5	1	-
Ramp	0.05	0.1	0.5	-

in this example (one year), even a single failure would represent a plant which is inadequately robust to weather variation. The need for oversizing differs between sites - at the wind dominated site, with no oversizing, there are hundreds of failures per year; this number falls to around 2 for the hybrid site (in 2022), and the solar-dominated site can operate without any oversizing (as can the hybrid site in 2050) - this result is discussed further in Section 4.3.3.3.

The amount of oversizing needed falls as the forecast horizon increases - see panel (a) - although increasing the length of the horizon would stretch the capacity of weather forecasters to make plausible predictions. With only 12 hours of forecasting, the number of failures is large because the system cannot adequately manage the storage inventory. Notably, however, if the plant can operate without failures using only 12 hours of forecasting, then the production rate is significantly higher - see panel (b).

Panels (c) and (d) shed light on why this occurs - when the tuning parameter is wound downwards, the effect is the same as using a shorter horizon. In other words, because the 12-hour forecast model has less information than the 24-hour version, it is more 'reckless', because it has less capacity to predict the consequences of increasing ammonia production on the storage inventory. This is only a suitable operating mode when the design is sufficiently oversized to guard against emptying the storage; however, when it is effective, it enables the plant to operate more like the LP. This emphasises the need for careful plant tuning; ideally, the plant will occupy the mode where production is maximised (and is essentially operating exactly as designed), but without tipping into a failure.

Interestingly, production tends to decline as oversizing increases. This is an artefact of the tuning parameter and the overdesign method. As oversizing increases, the most significant changes to the plant design are to the hydrogen storage and battery capacities. The tuning penalty term is given by the product of the tuning parameter and the storage inventory; since the maximum value of the storage inventory has increased, the value of the penalty term also increases, and it therefore has more impact relative to the ammonia production terms. Maximising ammonia production is therefore weighted less heavily by the objective function. The exception is the site designed to be able to operate completely inflexibly. When the LP is solved for this mode, it oversizes components of the plant other than the storage, which means the impact of the tuning penalty rebalances slightly in the other direction.

The role of the ramping parameter is less significant - within the range considered here, it does not affect the likelihood of plant failures, and it has a relatively small impact on overall production. This parameter therefore needs to be set such that the ammonia plant ramps at an adequate rate, ideally by introducing a cost function that depends on the impact of catalyst cycling, so that the optimal balance can be struck between preventing cycling and

producing an adequate amount of ammonia.

Perhaps counter-intuitively, a higher ramping penalty (i.e. less ramping) increases the production rate. This is visible on Figure 4.6(f), although the impact is more significant on the solar-dominated site in Algeria (see Figure B.2(f)). The ramping penalty drives up production by effectively overwhelming the tuning penalty, and therefore incentivising the HB loop to stay at maximum production, even if it draws down the inventory; provided this does not lead to plant failure, it increases production.

4.3.3.3 Actual LCOA-P

As is perhaps obvious, and also clear from the right-hand plots of Figure 4.6, the plant operated with imperfect forecasting will produce less ammonia than was predicted in the design case by the LP, because it cannot manage its storage inventory as effectively.

The MPC approach enables the true LCOA-P from each plant to be estimated by scaling the design LCOA-P by a factor of ratio of the actual production to the design production. In other words, for a case in which the design LCOA is 400 USD/t and production is 1 MMTPA, then if the operating model produces only 0.8 MMTPA then the 'actual' LCOA-P would be 500 USD/t. For this section, oversizing was enforced by considering a design case whose MOR was 20% larger than was allowed during operation (i.e. if the LP MOR used for plant design was 60%, the MPC MOR used for plant operation was 40%). The actual production was then determined by running the MPC using an array of parameters, and selecting the case with maximum production and no failures. To enable fair comparison of the LP and MPC controllers, MPC production was downrated by a factor of $\frac{8760-2\times168}{8760-n_{horizon}}$; the discounting in the numerator relates to the two weeks of maintenance per year that are enforced on the LP, and the term in the denominator corrects for the hours at the end of the year which need to be excluded from the MPC's scope because there is inadequate forecast information. In both the MPC and the LP approaches, the discounting of production is conservatively applied to production over the whole year (rather than selecting a two week period in which production was likely to be low).

Only 24 hours of forecast were allowed, over which range renewable forecasts tend to be highly accurate, because production estimates are required for bidding into day ahead electricity markets.[185]

Figure 4.7 shows the results of this estimation approach. There are two sources of cost increase in the operating case compared to the design case: oversizing costs (shown using the dotted line, which is simply the design prediction translated to the left by a value of 0.2), and reduced production. The solid red line on the figure shows the combined impact of plant oversizing and reduced production.

For all locations, where the operating plant had very little HB flexibility (i.e. MOR > 80%), the production in the design and operating cases was very similar. Under these constraints, there are not many degrees of freedom in plant operation, so both the design and operating cases will tend to behave in a similar way.

Considering cases with more flexible HB plants and a large quantity of solar (the bottom two panels), actual production was almost equal to the design production - in other words, the MPC was able to replicate the perfor-

mance of the LP model which had perfect foresight. This is an unsurprising result for a solar dominated plant in a high-quality location; because the renewable resource cycles on a 24 hour basis, optimising with a 24-hour forecast is broadly adequate. By contrast, the wind dominated site shown in the top panel fares far worse; because periods of low or high wind production may last for significantly longer than 24 hours, the MPC will not track the LP model as accurately.

The exception to the strong performance of solar sites is the performance of the hybrid site at an HB MOR of 60%, where the MPC production is around 10% less than the LP forecast, creating a significant spike in the actual LCOA-P on the figure. For the other cases, the optimal MPC production occurred when the tuning parameter took a value of 0.1; however, when this value for the tuning parameter was used in the case where the HB MOR was 60%, 97 plant failures were observed. This is a location-specific effect, indicating that for this case, the additional 20% oversizing was inadequate to run the MPC with a loose storage penalty parameter. For that specific case, therefore, the figure shows the next best production option which used a tighter value for the tuning parameter of 0.5. This tighter parameter prevented plant failures but at the cost of reduced production. Better design of the MPC would identify a tuning parameter between 0.1 and 0.5 that may strike a superior balance between these two goals. The effect is similar to that observed on panel (b) of Figure 4.6 for the 12 hour horizon, which has excellent ammonia production but requires more oversizing.

Reducing the actual LCOA-P requires (i) the plant oversizing to be reduced as much as possible, and (ii) the production from the MPC to be equal to the LP. For the solar plants, the latter goal has already been achieved; doing the same in wind plants will require superior forecasting and improved tuning, which may require machine learning to tune appropriately on a case-by-case basis. Achieving goal (i) is more complex, and is a useful area for further research. The approach from this analysis - using a plant designed with reduced flexibility - is fairly crude; this could be improved at individual sites on a case-by-case basis by iteratively solving the design LP and the MCP in order to strike a tolerable balance between plant failure risk and meeting production goals. Additionally, less coarse steps in the HB MOR and in the MPC parameters would enable more precise tuning at a given location.

Figure 4.7 presents a more complex view on plant flexibility than that presented using only the LP results (Figure 4.1). In the case of the solar dominated plants, provided the MPC is well-tuned, the conclusions are broadly the same: there is some benefit to be gained from plant flexibility, but the majority of this benefit is associated with reducing the HB MOR to $\sim$60%, and not beyond it to a very low minimum $\sim$20%. Improving the estimate of the required plant oversizing (as discussed in the previous paragraph) would move the orange line on Figure 4.7 towards the solid blue line, weakening the relationship between flexibility and LCOA-P yet further. However, in the case of predominantly wind-dominated plants, the difficulty of long-term forecasting means HB flexibility is a more useful lever for the plant to use while it is operating, and the LCOA-P continues to fall linearly as flexibility increases.

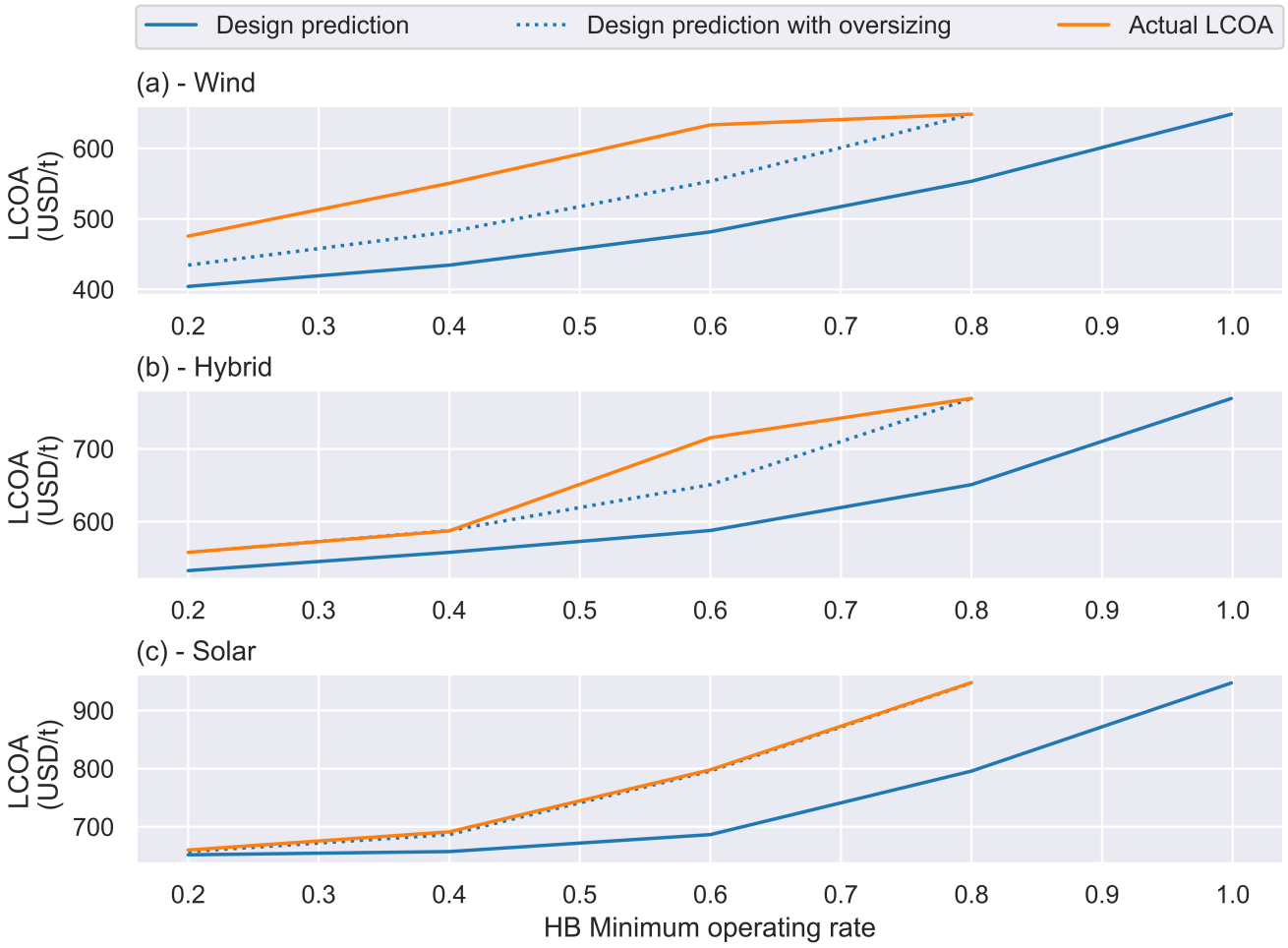

Fig. 4.7 Comparison of predicted LCOA-P from the design approach (LP) (**Blue**) and actual LCOA-P from the operating approach (MPC) (**Orange**) as a function of the Haber-Bosch Minimum Operating Rate (HB MOR). The lowest cost achievable is the design approach (**solid blue**); this has been constrained by oversizing, meaning the best cost achievable by the MPC is increased (**dotted blue**). Results are shown for 2022, for a wind-dominated site (**top**), a hybrid site (**middle**), and a solar-dominated site (**bottom**). The solar site tracks the design target very well; the hybrid site also tracks design performance well, with an exception at an MOR of 0.6 caused by imprecise tuning. The wind site performs poorly relative to both the design cases.

4.3.3.4 Long term operation

Until this point, this chapter has considered operation using weather data taken from the same year in which the plant was designed. To confirm that the parameters selected as optimum in the previous section would enable a green ammonia plant to operate robustly across longer time periods, the model was operated using 12 years of historical weather data (from the start of 2010 to the end of 2021; this period includes the design year which is 2019). Note that the historical weather data is used for both the 2022 and 2050 cases. The primary difference between the cases relates to equipment efficiency and CAPEX.

The MPC horizon is set to 24 hours, the ramping penalty is set to 0.1, and the tuning penalty is tuned based on the likelihood of failure observed in the sensitivity analysis: a tuning value of 1 for the wind site, 0.5 for the hybrid

site and 0.1 for the solar site. The plant design was selected by running the LP with an MOR of 40%; again, the MPC MOR was set to 20%.

No failures were observed across the 12 years of operation under these conditions. The results are shown in Figure 4.8. Evidently, the tuning of the MPC is best for the hybrid site, and may benefit from review in the other locations. However, in each 2022 case, production is within 10% of the design target, indicating that the MPC is robust when operated in unfamiliar weather profiles. For the 2050 cases, production is significantly less, indicating the tuning parameters are likely to be too conservative.

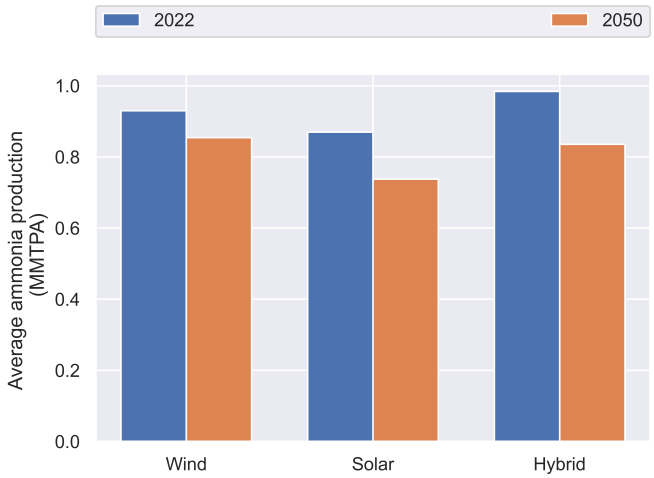

Fig. 4.8 Average annual production at three sites when operated over a long-time period, using the plant design for 2022 (**blue)** and for 2050 (**orange)**. For 2022, production is close to 1 MMTPA (i.e. the design target). For 2050, and for the solar site in 2022, the tuning parameters appear to be too conservative, since production is much lower than in the 2022 cases. There were no failures at any of the sites in either year.

4.4 Green ammonia operation summary

The general consensus in the literature is that enhanced flexibility is a prerequisite for affordable ammonia production. This chapter demonstrates that the true relationship between flexibility and green ammonia cost is more complex. While some flexibility is important, by 2050, reducing the MOR from 60% to 20% will improve the LCOA-P at the average site by less than 10%, even when constraints on storage equipment cycling are introduced; the benefits are even smaller at the best locations. It is therefore not likely that investing in more expensive technologies which enable more flexible operation (e.g. more robust catalysts or non-HB ammonia production technologies) will ultimately reduce the LCOA-P. There is significantly more to be achieved from (i) targeting reductions in equipment costs (particularly of Solar PV, which produces the cheapest ammonia in most production in the 2050 forecast), and (ii) improving the ability of operating plants to match the performance of optimally designed plants.

A technique for achieving the latter is demonstrated through an MPC model which is the first to consider how weather forecast limitations impact the operation and design of green ammonia plants: in summary, using plausible forecast horizons, sufficient plant overdesign, and careful MPC parameter tuning can manage the risk of plant

failure without sacrificing production. Production using imperfect forecasting at three locations as measured over a twelve year period was within 10% of the optimum production achievable using perfect forecasting for 2022; even better results may be achievable with more precise tuning. Only in circumstances where the VRE supply is less regular, such as a wind-dominated plant, is plant flexibility a useful lever for reducing ammonia costs. This study focussed on detailed analysis of three sites; further research should consider whether the results are consistent in other locations.

There is significant room for further research. Firstly, this approach provided very limited forecast information to the MPC (only up to a horizon at which the predictions had a high degree of confidence). Performance may be improved by including longer-term but higher uncertainty weather forecasts; the possibility of doing so should be investigated. Secondly, different approaches to plant oversizing should be considered, perhaps by iterating the LP and the MPC models to design optimal, robust plants. This research used quite coarse steps between different values of the HB minimum operating rate when determining the extent to which the plant should be oversized, and there may be merit to considering finer steps. Thirdly, the MPC approach should be extended to grid-connected plants, with a focus on the relationship between predictability of the grid cost and the opportunities posed by sector coupling. When a grid connection is used, plant flexibility may be more valuable than in the islanded case considered here, as it will enable the green ammonia plant to provide grid services. Fourthly, some of the 2050 cases produce considerably less ammonia in operating mode than targeted in design; more site-specific tuning studies should be conducted.

Chapter 5

Offshore green ammonia synthesis, and the impact of land constraints on global production capacity

The model provided in Chapter 3 enables the estimation of green ammonia costs given the weather data available at a given location; Chapter 4 validated that the model still provides reasonable results with imperfect forecasting.

However, the raw costs of green ammonia are not, on their own, a sufficient input into the global ammonia supply chain model whose development is the goal of this thesis. There needs to be some constraint on ammonia production capacity at a given location; otherwise the supply chain model will tend to import implausibly large volumes from single sites which can deliver very cheap ammonia. The literature review in Chapter 2 considered various constraints on green ammonia, and identified land as a potential constraint. This chapter estimates the land area which could be used for hypothetical production sites around the world; doing so allows the development of a global heat map of ammonia costs with high spatial granularity, including an estimate of the production capacity associated with each location.

Estimates of land constraints are not only useful in the context of the supply chain models used in later chapters; they are also applied in this chapter to provide an assessment of the potential value of offshore green ammonia production. This chapter starts by describing the potential drivers of offshore production (beyond land constraints), and its technical feasibility; the land constraints are then introduced to perform more rigorous technoeconomic modelling.

Assessment of offshore floating wind turbine costs is challenging and highly speculative. For that reason, sensible results cannot be derived from the cost forecasting model used in the previous (or subsequent) chapters for cost estimation in 2050. Instead, this chapter focusses on results for 2022; the implications of likely changes to the

relative costs of equipment on the results are considered, but not calculated in detail.

5.1 Rationale for offshore green ammonia production

The gas crisis caused by the war in Ukraine adds a layer of complexity to the challenge of decarbonisation: new energy systems must be not only cheap and reliable, but also secure in the face of global conflict. This is in stark contrast to the energy systems of many developed nations in Western Europe, which rely on energy imports from global hubs in the Middle East and Russia. Even net energy exporters like the US[186] and Australia[187] rely on imports of liquid fuels to meet demand in specific sectors, such as transport. As described in previous chapters, ammonia is well-placed to substitute demand for liquid fuels.

However, as described in chapter 2, production of green ammonia requires vast quantities of renewable energy, and therefore land. In more densely populated countries, green hydrogen and ammonia production must compete with both existing land use (predominantly for agriculture, but also for industry, urban areas, and protection of natural environments – see Figure C.3 to understand these constraints in Europe), and with new renewable energy deployment which will be required for domestic electricity consumption [188]. Beyond these practical constraints, political limitations on land use are considerable: in the UK, planning limitations for onshore wind were tightened in 2014, which has prevented any further development of onshore wind in the UK. Similar restrictions on construction near urban areas are less onerous in other countries, but may still seriously limit the total energy output available in areas with high potential for energy generation by wind [189].

Because of these land limitations, offshore wind development is expanding rapidly, although even offshore, easily accessible areas are filled quickly, and sites further from the coastline must be considered. In Scotland, this shortage of near-shore resources has led to the deployment of the first floating wind turbines [190], which can be used in water with depths greater than 100 m. However, as the distance from the shore increases, so does cost. For example, cabling of electricity to the shore typically represents between 15-20% of total project capital costs. Moreover, the longer these cables become, the higher the transmission energy losses [191]. Where energy produced from ammonia could be dispatched on-demand, energy delivered through electrical transmission is intermittent.

Considering all of these factors, there is a clear solution that has received little research attention: production of green ammonia on the ocean (Figure 5.1, adapted from Ottinger et al.[192]). Electricity which does not require storage (for instance to power the domestic grid) should be prioritised in onshore and near-shore renewable energy generation, where transmission costs are low. In contrast, energy which requires stockpiling (such as fuel for industrial processes which operate continuously, and seasonal energy balancing) should be produced further offshore. Compared to electricity transmission, transporting green ammonia in ships is cheap owing to its high energy density, and the energy losses associated with shipping are small.

Although there are inefficiencies inherent to ammonia production both on- and offshore, these cannot be avoided by an energy system that needs chemical energy storage. Meanwhile, once the sources of renewable power for an

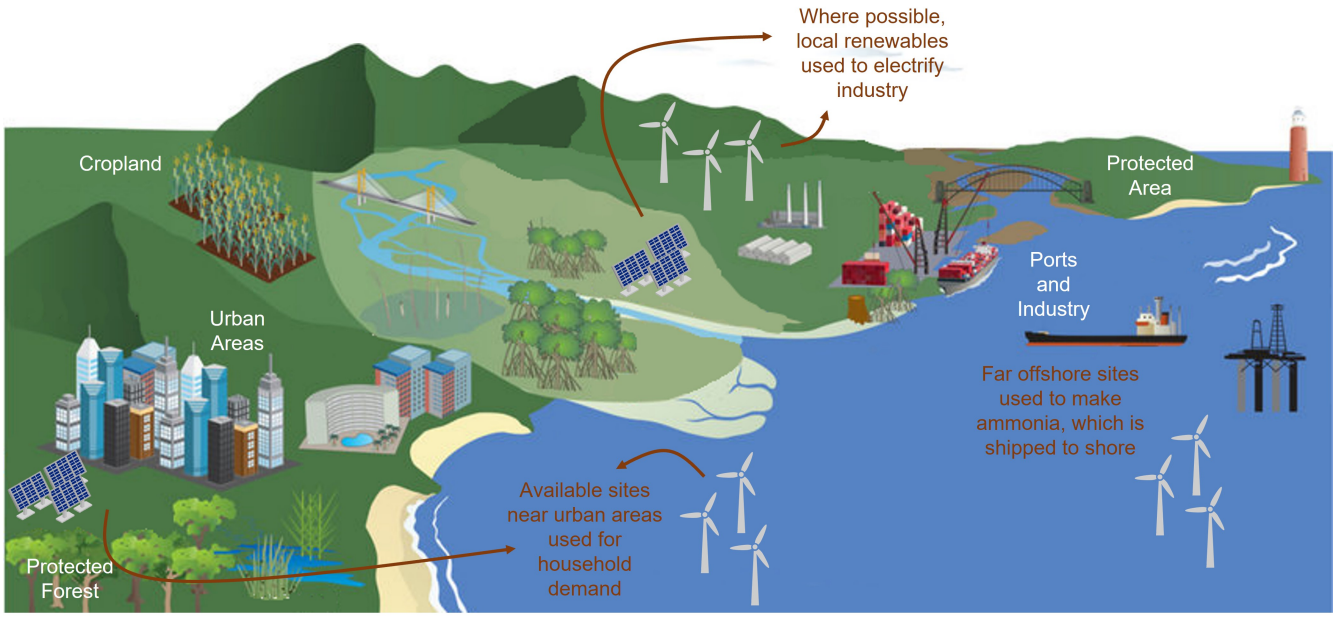

Fig. 5.1 Concept for an energy system including offshore ammonia production. Onshore land has a range of competing existing uses, meaning only a portion can be dedicated to renewable energy. The figure shows local renewable energy resources (which are finite) being used for decarbonisation of the national grid and industry which can be electrified. Meanwhile, ammonia is produced far offshore for the fertilizer industry, to use as a maritime fuel, and for industry which cannot be easily electrified.

energy system have been determined, the system-wide efficiency is maximized when electricity transport distances are minimized; by contrast, system-wide efficiencies do not depend strongly on ammonia transport distances.

The end-to-end efficiency of hydrogen or ammonia fuel in comparison to direct electrification is low in applications where the options are directly substitutable (for instance in light commuter vehicles)[193]. That inefficiency is compounded when the hydrogen is converted to ammonia, because the reaction is exothermic and it may not be possible to capture the heat released. Where land is constrained, overall efficiency is an important consideration in decision making because the total amount of renewable energy which can be produced is limited. However, by expanding ammonia production into oceans, site area constraints are relaxed considerably and efficiency is significant only insofar as it relates to project costs (since energy production potential will far exceed demand). The total global ocean area is almost triple the total land area, and competition from other applications is likely to be negligible in the deep ocean[58].

This chapter assesses the system-wide implications of green ammonia production on the ocean. Although this includes a technoeconomic analysis, it is not solely technoeconomics which can drive offshore production: in a context in which the possibility of generating renewable energy is constrained by land availability, large-scale ammonia production will be required for a range of applications, and energy security considerations encourage local production of renewable fuels, then the most sensible allocation of resources may require production of ammonia on the ocean.

For instance, in a context in which (for energy system security) a decision has been made to invest in an

offshore wind farm, using the energy from that farm to make ammonia rather than transmitting electricity will be profitable at large distances from population centres. Cost estimates described in the next chapter indicate that the transport cost of ammonia (which is largely the cost of fuel and the chartering of the ship) is in the order of 5 x 10^{-7} USD/kWh/km. Meanwhile, adapting the results for electrical transmission line costs reported by Crozier and Baker[194], and conservatively assuming full load operation for 25 years at a discount rate of 7%, the transport cost for high voltage direct current electricity is in the order of 8 x 10^{-6} USD/kWh/km; i.e. more than an order of magnitude higher than ammonia transport costs (there will also be costs which are independent of distance such as ports and mooring for ammonia transport ships, and substations, inverters and transformers for electricity transmission, but these are comparable in both instances). In other words, where chemical fuels are needed for energy security, it is best to pair production with the resources furthest from population centres, avoiding the need for expensive interconnection.

To that end, several projects are emerging which will produce green hydrogen and ammonia using an offshore resource: Yara and Ørsted will produce ammonia onshore in Norway using offshore wind [195]; Siemens is developing a wind turbine which integrates a floating water electrolyser [196]; the PosHyDon project will install a small water electrolyser on an existing oil and gas platform powered by offshore wind [197]. In the longer term, consortia in the Netherlands and Germany have both announced intentions to produce green hydrogen in the GW scale using offshore wind by 2030; some of the P2G infrastructure will be on land, but the German group has explicitly stated an intention to produce 290 MW of hydrogen on an offshore platform by 2028 [198]. The Thang Long offshore wind farm in Vietnam is investigating the construction of an offshore mounted structure from which electricity, hydrogen, ammonia could be exported [199].

5.2 Technical requirements for offshore synthesis

The concept of hydrogen and ammonia production from renewables on the ocean is not new. As far back as the 1970s[200], the use of thermal ocean gradients as a source of power was considered. More recent approaches have shown that the cost of using floating offshore wind is gradually becoming competitive with fossil-fuel alternatives [201]. Since the only production inputs are air, power, and water, the number of raw materials required is small. This section describes the technical differences between onshore and offshore production, and how they will best be met.

5.2.1 Offshore energy and hydrogen storage

Where Chapter 3 considered the role of grid-connected green ammonia production, this is clearly not possible offshore. As discussed in detail in earlier chapters, energy storage with associated back-up power is required in the absence of a grid connection. Offshore, the impacts of storage go beyond increased equipment costs; additional storage increases total plant weight and footprint, which will be significant factors for offshore operation. Therefore, where the importance of plant flexibility was called into question for onshore production in the previous chapter,

it may have more significance offshore. This will in turn increase the benefits of technologies that can improve flexibility, like novel catalyst designs [202] and alternative synthesis processes [19].

Assuming that perfect flexibility in the plant is not possible, around 70 tons of hydrogen storage are typically required for 1,000 tons per day of ammonia production - based on the average for results presented later in this chapter (although at very good sites on the ocean, this may be significantly lower owing to the reliable sources of renewable energy offshore). The literature normally predicts that hydrogen storage will be most economically achieved using buried pipelines (assuming that geological features that are currently used for natural gas storage like salt caverns are not available, which they will not be offshore) [80]. For a 1.5 m diameter pipeline with a working pressure range of around 80 bar, around 7 km of pipeline is required for 70 tons of hydrogen storage (based on NIST data[15]), which may be cost prohibitive to construct in deep-sea marine environments. As a baseline, the cost for hydrogen storage in pipes typically ranges between 500 and 1,000 USD/kg for onshore plants[80, 177], and contributes between 0.5 and 10% of the project cost, although the proportion of cost at offshore wind sites is likely to be lower because they tend to be highly reliable. There are two possible alternatives to pipeline hydrogen storage – either storage in spherical tanks on the surface, or metal hydride storage.

If hydrogen were to be stored in spherical tanks on the surface, eight tanks of around 15 m in diameter would be required. These could also be used to assist in floating the plant, although doing so may pose complications as the storage levels (and thus the buoyancy) in the tanks fluctuate during operation. Cost estimation for tank-based storage is very difficult because they are not widely used at present. On a much smaller scale, estimates for high pressure hydrogen storage in the Toyota Mirai are around $550 USD/kg of hydrogen[203]. Although there may be cost increases associated with increases in scale, much lower pressures can be used here since the abundance of space in the ocean means larger tanks can be used.

Alternatively, complex metal or intermetallic hydrides such as sodium alanate ($NaAlH_4$) can be used to store hydrogen. Hydrogen can be adsorbed and desorbed as required, improving volumetric density at the cost of gravimetric density (hydrogen composition by weight is $\sim$2% in metal hydrides[204], and would therefore increase the weight of the plant by around 3,000 tons. This increase is significant, but not infeasible; for comparison, the deadweight tonnage of a Panamax-sized container ship is $\sim$80,000 tons[104]. In some cases, desorption can occur at relatively low temperatures ($\sim$100°C)[204] and could therefore be achieved using waste heat from the ammonia plant. Cost estimation is challenging because of the wide range of hydride prices reported, from 200 USD/kg of hydrogen [204] up to 2,000 USD/kg of hydrogen[203].

Although hydrogen tanks and metal hydrides are not simple options for hydrogen storage or particularly low cost, they are unlikely to be substantially more expensive than the buried pipeline option typically considered for onshore production. Therefore, they are not likely to contribute to a wide cost differential associated with moving offshore.

5.2.2 Incorporation of desalination

Although some onshore green ammonia production may have adequate access to fresh water, desalination is likely to be the primary source of water for most plants given the high water demands of the process. Here, four concepts for operation using sea water are described (Figure 5.2): reverse osmosis (RO) in panel (a); multi-effect distillation (MED) in panel (b); direct sea water electrolysis in panel (c), and direct evaporation in panel (d).

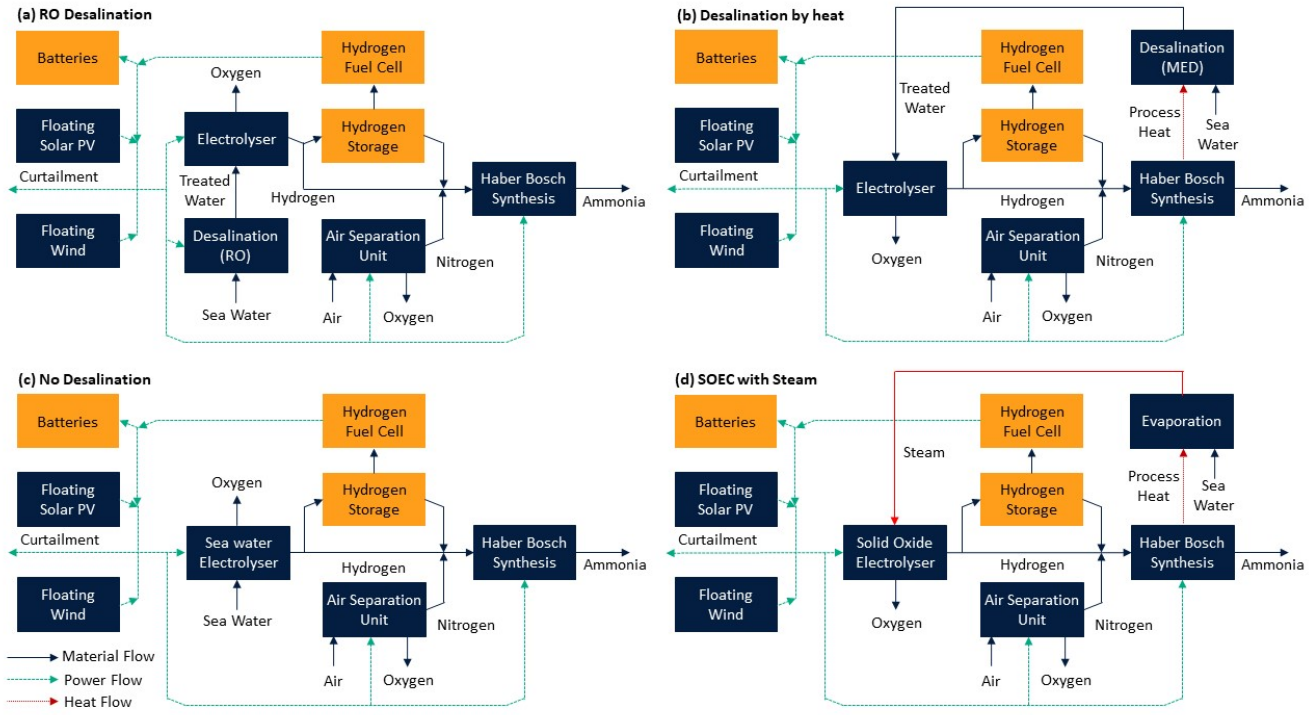

Fig. 5.2 Four synthesis concepts for offshore ammonia production. Dark blue blocks are equipment strictly required for standard operation of ammonia plants, whereas only some (but not necessarily all), of the orange blocks are required for optimum operation by providing back-up power and interim product material storage. **(a) - Top left**: A conventional concept which is also likely to be adopted onshore. It uses reverse osmosis (RO) powered by the renewables to produce fresh water from sea water. **(b) - Top right**: Process heat is used to drive a multi-effect distillation unit. This is less efficient than RO, but exploits waste heat from the Haber-Bosch process. **(c) - Bottom left**: This option dispenses with a separate desalination unit altogether, in favour of an electrolysis unit which is able to accept sea water as an input. **(d) - Bottom right**: Desalination in this option is achieved by direct evaporation of sea water. This evaporation is highly energy intensive, but the energy can be recovered using a solid oxide electrolyser cell, which operates at high temperatures and can accept steam as an input.

For onshore plants, the RO process for water desalination is the most likely to be adopted. This can be easily translated into offshore operation, in which case the only significant difference caused by moving offshore would be the presence of floating rather than fixed base renewables (Figure 5.2 a). As for onshore production, electricity is generated either from these in-situ renewables, or from back-up power supply, and is used for three purposes: hydrogen generation, powering the Haber-Bosch plant, and operating the RO plant.

As described in Chapter 2, the power demands of the RO plant are a very small fraction of the total plant demand. However, RO plants typically have high maintenance requirements – predominantly membrane replacement – and

rely upon skilled operating personnel [205], which is not suitable for far offshore operation where staffing costs are high and bringing parts for maintenance is challenging.

For that reason, there may be advantages to adopting a thermal approach to desalination offshore(Figure 5.2 b). In terms of global deployment of desalination, these are far less common than RO [206], partially because energy demands are much higher – in the order of 100 kWh of thermal energy per m^3[207] However, they rely on evaporation rather than membrane separation, so waste heat from the ammonia plant can be used in place of electrical energy from the renewables. Using this heat as a process input, rather than rejecting it to the environment, may also prevent localised increases in sea water temperature that contribute to thermal pollution and affect aquatic life[208]. The most suitable mode of thermal desalination is MED, which uses a series of evaporation stages (effects) at below atmospheric pressure with counter-current flow of desalinated water as steam to minimise heat input. MED is comparatively more flexible in operation than the more common multi-stage flash (MSF)[207], and therefore pairs better with variable ammonia production. The maximum heat available from Haber-Bosch ammonia synthesis is 2.7 GJ/ton[169], which would approximately enable the desalination of 7.5 tons of water via thermal methods (the stoichiometric water requirement is around 1.6 tons of water per ton of ammonia). Therefore, there is theoretically sufficient waste heat to desalinate all water needed by the process, although if the plant is operating at minimum rates or the plant is reliant on metal hydrides for hydrogen storage, then the overall plant heat balance may have less slack. This could be resolved by onboard storage of desalinated water. The maintenance requirements of MED are comparatively low compared to RO – they have few moving parts, can be operated with minimal operator intervention, and consume fewer chemicals, biocides and anti-scalants than other desalination technologies [209] Their footprint is sufficiently small that consuming space offshore is unlikely to pose a civil engineering challenge [210].

The third option is the adoption of direct sea water electrolysis (Figure 5.2 c). Compared to the desalination routes, direct sea water electrolysis has a low technology readiness level (TRL) because of the technical challenge of avoiding the chlorine evolution reaction (CER) when using sea water as a feed. The CER would both parasitically consume energy and require downstream separation equipment. However, Dresp et al.[211] were able to demonstrate that by using a NiFe-layered double hydroxide at the anode and platinum nano-particles at the cathode enabled sea water electrolysis without chlorine production. However, slightly higher overpotentials than would typically be used in Alkaline or PEM electrolysis were required[212], which compromises equipment efficiency. Given the very low real energy demands of desalinating water, sacrificing electrolyser energy efficiency solely to eliminate desalination energy consumption is not justifiable, unless significant capital cost savings can be realised. To some extent, these capital savings may originate from a streamlined plant design that does not require additional desalination equipment, although there is a risk that the more complex catalysts required by the direct sea-water electrolysers to prevent the CER would offset the savings from streamlining.

Finally, solid oxide electrolyser cells (SOECs) can be used for hydrogen production (Figure 5.2 d). SOECs operate

at high temperatures (∼700°C) and can, therefore, accept steam as an input, rather than liquid water [213]. At these high temperatures, the energy required for water splitting is reduced, enabling very high electrical efficiencies. In other words, SOECs enable thermal energy to be used to reduce the burden on renewable power generation. Boiling sea water using waste heat from the ammonia plant to separate out the dissolved salts and then using the product steam as the electrolyser feed could achieve high efficiencies and reduced costs. However, the exothermicity of the Haber-Bosch process alone is not enough; even if the water were pure, the 2.7 GJ/ton of heat produced could only evaporate around 1.05 tons of water at atmospheric pressure (i.e. less than the stoichiometric requirement of 1.6 tons). In the context of a marine environment, the additional energy demand of boiling sea water would reduce this number further. Therefore, additional desalinated water would need to be produced to supply the SOEC, most efficiently by RO. This route would increase plant complexity but may be justified given the improvements in efficiency. The stability of SOECs under thermochemical cycling is less-well understood than alkaline and PEM electrolysis [116]. SOECs may therefore require larger back-up power supplies in order to maintain temperature and therefore operating rates. However, the manufacturer Topsoe reports that a turndown to 10% is possible using SOECs, which may enable competition on cost with other types of electrolysers[213]. Operating SOECs reversibly is also technically possible, which may further reduce the cost of plants which use them by removing the need for a fuel cell [137].

5.2.3 Other technical challenges

This section considers a number of other technical challenges which may arise and would need to be addressed: civil infrastructure developments, operation and maintenance, and biodiversity impacts.

Civil infrastructure developments will be needed to enable both renewable energy and ammonia production equipment to float. Most significant of these is the substructure beneath turbines to enable their installed costs per MW to approach onshore costs (discussed in more detail in Section 5.4.1.1). However, floating platforms or production ships will also be required for the electrolysis and Haber-Bosch synthesis. Based on experience from floating natural gas plants, these platforms are technically feasible but their costs may be considerable. Whether ocean production is viable depends on whether the cost saving achieved by transporting ammonia rather than electricity to shore outweighs the cost of such platforms. In the short term, existing oil and gas platforms are likely to be convertible into green production facilities; in the longer term, new platforms are likely to be required[201]

Operation and maintenance studies will be needed to verify that ammonia plants can be operated in a challenging marine environment. These will involve consideration of wave action, local weather conditions and site vibration, and should be conducted on a case-by-case basis. Although these are significant technical challenges, they are surmountable. Firstly, operation of green ammonia plants is likely to be relatively simple; apart from gas compression, there are few moving parts which could be damaged by offshore weather, and although synthesis temperatures and pressures are high, they are not extreme. Secondly, offshore plants can learn from maintenance

strategies used in the oil and gas industry, which demonstrates that offshore operation is possible in marine environments. Remote monitoring developments will enable plants to be operated from shore with minimal personnel onsite, which will reduce costs and improve plant safety. The operation of hydrogen electrolysis plants is relatively simple, meaning remote control rooms will be able to operate provided adequate information is gathered from sophisticated onsite monitoring and drone surveillance (which is already used to reduce operating costs of some solar plants).

Biodiversity impacts of offshore production must also be considered because of the fragility of ocean ecosystems. Little research has been conducted in the field, and more will be required on a project-by-project basis to demonstrate that the impact on marine life will be limited. However, there is some evidence that there are positive impacts of offshore production. Although more research is required, offshore wind and solar installations may act as protection for some sea life, as a foundation for bivalves, and as a resting place for migrating sea birds [214, 215] At the same time, offshore production may avoid onshore environmental effects, which can be significant if suitable land is not available; as described in Chapter 2, these can be significant.

5.3 Technoeconomic considerations

The previous sections laid out the rationale for offshore production, and outlined the technical developments that would be required to enable such production. This section applies the model described in Chapter 3 to determine the extent to which offshore production would be economic. It does so in several stages: it firstly considers the production cost in isolation; it then estimates the impact of land availability; it finally incorporates the costs of offshore platforms and of ammonia transport to shore.

5.3.1 Technoeconomic literature

While a number of authors have conceptually considered production of hydrogen or one of its derivatives offshore [216], this rarely includes conversion to green ammonia (although this may significantly reduce project costs). Babarit et al [58] estimated the cost of offshore hydrogen production with transport to shore on ships; however, in this initial stage analysis, they assumed a fixed cost of electricity delivered with a fixed load factor, and estimate quite high costs because of the difficulties of hydrogen transport. Loisel et al. [217] and Singlitico et al. [218] also consider hydrogen production from offshore wind at a location near France; however, they only produce hydrogen using curtailed electricity, meaning one key benefit of offshore production (namely, the absence of an expensive transmission line) is not achieved.

Some authors did consider ammonia in more depth: Morgan [219] considered the onshore production of ammonia from offshore wind, and Parmar et al. [220] extended that analysis to offshore production, attaining flexibility through modularised reactors. However, because they did not consider the use of batteries or any improvements in flexible operation of ammonia plants, they estimate very high costs of production. Panchal et al. [221] considered hydrogen production using thermal gradients in the ocean; however, because this technology has yet to be used on

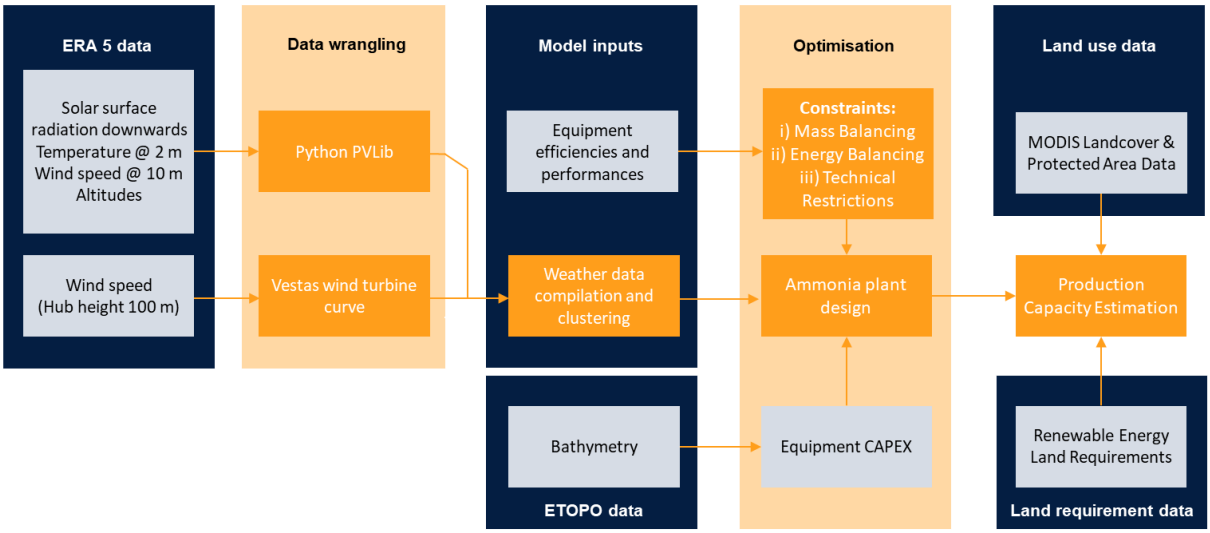

Fig. 5.3 Data flow through optimisation model at global scale, showing how land data is incorporated. Input data is shown in pale blue (and broadly clustered into dark blue themes); model processes are shown in yellow (and are broadly clustered into pale yellow themes)

very large scales, it is not considered further here.

Wang et al. [201] provide the most robust optimisation of ammonia costs considering offshore wind that is known to the author. This analysis used a synthetic wind profile to estimate project costs, which used a 'representative day' of electricity production from each month in a nominated year. However, as described in Section 3.2.2 of Chapter 3, using representative days can oversimplify production costs and underestimate the true energy storage requirements, and indeed, that paper found very small energy and hydrogen storage equipment was required. Moreover, the synthetic profiles they considered used two average wind speeds - 7 m/s and 11 m/s; however, much higher wind speeds are observed in the actual historical weather data used in this analysis - the best site has an average wind speed of 19 m/s, and the average speed is greater than 11 m/s at about 16% of sites - indicating that the synthetic profiles neglect locations in which very cheap production may be possible.

5.4 Methodology

The technoeconomic methodology is shown in Figure 5.3, which is an updated version of Figure 3.2, showing how land data is incorporated into the optimisation both pre- and post-processing.

The optimisation model is the same as that described in Chapter 3 (the LP model in Chapter 4), although it is here extended to a much larger number of locations; where Chapter 3 considered 700 locations for the analysis of Australia, this chapter considers over 60,000 locations.

As for chapter 3, weather data were sourced from the ERA5 reanalysis dataset; these were clustered into 4-hour time steps[141]. However, for bathymetry data, the ETOPO Global Relief Model was used instead, since it provides more granular data to larger water depths [222]; that data set was also used to estimate land slope for assessing the suitability of renewable energy production. Locations which were very close to the poles (i.e. latitude $< -85^{\circ}$

or latitude > 85°) were excluded, since environmental considerations likely exclude these sites; similarly, sites in Antarctica were excluded, even if they fell within the acceptable latitude range, for the same reason.

5.4.1 Offshore cost estimation

The most significant adjustment to the model for this chapter was an updated cost estimation to reflect the increased costs of offshore operation. While the costs of offshore installation as a function of distance to shore and depth are considered, we do not consider here regional differences in cost (i.e. we use the same installed cost of solar panels in India and Europe, even though installed costs are much lower in India). This is because (i) it is not possible to obtain meaningful estimates of the installed costs for each country considered individually, and (ii) the purpose of this analysis is to meaningfully compare ocean and land based sites based on the quality of their resource, rather than by the local financial conditions. For that reason, costs for land based applications were taken directly from the IRENA Renewable Cost estimation report [223], which considers a wide range of renewable projects, and reports the average and range of total project costs in 2020. Since their estimates refer to the total project cost, they include an average cost of purchasing land, which is highly variable globally, but is estimated to be around 3% of CAPEX in the US, based on the 0.03 USD/W published by NREL [224] (although it may be less if the site leases, rather than purchases, the land in question).

5.4.1.1 Offshore wind cost estimation

Offshore wind turbines fall into two categories: fixed bottom and floating. Many fixed-bottom turbines have already been installed, and are used for shallow water applications (<50 m). Because they are in common usage, their costs are widely reported; for this analysis, an installed cost of 2,644 USD/MW was used[223]; this is reflective of the global average installed cost minus the cost of high voltage power transmission to shore (which is about 17% of the total installed cost).

For water depths of greater than 50 m, it is not practical to install a fixed-bottom wind turbine, and the wind turbines will need to float [225]. While the literature is in general consensus that floating turbines will cost considerably more than ground mounted turbines[58], only a comparatively small number of authors provide meaningful cost estimates for this technology. The difficulty of estimating costs is further complicated by (i) the rapid reduction in the cost of renewable energy, meaning estimates are quickly outdated, and (ii) the relationship between the wind turbine cost and both the water depth and the distance to shore. Table 5.1 summarises all known data from the literature which reports a meaningful breakdown of floating wind turbine CAPEX.

The table demonstrates there is a wide range in reported costs of floating offshore wind, from between 3.5 million USD/MW to almost 6 million USD/MW. However, the transmission line to the shoreline often represents a substantial cost; if this were not required because of co-locating a green ammonia plant, then prices could fall to around 3 million USD/MW. Instead, the user must pay ammonia transport costs, but these are comparatively small because of ammonia's high density; these are discussed in Section 5.5.3.

Table 5.1 List of cost estimates for floating wind turbines. All costs listed are in millions of USD; where currency conversion was required to EUR, a factor of 1.12 €/USD was used, which is the approximate long term average. Where an author reported the costs of multiple technologies for floating turbines, the cheapest technology was selected for this work. Where available, present day costs are reported in preference to prospective future costs.

Author	Region	Year	Size (MW)	Turbine + Platform	Installation	Anchors	Mooring	Balance	Transmission	Cost/MW with transmission	Cost/MW without transmission
Ghigo et al. [226]	Italy	2020	10	28	16.8	0.1	0.5	-	13.4	5.9	4.5
Myhr et al. [227]	Generic	2014	1	1.8	0.34	In platform	0.6	0.28	1.1	4.1	3
Carbon Trust * [228]	Scotland	2015	1	2.1	0.43	0.07	0.2	0.13	0.4	3.3	2.9
NREL [191]	US	2019	1	2.7	0.48	In platform	In platform	1.1	0.98	5.3	4.3
NREL [229]	California	2020	1	2.5	0.2	In platform	In platform	1	0.8	4.5	3.7
Katsouris & Marina [190]	Netherlands	2016	4	10.5	0.39	0.30	0.30	1.35	2.24	3.7	3.2
Heidari [230]	Generic	2016	1	1.82	0.58	In mooring	0.06	0.53	0.48	3.5	3
Martinez & Iglesias [225] †	Europe	2021	1	3.7	0.27	0.11	0.06	0.48	0.81	5.4	4.6

* This publication used forecast pricing for 2030, rather than present day costs.
† Costs in this publication are a function of distance to shore and water depth. Values of 1,000 km to shore and 500 m depth were used for the calculations in this table only.

In general, the approach of Martinez and Iglesias [225] was adopted to estimate the cost of wind turbines, since (i) their work is the most recent, (ii) their work most clearly estimates costs as a function of water depth and distance to shore, and (iii) their work provides reasonable estimates compared to those offered by other works.

However, three modifications are made to their estimate. Firstly, and most importantly, the costs of the transmission line and onshore substation are not included, since they are not required. Secondly, the turbine costs indicated in their work are considerably higher than those considered by other authors, and may not adequately factor the falling cost of wind energy. For that reason, only the cost of the turbine component is taken from the IRENA average cost of a turbine from 2020. Thirdly, the time allowed for turbine transport in that work does not appear to take into account the low operational windows that may be present for ships in offshore wind farms, which Myhr et al. [227] argue can increase costs, because hired equipment for installation must wait in port until the weather conditions are safe. For that reason, the time taken for turbine transport was considered to be three times the one-way journey time (i.e. a return journey with an operational window of $\sim$67 %), and the costs are adjusted accordingly.

Table 5.2 shows the turbine cost estimates used in this work for three different turbine sizes. Clearly, the

total cost is a strong function of the wind turbine size; predominantly, this is caused by the considerable cost of the moorings, which has a relatively weak dependence on turbine size (although is also the largest source of uncertainty, since these moorings are not widely deployed). While turbines 10 MW in size are beginning to be deployed, we conservatively assume in the model that the largest turbines available are 7.5 MW, although clearly increasing turbine size is an avenue for future cost reduction.

Although Table 5.2 uses a distance to shore of 1,000 km and a water depth of 500 m, the completed plant model uses the actual distance and depth to determine installed costs per MW, although the relationship between these variables and the total cost is small, because of the large contribution made by the turbine and platform.

Table 5.2 Installed floating offshore wind costs for different turbine sizes; a depth of 500 m and a distance to shore of 1,000 km are used for demonstration purposes. Note costs are in USD unless otherwise specified.

Component	Description	5 MW	7.5 MW	10 MW
Turbine	1.28M USD/installed MW	6.40	9.60	12.80
Platform	8 M€ /turbine	8.96	8.96	8.96
Interarray cable	191.6 km for 100 turbines @ 0.3035 M€/km	0.65	0.65	0.65
Turbine Transport	0.0195 M€/day; 2 day install plus journey time @ 20 km/h	0.18	0.18	0.18
Turbine installation	0.24 M€/turbine (includes mooring installation)	0.27	0.27	0.27
Cable installation	0.213 M€/km (Interarrary cable only considered here)	0.46	0.46	0.46
Anchors	0.123 M€/anchor, 4 anchors/turbine	0.55	0.55	0.55
Mooring	Catenary wire (50 €/m wire) + chain (270 €/m) for 50 m	0.31	0.31	0.31
Site selection	0.21 M€/MW	1.18	1.76	2.35
Offshore substation	0.117 M€/MW	0.66	0.98	1.31
Decommissioning	70% of turbine transport, 10% of cable installation, 90% of balance of installation costs	0.41	0.41	0.41
	Total cost per installed MW (USD)	4.00	3.22	2.83

5.4.1.2 Offshore solar cost estimation

Offshore solar PV technology is an increasingly attractive option for land-restricted locations. To date, the majority of applications have occurred on inland water-bodies (which are technically simpler than marine applications); in these instances, the panel can reduce evaporation rates from the pond, while operating with increased efficiency because of the cooling effect from the water [231] (although obviously these effects partially cancel each other out). There are a host of other benefits: land preparation costs are not accrued; there is unlikely to be shading from nearby buildings, trees or mountains; and O&M costs may reduce because ocean areas are considerably less dusty [232]. Although more research is required, preliminary estimates indicate that the local environmental impacts

(e.g. biodiversity loss) may be lesser from floating panels than from land-mounted ones[231]. Additionally, for the application of ammonia which requires steady operation, solar may have a different seasonal profile to wind, and thus there may be synergies from including a second source of power.

Although the majority of floating PV has been installed on inland lakes and reservoirs, pilot projects have been constructed in marine environments in the North Sea [233] and the Strait of Johor [234]. These projects are more technically complex because (i) the salt water is corrosive and will degrade the panels over time, and (ii) wave action may damage the panels and support structures over time. This wave action may also reduce the efficiency of the panel, although Golroodbari et. al [235] estimate that the effects of panel cooling outweigh those of wave action. For this analysis, it is conservatively assumed that the effects cancel each other out, and that the efficiency of a floating panel is comparable to that of a land-mounted panel.

As was the case for floating wind turbines, it is difficult to estimate the costs of marine PV applications, although the challenge here is further complicated by the lack of consensus among operators as to the best panel superstructure to adopt (for instance, gable structures, solar trees and structures floating on tires have all been considered). Further, the majority of authors considering floating applications typically perform their analysis on inland reservoirs, and do not consider the additional costs for offshore application, although costs reported are typically between 1,000 and 2,000 USD/kW [235, 236]. For this analysis, the installed cost of floating solar panels are estimated at twice the cost of a land-based solar panel (i.e. 2×825 USD/kW = 1,650 USD/kW). While this nascent technology may well be more expensive in the short term, it is unlikely that it will be widely deployed until it falls below this cost.

5.4.2 Land restrictions

The approach of the previous section enables the minimum cost of ammonia production to be determined in all locations globally. This section determines how much ammonia can be made in each of those sites. The method is summarised in Figure 5.4.

This section breaks down land constraints into two categories: land availability, and land competition. *Land availability* here refers to restrictions on land that prevent the installation of renewable energy, because of (i) requirements for other land uses (predominantly agriculture, but also forests, as well as urban and built up land [237]), (ii) land protection legislation in areas of environmental/cultural significance (e.g. National Parks), or (iii) land with a steep gradient. *Land competition* here refers to an inability to use land specifically for green ammonia production because it is needed by other emerging renewable energy applications.

Land availability is determined using the Land Cover Type 1 layer from the MODIS6 dataset, which was obtained for each grid square considered in the optimisation [238]. This dataset classifies land into one of seventeen categories. Different approaches have been considered in the literature for determining whether solar and wind installation is possible on different land categories. For instance, van de Ven et al.[239] allow 'free' construction in

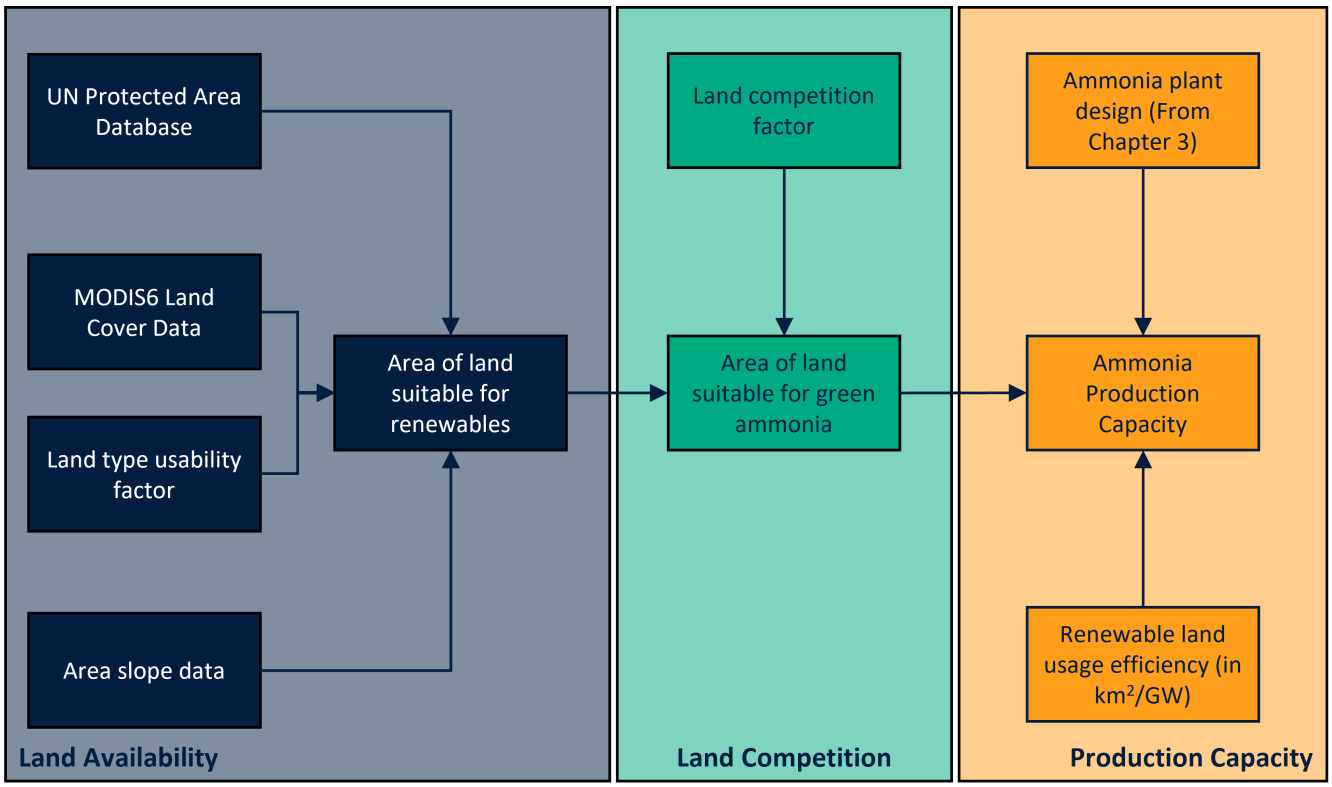

Fig. 5.4 Method for estimating ammonia production capacity. Land availability (i.e. fraction of land which can be used for renewable energy generation) is calculated using land cover data and factors for installation capacity based on land cover type; areas designated as protected by the UN and steeply sloping areas are excluded. Actual land which can be used for green ammonia specifically is a fraction of the total available land, dependent on land competition - which refers to the need to build other renewable sources. Method I for estimating land competition is shown in this figure; Method II incorporates an additional land cost. Based on the suitable land area for green ammonia, the optimal plant design, and the land-use efficiency of renewables, the actual production capacity is estimated.

unused areas (e.g. desserts, shrublands, some urban rooftops), and use a competition based model which allows some construction of solar panels in locations with existing uses (e.g. cropland, savanna), but prevents installation in areas that are likely to be environmentally protected such as forests. Deng et al. [188] also prevents construction of solar PV in forests, but allows wind turbines with ∼20% of the land efficiency that they have in other locations. In general, they predict far less land use than other analyses, because of the assumption of an 'availability factor'. This factor varies across countries and land uses, and significantly constrains their estimate of land availability.

Here, we use a hybrid of these approaches, which allows unlimited construction on barren land, and a fraction of construction on other land, depending on its current usage. The fractions adopted are reported in Table C.1 in Appendix C. A base, low and high land availability are modelled in order to estimate the possible range of productions. In all cases, construction is not allowed in protected areas, as listed in the UN database [240]. Construction is also excluded if a site has a slope of greater than 15° (to a granularity of 0.016 degrees). For offshore sites, it is assumed that all ocean area which is not designated as protected is available.

The MODIS dataset, protected land areas, and slope data, is more granular than the weather data that was used for estimation of ammonia LCOA. For each of these measures, land availability was estimated at the finest

granularity; the cumulative available area within each of the larger grid squares used for ammonia LCOA estimation was then used to calculate maximum available ammonia production.

Land competition factors the role of competing renewable applications. At present, there is little competition for available land, as renewable energy represents a small fraction of total energy consumption; however, in a fully decarbonised economy, this competition is likely to be considerable. Prediction of land competition in this context is challenging, as the composition of carbon neutral energy systems remains uncertain. Therefore, two different approaches are used to estimate land competition, which are designated **Method I** and **Method II**.

In **Method I**, it is assumed that the land competition faced by ammonia is proportional to its fraction of global energy demand to ensure there is sufficient land for other sectors to be decarbonised. At present, ammonia production for fertilisers represents 2% of global energy demand [90], which is taken as a base case; a minimum availability of 1.5% and a maximum availability of 3% are considered as sensitivities. Note that this competition factor is not equivalent to the availability factor proposed by Deng et al.[188]; the estimate is therefore conservative in assessing the performance of ocean based ammonia by allowing generous use of land. The competition factor is applied evenly to on− and offshore sites. In theory, as ammonia production expands to alternative end-uses, demand would increase, and the competition factor would increase to match it (i.e. if shipping were to be completely decarbonised by green ammonia, demand would be some multiple of present demand, but so too would the fraction of global energy associated with ammonia as an end use, and therefore the amount of land which could be used to produce the ammonia by the factor used in this method).

In **Method II**, it is assumed that land competition manifests as increased costs for onshore sites only. This method calculates how large those costs would need to be in order to drive different percentages of production offshore. Costs are expressed in USD/MWh, to provide easy comparison to other renewable energy production projects. Equation (5.1) links the increased costs of electricity to an increase in the LCOA-P.

The equation is essentially a unit conversion - the product of the annual operating hours, load factor and renewable installation gives the MWh per MMTPA of ammonia produced; when this is multiplied by the increased costs per MWh of electricity, it is translated into the increased costs per ton of ammonia produced each year. Results for Method II are shown in Appendix C (Figure C.2).

$$\text{Increase in LCOA-P} = \text{Increased costs in USD/MWh} \times \text{Annual Operating Hours} \times \frac{MMTPA}{10^6 tons NH_3} \times$$

$$\times \left[\sum_{\text{Renewables}} \text{Renewable load factor} \times \text{Renewable installation in MW required for 1 MMTPA of capacity} \right] \quad (5.1)$$

5.4.2.1 Renewable energy land requirements

Estimates for wind turbine land use requirements vary from 100 to 200 km^2/GW of installed capacity. In order to minimise wake effects, we assume a space efficiency of 200 km^2/GW[104].

Estimates for solar land use requirements also vary from different authors - we adopt the method from van de Ven et al. [239], which varies the packing of solar panels on the basis of latitude to maximise efficiency (since at higher latitudes panels must be further apart to prevent shading). The method is modified to report the land usage in km^2/GW by using the space efficiency of a standard solar panel [241].

To convert renewable energy land requirements into ammonia production capacity, we assume that complete overlap is allowed between wind and solar farms. In reality, access roads required by wind turbines, and the shading effect of these turbines, will prevent this idealised overlap; however, it provides the largest possible estimate of land production capacity and is therefore conservative for the assessment of ocean performance. For similar reasons, the area of the hydrogen and ammonia production itself is considered to be negligible in comparison to the area of the renewable energy farm.

5.5 Offshore wind results

This section of results is divided into three subsections. In the first subsection, the costs of production are presented without land limitations; these are factored into the second subsection as limitations on ammonia production at each of the sites, which enables an assessment of the relationship between cumulative global production and LCOA-P. The final subsection includes the costs of additional infrastructure requirements associated with offshore production (floating platforms and ships to ports) and onshore production (pipelines to ports).

5.5.1 Production costs

Two cases were considered for the production costs: a hypothetical case in which costs were equal on- and offshore, whose purpose is to show the quality of the ocean resource; and a more realistic case in which solar installation is allowed on land, and the additional costs of offshore renewable installation are included in the estimate. The reason these 'hypothetical' results are included is to demonstrate that, although the main driver explored in this chapter for moving offshore is land availability, the offshore resource quality is also a substantial driver. Cost reductions which enable floating wind turbine costs to be bought towards fixed-bottom turbine costs would make offshore production highly competitive. The results of the two cases are shown in Figure 5.5.

There are two points which are noteworthy for the hypothetical wind only cases. Firstly, the model cannot converge at many land-based sites; this occurs because there is a maximum cap on the wind turbine installation of 20 GW in order for the model to converge more quickly - although it sometimes causes the model to fail to return results, this will only occur in locations where the ammonia cost would have been extremely high, meaning they are unlikely to be used to produce ammonia in the future. Secondly, in this raw comparison of wind resources which

neglects the realistic costs of a floating plant, the ocean sites far outperform land based sites. In particular, the wind band at very southerly latitudes (from about -65° to -45°) has extremely cheap ammonia. This demonstrates that the wind resource quality in the oceans is superior for ammonia production to that available on land.

(a) - Wind only, onshore and offshore costs equal

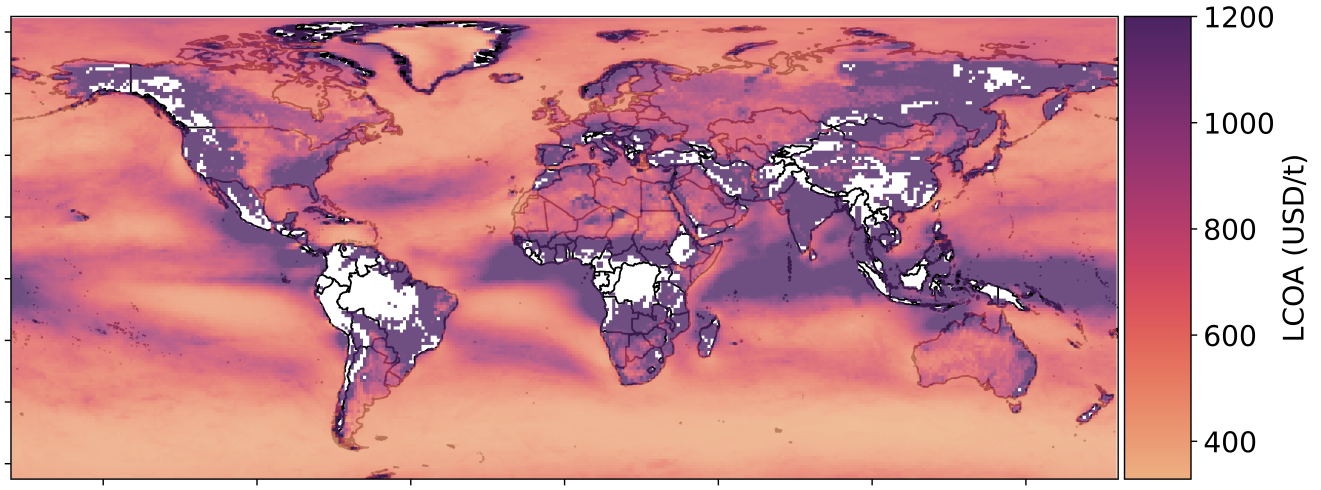

(b) - Wind and solar, true onshore and offshore costs

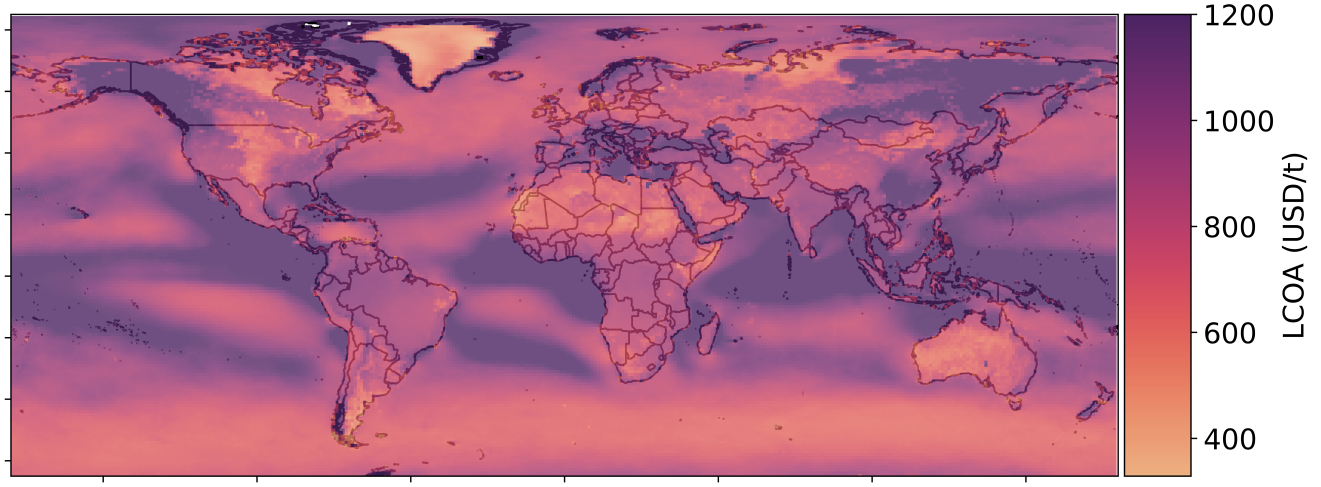

Fig. 5.5 Heat maps for global green ammonia cost estimates. **(a) - Top**: Wind only, with equal costs on and offshore, purely for demonstration of offshore wind potential; **(b) - Bottom**: True costs for on and offshore wind and solar. In order to maintain a readable colour gradient, locations with an LCOA-P > 1,200 USD/t were shown using the same colour as those with LCOA-P = 1,200 USD/t. In locations that are uncoloured, the model could not solve, indicating green ammonia produced there would be very expensive.

However, this performance is not replicated when the true costs of offshore wind installations are also considered, as is evident in Panel (b) of Figure 5.5. Figure 5.6 shows the comparison more clearly, by showing the cumulative production at a given price point for the two cases shown in the heat maps. One additional hypothetical case is included, in which cheap solar and electrolysers are available on- and offshore. This latter case represents a likely future in which the costs of solar PV and electrolysers fall more rapidly than the cost of wind turbines. As described in Chapter 4, cheap electrolysis will typically benefit solar dominated sites more than wind dominated

sites. Since, in general, the solar resource is superior onshore, this reduced cost of solar panels will typically benefit onshore locations more than offshore locations. (Note that for this section, it was assumed that the entire area demarcated by a location could be covered in renewables unaffected by land constraints) [104]

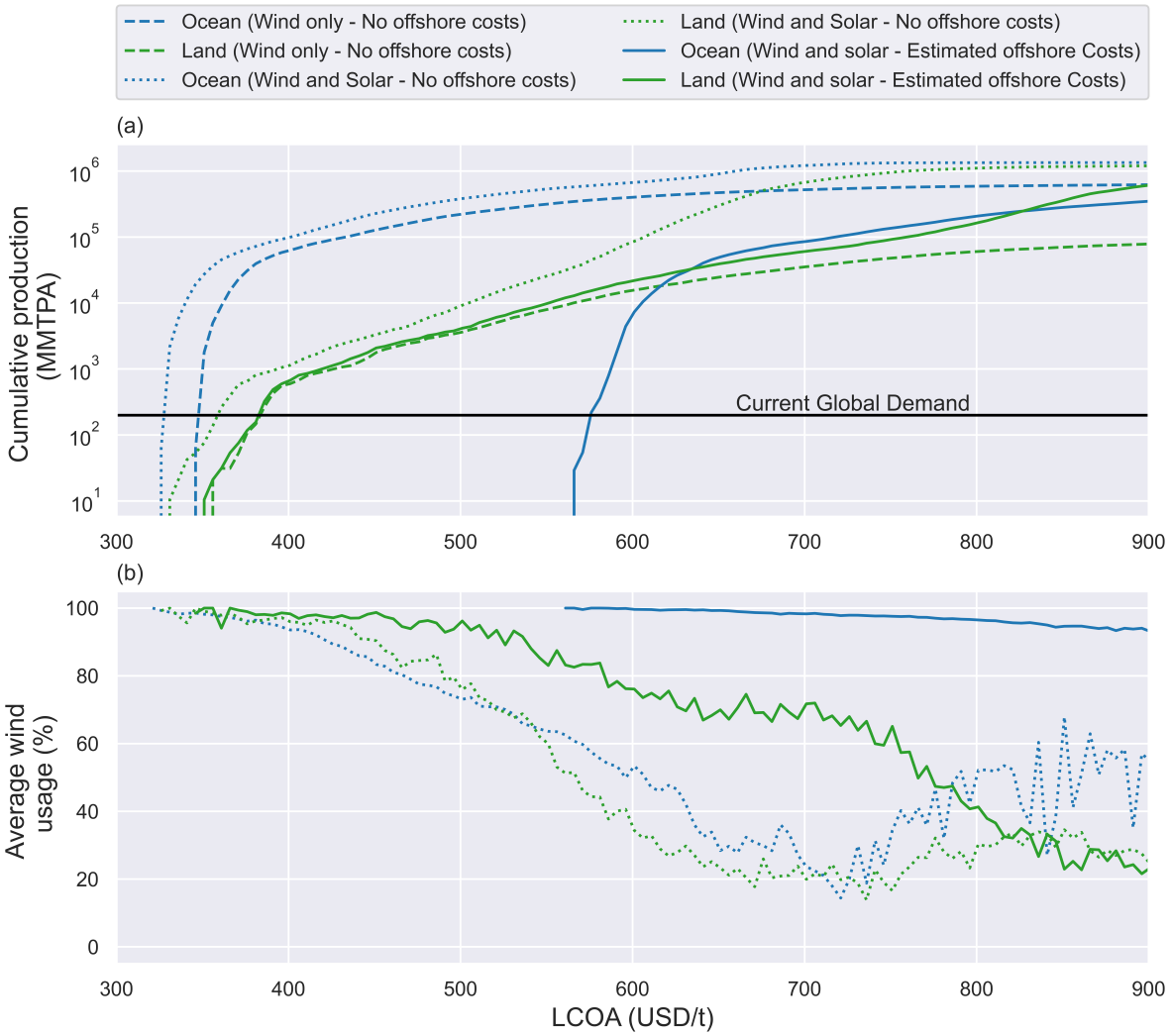

Fig. 5.6 Comparison of cases by cumulative production. Three cases are presented: two sets are hypothetical cases, in which onshore (**green**) and offshore (**blue)** equipment CAPEX is equal. In the first hypothetical case (**dashed**), only wind is allowed, and in the second (**dotted**), both wind and cheap solar/electrolysers are also allowed. The third case is the realistic case (**solid**), using the estimated actual costs of on- and offshore installation.**(a) - Top**: Comparison of marginal LCOA-P at a nominated global production, without land restrictions. Note that the inclusion of cheap solar benefits land production (**dotted green**), but not so much that it outperforms the corresponding ocean case (**dotted blue**). **(b) - Bottom**: Comparison of wind usage at top sites. Even when cheap solar installation is allowed, the best sites are still wind-dominated.

Figure 5.6(a) demonstrates that the superior ocean resource means that it produces considerably more very cheap ammonia than land based-sites, all equipment CAPEX costs being equal (as shown by the dashed blue line crossing the global demand line about 40 USD/t cheaper than the dashed green line). However, factoring in the increased costs of floating wind farms significantly increases the LCOA of the associated ammonia; it cannot compete with land-based ammonia in this regime (for the solid lines, the green land line crosses global demand almost 200

USD/t cheaper than the blue ocean line) - for it to be competitive, the global ammonia demand would need to be in the order of 10^4 MMTPA, or around 100 times larger than demand today (which is marked on the figure as approximately 200 MMTPA).

The cost increase across offshore sites between the hypothetical and realistic cases is fairly uniform, in the order of 40%. A 40% cost increase is consistent with expectations; although the turbines themselves have increased in cost by more than a factor of 2, there are many other components in the ammonia production process (i.e. electrolysers, Haber-Bosch) with significant costs that are largely unchanged in this mode (although the infrastructure required for this downstream equipment to float may also be expensive - see Section 5.5.3 for cost estimates).

5.5.1.1 Changing solar costs

As described in the introduction to this chapter, the analysis for floating offshore wind has been conducted using 2022 data to avoid the compounded uncertainty of floating turbine costs and cost forecasting. This is constraining to the analysis, as it is likely that the costs of solar PV will fall more quickly than the costs of on- or offshore wind. Aided by cost reductions in batteries and electrolysers, this will lead to the cheapest forms of ammonia production relying on solar, rather than wind (see Figure 6.4 in Chapter 6).

If the cost reductions in solar relative to wind are very large, then offshore wind will not be competitive from an economic perspective. High-land efficiency solar will generate adequate energy and offshore ammonia will not be needed. However, the change in the relative costs would need to be very large. Figure 5.6 gives an indication of how this cost balance may shift in response to a 30% reduction electrolyser costs, batteries, and the relative cost of wind and solar compared to the base case (rather than almost 50%, as is used in the other chapters based on Oxford INET forecasts[2]). In this case, the cheapest ocean and land sites become even cheaper than in the previous wind and solar case, but this difference is attributable to the reduction in the cost of electrolysis units, since the cheapest sites are still the ones with an excellent wind resource. Consequently, the cheapest land and ocean sites do not substantially change in cost relative to each other. Panel (b) indicates that most of the influence of the reduction in price of solar panels is felt at sites with an LCOA greater than 400 USD/t (in the hypothetical cases); this is where the most deviation is observed between the lines for the land cases comparing real and hypothetically low solar prices. The relationship between LCOA and wind usage is approximately the same at both land and ocean sites. Evidently, the switch to solar based sites which is observed in the next chapter requires a cost reduction of greater than 30%.

At the cheapest sites in the ocean, floating solar is not installed, even though it is allowed, because the wind resource is so superior to the solar resource (many of the best locations are at absolute latitudes greater than 40°). Land sites make greater use of solar, but it is still only enables a fairly small reduction in cost at the best sites - in the order of 5 USD/t.

There are some interesting results at comparatively poorly performing sites (i.e. LCOA > 600 USD/t for the hypothetical cases); in these locations, because the capacity of solar panels to generate far more electricity per area

of land, the total production capacity increases markedly; in fact, it becomes almost as high on land as in the ocean, even though the total area of the ocean is almost triple that of land.

5.5.1.2 Impact of ocean depth

Figure 5.7 shows the relationship between the cost of ammonia and how far a site is from the shore for the realistic case.

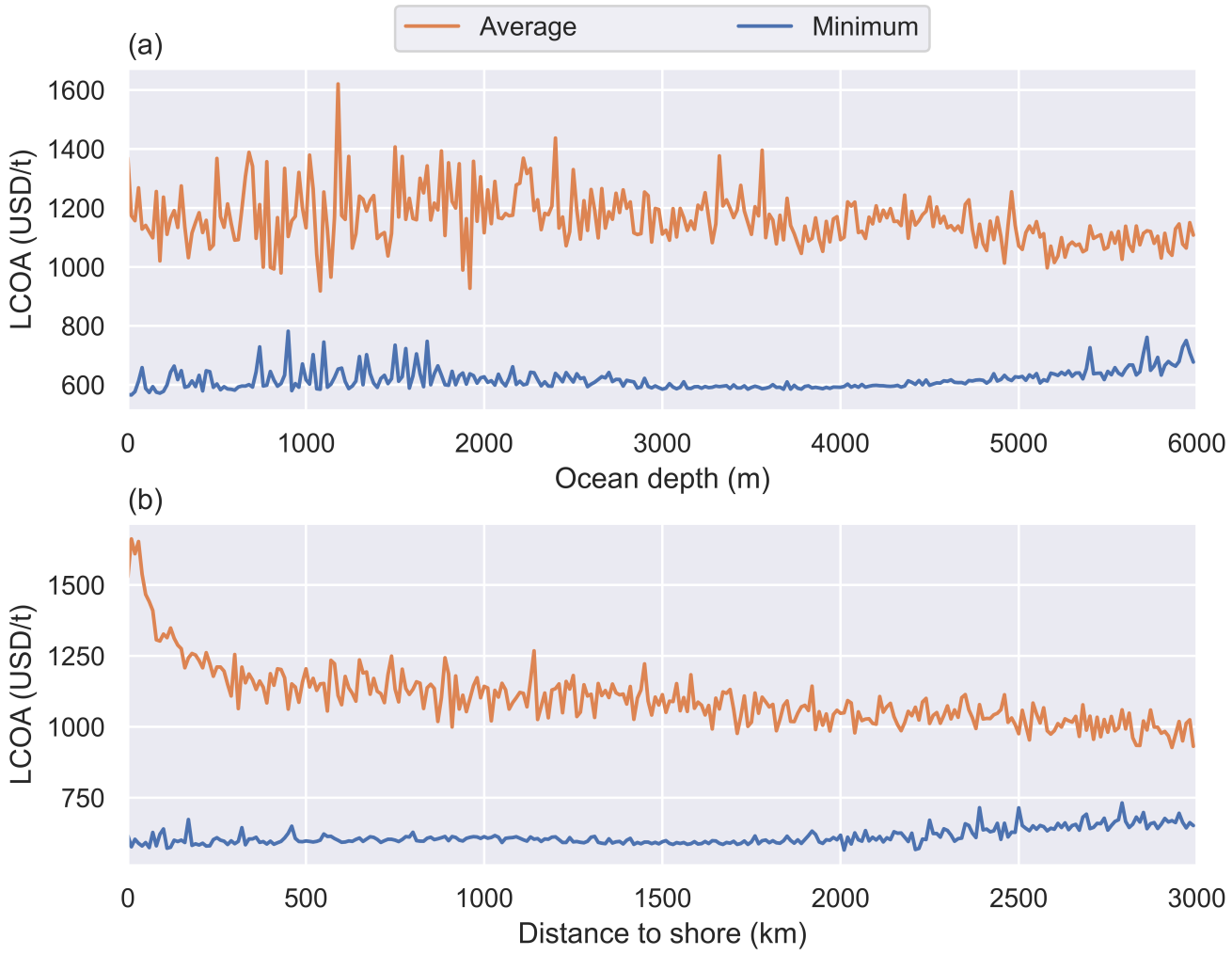

Fig. 5.7 Impact of ocean depth and distance to shore on average and minimum ammonia cost. **(a) - Top**: Impact of depth, which is not strongly correlated to cost. **(b) - Bottom**: Impact of distance, for which there is a surprising inverse correlation with the LCOA-P for the average site; even though sites further offshore are typically more expensive (because they are more likely to be in deep water, preventing fixed-bottom turbine installation) the associated LCOA is on average lower. This is driven by better wind resource quality further offshore

As outlined in Section 5.4.1.1, the total cost of the wind turbine is a function of water depth and distance to shore; however, the plot demonstrates that these variables have little dependence on either the minimum or the average LCOA-Ps observed at a nominated ocean depth or distance to shore. This is because the fraction of floating wind turbine costs associated with mooring and installation (which vary as a function of depth) is small

compared to the turbine and floating substructure (which do not depend on depth). The small increase in cost of the turbine does not translate to a meaningful increase in the cost of ammonia, as the quality of the wind resource is of greater significance. For locations comparatively close to shore (< 500 km), there is an inverse relationship between distance and LCOA, indicating that in general, better resources are available further from the shore; this is likely also the reason that the LCOA at depths < 50m (where cheaper fixed bottom turbines can be used) is not significantly less than the LCOA-Ps at greater depths.

The upper limit on ocean depth for floating wind turbine installation is not well-understood. As the ocean depth becomes larger, the strength of the mooring cables will need to increase, which will impose a maximum limit on water depth. The World Bank reports a maximum depth of around 1 km [242], which would cover around 80% of the world's ocean. Because of the high degree of uncertainty associated with the maximum depth, no sites are excluded here on the basis of a technical limit that may be beaten; because Figure 5.7 indicates the LCOA-P does not depend strongly on depth, this is not likely to have a major impact on results.

5.5.2 Land Constraint Results

The previous subsection compared the quality of the resources, and demonstrated that the costs of floating renewable energy generation are too large to enable ammonia to be produced on the ocean that is cheaper than that produced on land, despite the superior wind resource in the ocean. Even a potential increase in demand by a factor of 5 to 10^3 MMTPA (which would provide enough extra ammonia to supply the maritime industry and some energy/hydrogen trade via ammonia) would not justify the use of ocean sites, since the ammonia cost at that production rate still exceeds the cost on land by $\sim$160 USD/t.

However, the results in Figure 5.6 (a) assume all land can be used ammonia production, which is not realistic. For instance, it appears on Figure 5.5 (b) that Greenland would be a suitable location for production, but given environmental concerns with production in protected areas, it is not likely that it would be suitable for large scale chemical production; this land would not be available for renewables based on the description provided in Section 5.4.2.

As described in Section 5.4.2, there are two methods for calculating the impact of land competition (i.e. constraints on renewable installation for ammonia production because of other electricity usage); Figure 5.8 uses Method I, and Method II is shown in Appendix C. Three cases were considered for land use restrictions - a base case, as well as a low and a high land use case. This figure assumes construction of both wind and solar, identical to the "realistic" case shown on Figure 5.6.

Considering land constraints, the economic case for ocean-based ammonia production becomes considerably more attractive, and begins to become competitive with land based production around the current global ammonia production rate. In the base case (Figure 5.8b), around 15% of ammonia is made most profitably in the ocean (measured by the vertical distance between the orange and green lines where the orange line crosses the global

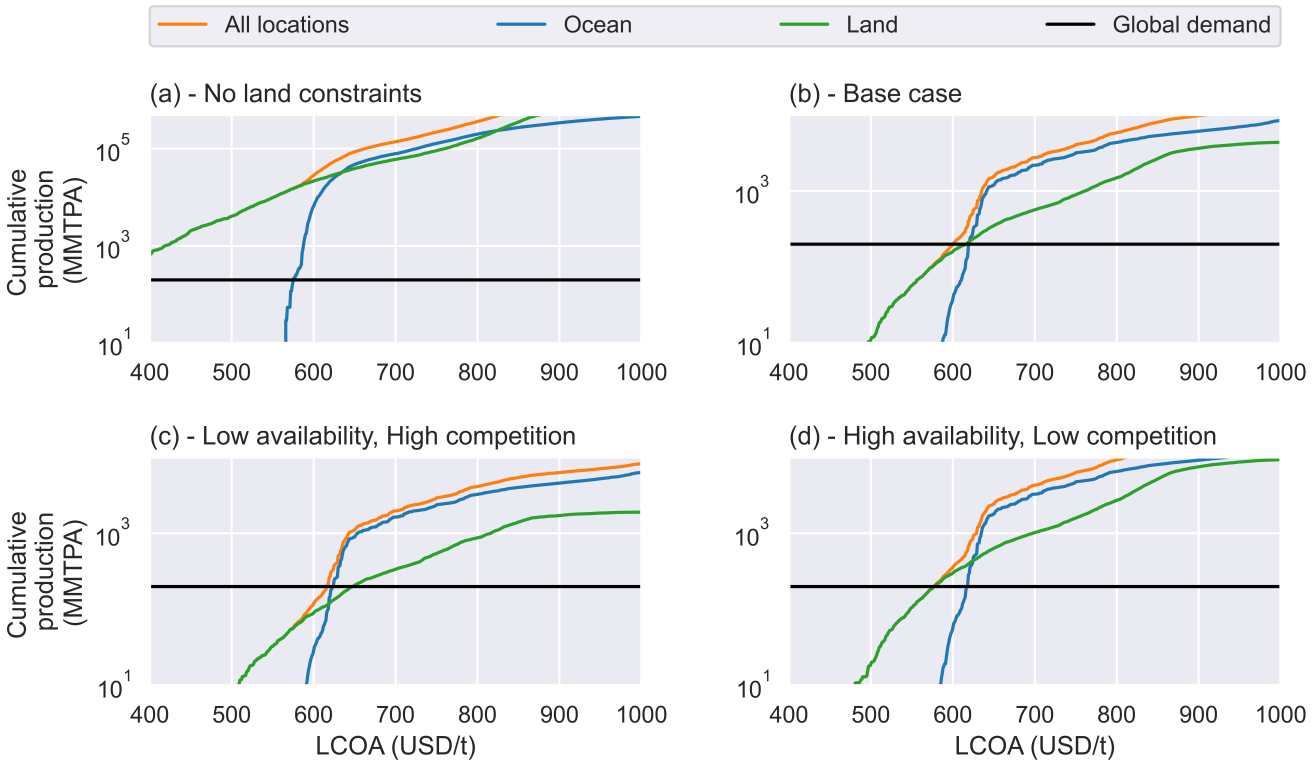

Fig. 5.8 Impact of land availability and competition on ammonia production costs. Competition is calculated using Method I, in which a factor is applied to available land in order to determine the impact of competition from other renewables. **(a) - Top left**: No land constraints; **(b) - Top right**: Base case; **(c) - Bottom left**: Low land use (i.e. low availability and high competition); **(d) - Bottom right**: High land use (i.e. high availability and low competition). Note the scaling on the y-axis of panel (a) differs from the other three plots. Where there are no land-constraints, onshore sites clearly outperform offshore sites. Including land constraints, offshore production goes some way to meeting global demand.

demand); in the low land availability case (Figure 5.8c), this rises to as high as 33%. Even in the high land availability case (Figure 5.8d), a small amount of ammonia (around 1 MMTPA) would also be profitably produced offshore.

The results in Figure 5.8 are calculated for the whole globe; in specific regions, the incentive for ammonia production on the ocean may be greater. For instance, the UK has both high population density and a sizable agricultural industry, meaning it has little available land but large fertilizer demand (compared to its fraction of the global population). The UK specific results are shown in Appendix C (Figure C.1), and demonstrate that even in the base case, as much as 50% of its ammonia may be produced offshore. Because of the very restrictive land restrictions for onshore wind farms in the UK[189], the low availability case is more likely, in which case almost 100% of ammonia will be produced offshore. While importation is also an option for the UK and other similar regions, near offshore production may be preferable to maintain energy security, and to avoid long distance shipping costs for fuel.

Using Method II for land competition estimation, we estimate that if land costs accrue which increase the levelised cost of electricity production by 10 USD/MWh, then about 15% of production will move offshore (the same as in the base case for the first approach). This is approximately equal to the costs of moving a wind farm

from a site with a load factor of 40% to one with a load factor of 30%, or to the cost of moving a solar farm from a site with a load factor of 25% to one with a load factor of 18%. In other words, it is similar in magnitude to relocating renewable energy production from an excellent site to an above average site, and is therefore a plausible estimate for the cost of land competition.

5.5.3 Infrastructure Requirements

An important consideration which has yet to be factored into the above analysis relates to the broader infrastructure requirements to enable ammonia to be produced on a floating plant: these include the platform on which the ammonia is produced and the cost of transport to shore (the costs of floating the wind turbines themselves have already been factored into the cost of equipment). Production on platforms should be technically achievable using similar technologies to those already employed by the offshore oil and gas industry. Having been produced, the ammonia could be delivered to the nearest point on the shore, but it would be more practical to deliver ammonia to a nearby demand centre. In that more realistic case, transport costs also accrue for ammonia produced onshore, in pipelines to ports, and shipping to demand centres. The purpose of this section is to understand how offshore production impacts the costs of delivery, on top of the cost of production. In order to do so, it considers delivery to two demand centres: Hamburg in Germany and Yokohama in Japan. Both countries have announced intention to import ammonia as fuel in the future, and these ports are also useful proxies for significant future demand for ammonia in Europe and East Asia respectively.

Costs for constructing offshore equipment may be significant, but are usually confidential. In a small number of cases they may be avoided if (a) there is shallow water or an island nearby on which to base an ammonia plant, or (b) there is an oil and gas rig which can be repurposed for hydrogen production. However, in the majority of cases, a new floating structure will be required. There are a range of possibilities available for a floating plant: it could be either a platform or a production ship. Wang et al. estimate a cost of 100 million USD per platform [201], which is considerably less than the $\sim$500 million USD estimated by Kaiser et al.[243] (for a semi-submersible platform, averaged between 2008 and 2013), although this figure is for an entire drilling rig, inclusive of equipment, and therefore represents an upper bound on the true cost. The cost of an offshore platform is therefore conservatively taken to be 200 million USD.

The impact of this additional cost on the LCOA naturally depends on production capacity; based on the weights of electrolysers specified by NREL [244], and the weight tolerances specified in Kaiser et al.[243], the approximate capacity of these platforms would be 1 MMTPA, meaning the increase to LCOA from platform operation would be approximately 15 USD/t. For comparison, a 600 km ammonia pipeline (the average distance from the coastline for land locations with an LCOA $<$ 600 USD/t and which are therefore competitive according to Figure 5.8) at that capacity would have a cost of around 12 USD/t[104]; that cost may be doubled if desalinated water must be pumped from the coast line, although that cost is not included here (i.e. it is assumed land based sites have access

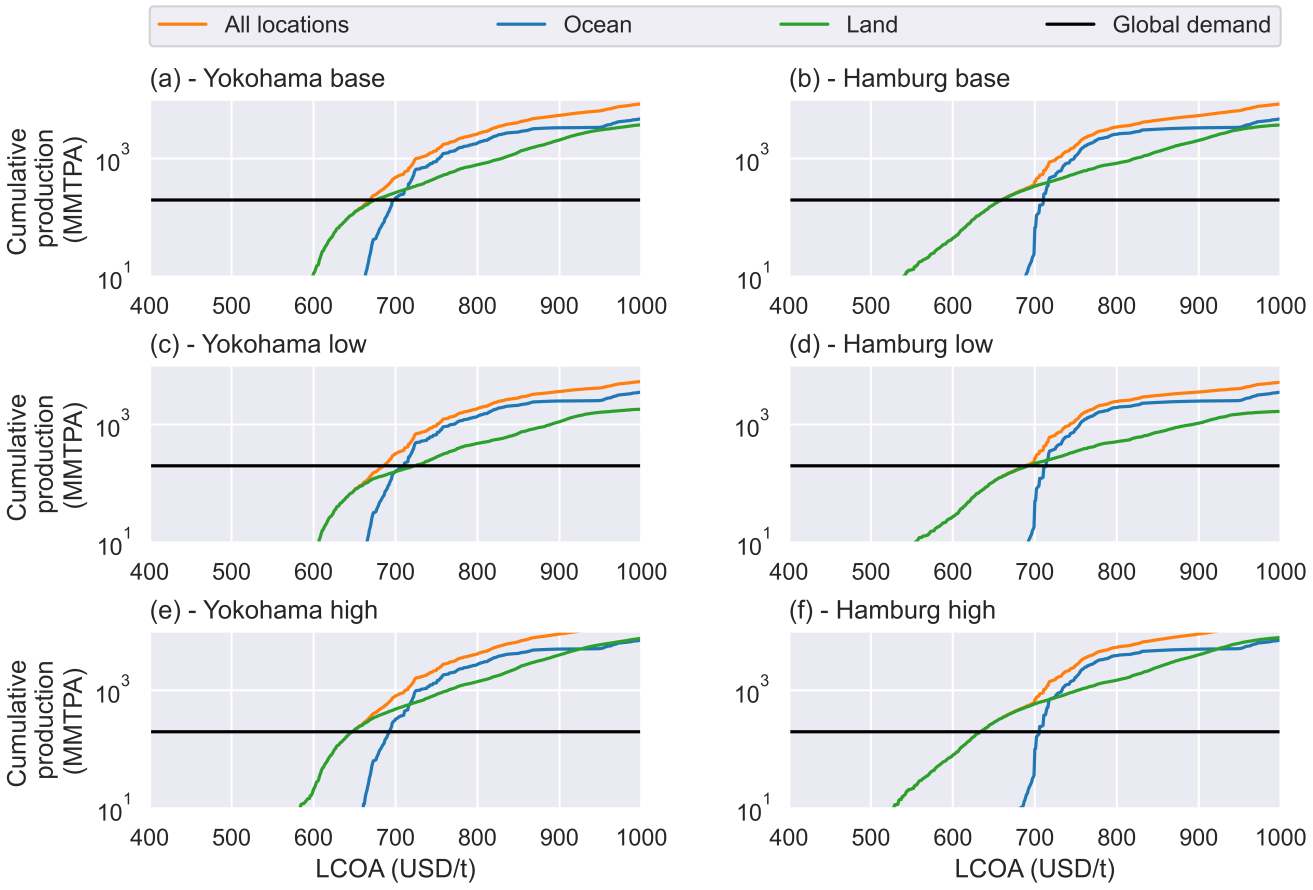

Fig. 5.9 Impact of infrastructure constraints and land availability on delivered costs of ammonia. Left plots show delivered costs to Yokohama; right plots show delivered costs to Hamburg. All three sensitivities on land availability are also shown, using Method I. Including transport costs may reduce the competitiveness of offshore sites; regardless of land constraints in Hamburg, offshore production is not the cheapest option at or below the level of global demand. In Yokohama, they are only competitive where land restrictions are very tight.

to water). The land and ocean based infrastructure requirements are therefore of a similar order of magnitude, although a significant uncertainty remains.

Shipping cost advantages should also be considered. These will differ for different countries; however, in some cases, ocean locations may hold considerable opportunity to reduce shipping costs. For instance, the majority of very cheap land locations are in the Western hemisphere (i.e. Northern Africa and South America); these will have very large shipping distances to Japan, which is forecast to be a major demand centre. The shipping distances from the very good marine locations in the Southern Ocean are about half that distance, which would amount to savings of ∼20 USD/t (see Chapter 6 for the methodology used to estimate shipping costs); on the other hand, those savings would be reversed for Germany (which has also stated its intention to import hydrogen in the form of ammonia), which would be better off importing from Morocco than the Southern Ocean.

To factor in these infrastructure costs, a delivered cost of ammonia to both Hamburg and Yokohama was estimated for each potential production location. Land transport costs were factored using a cost of 2.56 USD/t/100 km of pipeline (see Chapter 6), and land transport distances were calculated to the nearest port (with an overdesign

factor of 20%). Maritime distances between pairs of ports were estimated using shipping routes available in the AIS database. Maritime distances between offshore production sites and ports were estimated using the PortWorld online calculator. Shipping cost estimation is described in Chapter 6. It is assumed that the ships are powered using the onboard ammonia. The results are reported in Figure 5.9.

The infrastructure costs reduce the economic case for offshore production, although it may still be viable for shipping to east Asia in the base case, representing around 7% of production (and more than 25% of production in the low land availability case). However, for shipping to Europe, because of the proximity of cheap land production sites in West Africa, it is always preferable to used land based production. For the East Asia case, all ammonia is produced in deep water far from the shore; the average distance for the cheapest 200 MTPA of ammonia is 180 km from shore (compared to a global average of 30 km for offshore wind today), and the average water depth is approximately 400 m (well more than the typical depth of < 50 m for most offshore wind farms today).

5.6 Land availability and offshore production summary

This chapter has assessed the viability of ammonia synthesis on the ocean. It explained the rationale behind exploiting this resource, and considered various technologies which may enable offshore production. Although the renewable resource quality on the ocean is superior to that onshore, the vastly increased cost of exploiting that resource in general make land-based production more competitive. However, given the limitations on onshore production imposed by land-constraints, offshore production may be competitive at very high-production rates.

A major limitation of this research is the difficulty of forecasting the cost of floating offshore wind into the future. Offshore production is likely to become less competitive in the future: although floating wind turbines will fall in price, so too will solar panels, which are significantly more efficient users of land than wind turbines on an area/GW basis. This will enable increased onshore production. However, in specific regions like the UK, land limitations are more significant, and floating production may be required for energy security. Therefore, while the techno-economic analysis does not definitively show that offshore production will be the cheapest option for green ammonia production in the future, it does demonstrate that consideration of land limitations is important in determination of the composition of an energy system which uses chemical energy vectors. These land limitations are an important input to the model described in Chapter 6.

The final section of this chapter explored the role of transport costs in determining the delivered levelised cost of ammonia (LCOA-D), as opposed to only the levelised production cost (LCOA-P). The upcoming chapter explores the interplay between transport and production costs in more detail, and how they interact with various forecasts for ammonia demand.

Chapter 6

Optimising supply chains for ammonia transport

The previous chapters have provided a comprehensive assessment of how much it costs - and will cost in the future - to produce green ammonia, as well as providing a method to assess the amount of green ammonia which can be sustainably produced given land constraints.

This chapter integrates this supply information with two measures of ammonia demand, in order to estimate the 'globally optimal' distribution of production and supply (as determined by the minimum cost).

On a basic level, considering the supply chain costs is an important component of the optimisation: as this chapter will show, transport costs of ammonia are not negligible, and considering only the cheapest production location without regard to the costs of transport will not result in the cheapest ammonia. On a more sophisticated level, the integrated supply chain model provides a blueprint for ammonia production and distribution networks in the future. It enables identification of the core drivers of cost, and prediction of likely bottlenecks.

This chapter is divided into three parts: the first part explains how the model which integrates production and supply functions. There are then two case studies: the first focusses on global demand for ammonia as a maritime fuel, and the second focusses on using ammonia to supply back-up energy to electricity grids.

6.1 Methodology

There are two parts to this supply-chain methodology: the first explains how supply chain costs for ammonia are estimated, and the second explains the optimisation approach used to minimise the overall delivered cost of ammonia.

6.1.1 Transport and storage costs

In order to deliver ammonia from production locations to consumption locations, it must be transported over land, and, in many cases, by sea. Where it travels by sea, it must go via a port; this thesis considers only existing ports. Buffer storage is required at each production stage: at the supply site, the demand site, and any ports at which the ammonia stops at on the way. A summary of the input values is shown in the Appendix in Table D.2; this section describes how those values were reached.

6.1.1.1 Land transport

Pipelines are used to transport ammonia from production sites to local ports. Although trucking ammonia is also possible, pipelines are far more cost effective for all distances at large scales [31], and are already in wide use - there are over 4,500 km of pipeline installed in the US [245]. Both 'warm' and 'cold' pumping are possible (depending on whether the ammonia is in the liquid state due to pressure or temperature, respectively); which option is chosen will depend on local conditions.

Determining the cost of this pipeline is an important component of estimating the supply chain cost. These will naturally vary significantly based on local conditions; however, the purpose of the calculation in this chapter is not to determine the exact pipeline cost, but instead an order of magnitude estimate which is suitable for inclusion in the optimisation model. For inclusion of pipeline costs into the model, costs are expressed in USD/levelised ton of ammonia/km; these depend on the pipeline CAPEX, OPEX and discount rate.

The size of the pipe is determined iteratively based on the flow and the associated pipeline NPV. The calculation guesses a pipeline size and calculates the associated NPV; it then checks similar nearby sizes to check if its guess was optimal; if not it guesses again and re-iterates. The OPEX is determined by the power demand, which is dependent on the head loss using that pipeline size. The CAPEX is estimated based on the pipeline material demand, using a steel cost of 700 USD/t; the Lang factor was then calibrated to match the tariff (5 USD/levelised t ammonia/100 km at a flowrate of 1.5 MMTPA) reported in Nayak-Luke et al. [140]. The optimum speeds determined using this method are typically between 1.5 and 3 m/s, which is standard for pumped liquids [246].

One significant hurdle raised by the calculation is that the costs of ammonia transport by pipeline are not linear with production capacity; they tend to fall from around 5 USD/t/100 km for production scale in the order of 1 MMTPA to less than 2.5 USD/t/100 km at production rates of around 10 MMTPA (see Figure 6.1). This is unsurprising, since there are major costs associated with pipeline easements, and the pipeline material used per ton falls with increasing scale. This non-linearity will pose issues for optimisation using linear programming, which requires a fixed pipeline cost per unit mass of ammonia. This could be resolved by using integer variables within the MILP framework to approximate the impact of the non-linearity; however, doing so will significantly reduce the speed of the calculation. Instead, a linear regression (with intercept equal to 0) was used to estimate the best fit relating the flow to total pipeline cost across the value range; the gradient of the regression is used as the input to

the MILP model. This will tend to underestimate costs at small production and overestimate at high production; however, given the large scale of regional variation between pipeline costs, this option provides a reasonable order-of-magnitude estimate.

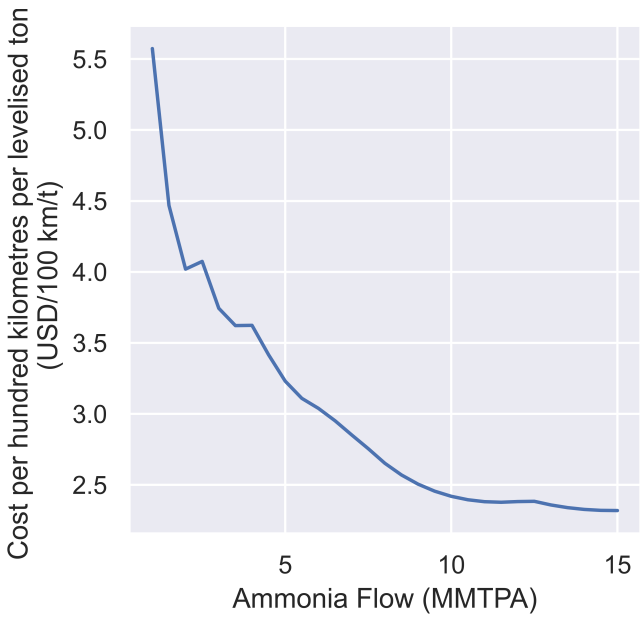

Fig. 6.1 Impact of ammonia production on ammonia pipeline cost; because the cost is not constant, small errors are introduced in the MILP optimisation

6.1.1.2 Ocean transport

The main costs of ocean transport of ammonia are the chartering of the ship (which includes labour costs) and shipping fuel, although there are other smaller costs such as port berthing and insurance. These components convert linearly into a shipping cost for ammonia based on the total number of trips required each year. In this section, it is assumed that ships carrying ammonia must pay for a return journey.

The ships used for transporting ammonia are expected to be comparable to those used for liquid propane gas (LPG), which has a similar boiling point to ammonia of $-42°C$ [15], although LNG ships can also be used for ammonia transport. Data extracted from the global Automatic Identification System (AIS) indicate there are presently over 2,500 ships capable of transporting LPG or LNG, the precise characteristics and nomenclature of which vary between ship builders. The largest of these ships (Panamax) is typically used only for LNG (not LPG) at present, but it is reasonable to assume that a global ammonia economy would make use of this size to minimise costs. These larger ships will be fully refrigerated [247]. There may be benefits associated with using smaller ships in some settings (see Section 6.2), but for simplicity this modelling only considers very large ships. This may pose technical issues for loading and unloading in small or shallow ports; however, loading and unloading ammonia is relatively simple, and, in extreme cases, can be achieved without the ship itself berthing at the port using a 'jettyless' terminal [248].

Chartering of ships is the most common method for international transport of liquid fuels. It is not common for energy exporters to own their own ships; doing so carries substantial capital risk and requires maritime expertise which energy producers may not possess. Chartering also enables more flexibility of production schedules. The chartering rates of maritime vessels are highly volatile; in 2020, for instance, LNG charters for 160,000 m^3 ships ranged from between 20,000-120,000 USD/day [249]. To some extent this volatility was caused by the COVID-19 pandemic, but it is also typical for the industry, in which changing ship availability and seasonal energy needs cause significant price fluctuations. Charter costs are estimated using the method described in Rogers [250] and capital costs reported by the ERIA [251], which also provides estimates of berthing costs. An additional 2% was added to the chartering costs for brokerage fees, and a further 2,600 USD/day were added for insurance.

It is assumed that the ships burn ammonia for fuel in a two stroke engine. The cost of that fuel on a per ton basis is taken as the global average of the top 1,000 production sites. The fuel use of these ships is estimated by Ash and Scarbrough [11] whose estimates are based on slow steaming (around 18 nautical miles/h); this slow rate tends to be more economical when fuel costs are high, which they are expected to be using renewable fuels. This is not the same as the basis for the fuel consumption estimate used for the shipping sector in general; that is described in more detail in the Maritime Case Study (Section 6.2). The total ammonia transported by a ship is given by the usable capacity of the ship minus the fuel used in transport. The usable capacity of the ship is 94% of its total capacity; this accounts for a filling limit of 98% at the supply port to prevent overpressure of the vessel, and a heel remaining in the vessel at the demand port of 4%. Shipping distances were provided by the Oxford Department of Geography which calculated the values using the AIS database.

6.1.1.3 Ammonia storage

Ammonia storage is required at the supplier, the demand site, and interim ports. At large scales, it is most cost-effective to store ammonia in insulated tanks at $-33°$C and atmospheric pressure; storage at atmospheric temperature under pressure requires far more steel to withstand the static pressure of the fluid, and is thus more costly (even though no refrigeration unit is required to recondense any boil off). The CAPEX of these tanks is reported in Leighty and Holbrook [30], and confirmed by Bartels [16]. The cost of recondensing boiled-off ammonia is estimated assuming a boil-off rate of 0.05%/day [252], a COP for the refrigeration unit of 2, an average tank level of 50%, and an electricity price of 80 USD/MWh at the port (all relatively conservative assumptions). Storage volumes forecast by the model are comparable to existing very large ammonia tanks ($\sim$ 60,000 t) [30]; around this scale, increasing storage requires the production of additional tanks. Consequently price reductions per tonne will not be observable as production rates increase, and linearising storage costs will not introduce error.

6.1.1.4 Integrated costs

Considering the transport costs outlined here and production costs outlined in previous chapters, it is now possible to estimate the delivered cost of ammonia.

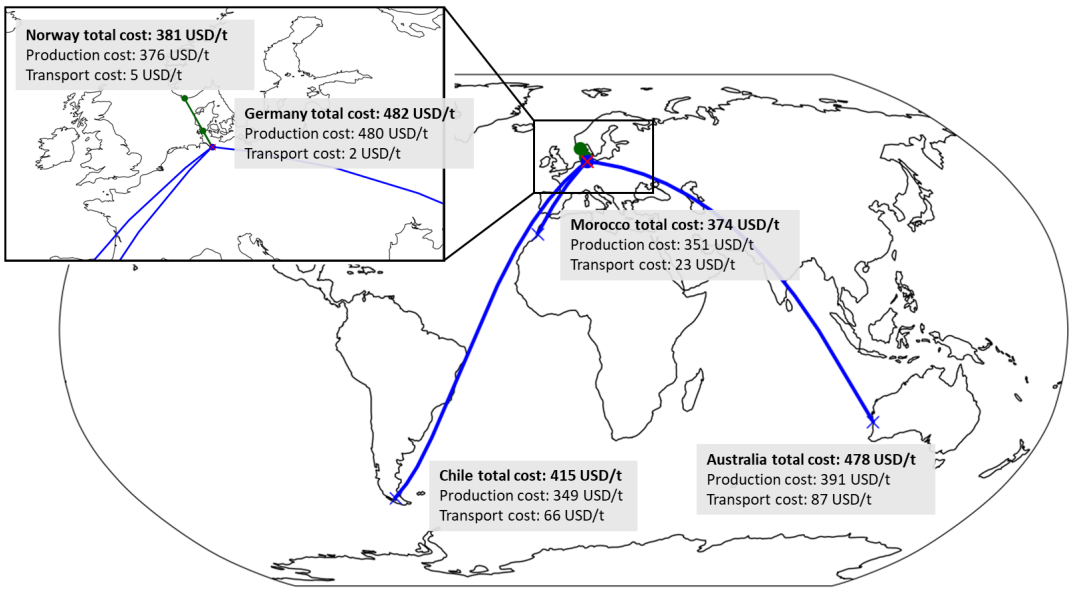

Fig. 6.2 Role of transport costs in determining delivered costs. Five example production sites are considered (**blue crosses**), along with the associated cost of delivery to the port of Hamburg (**red cross**). Some nearby sites in Germany and Norway can deliver via pipeline only (**green lines**), but more distant sites (in Chile, Morocco and Australia) need to deliver via pipelines and the ocean (**blue lines**). Although costs are dominated by production, and not transport, both need to be considered to obtain the cheapest ammonia, which comes not from the closest production sites in Germany or Norway, nor from the cheapest production site in Chile; rather it comes from Morocco, which offers a balance of cheap production and proximacy to the demand site considered.

Figure 6.2 demonstrates that considering both costs is necessary, comparing five production sites and the associated cost of transport to Germany. Local production in Germany is not affordable, with costs even higher than when ammonia is imported a very large distance from Australia. However, it is equally inappropriate to simply select the cheapest production site (Chile), because the transport costs are excessive. Regional production in either Norway or Morocco with short distance transport has a total cost that is around 10% cheaper than imports from Chile.

Although this system demonstrates the need to consider transport costs, real systems will contain far more demand sites which will compete for access to the cheapest ammonia. An optimisation approach is therefore required to determine the cheapest allocation of producer to supplier.

6.1.2 Optimisation approach

The optimal allocation of producers to suppliers is a classic example of a 'transport' problem, for which an MILP is the conventional mode for solution [253] - the same optimisation approach used for estimating ammonia costs in Chapter 3. The objective of the transport function is to minimise the NPV of the entire system while satisfying demand constraints.

In the transport problem, there are a number of supply nodes (in this case, the ammonia production locations) with an associated cost (the LCOA-P) and production capacity (as determined based on land constraints in Chapter

5). These need to be paired with demand nodes; in the maritime case study, these are ports which provide bunkering services to ships, and in the grid supply case study these are countries. In the classic version of the transport problem, there are simple costs associated with moving from each supplier to each consumer; in this version, while it is possible to take this direct route via pipeline transport, in most cases the ammonia must travel via pipeline to a transit port, after which it travels by sea. This version of the transport problem is further complicated by the need to incorporate buffer storage between nodes.

For each of the supply nodes, there are three constraints: a capacity constraint which sets the upper bound of production equal to the production capacity at that site; a mass-balance constraint, which requires that the total flow via pipeline from each production site to each port is equal to the production of ammonia at that site; and an 'activation' constraint, which is triggered if the site produces any ammonia at all, which will require the production of ammonia storage tanks on site; these must be able to buffer a week's worth of ammonia production.

In the maritime case study, the transit port nodes and the demand nodes are the same. This is managed using a mass-balance constraint: the difference between the total inflows to the port (both by pipeline and by ship) and the outflows (only by ship) must be equal to the demand at that port. In the maritime case study, the port demand is a parameter associated with that port.

In the grid case study, the demand nodes can be either ports or the geographical centroid of the country (this is required in order to satisfy demand in land-locked countries). The mass balance constraint at the centroid nodes is simply that the flow to the centroid must be greater than or equal to the centroid demand. The demand at the port and at the centroid in this case study is a decision variable (not a parameter). The relevant *parameter* is the country wide demand, and it must be equal to the sum of demands at (i) each of the ports in the country and (ii) the demand at the centroid. In other words, the model will allocate a country's demand to either the geographical centre of the country and/or to one or more of its ports, and will fulfill that demand at the location which minimises the delivered cost.

If there is any flow to a port node, then the port is 'activated' and storage requirements are triggered. There are two storage requirements. The first requirement is the same as storage at suppliers: the port must hold at least one week's worth of storage of the total inflows into the plant. The second requirement is that the tank must be able to hold more than 150% of the capacity of a single Panamax ship to ensure the tanks can load/unload a berthed ship as required.

The final additional constraint imposed in the optimisation model limits pipeline construction. In general, pipeline flow can occur between each supply node and each port node (in the maritime case study model). However, not all of these pipelines are realistic (there will not, for instance, be a pipeline between Australia and Germany). These unrealistic pipelines need to be prohibited not only to ensure sensible results but also to facilitate suitable solution times. For that reason, pipelines are banned if they (i) cross a country border and (ii) are more than 1,000 km long. Mathematically, this is incorporated after an instance of the model has been created but before it is solved;

flow between nodes which violates these rules is forced to be 0. This could also be achieved using constraints; however, this approach would increase the problem's complexity and therefore increase solution times. By contrast, the approach taken in which flow is forced to 0 before solution reduces the number of variables the model needs to solve and therefore accelerates solution. The pipeline constraint approach taken in the grid-optimisation case study is the same as that taken in the maritime decarbonisation study; the only difference is that there are now three sets of flows which can occur by pipeline (supplier to port, supplier to country centroid, and port to country centroid), but the logic behind the constraints is the same.

Having set up the optimisation model, it can now be applied to different demand cases. The following two sections explore two of these demand cases: they describe how demand was estimated, and then report the results of the associated optimisation.

6.2 Case study: Maritime decarbonisation

Maritime transport handles around 80% of global trade by volume[254], making it imperative for the global economy. However, maritime vessels currently run predominantly on cheap, energy-dense heavy fuel oils (HFO), which are responsible for around 2.9% of global anthropogenic greenhouse gas (GHG) emissions [255]. In 2018, the International Maritime Organization (IMO) committed to decarbonize the sector, aiming to reduce GHG emissions by 50% in 2050 compared to the 2008 baseline, alongside a set of other regulatory actions [255].

The shipping industry faces considerable hurdles to achieve the decarbonisation targets set, given long asset lifetimes, the price gap between HFO and green fuel options, and the large number of independent stakeholders which will need to coordinate (e.g. engine manufactures, ports, carriers, production facilities, investors) [128]. As such, there is considerable uncertainty in the cheapest path for decarbonising the maritime sector. This section considers whether ammonia would make a suitable target fuel for the sector, focussing on demand in 2050 when the sector should be deeply decarbonised.

To do so, the optimisation model introduced in the previous section is run using 1,360 ports, and 15,000 potential production locations. Two future decarbonisation scenarios are considered for 2050, a moderately ambitious (MOD-AMB) future scenario and highly ambitious (HIGH-AMB) future scenario, which are based on assumptions regarding future shipping trade (including overall growth in trade, and reduction in the quantity of fossil fuels that will be shipped in 2050), the levelised cost of ammonia production, and fleet adoption rate of ammonia-compatible maritime vessels (see Table 6.1 for a brief summary, and Table D.1 in the appendix for more detail on inputs to the ammonia cost estimation model). The overarching model is schematised in Figure 6.2.

Although 15,000 supply sites were considered (based on a 1 x 1 latitude-longitude grid, and including only onshore sites), allowing each of these to be used in the optimisation would have unduly slowed down the solution. Therefore sites were excluded if production capacity was less than 1 MMTPA (since these sites would not benefit from economies of scale, and would struggle to access suitable land). A heuristic of considering only the top 4,000

sites was then applied; this does not affect the model outcome, since the *production* cost at the 4,000th site is greater than the most expensive *delivered* ammonia in the model (meaning no more expensive production sites would ever be selected by the optimisation) but enables more rapid solving times. This is represented by the Site Selection Heuristics box on Figure 6.3.

Table 6.1 Scenarios considered for maritime decarbonisation case study

Description	MOD-AMB	HIGH-AMB
Socio-economic growth (SSP scenario)	Shared Socioeconomic Pathway 'Middle of the Road' (SSP2)	Shared Socioeconomic Pathway 'Sustainability' (SSP1)
Decarbonisation rate (RCP Pathway)	Representative Concentration Pathway 4.5 (RCP 4.5)	Representative Concentration Pathway 2.6 (RCP 2.6)
Fleet ammonia adoption rate	70%	90%
Levelized energy cost from solar PV with capacity factor = 20%	14.4 USD/MWh	10.7 USD/MWh
Levelized energy cost from onshore wind with capacity factor = 45%	21.9 USD/MWh	20.0 USD/MWh
Average Levelized ammonia production costs	260 USD/tonne	237 USD/tonne

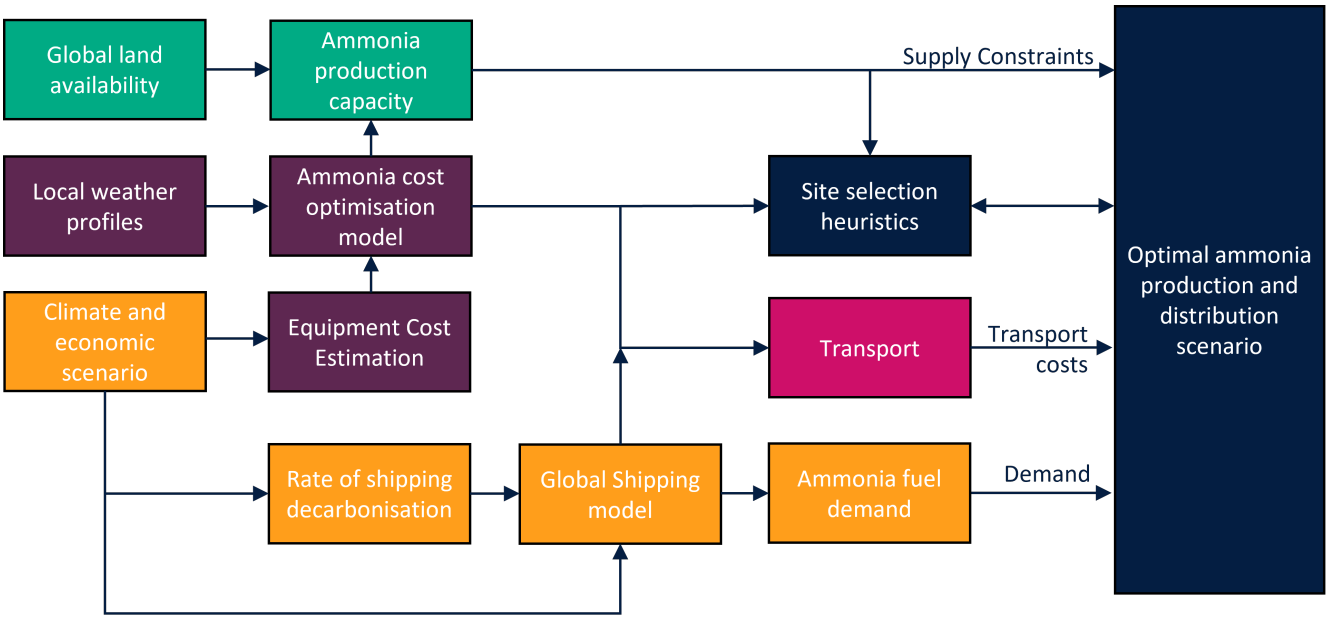

Fig. 6.3 Summary of information flow into maritime decarbonisation case study. Purple inputs come from Chapter 3, green inputs come from Chapter 5, pink transport costs are described earlier in the chapter (and depend on ammonia production costs because of shipping fuel consumption), dark blue boxes describe the optimisation model, and yellow boxes describe the demand information.

A small adjustment is made to the production model described in earlier chapters: a regional future cost of capital is incorporated, to take the risk associated with financing energy projects into consideration. To capture the differences in discount rate between potential production regions, data from was taken Ameli et al.[256]'s "Reduced scenario". It implies a high degree of trade between all countries and relatively small differences in discount rate compared to business-as-usual by 2050. Using that scenario is consistent with the SSP1 and SSP2 frameworks

which underpin the cases considered here.

Note also that in Chapter 5, the land competition factor in the calculation of ammonia production capacity was set to 2% to match the consumption of energy by the fertiliser sector. The consumption of energy by the maritime sector is roughly the same, based on the fuel demands calculated in the following subsection (223 MMTPA of HFO) and a total global energy consumption of around 420 EJ [257]. For land availability, the base case data from Chapter 5 is used.

Wang et al. [69] developed a similar optimisation strategy; however, their system was significantly lacking in detail: they considered far fewer potential ammonia production sites, they did not differentiate between land and ocean based transport, they did not sensibly measure ocean transport distances, their shipping dataset was far smaller, and they did not project costs out to 2050.

6.2.1 Demand estimation

Demand estimates for each port in the model were determined via a collaboration with the Oxford University Department of Geography. The Oxford Program for Sustainable Infrastructure Systems has a global model for shipping based on predicted patterns of trade and the AIS database. This enables a prediction of the number and size of ships which will travel between each of the ports in the model, based on the prevailing economic conditions. For instance, in the HIGH-AMB scenario, (i.e. SSP 1 and RCP 2.6), global models predict relatively little fossil-fuel usage and transport, so the model will not include significant allocation of shipping fuel to transporting coal, oil and natural gas.

This model was updated to estimate the fuel demand associated with each of these journeys. The fuel consumption was estimated based on a linear regression which depended on ship type, ship deadweight tonnage, ship installed power capacity, and the cube of the ship speed. The parameters were calibrated based on a dataset of 97,000 journeys. This enabled the calculation of the fuel consumption for each journey in the original model, which could then be allocated to the port at which the journey began. The model calibration data used heavy fuel oil (HFO) as the shipping fuel; this was converted to an ammonia demand assuming that the energy efficiency would be unchanged.

The model predicts that fuel demand expected to increase to 446 million tonnes million metric tons per annum (MMTPA) of HFO under the MOD-AMB scenario and 434 million tonnes MMTPA of HFO under the HIGH-AMB scenario in 2050. Assuming that only routes of more than 1,000 km ($\sim$94% of fuel demand) will be decarbonised by ammonia) this translates into a total demand of 595 million tonnes under the MOD-AMB scenario and 691 MMTPA under the HIGH-AMB scenario in 2050.

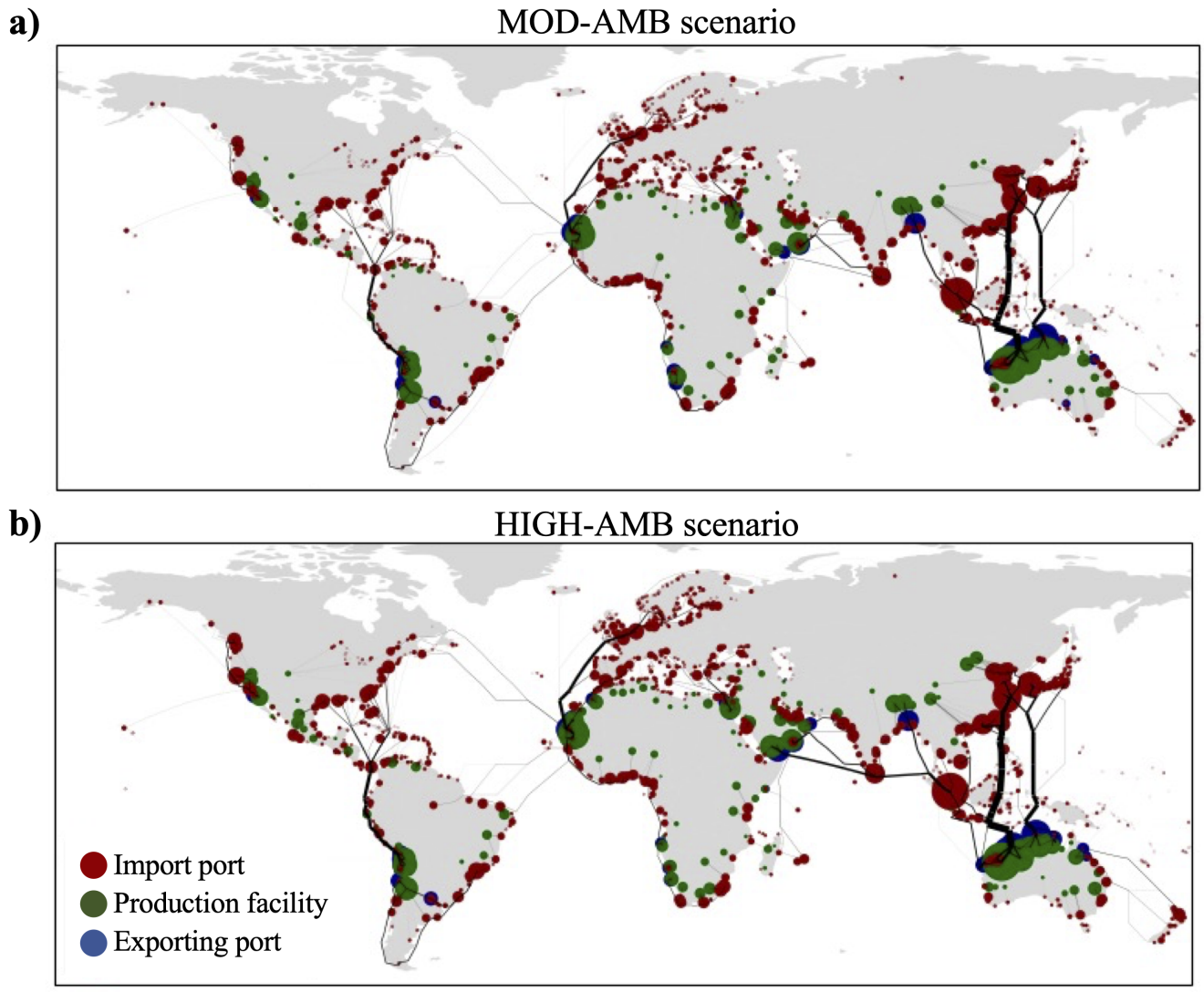

Fig. 6.4 Optimal spatial fuel supply to meet global port fuel demand. **(a) - Top**: Cost-optimal fuel supply-chain under the MOD-AMB scenario, with green markers indicating production locations, blue markers fuel exporting ports, red markers fuel demand ports, and the lines the fuel shipments from exporting to demand ports. **(b) - Bottom**: Same as (a) but under the HIGH-AMB scenario. Larger dots and thicker lines indicate larger ammonia flows.

6.2.2 Results

A representation of the ammonia distribution in both scenarios is shown in Figure 6.4. On average, the delivered ammonia cost is 237 USD/t for the HIGH-AMB case, and 260 USD/t for the MOD-AMB case. Because a greater fraction of ships are fuelled by ammonia in the HIGH-AMB scenario, its total investment requirements are higher, but only by 6% relative to the MOD-AMB scenario, despite 16% more ammonia being consumed.

A breakdown of the ammonia cost in each region is shown for both scenarios in Figure 6.5. The cost for each region is relatively similar – the largest difference is between East Asia and Northern Africa, but is only about 15% of the value of the fuel. Costs per levelised ton increase across the entire value chain in the MOD-AMB scenario compared to the HIGH-AMB – the model slightly compensates for increased production costs by

using supply locations which are further away, increasing transport costs. The exception is port storage costs, which depend on both demand and the size of the gas transporter used to export/import the ammonia. The latter constraint dominates at most ports, and therefore the total storage cost is equivalent across both scenarios and is therefore about 16% higher in the HIGH-AMB scenario.

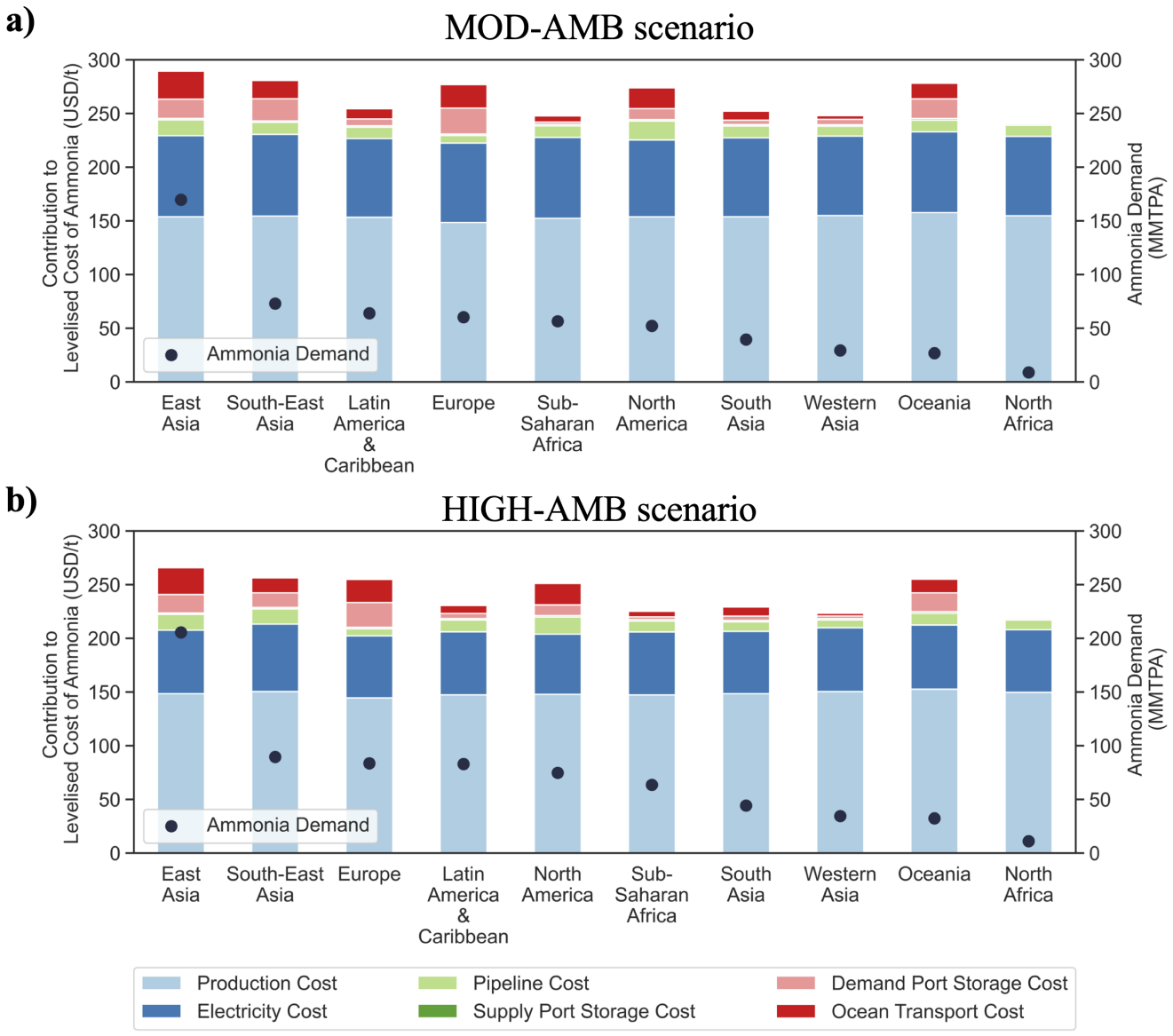

Fig. 6.5 Regional variations in levelised cost of ammonia and cost breakdown. **(a) - Top**: The total LCOA across geographic demand regions under the MOD-AMB scenario, including the cost breakdown in six cost components (production, electricity, pipelines, supply storage, demand storage and ocean transport). **(b) - Bottom** Same as (a) but under the HIGH-AMB scenario. The black markers indicate the total ammonia demand per region.

In both the MOD-AMB and HIGH-AMB scenarios, considering production alone, the cheapest production locations in 2050 predominantly rely on solar electricity. Although the capacity factor of solar (which is between 20 and 30% for most locations at latitudes $< 40^{\circ}$) is lower than the best wind sites, its CAPEX is very low: 184 USD/installed kW and 240 USD/installed kW for the HIGH-AMB and MOD-AMB scenarios respectively. The av-

erage production costs, weighted by production capacity at the top 4,000 sites, are 193 USD/t and 214 USD/t in the HIGH-AMB and MOD-AMB scenarios respectively. The cumulative production capacity across these sites is around 17,000 MMTPA in both instances; i.e., almost 25 times the predicted ammonia demand, despite the significant constraints imposed on land usage in determining production capacity. Evidently, using land-efficient solar for ammonia production will have much greater production capacity than forecast.

For both scenarios, shipping distances are generally quite short: for ammonia that is transported by ocean, the average maritime distance travelled is around 4,800 km, and only 0.03% of ammonia travels 10,000 km or more (which, for reference, is the approximate maritime distance from the Middle East to Western Europe). This is driven by (i) the relatively high cost of shipping ammonia compared to conventional fuels, and (ii) the abundance of high quality solar resources in all regions globally, which reduces the need for long distance transport.

The optimum export market predicted here is somewhat concentrated: 180 countries have ports which need to be supplied by fuel, but only 30 ports in 11 countries export fuel in the MOD-AMB scenario (which rises to 32 ports in 14 countries in the HIGH-AMB scenario). These exporting ports supply around 75% of the total ammonia demand in both scenarios, with the balance being provided by land transport, which is predominantly domestic (42 countries in the MOD-AMB scenario produce at least some of their ammonia themselves).

Australia is dominant in the international export market, contributing almost 50% of the total exported ammonia in both scenarios, and almost four times as much as the second largest exporter, Chile. Considering the costs of production only, it is not the best candidate. It has neither the cheapest production site selected by the model: of the 300 active production sites, its best is 48th (52nd) in the HIGH-AMB (MOD-AMB) scenario. Nor is its production remarkably cheap on aggregate: in both scenarios, it is only 19th on a ranking of all ammonia-producing nations by production cost, beating just two other exporting countries, and costing almost 10% more than the cheapest exporting country (Argentina).

This demonstrates the importance of robust consideration of both supply chains and land availability. Comparing north-western Australia and cheaper locations in South America and north-western Africa, the production cost difference is overcome by the relatively short shipping distance from Australia to the large hubs in Asia, which represent almost 50% of fuel demand in both scenarios. Land availability is also a significant consideration: in the MOD-AMB scenario, Singapore receives ammonia from both Australia and Bangladesh. Although the ammonia which originates in Bangladesh is slightly cheaper, it cannot meet Singapore's very large 33 MMTPA fuel demand alone, which means marginally more expensive ammonia must be sourced from Australia, which has much greater land availability.

The dominance of solar as an energy source is even more pronounced in the supply-chain model than in the production model. For instance, there are some very low-cost production locations in southern Chile and Argentina which are based entirely on wind, whose production cost is less than 210 USD/t, and are therefore competitive. However, because those sites fall mostly within the National Parks of Patagonia, they are excluded from producing

in this model. Similarly, the best potential sites in the UK are off the coast of Scotland, and would use mostly wind to produce ammonia for around 250 USD/t (HIGH-AMB). Ammonia storage, and a pipeline from northern Scotland to southern England, where port demand is concentrated, would add about 20 USD/t to the delivered cost. There is very little land available in the best wind regions in Scotland, so most of the wind would need to be sourced offshore, further pushing up the price – even if this could be done at a cost competitive with onshore wind, it would struggle to outcompete cheaper imports from north-western Africa, which are delivered to the UK at an average price of 235 USD/t in that scenario. In both scenarios, fewer than 20% of production nodes use any wind at all, and even at those sites, wind is not dominant: less than 1% of the installed energy capacity of the ammonia production infrastructure globally comes from wind.

Because of the low cost of solar, production tends to be clustered relatively close to the equator. The HIGH-AMB scenario has more production at locations with larger absolute latitudes; because a greater fraction of shipping fuels are decarbonised in that scenario, sites with less favourable weather profiles need to be used. However, the effect is fairly small: in both scenarios, less than 10% of ammonia is made at an absolute latitude of greater than 30°, and less than 2% is made at an absolute latitude of greater than 40°. As a consequence of this preference for solar, some regions produce very little ammonia themselves – Europe, for instance, consumes about 9% of ammonia demand in both scenarios, but produces less than 0.05% of the global supply.

Figure 6.6 shows the investment required to develop the ammonia supply chains. The vast majority of global investment is supply-side (i.e. ammonia production and land transport to transit ports - panels (a) and (b)) – only 8% is invested in ocean transport and storage at demand ports - panels (c) and (d). The total value of investment required is estimated to be in the order of 2 trillion USD.

6.2.3 Maritime decarbonisation summary

This section has provided a blueprint for the decarbonisation of the shipping industry. Such blueprints are vital for reducing the uncertainty which hinders the very large investments required.

The implications are striking. Current dependence upon oil-producing nations, with crude oil being shipped very long distances and being separated into HFO nearer to demand hubs, is likely to be replaced by a more regionalised industry; green ammonia will be produced near the equator in countries with high solar potential and abundant land, and shipped to regional centres of shipping fuel demand.

At present, the model optimizes for the least-supply cost in 2050. There are two factors which are likely to prevent the least-cost solution from being realised. Firstly, energy security requirements may lead to countries to adopt a non-optimal approach to sourcing ammonia: they may source it only from allies, require their ammonia to come from a variety of countries, or pay a premium for domestic production (as described in the previous chapter, this may drive production offshore). Secondly, this model presents a snapshot for 2050, and does not consider prior optimal solutions. For instance, it is likely that green ammonia will be produced using wind energy in Europe;

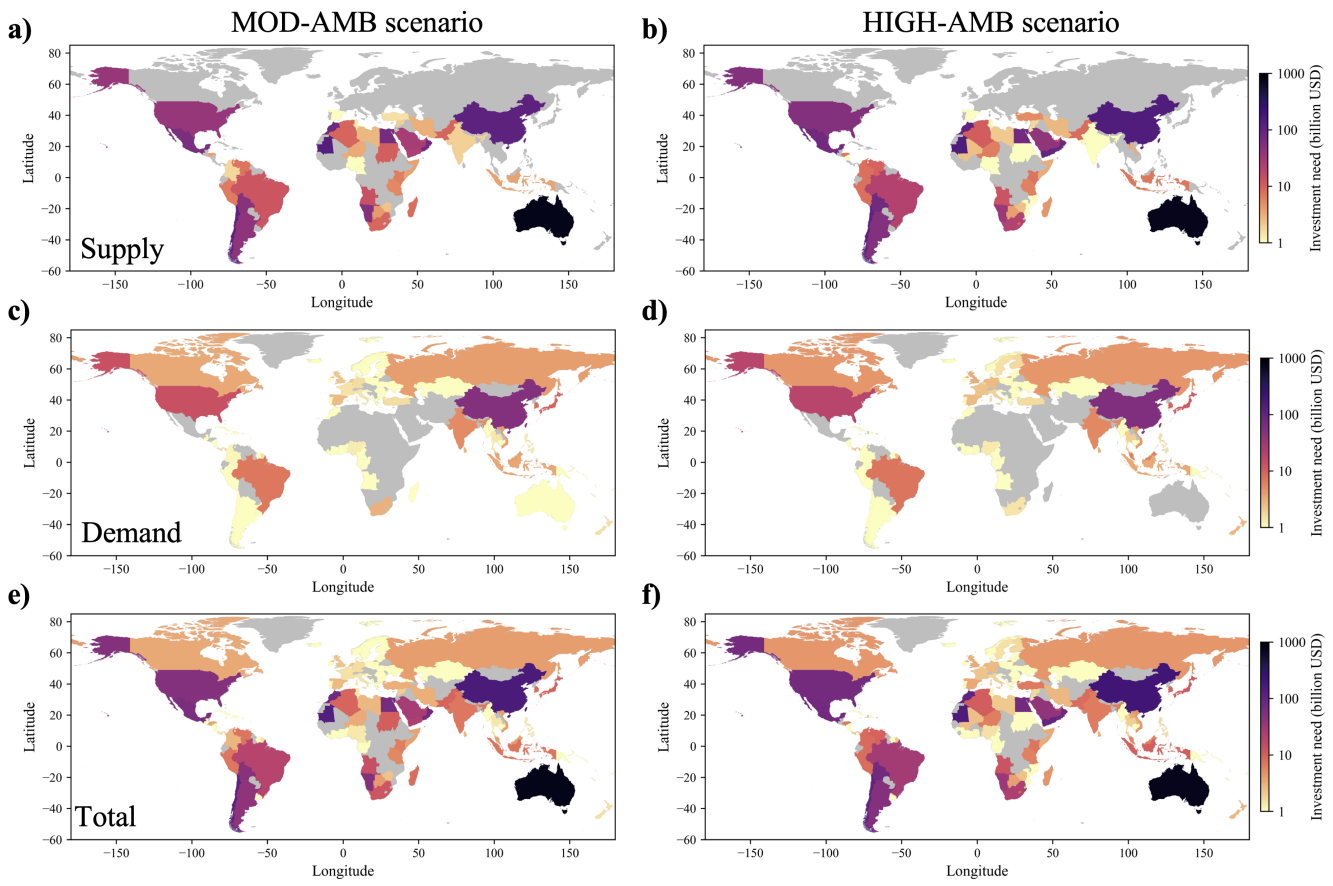

Fig. 6.6 Global supply and demand-side investment needs. **(a-b) - Top**: Total supply-side (production, electricity, pipelines and supply storage costs) investment need across countries under the MOD-AMB (a) and HIGH-AMB (b) scenario. **(c-d) - Middle**: Total demand-side (demand storage and ocean transport costs) investment need across countries under the MOD-AMB (c) and HIGH-AMB (d) scenario. **(e-f) - Bottom**: Total investment need (supply and demand-side) across countries under the MOD-AMB (e) and HIGH-AMB (f) scenario.

that production may be among the cheapest globally in the 2030s due to favourable project finance, government support, and high-quality wind resources. Although wind-based production will eventually be surpassed by solar production, those plants will still exist and will contribute to meeting global demand.

Future research should consider both of these factors, estimate how much deviation they may cause from the optimum, to determine the extent to which those deviations are justified.

At the same time, research outside the engineering space needs to consider how socio-economic structures can enable the optimal ammonia distribution to be achieved. In particular, this will require a clear regulatory environment, and strong financial support for ammonia production around the world, including lower- and middle-income countries, which require approximately 50% of the total global investment.

6.3 Case study: Dispatchable grid supply

Although the maritime sector will likely be responsible for the vast majority of ammonia consumption by 2050, the range of applications of ammonia will likely also see significant consumption in other sectors. This section demonstrates that the transport MILP developed in this chapter is also suitable for considering these other sectors,

and focusses in particular on back-up energy for the grid. As identified in earlier chapters, ammonia is well-suited for this duty where seasonal energy storage is required because it is liquid under mild conditions and relatively dense. This case study assumes that wind and solar are the primary source of energy for the grid, and that they can be easily stored for short periods using batteries; it identifies countries where these sources of energy will be inadequate to meet demand, and how much it would cost to fill the gap by using green ammonia.

There are, of course, many other options for energy production to meet electricity demand where wind and solar fall short: (i) alternative renewables (e.g. hydro, biomass, geothermal); (ii) nuclear energy; (iii) long-distance HVDC electricity cables; and (iv) efficiency improvements, and (v) demand-response policies are all likely to be used to some extent. This case-study provides a benchmark ammonia cost against which these other technologies and policies can be measured.

Developing robust electricity systems which can always meet demand is a complex problem which has already been, and will continue, to be the subject of a significant amount of research [82]. Therefore, while the purpose of the previous case-study on maritime usage was to provide a very detailed picture, the purpose of this case-study is instead to (i) demonstrate the applicability of the method, and (ii) form preliminary, high-level conclusions that can inform future work.

Like the previous case study, this section uses costs for 2050. This introduces a challenge of forecasting how both total electricity consumption and the profile of electricity consumption will change over time, since the electricity profiles considered relate to 2019. As a basic assumption, this section assumes that the electricity profiles themselves will not change between now and 2050; the implications of the changing profiles are discussed in Section 6.3.4.

The information flow through the model for this case study is slightly different to that used in the Maritime section - see Figure 6.7.

6.3.1 Demand Estimation

Hourly grid electricity consumption for 2019 was sourced for 52 countries [194]. The data contain some irregularities – Japan's demand, for instance, is incongruously low; the hourly grid consumption of all countries is therefore scaled so the total consumption matched that calculated by the IEA for 2019[133]; Japan is the only country whose cumulative energy demand was mismatched from the total by more than 10%. Where hourly data was not available for a country, the total annual electricity demand was taken from the IEA (adding 92 countries to the dataset), although in general, where only the total electricity demand was available, it did not translate into a positive ammonia demand.

Using the ERA5 and MODIS6 datasets described in Chapter 5, the maximum potential renewable energy production for each country was also calculated on an hourly basis. A country could also exploit offshore resources within 100 km of their border (where a potential production site was within 100 km of the shoreline of multiple countries, it was allocated to the most nearby country). At each location, the country can either install wind or

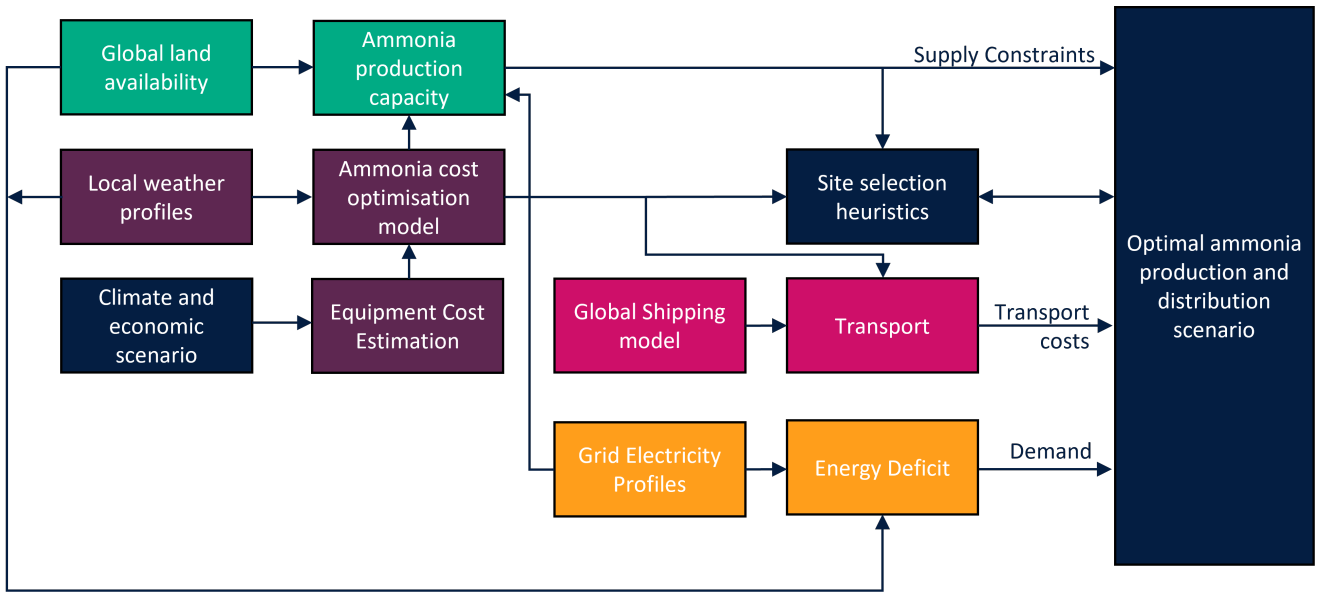

Fig. 6.7 Summary of information flow into the grid dispatch case study. As for Figure 6.3, purple boxes come from Chapter 3, green boxes come from chapter 5, yellow boxes are demand calculated in this chapter, and dark blue boxes are the optimisation model. In this case, renewable energy availability and land availability estimates, alongside grid energy consumption, inform the demand estimate. Grid electricity usage also constrains ammonia supply; it is assumed that ammonia production only occurs with any electricity available in excess once grid demand has been satisfied.

solar; considering both land availability and the capacity factor of the renewable in that location, it will select the technology which produces a greater total amount of energy each year.

Ammonia demand is particularly sensitive to the land competition factor outlined in Chapter 5. At present, electricity represents around 20% of total global energy consumption [257]. Obviously, that fraction will increase in the future as a range of sectors are electrified. This increase will cause new electricity demands that are not featured in the available grid data. 20% is therefore taken as the base-case land competition (in order to determine both ammonia demand based on renewable electricity availability, and to determine ammonia production capacity). 20% would not be an appropriate value for the land competition faced by all electricity by 2050, but it is an appropriate value for the land competition faced by the specific grid electricity usage represented by the data. Wide sensitivity ranges are considered, with a high-land competition case of (only 10% of land available for powering the grid) and a low land competition case (30% of land available for powering the grid).

Because highly efficient batteries will be widely available by 2050, the total renewable energy production will not need to exceed the grid consumption in every hour. However, since energy storage in batteries is expensive compared to ammonia, batteries will not be suitable for seasonal storage. It is therefore assumed that if there is a net energy deficit whose duration is greater than 24 hours (low battery scenario) or 72 hours (high battery scenario), then ammonia is required to fill the gap; it is assumed it can be converted into electricity with an efficiency of 60% [27]. The ammonia demand estimate is not as sensitive to battery storage duration as to land competition - the difference between the low and the high battery storage case is between 8% (high land competition) and 20% (low land competition).

The ammonia demands estimated between the cases span from 26 MMTPA (high battery, low land competition) to 202 MMTPA (low battery, high land competition); Figure 6.8 shows the breakdown of ammonia demand in the latter case. Consumption will therefore not be as high as the maritime sector, but could be very significant, and even exceed existing fertiliser demand. Demand is concentrated in Europe, although there are also major hubs in Singapore and Japan.

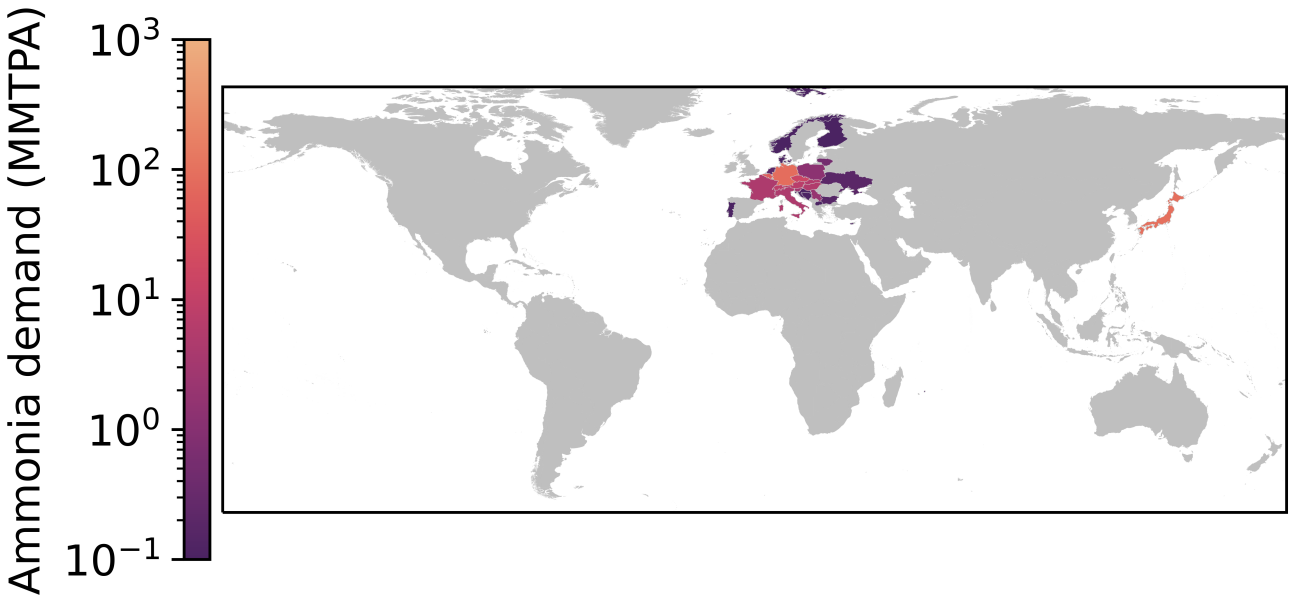

Fig. 6.8 Demand for ammonia as a back-up energy source, assuming a high land competition of 10% and low battery availability. Countries shown in grey have no ammonia demand; the vast majority of countries fall into this category because of the abundance of renewable energy. Only a small number of countries, predominantly in Europe, will struggle because of their high population densities (which lead to high grid demands and limited land availability) and relatively poor solar insolation.

6.3.2 Model adjustments

The most significant adjustment to the model for this case study was described in Section 6.1.2; this enables a country's ammonia demand to be satisfied either be delivery to any port in the country or to the geographical centroid of that country.

Additional constraints were also imposed on ammonia production capacity. If a country is unable to meet its domestic electricity needs, it is not likely to export more energy in the form of ammonia. Each country's total production capacity is therefore capped so as to not use more energy for ammonia production than the difference between the total renewable potential and the grid electricity demand (summed over the course of a year). It is therefore possible in the model for a country to produce its own ammonia domestically; this could occur in a location where there were a number of days on which renewable energy generation was particularly poor (creating demand for ammonia), but in which there was generally more renewable energy capacity than there was demand. In practice, though, where a country has an ammonia demand, no country produces that ammonia domestically in any of the cases considered; all countries with an ammonia demand opt to import.

6.3.3 Dispatchable grid supply results

Figure 6.9 shows the distribution of ammonia under this demand scenario.

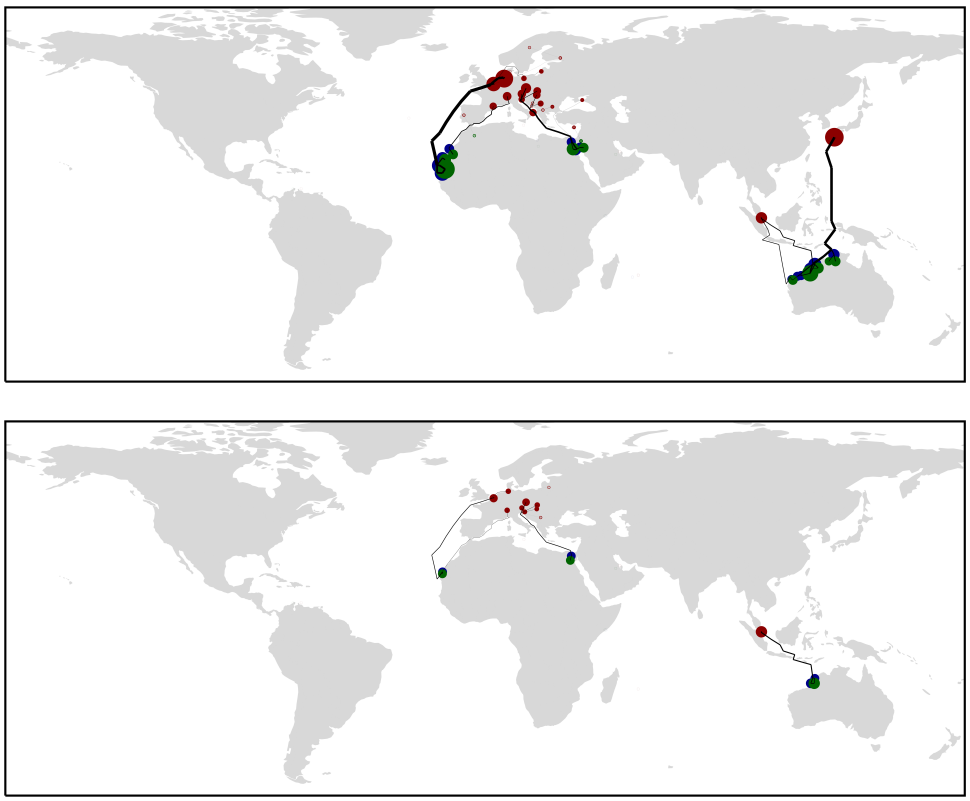

Fig. 6.9 Cost-optimal distribution of ammonia to operate as back-up power supply. As for Figure 6.4, green markers indicate production locations, blue markers indicate fuel exporting ports, and the lines are ammonia transport. Here, red markers indicate fuel demand locations which could be either a port inside the country which has an ammonia demand, or a country centroid. Larger dots and thicker lines indicate larger ammonia flows. **(a) - Top**: Low battery availability, high land competition; **(b) - Bottom**: High battery availability, low land competition.

In comparison to Figure 6.4 (the equivalent figure for the maritime demand case study), Figure 6.9 is relatively 'sparse', which is to say that demand is concentrated in a relatively small number of locations (alongside there being only around 30% of the absolute demand even in panel (a), the high demand scenario). The largest ammonia consumer in the maritime model is the port of Singapore, which represents around 5% of the total demand; by contrast, Japan, the largest consumer in this grid-dispatch model, consumes 30% of the total demand, followed closely by Germany which consumes 28%. However, even though the number of flows, as well as the total demand is relatively reduced in this grid case study, the locations in which ammonia is produced are broadly similar: Asia is supplied by north-western Australia, northern Europe is supplied by Morocco, and southern and central Europe by the Middle East. Again, solar dominates ammonia production. Even though the total flows are substantially reduced in the low demand scenario (panel (b)) compared to the high demand scenario, the ammonia production locations are the same. Where Australia was the primary source of ammonia production in the maritime model, the largest supplier in this grid model is Morocco; this is because the largest demand hub has moved from Asia (maritime model) to

Europe (grid-dispatch model). These results add weight to the core conclusions of the previous case-study: (i) the location of ammonia production must balance both low production costs and proximity to demand sites; and (ii) accurate estimates of land availability and competition are critical to form sensible predictions of future energy systems reliant on chemical fuels. To add more detail to point (ii): where land availability constrained ammonia production at the best supply sites in the maritime model, it played a different role in this case study, instead having a powerful influence over ammonia demand, rather than supply. In either case, the modelling indicates that, based on reasonable estimates for the demand of maritime fuel/back-up grid power, renewable energy generation in some locations will approach the maximum which would reasonably allowed while respecting existing and future land-uses, and managing those land constraints will be both a significant challenge for government policy and industry strategy.

There was very little variance in the LCOA-D across the cases - ranging from between 230 USD/t and 235 USD/t regardless of the size of the demand (using the HIGH-AMB inputs from the maritime case study section for ammonia cost estimation), which equates to an operating cost of approximately 60 USD/MWh. The extent to which this could be competitive with other technologies depends on the capacity factor and CAPEX of the ammonia turbine, but would likely be competitive with new build nuclear technology, which the IEA estimates will cost more than 100 USD/MWh in most developed economies in 2040 [258]. At these prices, using imported ammonia for back-up energy would be likely to be competitive in a number of countries.

6.3.4 Dispatchable grid supply conclusions

Although estimation of ammonia demand for the electricity sector is more complex than for the maritime sector, this section has demonstrated the significant sensitivity of back-up grid demand to land competition, and shown that electricity generated from imported green ammonia in 2050 can be competitive with other options for back-up power. It has added further evidence to the most significant findings of this chapter: the need to consider whole of supply chain costs, and the importance of land availability in designing energy systems reliant on ammonia.

This model would benefit from the same improvements described for the maritime case study. There are also three additional areas in this specific model which need further work. Firstly, energy sources other than wind and solar (nuclear, hydro, biomass, interconnection to other countries etc.) should be included. However, the model is still somewhat useful even where it has neglected those sources; it provides a baseline cost for dispatchable energy from ammonia which is useful for comparison to any other means of supplying back-up power.

The model's second major limitation is that it does not consider future changes to the grid. Including these changes will need to factor changes to both total electricity consumption, and to patterns of electricity consumption. Changes to total electricity consumption are impacted by growing access to electricity in developing nations, efficiency improvements, and electrification of transport and heat. Changing patterns of consumption will be driven by smart grids, demand-response, and electric vehicle charging (on a daily level); and by increased use of heat

pumps/air conditioning, and climate change itself (on a seasonal level). These should be considered in further work.

Finally, when determining the renewable energy generation capacity of a country (which ultimately determines ammonia demand), the model chooses, between wind and solar, the technology which will produce more energy in a given location. In general, this causes the model to select solar, because solar energy is significantly more land-efficient than wind. This may not always be the sensible choice; sometimes it will be preferable to install wind even if it produces less total energy, if that energy is produced at useful times of the year. For instance, solar generation in northern European winter is typically very low, which may have lead to artificially high estimates of ammonia demand during that season where solar was installed in place of wind.

6.4 Ammonia Supply Chains Summary

This chapter is the capstone of the thesis: it brings together the ammonia cost estimation results from chapters 3 and 4, the land availability estimation from chapter 5, and a new model introduced for combining supply and demand.

This new model was used for two case studies, from which a large number of conclusions can be drawn. Among the most significant: (i) the cheapest ammonia both for production and delivery will originate near the equator in locations with high solar radiation (independent of the land-use case); (ii) appropriate determination of ammonia supply sites depends on the costs of both production and transport, and neglecting either will lead to a non-optimal solution; (iii) because of ammonia's lower density compared to some fossil fuels and the large number of viable ammonia production regions globally, trade in ammonia is likely to be more regional than present-day energy markets; and (iv), land limitations will influence ammonia production and distribution, potentially on both supply and demand side depending on the end-use case.

Specific model tweaks and improvements were described in the individual case-studies, but there is a much more significant area of further work to be embarked upon: enabling the optimal solution identified in this chapter to become a reality. Most importantly, the low values of the LCOA-D in the future rely on significant cost reductions for production technology. Those cost reductions will be driven by the uptake of that technology itself. This will require ambitious first-movers in the production space, offtake commitments from consumers and governments, a transparent regulatory environment, and global cooperation on a range of issues from project financial support, open technology flow and trade.

Chapter 7

Conclusions

7.1 Summary of thesis

This thesis develops what is, essentially, a pre-feasibility study for a global system for green ammonia delivery. The core output of the research, presented in Chapter 6, was an optimisation model which considered both the supply and demand of green ammonia, and optimised the overall system of production and transport to minimise the levelised cost of delivered ammonia. The earlier chapters in this thesis focussed on developing the necessary inputs to that model, predominantly on the supply side.

Chapter 3 developed a model that determines the cost of green ammonia produced from wind and solar resources. This modelling is complicated by the need to optimise production facilities created by the inherent variability of wind and solar energy, and by the limited flexibility of green ammonia production. In developing this method, this chapter also considered the potential impact of the electricity network, and various techniques which might be used to accelerate the solution of the model to enable it to be solved on a global scale in a manner which was computationally tractable.

Chapter 4 marks a slight deviation from the trajectory of the thesis, and its main purpose is to validate the methods used in Chapter 3. Although the Mixed Integer Linear Programming approach used in Chapter 3 is increasingly widely used in energy system design, it relies on perfect forecasting and runs the risk of overfitting the system design to the precise conditions considered by the optimisation problem. Chapter 4 tackles this limitation by demonstrating that tweaking the optimisation function using a model predictive control approach can enable green ammonia plants to operate without perfect foresight of long-term weather patterns.

Estimating the cost of green ammonia alone is insufficient for developing a global supply network model, as the optimisation will simply source all of the product ammonia from the cheapest supply site. It was therefore necessary to develop an estimate of the largest constraints to green ammonia supply, and this was the purpose of chapter 5, which focussed particularly on the limitation posed by the area required for large scale green ammonia production. It used satellite data to assess land availability, and used that data to determine the capacity of renewables which

could be installed at a given location, which was then translated into an approximate ammonia production capacity. Land limitations might imply benefits to offshore production, and this chapter also investigated the potential benefits of producing ammonia from floating offshore wind, demonstrating that in some regions, offshore resources may be an economically feasible option.

Having developed a detailed supply model in the early chapters, chapter 6 integrates these inputs into the optimisation model. To estimate ammonia demand, the model considers two cases. The more significant focusses on decarbonising the shipping industry using ammonia, for which fuel demand was estimated by considering future trade requirements in collaboration with the Department of Geography. Including that information in the optimisation model showed a strong bias towards green ammonia production from solar electricity, and that transport of energy via ammonia in the future is more likely to occur on regional length scales than intercontinental ones. The second smaller case study considered the role of ammonia in decarbonising energy grids; using the land availability forecasts from chapter 5 and published data on grid demand, it determined which countries would face a shortfall in renewable energy from wind and solar, and estimated the cost of filling that shortfall using green ammonia. The purpose of this case study was not scenario modelling; it was instead to provide an estimate of the potential value of ammonia as an energy vector for achieving stability in electricity grids.

7.1.1 Answer to research question

The core question posed by this thesis was "What are the core features of a global system for the production and distribution of green ammonia?". The simplest answer to this question provided by this thesis would have three key tenets:

1. The future global energy system is likely to require significantly more green ammonia than is used today, with a production increase by a factor of 5 likely required for an ambitious decarbonisation required.

2. By 2050, the cheapest means of producing green ammonia will be solar PV, and it will dominate the means of production.

3. Producing ammonia locally to meet local demand will not be the most cost-effective means of delivering energy; however, nor will production in just one or two highly centralised global hubs. Given the impacts of land constraints and the relatively high cost of ammonia transport compared to liquid fossil fuels, the optimal system will regionally distribute production to the many areas globally with high quality renewable resources.

The more complex answer to this question is provided in each of the chapters: Chapter 3 shows that a global system will, in the short term, benefit from electricity grids, and that local optimisation of production is important to bring down costs; Chapter 4 shows the importance of weather forecasting and questions the role of ammonia plant flexibility in the long term; Chapter 5 shows that land limitations could drive production offshore.

7.2 Critical Review

Although considerable care was taken to include a high degree of detail, the overarching goal of the thesis (a global pre-feasibility study for a green ammonia system) necessarily required a degree of simplification of details that may impact specific regions or projects. Chapter 3, in particular, provided high level estimates of production costs, but there are many features which are location-specific which would need to be considered by project developers. For instance:

1. Water costs were estimated based on desalination; however, for inland locations there may be significant transport costs that were not considered. The pipeline costs shown in Chapter 6 for ammonia were not large, implying that water transport costs would be similarly not large, but individual projects could be significantly affected.

2. Wind production was estimated using a simple wake factor and a single wind-turbine curve. Real wind projects optimise the layout of wind turbines, and may use turbines that are more suitable to operating at low speeds at the back of the array to minimise the losses caused by the wind wake. Capturing this detail requiresreal wind measurements, and complex wind farm optimisations that need to be performed on a site-by-site basis.

3. Combusting ammonia for energy is not widely performed at the moment, but may be a cheaper alternative to batteries and hydrogen fuel cells for maintaining the supply of back up power to the ammonia plant; again, this would depend on the specific wind profile and would need to be considered on a site-by-site basis.

4. There is significant uncertainty in many of the input parameters used in this chapter; most significantly the electrolyser cost and the discount rate. Although this chapter performed a sensitivity analysis when discussing the role of the grid, the many contributors to the ammonia cost means that there is uncertainty in the specific values provided for ammonia costs in that chapter.

Similar limitations emerge in other chapters:

1. Estimates of land availability and land competition in Chapter 5 used global averages, but in reality will differ meaningfully between countries and within countries. More regionally specific future studies could feature this detail with a clearer understanding of specific local conditions.

2. A core driver of green ammonia production is policy, and subsidies are likely to drive production in the next decade that will continue to impact the supply distribution in 2050. For instance, the Inflation Reduction Act in the US provides generous subsidies to producers of hydrogen and hydrogen derivatives, which is likely to drive production into the US.

3. The core conclusions in Chapter 6 relate to the dominance of solar PV, which depends on significant cost reductions in that technology that are forecast to occur before 2050. Although those forecasts are based on

sound economic principles, they carry significant uncertainty, and should they not eventuate, the production and distribution landscape for ammonia will depend more strongly on wind.

A direct comparison of the results of this thesis to other authors is not straightforward because few studies of this magnitude have been attempted. However, some of the core points are echoed in other research: Wang et al. [69] used a much less granular approach to cost modelling but found green ammonia production would occur in similar locations to those predicted in Chapter 6, and Fasihi et al. [80] also predicted that solar would come to dominate green ammonia production. Both of those authors also found that production would be focussed regional hubs (as opposed to highly distributed adjacent to users or highly concentrated in a single global location) because of the significant contribution of both production and transport costs identified in Chatper 6. Where different results are obtained for ammonia costs, the most common reason is variation in input values, underlining the importance of using sensible data and carefully considered cost forecasts as outlined by Way et al. [2].

7.3 Significance of research

The significance of each chapter was described in the body of the text, and the core findings are summarised in Table 7.1.

The goal of this thesis was to produce an optimisation model for the entire supply chain of green ammonia. This was achieved in Chapter 6, with case studies describing ammonia usage in the maritime sector, and for back-up electricity supply during periods of low renewable energy generation. This model provides a blueprint for policy makers: it enables us to understand the key drivers of ammonia's use as an energy vector, and to estimate how much delivered ammonia will cost in different social and environmental scenarios.

Although chapters 2 to 5 provided the necessary inputs into chapter 6, they had their own findings, which are of independent significance: chapter 2 showed that a global supply chain model such as that presented in chapter 6 was missing from the literature; chapter 3 showed the value of grid connection in reducing ammonia cost, and how data clustering can be used to accelerate models for green ammonia cost estimation; chapter 4 presented an algorithm through which green ammonia plants can be operated with limited forecast information, and called into question the assumption that increased plant flexibility will always reduce the cost of ammonia; and chapter 5 argued the merits of offshore green ammonia production, particularly in a context in which floating offshore wind is already being installed for some energy grids.

7.4 Further work

As identified in Chapter 6, the most significant further work required beyond this thesis is in realising the future which this thesis predicts, and the task is monumental: it will require order of magnitude increases in solar energy, wind energy, hydrogen production, and supply-chain systems. Today, the cost of green ammonia production is quickly becoming competitive with grey alternatives due to the rapid fall in renewable energy costs and the rapid rise in global gas prices; the findings of the third chapter of this thesis (that a grid connection made could further

Table 7.1 Significant contributions grouped by chapter

Chapter	Title	Significant findings
3	Optimisation of green ammonia plant design	1. Grid connection of green ammonia plants in Australia can reduce the size of storage equipment and therefore reduce the LCOA-P.
		2. The suitability of grid connection is strong function of the distance of a green ammonia plant from the grid.
		3. Data clustering can improve the speed of MILP based optimisation of green ammonia plant design without significantly sacrificing accuracy.
4	Operating green ammonia plants with imperfect forecasts and partial flexibility	1. Even if an ammonia plant is designed using perfect foresight, it is possible to operate such a plant with real-time weather forecasting; depending on the location, the plant storage equipment may need to be oversized to achieve that goal.
		2. Although HB flexibility may improve ammonia costs to some extent, the benefits of improving plant design design so that the minimum operating rate of a HB unit falls below 60% are limited. Therefore it is not likely that alternative ammonia synthesis technologies will overtake HB unless they have a lower CAPEX.
		3. Operating models for green ammonia plants must be carefully tuned; this tuning will differ by location.
		4. It may be easier to operate a plant with limited foresight if that plant is dominated by solar rather than wind.
5	Offshore green ammonia synthesis, and the impact of land constraints on global production capacity	1. The techno-economic case for green ammonia production offshore is, on its own, weak; however, because land restrictions limit onshore production, it may be the most cost-competitive option for ammonia production.
		2. In specific regions where land is highly constrained, offshore green ammonia production offers energy security and is a sensible allocation of energy produced from offshore resources.
6	Optimising supply chains for ammonia transport	1. Solar energy will produce the cheapest green ammonia in 2050 by a significant margin.
		2. The best ammonia production sites in the future will be determined by production cost, production capacity, and proximity to demand.
		3. Maritime fuel and back-up power delivered by green ammonia in 2050 are likely to be cost competitive with current fossil fuel technologies
		4. Energy transport in the future is likely to be more highly regionalised than today.

reduce ammonia costs) can accelerate the present-day transition. In the future, this modelling has shown that ammonia will be able to provide reliable, affordable energy to a range of sectors.

To some extent, further research could involve completing hundreds of smaller research tasks. That could involve several smaller, more regional studies in which cost-estimates could be more precise; it could involve incorporating other zero-carbon energy sources like hydro or nuclear; it could involve considering other renewable energy vectors like methanol. The potential list of further studies is long.

However, when looking for larger research prospects, a common thread emerges across chapters 3, 5 and 6,

which is a need for broader energy systems modelling. Chapter 3 considered the role of the electricity grid in green ammonia production, but there are endogenous impacts of this sector coupling which need to be studied at a broader level. Chapter 5 introduced a land-competition factor, to which the modelling was highly sensitive, in order to model the impact of other renewables on land usage - this could be more accurately captured with broader energy systems models. Whether or not the offshore ammonia proposed in that chapter would be sensible depends on the design and goals of national energy systems as a whole. In the section on back-up energy for grids, Chapter 6 also considered the interaction between energy systems and green ammonia, but again it treated back-up grid demand as exogenous to ammonia cost, which is a simplification. These common threads suggest that further work needs to incorporate more energy sectors into integrated models to continue the task of understanding how ammonia will fit into system design.

Beyond adding detail to the global pre-feasibility study, further research could also focus on answering specific regional questions, also considering the whole of the energy system. For instance, in prospective supply countries, what is the impact of using partially flexible green ammonia production on the energy system as a whole? Are there synergies between providing reliable energy supply to domestic consumers and a robust energy export inidustry exploiting green ammonia; or will these two energy consumers compete for finite land required for renewable power generation? In demand countries, is there a role for green ammonia, or is the plausible range of operating costs too high to justify its consumption? Will green ammonia be available when demand countries require it, or will global shortages strike concurrently and cause price shocks? Each of these questions is too specific to answer on a global level, but regional detail can be incorporated in more specific models and meaningful answers could be developed, which should be the focus of further research.

There is much work left to be done, but this thesis has advanced our understanding of how green ammonia can be used to combat climate change. It offers great promise as one of many solutions for the immense challenge of decarbonisation.

References

[1] International Renewable Energy Agency. *Renewable Power Generation Costs in 2021*. Web Page. 2022. URL: https://www.irena.org/publications/2022/Jul/Renewable-Power-Generation-Costs-in-2021.

[2] Rupert Way et al. "Empirically grounded technology forecasts and the energy transition". In: *Joule* 6.9 (2022), pp. 2057–2082. ISSN: 2542-4351. DOI: https://doi.org/10.1016/j.joule.2022.08.009. URL: https://www.sciencedirect.com/science/article/pii/S254243512200410X.

[3] International Renewable Energy Agency. *Hydrogen: a renewable energy perspective*. Web Page. 2019. URL: https://www.irena.org/publications/2019/Sep/Hydrogen-A-renewable-energy-perspective.

[4] W.L. Ahlgren. "The Dual-Fuel Strategy: An Energy Transition Plan". In: *Proceedings of the IEEE* 100.11 (2012), pp. 3001–3052. ISSN: 0018-9219 1558-2256. DOI: 10.1109/jproc.2012.2192469.

[5] J. Schmidt et al. "A new perspective on global renewable energy systems: why trade in energy carriers matters". In: *Energy & Environmental Science* 12.7 (2019), pp. 2022–2029. ISSN: 1754-5692. DOI: 10.1039/c9ee00223e. URL: https://dx.doi.org/10.1039/c9ee00223e.

[6] IEEJ. *IEEJ Outlook 2019*. Web Page. 2019. URL: https://eneken.ieej.or.jp/data/8122.pdf.

[7] Alexandra Devlin and Aidong Yang. "Regional supply chains for decarbonising steel: Energy efficiency and green premium mitigation". In: *Energy Conversion and Management* 254 (2022), p. 115268. ISSN: 0196-8904. DOI: https://doi.org/10.1016/j.enconman.2022.115268. URL: https://www.sciencedirect.com/science/article/pii/S0196890422000644.

[8] Sebastian Franz et al. "Requirements for a maritime transition in line with the Paris agreement". In: *iScience* 25.12 (2022), p. 105630. ISSN: 2589-0042. DOI: https://doi.org/10.1016/j.isci.2022.105630. URL: https://www.sciencedirect.com/science/article/pii/S2589004222019022.

[9] Sebastian Franz, Marianna Rottoli, and Christoph Bertram. "The wide range of possible aviation demand futures after the COVID-19 pandemic". In: *Environmental Research Letters* 17.6 (2022), p. 064009. DOI: 10.1088/1748-9326/ac65a4. URL: https://dx.doi.org/10.1088/1748-9326/ac65a4.

[10] D.R. MacFarlane et al. “A Roadmap to the Ammonia Economy”. In: *Joule* 4.6 (2020), pp. 1186–1205. ISSN: 25424351. DOI: 10.1016/j.joule.2020.04.004.

[11] N. Ash and T. Scarbrough. *Sailing on Solar: Could green ammonia decarbonise international shipping?* London: Environmental Defense Fund, 2019, pp. 56–57.

[12] Z. Cesaro, J. Thatcher, and R. Banares-Alcantara. “Techno-Economic Aspects of the use of ammonia as an energy vector”. In: *Green Ammonia*. Elsevier, 2020. Chap. 9, pp. 209 –220.

[13] Nicholas Salmon and René Bañares-Alcántara. “Green ammonia as a spatial energy vector: a review”. In: *Sustainable Energy Fuels* 5 (11 2021), pp. 2814–2839. DOI: 10.1039/D1SE00345C. URL: http://dx.doi.org/10.1039/D1SE00345C.

[14] A.T. Wijayanta et al. “Liquid hydrogen, methylcyclohexane, and ammonia as potential hydrogen storage: Comparison review”. In: *International Journal of Hydrogen Energy* 44.29 (2019), pp. 15026–15044. ISSN: 0360-3199. DOI: https://doi.org/10.1016/j.ijhydene.2019.04.112. URL: http://www.sciencedirect.com/science/article/pii/S0360319919315411.

[15] National Institute for Standards and Technology. *Chemistry Webbook*. Web Page. 2020. URL: https://webbook.nist.gov/chemistry/.

[16] J. Bartels. “A feasibility study of implementing an Ammonia Economy”. MSc Thesis. Iowa State University, 2008.

[17] A. Valera-Medina et al. “Ammonia for power”. In: *Progress in Energy and Combustion Science* 69 (2018), pp. 63–102. ISSN: 0360-1285. DOI: 10.1016/j.pecs.2018.07.001. URL: http://orca.cf.ac.uk/115540/1/180910%20JPECS%20Ammonia.pdf.

[18] R. Nayak-Luke and R. Bañares-Alcántara. “Techno-economic viability of islanded green ammonia as a carbon-free energy vector and as a substitute for conventional production”. In: *Energy & Environmental Science* 13.9 (2020), pp. 2957–2966. ISSN: 1754-5692. DOI: 10.1039/d0ee01707h. URL: https://dx.doi.org/10.1039/D0EE01707H.

[19] C. Smith, A.K. Hill, and L. Torrente-Murciano. “Current and future role of Haber–Bosch ammonia in a carbon-free energy landscape”. In: *Energy & Environmental Science* 13.2 (2020), pp. 331–344. ISSN: 1754-5692. DOI: 10.1039/c9ee02873k. URL: https://dx.doi.org/10.1039/C9EE02873K.

[20] DNV GL. *Hydrogen as an energy carrier*. Web Page. 2018. URL: https://www.dnvgl.com/oilgas/download/hydrogen-as-an-energy-carrier.html.

[21] C. Stiller et al. “Options for CO2-lean hydrogen export from Norway to Germany”. In: *Energy* 33.11 (2008), pp. 1623–1633. ISSN: 0360-5442. DOI: https://doi.org/10.1016/j.energy.2008.07.004. URL: http://www.sciencedirect.com/science/article/pii/S0360544208001692.

[22] C. Hank et al. “Energy efficiency and economic assessment of imported energy carriers based on renewable electricity”. In: *Sustainable Energy & Fuels* 4.5 (2020), pp. 2256–2273. ISSN: 2398-4902. DOI: 10.1039/d0se00067a. URL: https://doi.org/10.1039/D0SE00067A.

[23] T. Hijikata. “Research and Development of international clean energy network using hydrogen”. In: *International Journal of Hydrogen Energy* 27 (2002), pp. 115–129.

[24] International Energy Agency. *Hydrogen Report*. Web Page. 2019. URL: https://www.iea.org/reports/hydrogen.

[25] Y. Zhao et al. “An Efficient Direct Ammonia Fuel Cell for Affordable Carbon-Neutral Transportation”. In: *Joule* 3.10 (2019), pp. 2472–2484. ISSN: 25424351. DOI: 10.1016/j.joule.2019.07.005.

[26] C. Hank et al. “Economics & carbon dioxide avoidance cost of methanol production based on renewable hydrogen and recycled carbon dioxide – power-to-methanol”. In: *Sustainable Energy & Fuels* 2.6 (2018), pp. 1244–1261. ISSN: 2398-4902. DOI: 10.1039/c8se00032h.

[27] Z. Cesaro et al. “Ammonia to power: Forecasting the levelized cost of electricity from green ammonia in large-scale power plants”. In: *Applied Energy* 282 (2021), p. 116009. ISSN: 0306-2619. DOI: 10.1016/j.apenergy.2020.116009. URL: https://dx.doi.org/10.1016/j.apenergy.2020.116009.

[28] International Energy Agency. *Country report: Japan*. Web Page. 2020. URL: https://www.iea.org/countries/japan.

[29] Z. Hafsi, M. Mishra, and S. Elaoud. “Hydrogen embrittlement of steel pipelines during transients”. In: *Procedia Structural Integrity* 13 (2018), pp. 210–217. ISSN: 2452-3216. DOI: 10.1016/j.prostr.2018.12.035. URL: https://dx.doi.org/10.1016/j.prostr.2018.12.035.

[30] W.C. Leighty and J.H Holbrook. “Alternatives to Electricity for Transmission, Firming Storage, and Supply Integration for Diverse, Stranded, Renewable Energy Resources: Gaseous Hydrogen and Anhydrous Ammonia Fuels via Underground Pipelines”. In: *WHEC 2012 Conference Proceedings – 19th World Hydrogen Energy Conference*. Vol. 29. Toronto: JPdL International, 2012, pp. 332–346. ISBN: 18766102. DOI: 10.1016/j.egypro.2012.09.040.

[31] C. Yang and J. Ogden. “Determining the lowest-cost hydrogen delivery mode”. In: *International Journal of Hydrogen Energy* 32.2 (2007), pp. 268–286. ISSN: 0360-3199. DOI: 10.1016/j.ijhydene.2006.05.009. URL: https://dx.doi.org/10.1016/j.ijhydene.2006.05.009.

[32] M.J. Palys et al. “A novel system for ammonia-based sustainable energy and agriculture: Concept and design optimization”. In: *Chemical Engineering and Processing - Process Intensification* 140 (2019), pp. 11–21. ISSN: 02552701. DOI: 10.1016/j.cep.2019.04.005.

[33] A. Afif et al. “Ammonia-fed fuel cells: a comprehensive review”. In: *Renewable and Sustainable Energy Reviews* 60 (2016), pp. 822–835. ISSN: 1364-0321. DOI: 10.1016/j.rser.2016.01.120.

[34] H. Kwon, M. Ryu, and S.-K. An. “Technical and economic feasibility study for commercial ships with HFO, LNG, and NH_3 as fuel”. In: *AIChE Annual Meeting Conference*. Orlando, 2019.

[35] T. Ben Brahim, F. Wiese, and M. Münster. “Pathways to climate-neutral shipping: A Danish case study”. In: *Energy* 188 (2019), p. 116009. ISSN: 0360-5442. DOI: 10.1016/j.energy.2019.116009.

[36] R. Lan and S. Tao. “Ammonia as a Suitable Fuel for Fuel Cells”. In: *Frontiers in Energy Research* 2 (2014). ISSN: 2296-598X. DOI: 10.3389/fenrg.2014.00035. URL: https://dx.doi.org/10.3389/fenrg.2014.00035.

[37] G. Cinti, L. Barelli, and G. Bidini. “The use of ammonia as a fuel for transport: Integration with solid oxide fuel cells”. In: *Second International Conference on material science, smart structures and applications*. Erode, India: AIP Publishing, 2019. DOI: 10.1063/1.5138781.

[38] O. Kurata et al. “Development of a wide range-operable, rich-lean low-NOx combustor for NH_3 fuel gas-turbine power generation”. In: *Proceedings of the Combustion Institute* 37.4 (2019), pp. 4587–4595. ISSN: 1540-7489. DOI: 10.1016/j.proci.2018.09.012. URL: https://dx.doi.org/10.1016/j.proci.2018.09.012.

[39] A. Valera-Medina et al. “Premixed ammonia/hydrogen swirl combustion under rich fuel conditions for gas turbines operation”. In: *International Journal of Hydrogen Energy* 44.16 (2019), pp. 8615–8626. ISSN: 0360-3199. DOI: 10.1016/j.ijhydene.2019.02.041.

[40] Hydrogenious LOHC Technologies. *Hydrogen infrastructure solutions*. Web Page. 2020. URL: https://www.hydrogenious.net/wp-content/uploads/2018/08/Hydrogenious-LOHC-Technologies-Product-Brochure_short.pdf.

[41] D. Teichmann, W. Arlt, and P. Wasserscheid. “Liquid Organic Hydrogen Carriers as an efficient vector for the transport and storage of renewable energy”. In: *International Journal of Hydrogen Energy* 37.23 (2012), pp. 18118–18132. ISSN: 03603199. DOI: 10.1016/j.ijhydene.2012.08.066.

[42] B. Lin, T. Wiesner, and M. Malmali. “Performance of a Small-Scale Haber Process: A Techno-Economic Analysis”. In: *ACS Sustainable Chemistry & Engineering* 8.41 (2020), pp. 15517–15531. ISSN: 2168-0485 2168-0485. DOI: 10.1021/acssuschemeng.0c04313.

[43] G. Ondrey. “Ammonia as a H2 carrier enabled by a catalytic membrane”. In: *Chemical Engineering* 124.9 (2017), p. 8. ISSN: 00092460.

[44] CSIRO. *Metal membrane for hydrogen separation*. Web Page. 2019. URL: https://www.csiro.au/en/Research/EF/Areas/Renewable-and-low-emission-tech/Hydrogen/Hydrogen-membrane.

[45] CertifyHy. *SD Hydrogen Criteria*. Web Page. 2020. URL: https://www.certifhy.eu/images/media/files/CertifHy_2_deliverables/CertifHy_H2-criteria-definition_V1-1_2019-03-13_clean_endorsed.pdf.

[46] Y. Bicer and I. Dincer. "Life cycle assessment of ammonia utilization in city transportation and power generation". In: *Journal of Cleaner Production* 170 (2018), pp. 1594–1601. ISSN: 0959-6526. DOI: 10.1016/j.jclepro.2017.09.243.

[47] J. Fuhrmann, M. Hülsebrock, and U. Krewer. "Energy Storage Based on Electrochemical Conversion of Ammonia". In: *Transition to Renewable Energy Systems*. 2013, pp. 691–706. DOI: https://doi.org/10.1002/9783527673872.ch33. URL: https://onlinelibrary.wiley.com/doi/abs/10.1002/9783527673872.ch33.

[48] Y. Bicer and I. Dincer. "Evaluation of Renewable and Conventional Ammonia as a Potential Solution". In: Springer, 2017, pp. 119–127. ISBN: 97833194565849783319456591.

[49] O. Siddiqui and I. Dincer. "A review and comparative assessment of direct ammonia fuel cells". In: *Thermal Science and Engineering Progress* 5 (2018), pp. 568–578. ISSN: 2451-9049. DOI: 10.1016/j.tsep.2018.02.011.

[50] Hellenic Shipping News. *Once a niche segment, LPG carrier market is now a boon for ship owners*. Web Page. 2019. URL: https://www.hellenicshippingnews.com/once-a-niche-segment-lpg-carrier-market-is-now-a-boon-for-ship-owners/.

[51] Hydrogen import coalition. *Shipping sun and wind to Belgium is key in climate neutral economy*. Web Page. 2020. URL: https://www.portofantwerp.com/sites/default/files/Hydrogen%20Import%20Coalition.pdf.

[52] Y. Ishimoto et al. "Large-scale production and transport of hydrogen from Norway to Europe and Japan: Value chain analysis and comparison of liquid hydrogen and ammonia as energy carriers". In: *International Journal of Hydrogen Energy* (2020). ISSN: 03603199. DOI: 10.1016/j.ijhydene.2020.09.017.

[53] M. Wietschel and U. Hasenauer. "Feasibility of hydrogen corridors between the EU and its neighbouring countries". In: *Renewable Energy* 32.13 (2007), pp. 2129–2146. ISSN: 09601481. DOI: 10.1016/j.renene.2006.11.012.

[54] Y Kawakami, S. Endo, and H. Hirai. *A feasibility study on the supply chain of CO_2 free ammonia with CCS and EOR*. Web Page. 2019. URL: https://eneken.ieej.or.jp/data/8371.pdf.

[55] C. Fúnez Guerra et al. "Technical-economic analysis for a green ammonia production plant in Chile and its subsequent transport to Japan". In: *Renewable Energy* 157 (2020), pp. 404–414. ISSN: 09601481. DOI: 10.1016/j.renene.2020.05.041.

[56] International Energy Agency. Web Page. 2020. URL: https://www.iea.org/reports/world-energy-outlook-2020.

[57] P.-M. Heuser et al. “Techno-economic analysis of a potential energy trading link between Patagonia and Japan based on CO_2 free hydrogen”. In: *International Journal of Hydrogen Energy* 44.25 (2019), pp. 12733–12747. ISSN: 03603199. DOI: 10.1016/j.ijhydene.2018.12.156.

[58] A. Babarit et al. “Techno-economic feasibility of fleets of far offshore hydrogen-producing wind energy converters”. In: *International Journal of Hydrogen Energy* 43.15 (2018), pp. 7266–7289. ISSN: 03603199. DOI: 10.1016/j.ijhydene.2018.02.144.

[59] S. Kamiya, M. Nishimura, and E. Harada. “Study on introduction of CO_2 free energy to Japan with liquid hydrogen”. In: *Physics procedia* 67.C (2015), pp. 11–19. ISSN: 1875-3892. DOI: 10.1016/j.phpro.2015.06.004.

[60] T. Watanabe et al. “Cost Estimation of Transported Hydrogen, Produced by Overseas Wind Power Generation”. In: *18th World Hydrogen Energy Conference 2010*. Vol. 78-3. Essen, 2010, pp. 547–557. ISBN: 978-3-89336-653-8.

[61] J. Gretz et al. “Status of the hydro-hydrogen pilot project (EQHHPP)”. In: *International Journal of Hydrogen Energy* 19.2 (1994), pp. 169–174. ISSN: 0360-3199. DOI: https://doi.org/10.1016/0360-3199(94)90123-6. URL: https://www.sciencedirect.com/science/article/pii/0360319994901236.

[62] Kenneth Engblom. “LNG to Power in remote locations-the optimal way”. In: Seoul: Power Gen Asia 2016, 2016.

[63] J. Armijo and C. Philibert. “Flexible production of green hydrogen and ammonia from variable solar and wind energy: Case study of Chile and Argentina”. In: *International Journal of Hydrogen Energy* 45.3 (2020), pp. 1541–1558. ISSN: 03603199. DOI: 10.1016/j.ijhydene.2019.11.028. URL: https://doi.org/10.1016/j.ijhydene.2019.11.028.

[64] O. Osman, S. Sgouridis, and A. Sleptchenko. “Scaling the production of renewable ammonia: A techno-economic optimization applied in regions with high insolation”. In: *Journal of Cleaner Production* 271 (2020), p. 121627. ISSN: 09596526. DOI: 10.1016/j.jclepro.2020.121627. URL: https://doi.org/10.1016/j.jclepro.2020.121627.

[65] D. Kim et al. “Unveiling electrode–electrolyte design-based NO reduction for NH_3 synthesis”. In: *ACS Energy Letters* 5.11 (2020), pp. 3647–3656. DOI: 10.1021/acsenergylett.0c02082. URL: https://doi.org/10.1021/acsenergylett.0c02082.

[66] CSIRO. *Hydrogen Research, Development and Demonstration*. Web Page. 2019. URL: https://www.csiro.au/en/research/technology-space/energy/Energy-and-Resources.

[67] A. Hauch et al. “Recent advances in solid oxide cell technology for electrolysis”. In: *Science* 370.6513 (2020). ISSN: 1095-9203 (Electronic) 0036-8075 (Linking). DOI: 10.1126/science.aba6118. URL: https://www.ncbi.nlm.nih.gov/pubmed/33033189.

[68] O. Posdziech, K. Schwarze, and J. Brabandt. “Efficient hydrogen production for industry and electricity storage via high-temperature electrolysis”. In: *International Journal of Hydrogen Energy* 44.35 (2019), pp. 19089–19101. ISSN: 0360-3199. DOI: 10.1016/j.ijhydene.2018.05.169.

[69] Hanchu Wang, Prodromos Daoutidis, and Qi Zhang. “Ammonia-based green corridors for sustainable maritime transportation”. In: *Digital Chemical Engineering* 6 (2023), p. 100082. ISSN: 2772-5081. DOI: https://doi.org/10.1016/j.dche.2022.100082. URL: https://www.sciencedirect.com/science/article/pii/S2772508122000734.

[70] Eric R. Morgan, James F. Manwell, and Jon G. McGowan. “Sustainable ammonia production from U.S. offshore wind farms: a techno-economic review”. In: *ACS Sustainable Chemistry & Engineering* 5.11 (2017), pp. 9554–9567. DOI: 10.1021/acssuschemeng.7b02070. URL: https://doi.org/10.1021/acssuschemeng.7b02070.

[71] P. Tunå, C. Hulteberg, and S. Ahlgren. “Techno-economic assessment of nonfossil ammonia production”. In: *Environmental Progress & Sustainable Energy* 33.4 (2014), pp. 1290–1297. ISSN: 19447442. DOI: 10.1002/ep.11886.

[72] E. Morgan, J. Manwell, and J. Mcgowan. “Wind-powered ammonia fuel production for remote islands: A case study”. In: *Renewable Energy* 72 (2014), pp. 51–61. ISSN: 0960-1481. DOI: 10.1016/j.renene.2014.06.034.

[73] M. Rivarolo et al. “Clean hydrogen and ammonia synthesis in Paraguay from the Itaipu 14 GW hydroelectric plant”. In: *ChemEngineering* 3.4 (2019), p. 87. ISSN: 2305-7084. DOI: 10.3390/chemengineering3040087.

[74] J. Moore and N. Meeks. “Hourly modelling of Thermal Hydrogen electricity markets”. In: *Clean Energy* 4.3 (2020), pp. 270–287. ISSN: 2515-4230. DOI: 10.1093/ce/zkaa014.

[75] Hui Chen, Fangyuan Dong, and Shelley D. Minteer. “The progress and outlook of bioelectrocatalysis for the production of chemicals, fuels and materials”. In: *Nature Catalysis* 3.3 (2020). ID: Chen2020, pp. 225–244. DOI: 10.1038/s41929-019-0408-2. URL: https://doi.org/10.1038/s41929-019-0408-2.

[76] David L. Boucher et al. “An investigation of the putative photosynthesis of ammonia on iron-doped titania and other metal oxides”. In: *Journal of Photochemistry and Photobiology A: Chemistry* 88.1 (1995), pp. 53–64. ISSN: 1010-6030. DOI: https://doi.org/10.1016/1010-6030(94)03994-6. URL: https://www.sciencedirect.com/science/article/pii/1010603094039946.

[77] G. Wang, A. Mitsos, and W. Marquardt. “Conceptual design of ammonia-based energy storage system: System design and time-invariant performance”. In: *AIChE Journal* 63.5 (2017), pp. 1620–1637. ISSN: 0001-1541. DOI: 10.1002/aic.15660. URL: https://aiche.onlinelibrary.wiley.com/doi/abs/10.1002/aic.15660.

[78] S.S. Beerbühl, M. Fröhling, and F. Schultmann. “Combined scheduling and capacity planning of electricity-based ammonia production to integrate renewable energies”. In: *European Journal of Operational Research* 241.3 (2015), pp. 851–862. ISSN: 0377-2217. DOI: 10.1016/j.ejor.2014.08.039. URL: https://dx.doi.org/10.1016/j.ejor.2014.08.039.

[79] S.S. Beerbühl et al. “Ammoniaksynthese als Beispiel einer stofflichen Nutzung von intermittierend erzeugtem Wasserstoff”. In: *Chemie Ingenieur Technik* 86.5 (2014), pp. 649–657. ISSN: 0009286X. DOI: 10.1002/cite.201300167. URL: https://doi.org/10.1002/cite.201300167.

[80] Mahdi Fasihi et al. “Global potential of green ammonia based on hybrid PV-wind power plants”. In: *Applied Energy* 294 (2021), p. 116170. ISSN: 0306-2619. DOI: https://doi.org/10.1016/j.apenergy.2020.116170. URL: https://www.sciencedirect.com/science/article/pii/S0306261920315750.

[81] J.R. Gomez, J. Baca, and Fernando Garzon. “Techno-economic analysis and life cycle assessment for electrochemical ammonia production using proton conducting membrane”. In: *International Journal of Hydrogen Energy* 45.1 (2020), pp. 721–737. ISSN: 03603199. DOI: 10.1016/j.ijhydene.2019.10.174.

[82] M.J. Palys and P. Daoutidis. “Using hydrogen and ammonia for renewable energy storage: A geographically comprehensive techno-economic study”. In: *Computers & Chemical Engineering* 136 (2020), p. 106785. ISSN: 00981354. DOI: 10.1016/j.compchemeng.2020.106785. URL: https://doi.org/10.1016/j.compchemeng.2020.106785.

[83] G. Wang, A. Mitsos, and W. Marquardt. “Renewable production of ammonia and nitric acid”. In: *AIChE Journal* 66.6 (2020). ISSN: 0001-1541. DOI: 10.1002/aic.16947.

[84] H. Zhang et al. “Techno-economic comparison of green ammonia production processes”. In: *Applied Energy* 259 (2020). ISSN: 03062619. DOI: 10.1016/j.apenergy.2019.114135.

[85] A. Allman, M.J. Palys, and P. Daoutidis. “Scheduling-informed optimal design of systems with time-varying operation: A wind-powered ammonia case study”. In: *AIChE Journal* 65.7 (2019). ISSN: 00011541. DOI: 10.1002/aic.16434.

[86] W.W. Tso et al. “Energy Carrier Supply Chain Optimization: A Texas Case Study”. In: *Proceedings of the 9th International Conference on Foundations of Computer-Aided Process Design*. Computer Aided Chemical Engineering. Elsevier, 2019, pp. 1–6. ISBN: 9780128185971. DOI: 10.1016/b978-0-12-818597-1.50001-1.

[87] C. D. Demirhan et al. “Sustainable ammonia production through process synthesis and global optimization”. In: *AIChE Journal* 65.7 (2019). ISSN: 00011541. DOI: 10.1002/aic.16498.

[88] Fraunhofer IFI. *What are the opportunities and challenges of importing green hydrogen?* Web Page. 2019. URL: https://www.isi.fraunhofer.de/en/presse/2020/presseinfo-26-policy-brief-wasserstoff.html.

[89] J. Ikaheimo et al. “Power-to-ammonia in future North European 100% renewable power and heat system”. In: *International Journal of Hydrogen Energy* 43.36 (2018), pp. 17295–17308. ISSN: 03603199. DOI: 10.1016/j.ijhydene.2018.06.121.

[90] R. Nayak-Luke, R. Bañares-Alcántara, and I. Wilkinson. ““Green” ammonia: impact of renewable energy intermittency on plant sizing and levelized cost of ammonia”. In: *Industrial & Engineering Chemistry Research* 57.43 (2018), pp. 14607–14616. ISSN: 0888-5885. DOI: 10.1021/acs.iecr.8b02447. URL: https://dx.doi.org/10.1021/acs.iecr.8b02447.

[91] M.J. Palys, A. Allman, and P. Daoutidis. “Exploring the Benefits of Modular Renewable-Powered Ammonia Production: A Supply Chain Optimization Study”. In: *Industrial & Engineering Chemistry Research* 58.15 (2018), pp. 5898–5908. ISSN: 0888-5885 1520-5045. DOI: 10.1021/acs.iecr.8b04189.

[92] ISPT. *Power to Ammonia: From renewable energy to CO_2-free ammonia as chemical feedstock and fuel*. Web Page. 2017. URL: https://ispt.eu/news/power-ammonia-renewable-energy-co2-free-ammonia-chemical-feedstock-fuel/.

[93] P.H. Pfromm. “Towards sustainable agriculture: Fossil-free ammonia”. In: *Journal of Renewable and Sustainable Energy* 9.3 (2017), p. 034702. ISSN: 1941-7012. DOI: 10.1063/1.4985090.

[94] A. Sanchez and M. Martín. “Optimal renewable production of ammonia from water and air”. In: *Journal of Cleaner Production* 178 (2018), pp. 325–342. ISSN: 09596526. DOI: 10.1016/j.jclepro.2017.12.279.

[95] R. Bañares Alcántara et al. *Analysis of Islanded Ammonia-based Energy Storage Systems*. Web Page. 2015. URL: http://www2.eng.ox.ac.uk/systemseng/publications/Ammonia-based_ESS.pdf.

[96] M. Matzen, M. Alhajji, and Y. Demirel. “Technoeconomics and Sustainability of Renewable Methanol and Ammonia Productions Using Wind Power-based Hydrogen”. In: *Journal of Advanced Chemical Engineering* 5.3 (2015). ISSN: 20904568. DOI: 10.4172/2090-4568.1000128.

[97] P. Trop and D. Goricanec. “Comparisons between energy carriers’ productions for exploiting renewable energy sources”. In: *Energy* 108 (2016), pp. 155–161. ISSN: 03605442. DOI: 10.1016/j.energy.2015.07.033.

[98] K. H. Rouwenhorst et al. “Islanded ammonia power systems: Technology review & conceptual process design”. In: *Renewable and Sustainable Energy Reviews* 114 (2019), p. 109339. ISSN: 1364-0321. DOI: 10.1016/j.rser.2019.109339.

[99] M. Malmali et al. “Better Absorbents for Ammonia Separation”. In: *ACS Sustainable Chemistry & Engineering* 6.5 (2018), pp. 6536–6546. ISSN: 2168-0485 2168-0485. DOI: 10.1021/acssuschemeng.7b04684.

[100] O. A. C. Hoes et al. “Systematic high-resolution assessment of global hydropower potential”. In: *PLOS ONE* 12.2 (2017), e0171844. ISSN: 1932-6203. DOI: 10.1371/journal.pone.0171844. URL: https://dx.doi.org/10.1371/journal.pone.0171844.

[101] B. Steffen. “Estimating the cost of capital for renewable energy projects”. In: *Energy Economics* 88 (2020). ISSN: 01409883. DOI: 10.1016/j.eneco.2020.104783.

[102] Bloomberg New Energy Finance. *Sector coupling in Europe: Powering decarbonization*. Report. 2020. URL: https://assets.bbhub.io/professional/sites/24/BNEF-Sector-Coupling-Report-Feb-2020.pdf.

[103] A. Mayyas et al. *Manufacturing Cost Analysis for Proton Exchange Membrane Water Electrolyzers*. Web Page. 2019. URL: https://www.nrel.gov/docs/fy19osti/72740.pdf.

[104] Nicholas Salmon, René Bañares-Alcántara, and Richard Nayak-Luke. “Optimization of green ammonia distribution systems for intercontinental energy transport”. In: *iScience* 24.8 (2021), p. 102903. ISSN: 2589-0042. DOI: https://doi.org/10.1016/j.isci.2021.102903. URL: https://www.sciencedirect.com/science/article/pii/S2589004221008713.

[105] Asian Renewable Energy Hub. Web Page. 2020. URL: https://asianrehub.com/about/.

[106] The Economist. *Green Energy Oman project to boost renewable energy*. 2021. URL: https://www.emis.com/php/search/doc?pc=OM&dcid=739116571&primo=1.

[107] A. Vasquez and B. Hapes. *Europe’s largest single-train ammonia plant successfully started up with KBR technology*. Web Page. 2019. URL: https://www.kbr.com/en/insights-events/press-release/europes-largest-single-train-ammonia-plant-successfully-started-kbr.

[108] European Commission and Joint Research Centre and Alves Dias, P and Pavel, C and Plazzotta, B and Carrara, S. *Raw materials demand for wind and solar PV technologies in the transition towards a decarbonised energy system*. Web Page. 2020. DOI: 10.2760/160859. URL: https://ec.europa.eu/jrc/en/publication/raw-materials-demand-wind-and-solar-pv-technologies-transition-towards-decarbonised-energy-system.

[109] Zhehan Weng et al. “A Detailed Assessment of Global Rare Earth Element Resources: Opportunities and Challenges”. In: 110.8 (2015), pp. 1925–1952. ISSN: 0361-0128. DOI: 10.2113/econgeo.110.8.1925. URL: https://dx.doi.org/10.2113/econgeo.110.8.1925.

[110] J. Brauns and T. Turek. “Alkaline Water Electrolysis Powered by Renewable Energy: A Review”. In: *Processes* 8.2 (2020), p. 248. ISSN: 2227-9717. DOI: 10.3390/pr8020248.

[111] F. Hegge et al. “Efficient and stable low iridium loaded anodes for PEM water electrolysis made possible by nanofiber interlayers”. In: *ACS Applied Energy Materials* 3.9 (2020), pp. 8276–8284. ISSN: 2574-0962. DOI: 10.1021/acsaem.0c00735.

[112] Rebecca R. Beswick, Alexandra M. Oliveira, and Yushan Yan. “Does the Green Hydrogen Economy Have a Water Problem?” In: *ACS Energy Letters* 6.9 (2021), pp. 3167–3169. DOI: 10.1021/acsenergylett.1c01375. eprint: https://doi.org/10.1021/acsenergylett.1c01375. URL: https://doi.org/10.1021/acsenergylett.1c01375.

[113] P. Moriarty and D. Honnery. “What is the global potential for renewable energy?” In: *Renewable and Sustainable Energy Reviews* 16.1 (2012), pp. 244–252. ISSN: 13640321. DOI: 10.1016/j.rser.2011.07.151.

[114] Dirk-Jan van de Ven, Mikel Gonzalez-Eguino, and Inaki Arto. *Land-use impacts from renewable energy policies*. Web Page. 2017. URL: http://transrisk-project.eu/sites/default/files/Documents/4.4.6_Land-use%20impacts%20from%20renewable%20energy%20policies.pdf.

[115] E. Rowan, L. Seabrook, and C. Mcalpine. “Global prioritisation of renewable nitrogen for biodiversity conservation and food security”. In: *Journal of Geographical Sciences* 28.11 (2018), pp. 1567–1579. ISSN: 1009-637X. DOI: 10.1007/s11442-018-1561-2.

[116] International Renewable Energy Agency. *Global landscape of renewable energy finance*. Web Page. 2020. URL: irena.org/publications/2020/Nov/Global-Landscape-of-Renewable-Energy-Finance-2020.

[117] S. Carley et al. “Energy infrastructure, NIMBYism, and public opinion: a systematic literature review of three decades of empirical survey literature”. In: *Environmental Research Letters* 15.9 (2020), p. 093007. ISSN: 1748-9326. DOI: 10.1088/1748-9326/ab875d.

[118] J. Rand and B. Hoen. “Thirty years of North American wind energy acceptance research: What have we learned?” In: *Energy Research & Social Science* 29 (2017), pp. 135–148. ISSN: 2214-6296. DOI: 10.1016/j.erss.2017.05.019. URL: https://escholarship.org/content/qt3747t3q4/qt3747t3q4.pdf?t=otna92.

[119] S. Chapman and F. Crichton. “Opponents of windfarms in Australia”. In: *Wind Turbine Syndrome*. A Communicated Disease. Sydney University Press, 2017, pp. 179–224. ISBN: 9781743324967. DOI: 10.2307/j.ctt1zrvhrt.12. URL: http://www.jstor.org/stable/j.ctt1zrvhrt.12.

[120] H. Gavin. *Integrating renewable energy: opportunities and challenges*. Web Page. 2019. URL: https://www.research.ox.ac.uk/Article/2019-12-13-integrating-renewable-energy-opportunities-and-challenges.

[121] K. Ono and K. Tsunemi. "Identification of public acceptance factors with risk perception scales on hydrogen fueling stations in Japan". In: *International Journal of Hydrogen Energy* 42.16 (2017), pp. 10697–10707. ISSN: 03603199. DOI: 10.1016/j.ijhydene.2017.03.021.

[122] A. Schmidt and W. Donsbach. "Acceptance factors of hydrogen and their use by relevant stakeholders and the media". In: *International Journal of Hydrogen Energy* (2016). ISSN: 0360-3199. DOI: 10.1016/j.ijhydene.2016.01.058. URL: https://dx.doi.org/10.1016/j.ijhydene.2016.01.058.

[123] Peta Ashworth and Victoria Lambert. "Cautiously optimistic: Understanding the Australian public's response to the Hydrogen opportunity". In: (2019). URL: https://www.h2knowledgecentre.com/content/conference911#abstract_content.

[124] K. Itaoka, A. Saito, and K. Sasaki. "Public perception on hydrogen infrastructure in Japan: Influence of roll-out of commercial fuel cell vehicles". In: *International Journal of Hydrogen Energy* 42.11 (2017), pp. 7290–7296. ISSN: 0360-3199. DOI: 10.1016/j.ijhydene.2016.10.123.

[125] A. Guati-Rojo, C. Demski, and A. Valera-Medina. "Chapter 12 - Beyond the Technology: Public Perception of Ammonia Energy Technologies". In: *Techno-Economic Challenges of Green Ammonia as an Energy Vector*. Ed. by Agustin Valera-Medina and Rene Banares-Alcantara. Academic Press, 2021, pp. 277–302. ISBN: 978-0-12-820560-0. DOI: https://doi.org/10.1016/B978-0-12-820560-0.00012-6. URL: http://www.sciencedirect.com/science/article/pii/B9780128205600000126.

[126] Paul Wolfram et al. "Using ammonia as a shipping fuel could disturb the nitrogen cycle". In: *Nature Energy* 7.12 (2022), pp. 1112–1114. DOI: 10.1038/s41560-022-01124-4. URL: https://doi.org/10.1038/s41560-022-01124-4.

[127] International Renewable Energy Agency. *Navigating the way to a renewable future*. Web Page. 2019. URL: https://www.irena.org/publications/2019/Sep/Navigating-the-way-to-a-renewable-future.

[128] Laurens Van Hoecke et al. "Challenges in the use of hydrogen for maritime applications". In: *Energy Environ. Sci.* 14 (2 2021), pp. 815–843. DOI: 10.1039/D0EE01545H. URL: http://dx.doi.org/10.1039/D0EE01545H.

[129] J. Tattini and J. Teter. *International Shipping - IEA Tracking Report*. Web Page. 2020. URL: https://www.iea.org/reports/international-shipping-resources.

[130] *Engie-Yara Renewable hydrogen and ammonia deployment in Pilbara*. Web Page. 2020. URL: https://arena.gov.au/assets/2020/11/engie-yara-renewable-hydrogen-and-ammonia-deployment-in-pilbara.pdf.

[131] Zac Cesaro. *The role of green ammonia in sector coupling and seasonal electricity storage*. Web Page. 2021. URL: https://www.ammoniaenergy.org/wp-content/uploads/2021/11/20211105_ZCesaro_AEAConference_noappendix.pdf.

[132] World Steel Association. *World steel in figures 2022*. 2022. URL: https://worldsteel.org/steel-topics/statistics/world-steel-in-figures-2022/.

[133] International Energy Agency. *World Energy Outlook*. Web Page. 2020. URL: https://www.iea.org/reports/world-energy-outlook-2020.

[134] The Hydrogen Council. *Clean hydrogen monitor 2020*. Web Page. 2020. URL: https://hydrogeneurope.eu/sites/default/files/2020-10/Clean%20Hydrogen%20Monitor%202020_0.pdf.

[135] L. Easton and A. Feitz. *Mapping Australia's hydrogen future – release of the Hydrogen Economic Fairways Tool*. Web Page. 2021. URL: https://www.ga.gov.au/news-events/events/public-talks/public-talks-archive/mapping-australias-hydrogen-future.

[136] Stuart Walsh et al. *Evaluating the Economic Fairways for HydrogenProduction in Australia*. 2021. URL: https://eartharxiv.org/repository/view/2361/.

[137] Nicolas Campion et al. "Techno-economic assessment of green ammonia production with different wind and solar potentials". In: *Renewable and Sustainable Energy Reviews* 173 (2023), p. 113057. ISSN: 1364-0321. DOI: https://doi.org/10.1016/j.rser.2022.113057. URL: https://www.sciencedirect.com/science/article/pii/S1364032122009388.

[138] G. Hochman et al. "Potential Economic Feasibility of Direct Electrochemical Nitrogen Reduction as a Route to Ammonia". In: *ACS Sustainable Chemistry & Engineering* 8.24 (2020), pp. 8938–8948. DOI: 10.1021/acssuschemeng.0c01206. URL: https://doi.org/10.1021/acssuschemeng.0c01206.

[139] Carlos A. Fernandez and Marta C. Hatzell. "Editors' Choice—Economic considerations for low-temperature electrochemical ammonia production: achieving Haber-Bosch parity". In: *Journal of The Electrochemical Society* 167.14 (2020), p. 143504. ISSN: 1945-7111. DOI: 10.1149/1945-7111/abc35b.

[140] R. Nayak-Luke et al. "Techno-economic aspects of production, storage, and distribution of ammonia". In: *Techno-Economic Challenges of Green Ammonia as an Energy Vector*. London: Elsevier, 2020. Chap. 8, pp. 191–209.

[141] European Centre for Medium-Range Weather Forecasts. *ERA5*. Web Page. 2021. URL: https://www.ecmwf.int/en/forecasts/datasets/reanalysis-datasets/era5.

[142] Zac Cesaro. “The role of green ammonia in decarbonised energy systems”. DPhil Thesis. University of Oxford, 2022.

[143] J. Ambrose. *What caused the UK’s energy crisis?* Newspaper Article. 2021. URL: https://www.theguardian.com/business/2021/sep/21/what-caused-the-uks-energy-crisis.

[144] L. Dawkins. *Weather and Climate Related Sensitivities and Risks in a Highly Renewable UK Energy System: A Literature Review*. Web Page. 2019. URL: https://nic.org.uk/app/uploads/MetOffice_NIC_LiteratureReview_2019.pdf.

[145] Frauke Wiese et al. “Balmorel open source energy system model”. In: *Energy Strategy Reviews* 20 (2018), pp. 26–34. ISSN: 2211-467X. DOI: https://doi.org/10.1016/j.esr.2018.01.003. URL: https://www.sciencedirect.com/science/article/pii/S2211467X18300038.

[146] Bram van der Heijde et al. “Representative days selection for district energy system optimisation: a solar district heating system with seasonal storage”. In: *Applied Energy* 248 (2019), pp. 79–94. ISSN: 0306-2619. DOI: https://doi.org/10.1016/j.apenergy.2019.04.030. URL: https://www.sciencedirect.com/science/article/pii/S0306261919306622.

[147] Paolo Gabrielli et al. “Optimal design of multi-energy systems with seasonal storage”. In: *Applied Energy* 219 (2018), pp. 408–424. ISSN: 0306-2619. DOI: https://doi.org/10.1016/j.apenergy.2017.07.142. URL: https://www.sciencedirect.com/science/article/pii/S0306261917310139.

[148] Guangsheng Pan et al. “Cost and low-carbon competitiveness of electrolytic hydrogen in China”. In: *Energy & Environmental Science* (2021). ISSN: 1754-5692 1754-5706. DOI: 10.1039/d1ee01840j.

[149] Bloomberg. *AUD USD Exchange Rate*. Web Page. 2021. URL: https://www.bloomberg.com/quote/AUDUSD:CUR.

[150] Australian Energy Market Operator. *Aggregated price and demand data*. Web Page. 2020. URL: https://aemo.com.au/energy-systems/electricity/national-electricity-market-nem/data-nem/aggregated-data.

[151] Government of Australia. *Electricity transmission lines*. Web Page. 2021. URL: https://data.gov.au/dataset/ds-ga-1185c97c-c042-be90-e053-12a3070a969b/details?q=.

[152] Kelsey Jordahl et al. *geopandas/geopandas: v0.8.1*. Version v0.8.1. July 2020. DOI: 10.5281/zenodo.3946761. URL: https://doi.org/10.5281/zenodo.3946761.

[153] TasNetworks. *Prescribed Transmission Services Prices for 2021-22*. Web Page. 2021. URL: https://www.tasnetworks.com.au/config/getattachment/64d81498-67a5-4ae1-a1c1-dab70ae96d7e/2021-22-prescribed-transmission-services-prices.pdf.

[154] Powerlink Queensland. *Pricing and Revenue*. Web Page. 2021. URL: https://www.powerlink.com.au/pricing-and-revenue.

[155] Australian Energy Market Operator. *Shared transmission network services prices in Victoria – 1 July 2020 to 30 June 2021*. Web Page. 2020. URL: https://aemo.com.au/-/media/files/electricity/nem/participant_information/fees/2020/electricity-transmission-use-of-system-prices-1-july-2020--30-june-2021.pdf?la=en.

[156] International Renewable Energy Agency. *Renewable Power Generation Costs in 2019*. Abu Dhabi: International Renewable Energy Agency, 2019. ISBN: 978-92-9260-244-4. URL: https://irena.org/-/media/Files/IRENA/Agency/Publication/2020/Jun/IRENA_Power_Generation_Costs_2019.pdf.

[157] Jacqueline A. Dowling et al. "Role of Long-Duration Energy Storage in Variable Renewable Electricity Systems". In: *Joule* 4.9 (2020), pp. 1907–1928. ISSN: 2542-4351. DOI: https://doi.org/10.1016/j.joule.2020.07.007. URL: https://www.sciencedirect.com/science/article/pii/S2542435120303251.

[158] A. Sakti, R. Miller, and F. Brushett. *What's cost got to do with it?* Web Page. 2015. URL: https://energy.mit.edu/news/whats-cost-got-to-do-with-it/.

[159] G. Parkinson. *Tesla big battery adds new capacity and services on march to 100pct renewables grid*. Web Page. 2019. URL: https://reneweconomy.com.au/tesla-big-battery-adds-new-capacity-and-services-on-march-to-100pct-renewables-grid-55121/.

[160] T.S. Brinsmead, J. Hayward, and P. Graham. *Australian Electricity Market Analysis report to 2020 and 2030*. Web Page. 2014. URL: https://arena.gov.au/assets/2017/02/CSIRO-Electricity-market-analysis-for-IGEG.pdf.

[161] M. Pirolli. *Sustainable Energy Handbook*. Web Page. 2021. URL: https://europa.eu/capacity4dev/public-energy/wiki/sustainable-energy-handbook.

[162] K. Vaillancourt. *Electricity Transmission and Distribution*. Web Page. 2014. URL: https://iea-etsap.org/E-TechDS/PDF/E12_el-t&d_KV_Apr2014_GSOK.pdf.

[163] Australian Energy Market Commission. *Changing generation mix*. Web Page. 2021. URL: https://www.aemc.gov.au/energy-system/electricity/changing-generation-mix.

[164] W. Michael et al. *World Energy Investment 2020*. Web Page. 2020. URL: https://webstore.iea.org/download/direct/3003.

[165] Thomas Knight, Chao Chen, and Aidong Yang. “Embracing the era of renewable energy: model-based analysis of the role of operational flexibility in chemical production”. In: *Computer Aided Chemical Engineering*. Ed. by Yoshiyuki Yamashita and Manabu Kano. Vol. 49. Elsevier, 2022, pp. 1915–1920. ISBN: 1570-7946. DOI: https://doi.org/10.1016/B978-0-323-85159-6.50319-5. URL: https://www.sciencedirect.com/science/article/pii/B9780323851596503195.

[166] I. I. Cheema and U. Krewer. “Operating envelope of Haber-Bosch process design for power-to-ammonia”. In: *RSC Advances* 8.61 (2018), pp. 34926–34936. DOI: 10.1039/c8ra06821f. URL: https://www.scopus.com/inward/record.uri?eid=2-s2.0-85055098984&doi=10.1039%2fc8ra06821f&partnerID=40&md5=3495920e1b9b7dc6ef4ea97498f46583.

[167] Chao Chen and Aidong Yang. “Power-to-methanol: The role of process flexibility in the integration of variable renewable energy into chemical production”. In: *Energy Conversion and Management* 228 (2021), p. 113673. ISSN: 0196-8904. DOI: https://doi.org/10.1016/j.enconman.2020.113673. URL: https://www.sciencedirect.com/science/article/pii/S0196890420311997.

[168] Ronny Tobias Zimmermann, Jens Bremer, and Kai Sundmacher. “Optimal catalyst particle design for flexible fixed-bed CO_2 methanation reactors”. In: *Chemical Engineering Journal* 387 (2020), p. 123704. ISSN: 1385-8947. DOI: https://doi.org/10.1016/j.cej.2019.123704. URL: https://www.sciencedirect.com/science/article/pii/S1385894719331195.

[169] Collin Smith and Laura Torrente-Murciano. “Exceeding Single-Pass Equilibrium with Integrated Absorption Separation for Ammonia Synthesis Using Renewable Energy—Redefining the Haber-Bosch Loop”. In: *Advanced Energy Materials* 11.13 (2021), p. 2003845. ISSN: 1614-6832. DOI: https://doi.org/10.1002/aenm.202003845. URL: https://doi.org/10.1002/aenm.202003845.

[170] Emanuele Taibi et al. *Green Hydrogen Cost Reduction*. Report. International Renewable Energy Agency, 2020. URL: https://irena.org/-/media/Files/IRENA/Agency/Publication/2020/Dec/IRENA_Green_hydrogen_cost_2020.pdf.

[171] Michael J. Ginsberg et al. “Minimizing the cost of hydrogen production through dynamic polymer electrolyte membrane electrolyzer operation”. In: *Cell Reports Physical Science* 3.6 (2022), p. 100935. ISSN: 2666-3864. DOI: https://doi.org/10.1016/j.xcrp.2022.100935. URL: https://www.sciencedirect.com/science/article/pii/S2666386422002168.

[172] International Renewable Energy Agency. *Making the breakthrough: Green hydrogen policies and technology costs*. Web Page. 2021. URL: https://www.irena.org/-/media/Files/IRENA/Agency/Publication/2020/Nov/IRENA_Green_Hydrogen_breakthrough_2021.pdf?la=en&hash=40FA5B8AD7AB1666EECBDE30EF458C45EE5A0AA6.

[173] Pedro L. García-Miguel et al. “A Review on the Degradation Implementation for the Operation of Battery Energy Storage Systems”. In: *Batteries* 8.9 (2022), p. 110. DOI: 10.3390/batteries8090110.

[174] Yu-Shan Cheng et al. “A PSO-Optimized Fuzzy Logic Control-Based Charging Method for Individual Household Battery Storage Systems within a Community”. In: *Energies* 11.2 (2018), p. 469. DOI: 10.3390/en11020469.

[175] Pierre Berest. *Thermomechanical Aspects of high frequency cycling in salt storage caverns*. Conference Paper. 2011. URL: https://hal.archives-ouvertes.fr/hal-00654932/document.

[176] Shahrouz Nayebossadri and David Book. “Compositional effects on the hydrogen cycling stability of multicomponent Ti-Mn based alloys”. In: *International Journal of Hydrogen Energy* 44.21 (2019), pp. 10722–10731. ISSN: 0360-3199. DOI: https://doi.org/10.1016/j.ijhydene.2019.02.138. URL: https://www.sciencedirect.com/science/article/pii/S0360319919307578.

[177] Nicholas Salmon and René Bañares-Alcántara. “Sector Coupling of Green Ammonia Production to Australia’s Electricity Grid”. In: *Computer Aided Chemical Engineering*. Ed. by Yoshiyuki Yamashita and Manabu Kano. Vol. 49. Elsevier, 2022, pp. 1903–1908. ISBN: 1570-7946. DOI: https://doi.org/10.1016/B978-0-323-85159-6.50317-1. URL: https://www.sciencedirect.com/science/article/pii/B9780323851596503171.

[178] Nicholas Salmon and René Bañares-Alcántara. “Importance of interannual renewable energy variation in the design of green ammonia plants”. In: *Computer Aided Chemical Engineering*. Ed. by Yoshiyuki Yamashita and Manabu Kano. Vol. 49. Elsevier, 2022, pp. 757–762. ISBN: 1570-7946. DOI: https://doi.org/10.1016/B978-0-323-85159-6.50126-3. URL: https://www.sciencedirect.com/science/article/pii/B9780323851596501263.

[179] Kevin Verleysen et al. “How can power-to-ammonia be robust? Optimization of an ammonia synthesis plant powered by a wind turbine considering operational uncertainties”. In: *Fuel* 266 (2020), p. 117049. ISSN: 0016-2361. DOI: https://doi.org/10.1016/j.fuel.2020.117049. URL: https://www.sciencedirect.com/science/article/pii/S0016236120300442.

[180] Morgan T. Kelley, Tam T. Do, and Michael Baldea. “Evaluating the demand response potential of ammonia plants”. In: *AIChE Journal* 68.3 (2022), e17552. ISSN: 0001-1541. DOI: https://doi.org/10.1002/aic.17552. URL: https://doi.org/10.1002/aic.17552.

[181] Andrew Allman and Prodromos Daoutidis. “Optimal scheduling for wind-powered ammonia generation: Effects of key design parameters”. In: *Chemical Engineering Research and Design* 131 (2018), pp. 5–15. ISSN: 0263-8762. DOI: https://doi.org/10.1016/j.cherd.2017.10.010. URL: https://www.sciencedirect.com/science/article/pii/S0263876217305646.

[182] Matthew J. Palys and Prodromos Daoutidis. “Power-to-X: A review and perspective”. In: *Computers & Chemical Engineering* 165 (2022), p. 107948. ISSN: 0098-1354. DOI: https://doi.org/10.1016/j.compchemeng.2022.107948. URL: https://www.sciencedirect.com/science/article/pii/S009813542200285X.

[183] Prodromos Daoutidis et al. “Integrating operations and control: A perspective and roadmap for future research”. In: *Computers & Chemical Engineering* 115 (2018), pp. 179–184. ISSN: 0098-1354. DOI: https://doi.org/10.1016/j.compchemeng.2018.04.011. URL: https://www.sciencedirect.com/science/article/pii/S0098135418303132.

[184] Sergio Lucia et al. “Rapid development of modular and sustainable nonlinear model predictive control solutions”. In: *Control Engineering Practice* 60 (2017), 51–62. DOI: 10.1016/j.conengprac.2016.12.009.

[185] Alfredo Nespoli et al. “Day-Ahead Photovoltaic Forecasting: A Comparison of the Most Effective Techniques”. In: *Energies* 12 (2019), p. 9. DOI: 10.3390/en12091621.

[186] US Energy Information Administration. *World Oil Transit Chokepoints*. Web Page. 2017. URL: https://www.eia.gov/international/content/analysis/special_topics/World_Oil_Transit_Chokepoints/wotc.pdf.

[187] Audrey Quicke Liam Carter and Alia Armistead. *Over a barrel - Addressing Australia’s Liquid Fuel Security*. 2022. URL: https://australiainstitute.org.au/wp-content/uploads/2022/04/P1036-Over-a-barrel_liquid-fuel-security-WEB.pdf.

[188] Yvonne Y. Deng et al. “Quantifying a realistic, worldwide wind and solar electricity supply”. In: *Global Environmental Change* 31 (2015), pp. 239–252. ISSN: 0959-3780. DOI: https://doi.org/10.1016/j.gloenvcha.2015.01.005. URL: https://www.sciencedirect.com/science/article/pii/S0959378015000072.

[189] Rebecca Windemer. “Considering time in land use planning: An assessment of end-of-life decision making for commercially managed onshore wind schemes”. In: *Land Use Policy* 87 (2019), p. 104024. ISSN: 0264-8377. DOI: https://doi.org/10.1016/j.landusepol.2019.104024. URL: https://www.sciencedirect.com/science/article/pii/S026483771831915X.

[190] Georgios Katsouris and Andrew Marina. *Cost Modelling of Floating Wind Farms*. Web Page. 2016. URL: https://questfwe.com/wp-content/uploads/2018/02/Cost-Modeling-of-Floating-Wind-Farms-ECN-2016.pdf.

[191] Tyler Stehly, Philipp Beiter, and Patrick Duffy. *2019 Cost of Wind Energy Review*. Web Page. 2020. URL: https://www.nrel.gov/docs/fy21osti/78471.pdf.

[192] Marco Ottinger and Claudia Kuenzer. “Spaceborne L-Band Synthetic Aperture Radar Data for Geoscientific Analyses in Coastal Land Applications: A Review”. In: *Remote Sensing* 12.14 (2020). ISSN: 2072-4292. DOI: 10.3390/rs12142228. URL: https://www.mdpi.com/2072-4292/12/14/2228.

[193] Jake Whitehead, Joel P. Franklin, and Simon Washington. “Transitioning to energy efficient vehicles: An analysis of the potential rebound effects and subsequent impact upon emissions”. In: *Transportation Research Part A: Policy and Practice* 74 (2015), pp. 250–267. ISSN: 0965-8564. DOI: https://doi.org/10.1016/j.tra.2015.02.016. URL: https://www.sciencedirect.com/science/article/pii/S0965856415000336.

[194] Constance Crozier and Kyri Baker. “The effect of renewable electricity generation on the value of cross-border interconnection”. In: *Applied Energy* 324 (2022), p. 119717. ISSN: 0306-2619. DOI: https://doi.org/10.1016/j.apenergy.2022.119717. URL: https://www.sciencedirect.com/science/article/pii/S030626192201008X.

[195] Ørsted. *Ørsted and Yara seek to develop groundbreaking green ammonia project in the Netherlands*. Web Page. 2021. URL: https://orsted.com/en/media/newsroom/news/2020/10/143404185982536.

[196] Siemens Gamesa Renewable Energy. *Green hydrogen*. Web Page. 2021. URL: https://www.siemensgamesa.com/en-int/products-and-services/hybrid-and-storage/green-hydrogen.

[197] PosHyDon. *PosHyDon*. Web Page. 2021. URL: https://poshydon.com/en/home-en/.

[198] American Bureau of Shipping. *Offshore Production of Green Hydrogen*. Report. 2022. URL: https://absinfo.eagle.org/acton/attachment/16130/f-ef0106f5-bb6b-4fd6-b75a-99e7df5645da/1/-/-/-/-/ABS_Offshore%20Production%20of%20Green%20Hydrogen_2022.pdf.

[199] Thang Long Wind. *’One-stop’ offshore wind platform for green hydrogen and ammonia planned*. Web Page. 2022. URL: http://en.thanglongwind.com/news-events/onestop-offshore-wind-platform-for-green-hydrogen-and-ammonia-planned-2178.html.

[200] G.L. Dugger and E.J. Francis. “Design of an ocean thermal energy plant ship to produce ammonia via hydrogen”. In: *International Journal of Hydrogen Energy* 2.3 (1977), pp. 231–249. ISSN: 0360-3199. DOI: https://doi.org/10.1016/0360-3199(77)90020-9. URL: https://www.sciencedirect.com/science/article/pii/0360319977900209.

[201] Hanchu Wang, Prodromos Daoutidis, and Qi Zhang. “Harnessing the Wind Power of the Ocean with Green Offshore Ammonia”. In: *ACS Sustainable Chemistry & Engineering* 9.43 (2021), pp. 14605–14617. DOI: 10.1021/acssuschemeng.1c06030. URL: https://doi.org/10.1021/acssuschemeng.1c06030.

[202] John Humphreys, Rong Lan, and Shanwen Tao. “Development and Recent Progress on Ammonia Synthesis Catalysts for Haber–Bosch Process”. In: *Advanced Energy and Sustainability Research* 2.1 (2021), p. 2000043. DOI: https://doi.org/10.1002/aesr.202000043. eprint: https://onlinelibrary.wiley.com/doi/pdf/10.1002/aesr.202000043. URL: https://onlinelibrary.wiley.com/doi/abs/10.1002/aesr.202000043.

[203] Brian James et al. *Hydrogen Storage System Cost Analysis*. 2016. URL: https://doi.org/10.2172/1343975.

[204] J. Bellosta Von Colbe et al. “Application of hydrides in hydrogen storage and compression: Achievements, outlook and perspectives”. In: *International Journal of Hydrogen Energy* 44.15 (2019), pp. 7780–7808. ISSN: 0360-3199. DOI: 10.1016/j.ijhydene.2019.01.104. URL: https://dx.doi.org/10.1016/j.ijhydene.2019.01.104.

[205] Ahmed Alkaisi, Ruth Mossad, and Ahmad Sharifian-Barforoush. “A Review of the Water Desalination Systems Integrated with Renewable Energy”. In: *Energy Procedia* 110 (2017). 1st International Conference on Energy and Power, ICEP2016, 14-16 December 2016, RMIT University, Melbourne, Australia, pp. 268–274. ISSN: 1876-6102. DOI: https://doi.org/10.1016/j.egypro.2017.03.138. URL: https://www.sciencedirect.com/science/article/pii/S1876610217301686.

[206] Domenico Curto, Vincenzo Franzitta, and Andrea Guercio. “A Review of the Water Desalination Technologies”. In: *Applied Sciences* 11.2 (2021). ISSN: 2076-3417. DOI: 10.3390/app11020670. URL: https://www.mdpi.com/2076-3417/11/2/670.

[207] Huyen Trang Do Thi et al. “Comparison of Desalination Technologies Using Renewable Energy Sources with Life Cycle, PESTLE, and Multi-Criteria Decision Analyses”. In: *Water* 13.21 (2021). ISSN: 2073-4441. DOI: 10.3390/w13213023. URL: https://www.mdpi.com/2073-4441/13/21/3023.

[208] Priyom Roy et al. “Discharge water temperature assessment of thermal power plant using remote sensing techniques”. In: *Energy Geoscience* 3.2 (2022), pp. 172–181. ISSN: 2666-7592. DOI: https://doi.org/10.1016/j.engeos.2021.06.006. URL: https://www.sciencedirect.com/science/article/pii/S2666759221000317.

[209] AquaSwiss. *Multi-effect distillation*. 2010. URL: http://aquaswiss.eu/desalination-solutions/multi-effect-distillation/.

[210] Veolia Water Technologies. *Multiple Effect Distillation (MED)*. 2023. URL: https://www.veoliawatertechnologies.com/asia/en/solutions/technologies/multiple-effect-distillation-med.

[211] Sören Dresp et al. “Direct Electrolytic Splitting of Seawater: Activity, Selectivity, Degradation, and Recovery Studied from the Molecular Catalyst Structure to the Electrolyzer Cell Level”. In: *Advanced Energy Materials* 8.22 (2018), p. 1800338. DOI: https://doi.org/10.1002/aenm.201800338. eprint: https://onlinelibrary.wiley.com/doi/pdf/10.1002/aenm.201800338. URL: https://onlinelibrary.wiley.com/doi/abs/10.1002/aenm.201800338.

[212] Sören Dresp et al. “Direct Electrolytic Splitting of Seawater: Opportunities and Challenges”. In: *ACS Energy Letters* 4.4 (2019). doi: 10.1021/acsenergylett.9b00220, pp. 933–942. DOI: 10.1021/acsenergylett.9b00220. URL: https://doi.org/10.1021/acsenergylett.9b00220.

[213] Topsoe. *SOEC*. Web Page. 2023. URL: https://www.topsoe.com/our-resources/knowledge/our-products/equipment/soec.

[214] Hayley Farr et al. “Potential environmental effects of deepwater floating offshore wind energy facilities”. In: *Ocean & Coastal Management* 207 (2021), p. 105611. ISSN: 0964-5691. DOI: https://doi.org/10.1016/j.ocecoaman.2021.105611. URL: https://www.sciencedirect.com/science/article/pii/S096456912100096X.

[215] H J Lindeboom et al. “Short-term ecological effects of an offshore wind farm in the Dutch coastal zone; a compilation”. In: *Environmental Research Letters* 6.3 (2011), p. 035101. DOI: 10.1088/1748-9326/6/3/035101. URL: https://dx.doi.org/10.1088/1748-9326/6/3/035101.

[216] Bruce D. Patterson et al. “Renewable CO_2; recycling and synthetic fuel production in a marine environment”. In: *Proceedings of the National Academy of Sciences* 116.25 (2019), p. 12212. DOI: 10.1073/pnas.1902335116. URL: http://www.pnas.org/content/116/25/12212.abstract.

[217] Rodica Loisel et al. “Economic evaluation of hybrid off-shore wind power and hydrogen storage system”. In: *International Journal of Hydrogen Energy* 40.21 (2015), pp. 6727–6739. ISSN: 0360-3199. DOI: https://doi.org/10.1016/j.ijhydene.2015.03.117. URL: https://www.sciencedirect.com/science/article/pii/S0360319915007636.

[218] Alessandro Singlitico, Jacob Østergaard, and Spyros Chatzivasileiadis. “Onshore, offshore or in-turbine electrolysis? Techno-economic overview of alternative integration designs for green hydrogen production into Offshore Wind Power Hubs”. In: *Renewable and Sustainable Energy Transition* 1 (2021), p. 100005. ISSN: 2667-095X. DOI: https://doi.org/10.1016/j.rset.2021.100005. URL: https://www.sciencedirect.com/science/article/pii/S2667095X21000052.

[219] E. Morgan. “A Techno-economic Feasibility Study of Ammonia Plants Powered by Offshore Wind”. PhD Thesis. University of Massachusetts Amherst, 2013. URL: https://scholarworks.umass.edu/cgi/viewcontent.cgi?article=1704&context=open_access_dissertations.

[220] Vismay V Parmar. "Ammonia Production from a Non-Grid Connected Floating Offshore Wind-Farm: A System-Level Techno-Economic Review". MSc Thesis. University of Massachusetts Amherst, 2019. URL: https://scholarworks.umass.edu/masters_theses_2/750?utm_source=scholarworks.umass.edu\%2Fmasters_theses_2\%2F750\&utm_medium=PDF\&utm_campaign=PDFCoverPages.

[221] C.B. Panchal, P.P Pandolfini, and W.H Kumm. *Ocean Thermal Plantships for Production of Ammonia as the Hydrogen Carrier*. Report. Argonne National Laboratory, 2009. URL: https://publications.anl.gov/anlpubs/2009/12/65627.pdf.

[222] C. Amante and B.W. Eakins. *ETOPO1 1 Arcminute global relief model: procedures, data sources and analysis*. Web Page. 2009. URL: https://www.ngdc.noaa.gov/mgg/global/relief/ETOPO1/docs/ETOPO1.pdf.

[223] International Renewable Energy Agency. *Renewable power generation costs in 2020*. Web Page. 2021. URL: https://www.irena.org/-/media/Files/IRENA/Agency/Publication/2021/Jun/IRENA_Power_Generation_Costs_2020.pdf.

[224] David Feldman et al. *U.S. Solar Photovoltaic System and Energy Storage Cost Benchmark: Q1 2020*. Web Page. 2021. URL: https://www.nrel.gov/docs/fy21osti/77324.pdf.

[225] A. Martinez and G. Iglesias. "Mapping of the levelised cost of energy for floating offshore wind in the European Atlantic". In: *Renewable and Sustainable Energy Reviews* 154 (2022), p. 111889. ISSN: 1364-0321. DOI: https://doi.org/10.1016/j.rser.2021.111889. URL: https://www.sciencedirect.com/science/article/pii/S1364032121011564.

[226] Alberto Ghigo et al. "Platform Optimization and Cost Analysis in a Floating Offshore Wind Farm". In: *Journal of Marine Science and Engineering* 8.11 (2020), p. 835. ISSN: 2077-1312. DOI: 10.3390/jmse8110835. URL: https://doi.org/10.3390/jmse8110835.

[227] Anders Myhr et al. "Levelised cost of energy for offshore floating wind turbines in a life cycle perspective". In: *Renewable Energy* 66 (2014), pp. 714–728. ISSN: 0960-1481. DOI: https://doi.org/10.1016/j.renene.2014.01.017. URL: https://www.sciencedirect.com/science/article/pii/S0960148114000469.

[228] The Carbon Trust. *Floating Offshore Wind: Market and Technology Review*. Web Page. 2015. URL: https://prod-drupal-files.storage.googleapis.com/documents/resource/public/Floating\%20Offshore\%20Wind\%20Market\%20Technology\%20Review\%20-\%20REPORT.pdf.

[229] Philipp Beiter et al. *The Cost of Floating Offshore Wind Energy in California Between 2019 and 2032*. Web Page. 2020. URL: https://www.nrel.gov/docs/fy21osti/77384.pdf.

[230] Shayan Heidari. "Economic modelling of floating offshore wind power". MSc Thesis. Mälardalen University, 2016. URL: http://www.diva-portal.org/smash/get/diva2:1128321/FULLTEXT01.pdf.

[231] Sara Oliveira-Pinto and Jasper Stokkermans. “Marine floating solar plants: an overview of potential, challenges and feasibility”. In: *Proceedings of the Institution of Civil Engineers - Maritime Engineering* 173.4 (2020), pp. 120–135. DOI: 10.1680/jmaen.2020.10. URL: https://www.icevirtuallibrary.com/doi/abs/10.1680/jmaen.2020.10.

[232] S. Z. Sara M. Golroodbari and Wilfried van Sark. “Pooling the cable: A techno-economic feasibility study of integrating offshore floating photovoltaic solar technology within an offshore wind park”. In: *Solar Energy* 219 (2021), pp. 65–74. DOI: 10.1016/j.solener.2020.12.062.

[233] Oceans of Energy. Web Page. 2021. URL: https://oceansofenergy.blue/projects/.

[234] Joshua S Hill. *Sunseap completes offshore floating solar farm in Straits of Johor*. Web Page. 2021. URL: https://reneweconomy.com.au/sunseap-completes-offshore-floating-solar-farm-in-straits-of-johor/.

[235] S. Zahra Golroodbari and Wilfried van Sark. “Simulation of performance differences between offshore and land-based photovoltaic systems”. In: *Progress in Photovoltaics: Research and Applications* 28.9 (2020), pp. 873–886. ISSN: 1062-7995. DOI: https://doi.org/10.1002/pip.3276. URL: https://doi.org/10.1002/pip.3276.

[236] Marco Rosa-Clot and Giuseppe Tina. “Levelized Cost of Energy (LCOE) Analysis”. In: Elsevier, 2020, pp. 119–127. ISBN: 9780128170618. DOI: 10.1016/B978-0-12-817061-8.00010-5.

[237] Food and Agriculture Organisation of the UN. *FAOStat*. Web Page. 2021. URL: http://www.fao.org/faostat/en/#data/RL.

[238] M. Friedl and D. Sulla-Menashe. *MCD12Q1 MODIS/Terra+Aqua Land Cover Type Yearly L3 Global 500m SIN Grid V006*. Web Page. 2019. DOI: https://doi.org/10.5067/MODIS/MCD12Q1.006. URL: https://doi.org/10.5067/MODIS/MCD12Q1.006.

[239] Dirk-Jan van de Ven et al. “The potential land requirements and related land use change emissions of solar energy”. In: *Scientific Reports* 11.1 (2021), p. 2907. ISSN: 2045-2322. DOI: 10.1038/s41598-021-82042-5. URL: https://doi.org/10.1038/s41598-021-82042-5.

[240] UNEP-WCMC and IUCN. *Protected Planet Report 2020*. Report. UNEP-WCMC and IUCN, 2021. URL: https://livereport.protectedplanet.net/.

[241] First Solar, Inc. *First Solar Series 4™ PV Module*. Web Page. 2018. URL: https://www.firstsolar.com/en-Emea/-/media/First-Solar/Technical-Documents/Series-4-Datasheets/Series-4V3-Module-Datasheet.ashx.

[242] Energy Sector Management Assistance Program. *Going Global: Expanding Offshore Wind to Emerging Markets*. Report. Washington, DC, 2022. URL: https://openknowledge.worldbank.org/server/api/core/bitstreams/04db13ea-547f-5d69-a4ad-0963d9dff06d/content.

[243] Mark J. Kaiser and Brian Snyder. "The five offshore drilling rig markets". In: *Marine Policy* 39 (2013), pp. 201–214. ISSN: 0308-597X. DOI: https://doi.org/10.1016/j.marpol.2012.10.019. URL: https://www.sciencedirect.com/science/article/pii/S0308597X12002187.

[244] Mark Ruth, Ahman Mayyas, and Maggie Mann. *Manufacturing Competitiveness Analysis for PEM and Alkaline Water Electrolysis Systems*. Report. National Renewable Energy Laboratory, 2017. URL: https://www.nrel.gov/docs/fy19osti/70380.pdf.

[245] Sankara Papavinasam. "Chapter 2 - Oil and Gas Industry Network". In: *Corrosion Control in the Oil and Gas Industry*. Ed. by Sankara Papavinasam. Boston: Gulf Professional Publishing, 2014, pp. 41–131. ISBN: 978-0-12-397022-0. DOI: https://doi.org/10.1016/B978-0-12-397022-0.00002-9. URL: https://www.sciencedirect.com/science/article/pii/B9780123970220000029.

[246] J. Couper et al. "6 - Flow of Fluids". In: *Chemical Process Equipment*. Ed. by James R. Couper et al. Third. Boston: Butterworth-Heinemann, 2012, pp. 83–119. ISBN: 978-0-12-396959-0. DOI: https://doi.org/10.1016/B978-0-12-396959-0.00006-9. URL: https://www.sciencedirect.com/science/article/pii/B9780123969590000069.

[247] Wärtsilä. *Encyclopedia of marine technology*. Web Page. 2021. URL: https://www.wartsila.com/encyclopedia/term/gas-carrier-types.

[248] Imodco. *Jettyless Ammonia Terminal*. website. 2023. URL: https://imodco.com/new-energies/.

[249] H. Homan and C. Klass. *LNG freight rates*. Web Page. 2020. URL: https://www.argusmedia.com/en/hubs/lng.

[250] H Rogers. *The LNG shipping forecast: costs rebounding, outlook uncertain*. Web Page. 2018. URL: https://www.oxfordenergy.org/wpcms/wp-content/uploads/2018/02/The-LNG-Shipping-Forecast-costs-rebounding-outlook-uncertain-Insight-27.pdf.

[251] Economic Research Institute for ASEAN and East Asia. "Investment in LNG Supply Chain Infrastructure Estimation". In: *Formulating Policy Options for Promoting Natural Gas Utilization in the East Asia Summit Region Volume II: Supply Side Analysis*. Jakarta: ERIA, 2018. Chap. 6, pp. 67–80. URL: https://globallnghub.com/wp-content/uploads/2018/05/ERIA_RPR_FY2016_7b_Chapter_6.pdf.

[252] M. Al-Breiki and Y. Bicer. "Technical assessment of liquefied natural gas, ammonia and methanol for overseas energy transport based on energy and exergy analyses". In: *International Journal of Hydrogen Energy* 45 (2020), pp. 34927–34937. ISSN: 03603199. DOI: 10.1016/j.ijhydene.2020.04.181.

[253] Gurobi Optimization, LLC. *Gurobi Optimizer Reference Manual*. 2022. URL: https://www.gurobi.com.

[254] J. Verschuur, E. E. Koks, and J. W. Hall. "Ports' criticality in international trade and global supply-chains". In: *Nature Communications* 13.1 (2022). ID: Verschuur2022, p. 4351. DOI: 10.1038/s41467-022-32070-0. URL: https://doi.org/10.1038/s41467-022-32070-0.

[255] International Maritime Organisation. *Fourth IMO GHG Study 2020 Full Report*. Web Page. 2021. URL: https://www.imo.org/en/OurWork/Environment/Pages/Fourth-IMO-Greenhouse-Gas-Study-2020.aspx.

[256] Nadia Ameli et al. "Higher cost of finance exacerbates a climate investment trap in developing economies". In: *Nature Communications* 12.1 (2021). ID: Ameli2021, p. 4046. DOI: 10.1038/s41467-021-24305-3. URL: https://doi.org/10.1038/s41467-021-24305-3.

[257] International Energy Agency. *World Energy Balances*. 2022. URL: https://www.iea.org/data-and-statistics/data-product/world-energy-balances.

[258] International Energy Agency. *Nuclear Power in a Clean Energy System*. Paris, 2020. URL: https://www.iea.org/reports/nuclear-power-in-a-clean-energy-system.

Appendix A

Grid Cost case study inputs

A.1 Modelling data for Grid Case Study

Table A.1 Equipment Costs for Chapter 3

Equipment	CAPEX	Sensitivity
Solar PV	1,250 USD/kW [1]	± 30% (Electricity)
Wind	1,550 USD/kW [1]	± 10% (Electricity)
Electrolyser	700 USD/kW [2]	± 30% (Electrolyser)
HB CAPEX	7,444 USD/kW [2]	-
Hydrogen storage	500 USD/t [2]	± 20% (Storage)
Battery interface	271 USD/kW [3]	± 20% (Electricity)
Battery storage	500 USD/kWh [4]	± 200 USD/MWh (Storage)
Fuel cell	960 USD/kW [5]	± 20% (Storage)
TUOS fee	10 AUD/MWh [6]	± 5 AUD/MWh (Grid)
HV connection fee	55 million AUD [7]	-
LV connection fee	23 million AUD[7]	-
HV DC wire cost	2.1 million AUD/km [7]	-
HV AC wire cost	1.8 million USD/km [7]	-
LV wire cost	0.4 million AUD/km [7]	-
HV transformer efficiency	0.96 [8]	-
LV transformer efficiency	0.99 [8]	-
HVDC wire efficiency	3% loss/1000 km [9]	-
HVAC wire efficiency	4% loss/100 km [9]	-
LV wire efficiency	30% loss/100 km [9]	-

Table A.2 List of parameters used in the MILP production cost estimation model in Chatper 3 and their meaning.

Parameter	*Sets*	*Symbol*	*Meaning*	*Data value/source*
Power supply	Renewables, Time	$Z(R,t)$	The power provided by each renewable at a given time for each time (fraction between 0 and 1; 1 corresponds to the installed power of the equipment)	Transformed ERA5 data
Grid electricity cost	Days, Time	$Y(t)$	The cost of electricity provided by the grid for each time (in AUD/MWh)	AEMO [10]
Renewable installation Cost	Renewables	$Cost_R$	Installed cost of 1 MW of renewable capacity	IRENA [1]
Component Cost	Components	$Cost_C$	Installed cost of 1 MW of the nominated component	Nayak-Luke et al. [2]
Storage Cost	Storage Components	$Cost_{SC}$	Installed cost of 1 MWh of the nominated storage component	Nayak-Luke et al. [2]
Conversion Factors	Flows, Flows	CF	Amount of Flow 1 required to produce one unit of Flow 2	50 kWh/kg (hydrogen from electricity)[2]; 1.61 kWh/kg (HB + ASU operation from electricity)[2]; 0.98 kWh/kWh (Power out of battery from power into battery)[3]
Total days	None	G_{Days}	The total number of days in the data set	Dependent on number of years modelled
Battery self-discharge	None	$G_{Discharge}$	The fraction of energy lost by the battery each hour	Assumed 5% per month
Annual hours	None	G_{Hours}	The number of operating hours per year	8,424 (14 days offline/year)[2]
HB Minimum Operating Rate	None	$G_{HB_{Min}}$	The lowest rate at which the Haber-Bosch plant can be operated as a fraction of its rated design.	0.2[11]
HB Ramp down rate	None	$G_{HB_{\text{Ramp Down}}}$	The maximum rate at which the Haber-Bosch plant can ramp down as a fraction of its rated operation	0.2[12]
HB Ramp up rate	None	$G_{HB_{\text{Ramp Up}}}$	The maximum rate at which the Haber-Bosch plant can ramp up as a fraction of its rated operation	0.02[12]
Annual Production	None	F	The mass of ammonia produced per year	1 MMTPA
Water Cost	None	$Cost_W$	The cost per t of water	2 USD/t[13]
Operating and Maintenance Costs	None	$Cost_{OM}$	The operating and maintenance costs as a fraction of CAPEX	2%[2]

Appendix B

MPC inputs and results

B.1 List of symbols used for MPC

t	Time (h)
S_t	The set of all times
$\alpha(t)$	Total renewable energy available to the plant at time t in MWh
$\lambda(SC,t)$	Total charge accumulation in storage component SC at time t in MWh (Design only)
$\kappa(SC,t)$	State of charge of a storage component SC at time t in MWh (Design only)
x	State of plant in the MPC controller (Operating approach only)
$\pi_E(t)$	Total energy flow to the electrolyser at time t in MWh (MPC)
$\pi_{HB}(t)$	Total energy flow to the HB plant (MPC) at time t in MWh
$\beta_{In}(t)$	Energy flow to the battery at time t in MWh (MPC)
$\beta_{Out}(t)$	Energy flow from the battery at time t in MWh (MPC)
$\gamma(t)$	Energy flow from the fuel cell in MWh at time t(MPC)
η	Conversion efficiency
ε_B	Battery hourly self discharge rate
n	Forecast horizon of MPC controller
k_H	Hydrogen storage tuning parameter
k_B	Battery storage tuning parameter
k_R	Ramping tuning parameter

B.2 MPC Results

B.2.1 Plant operation under MPC

These figures are shown in the body of the report for a hybrid site that uses both wind and solar. The figures included here are at the other two sites which were analysed in detail, which use wind only (top) or solar only (bottom).

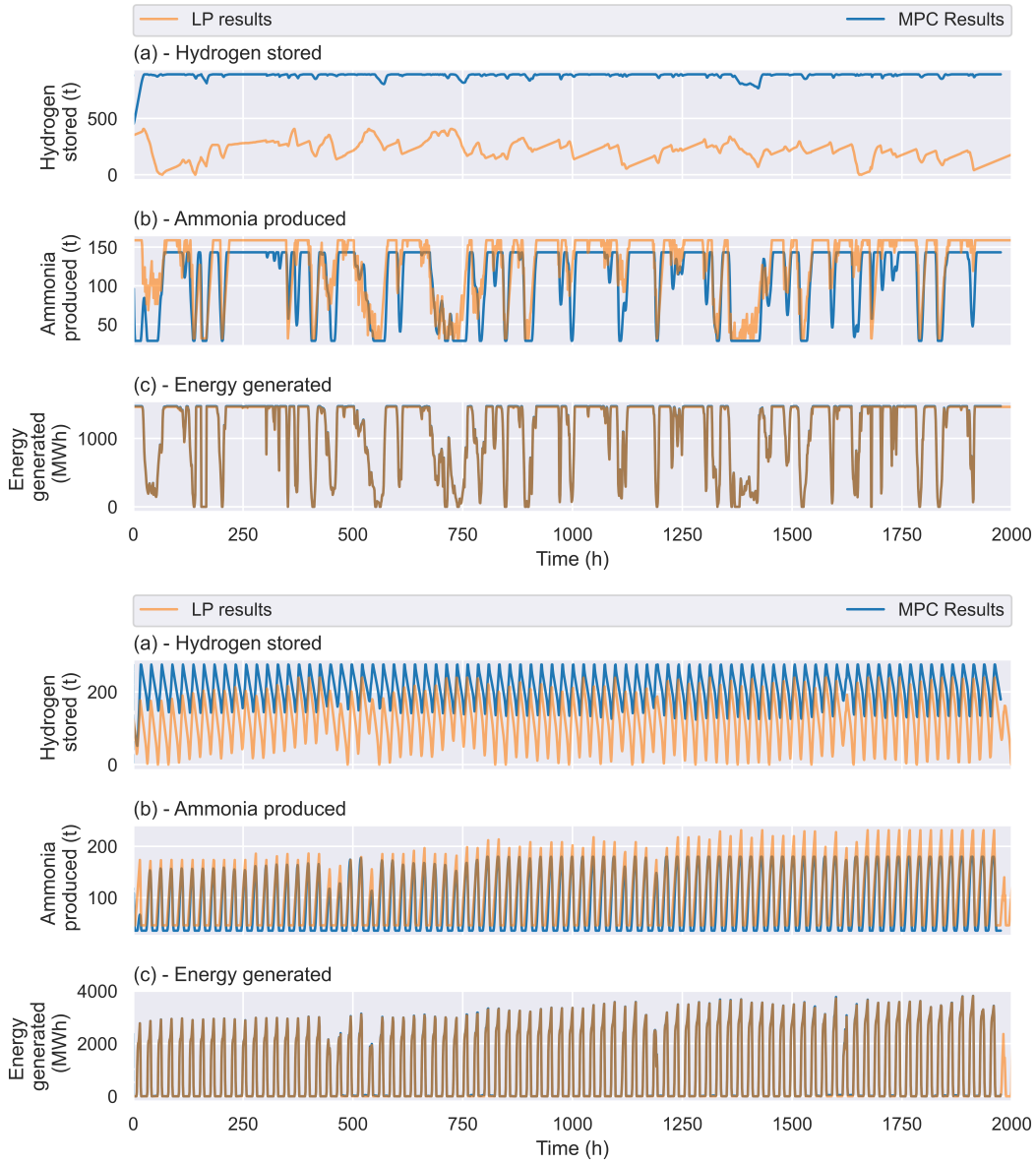

Fig. B.1 Plots comparing the operation of the MPC controller with the LP optimisation for a wind-dominated site (**top**) and a solar-dominated site (**bottom**), for 2022. These plots are produced without significant tuning of parameters which is described in the article; for instance the tuning penalty in both plots is most likely too high, as the hydrogen storage is emptying much less frequently than occurred for the LP case.

B.2.2 Plant failure frequency - 2022

Equivalent plots for a wind-only site in 2022 are included in the body text; these figures are for hybrid wind-solar and solar-only sites.

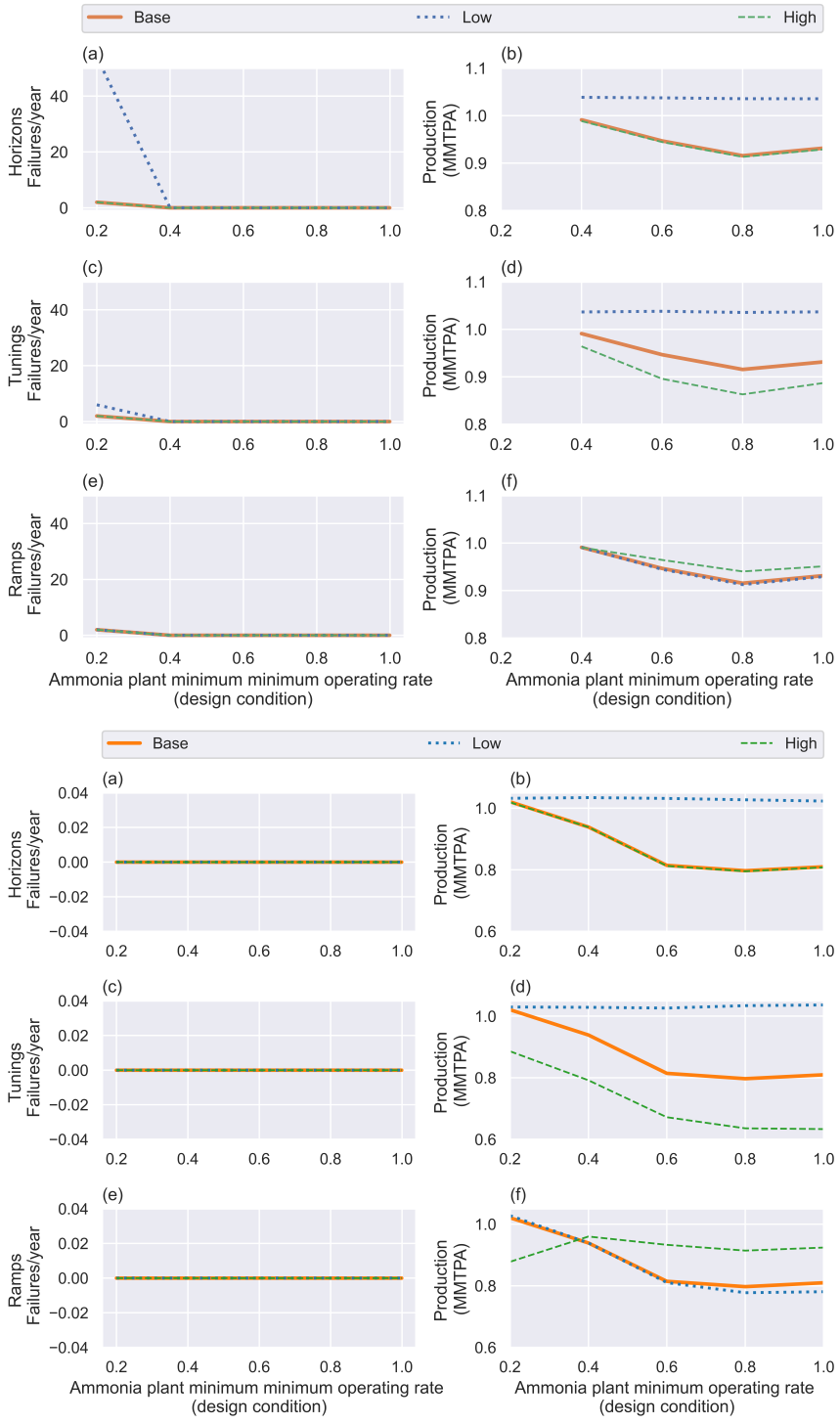

Fig. B.2 Plots of the failure frequency (**left**) and production (**right**) using the same parameters as described in Figure 4.6 for a hybrid wind/solar site (**top**) and a solar dominated site in 2022 (**bottom**)

B.2.3 Plant failure frequency - 2050

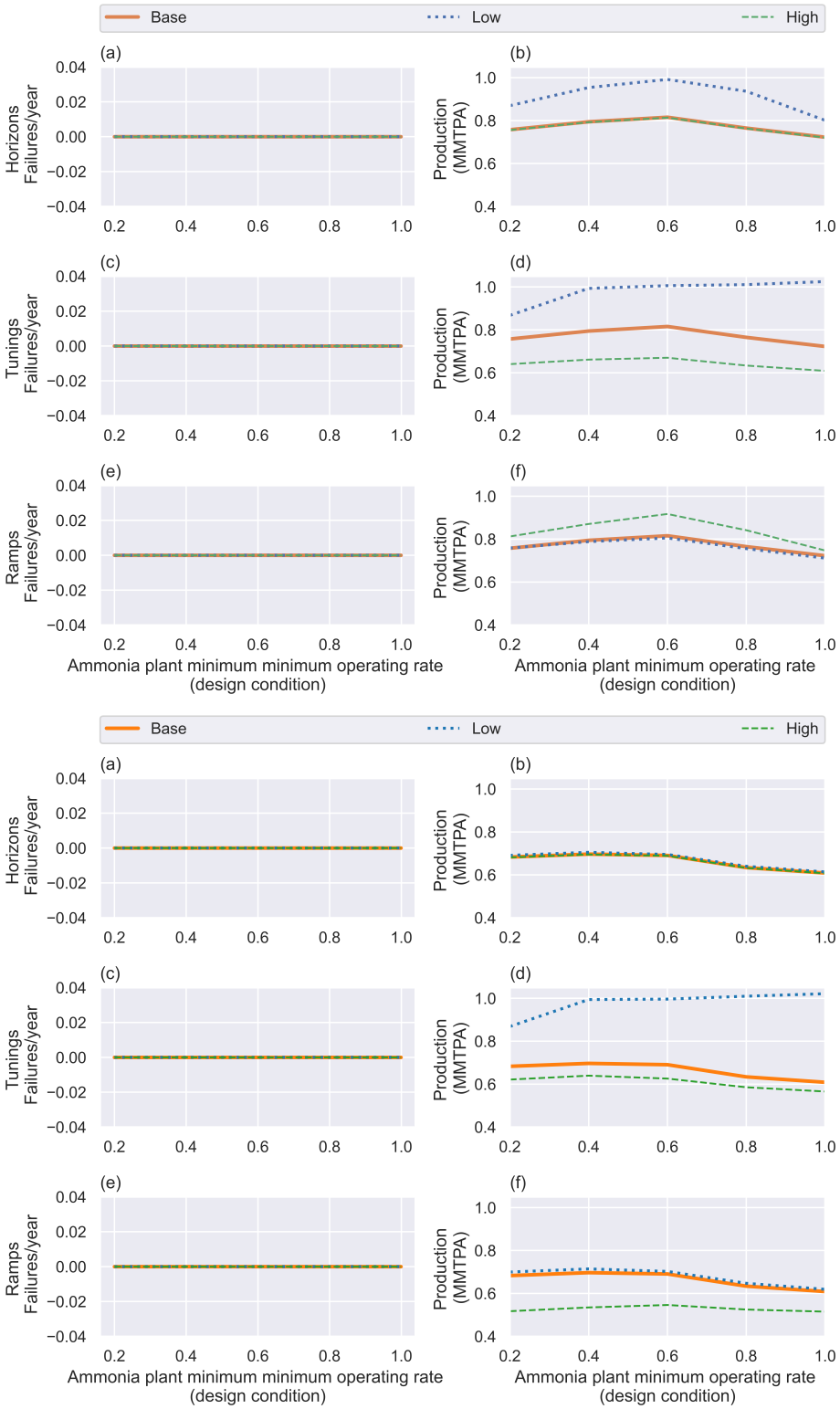

Fig. B.3 Identical plots to those shown on the previous page, except using data from 2050. Plots of the failure frequency (**left**) and production (**right**) using the same parameters as described in Figure 4.6 for a hybrid wind/solar site (**top**) and a solar dominated site in 2050 (**bottom**)

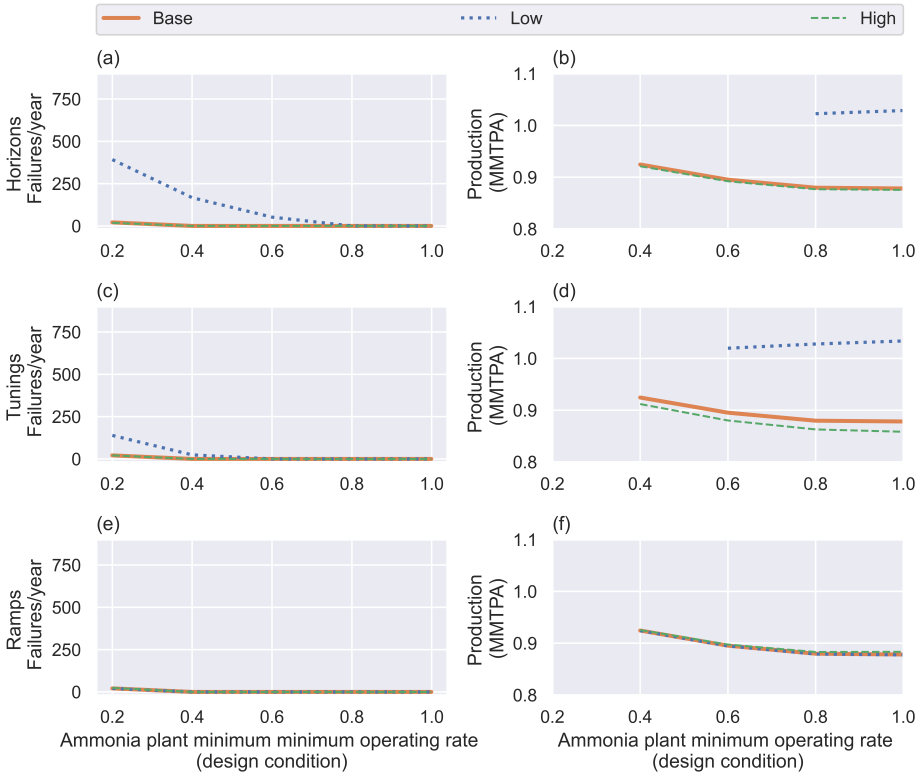

Fig. B.4 Plots of the failure frequency (**left**) and production (**right**) using the same parameters as described in Figure 4.6 for a wind site in 2050.

Appendix C

Offshore production supplementary data and results

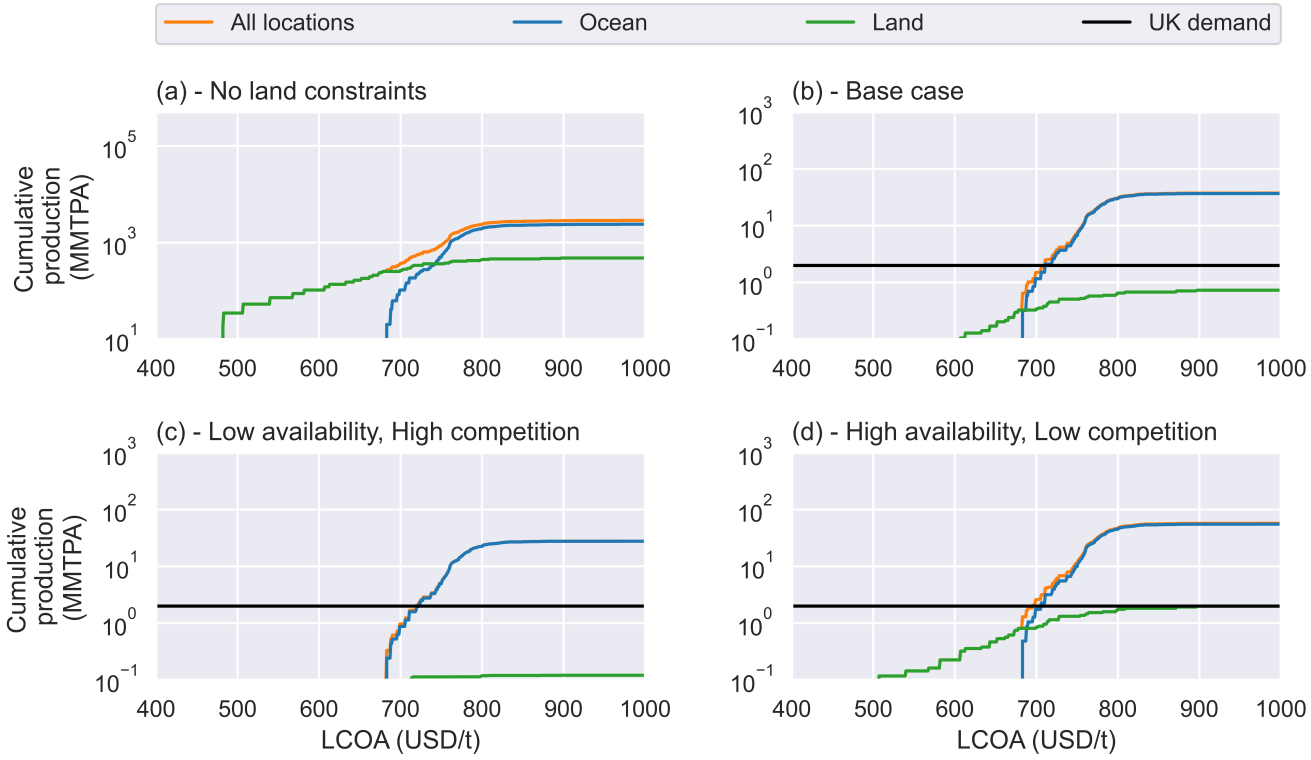

Fig. C.1 Land availability and competition for green ammonia production in the UK. Method I for land competition (i.e. capping land-use at a maximum percentage of available land based on relative energy demand) is used for this figure. Note the different y-axis scaling on panel (a) compared to the other panels. **(a) - Top left**: No land constraints; **(b) - Top right**: Base case; **(c) - Bottom left**: Low land use (i.e. low availability and high competition); **(d) - Bottom right**: High land use (i.e. high availability and low competition)

Land Cover Type	MODIS Number	Low land availability		Base case		High land availability	
		Wind	Solar	Wind	Solar	Wind	Solar
Evergreen Needleleaf Forests	1	-	-	-	-	0.1	-
Evergreen Broadleaf Forests	2	-	-	-	-	0.1	-
Deciduous Needleleaf Forests	3	-	-	-	-	0.1	-
Deciduous Broadleaf Forests	4	-	-	-	-	0.1	-
Mixed Forests	5	-	-	-	-	0.1	-
Closed Shrublands	6	0.25	0.25	0.5	0.5	0.75	0.75
Open Shrublands	7	0.25	0.25	0.5	0.5	0.75	0.75
Woody Savannas	8	0	0	0.2	0.2	0.4	0.4
Savannas	9	0	0	0.2	0.2	0.4	0.4
Grasslands	10	0	0	0.2	0.2	0.4	0.4
Permanent Wetlands	11	-	-	-	-	-	-
Croplands	12	0.1	-	0.1	-	0.1	-
Urban and Built-up Lands	13	-	0.03	-	0.03	-	0.03
Cropland, Natural Vegetation, Mosaic	14	0.1	-	0.1	-	0.1	-
Permanent Snow and Ice	15	-	-	-	-	-	-
Barren	16	1	1	1	1	1	1
Water Bodies	17	-	-	-	-	-	-

Table C.1 Allowable fraction of land usage in different sensitivity scenarios

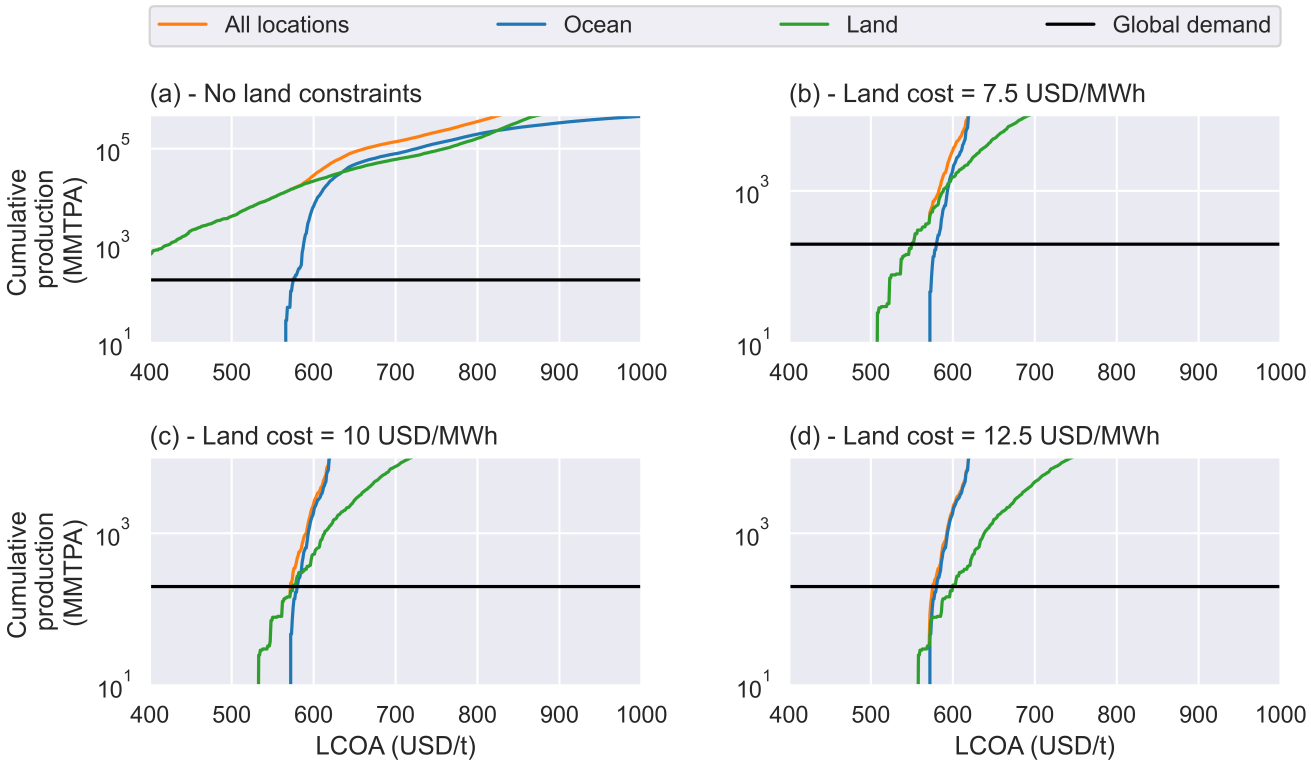

Fig. C.2 Land availability and competition using Method II. The land costs associated with Method II are expressed as an increase in the levelised cost of electricity in USD/MWh.

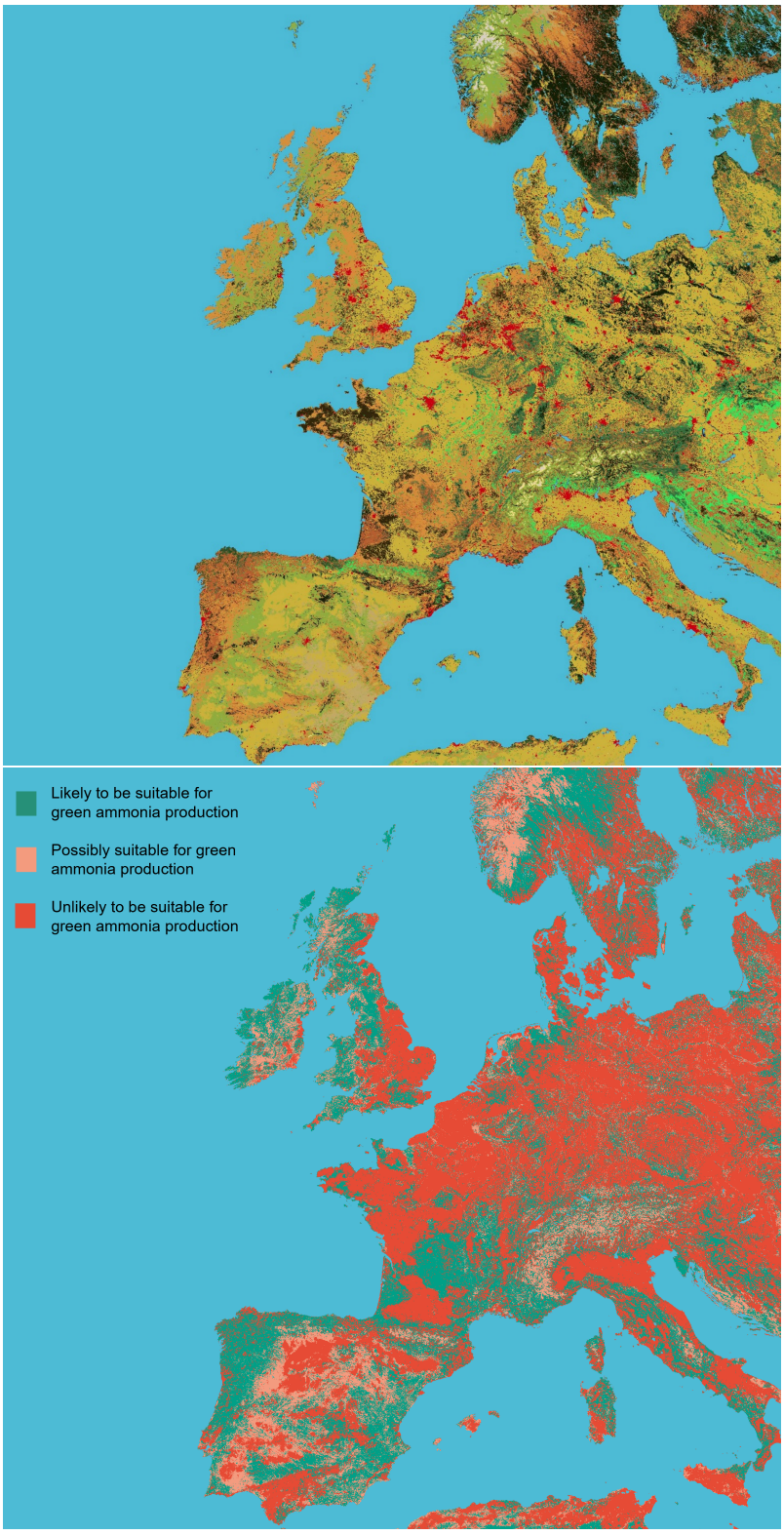

Fig. C.3 Land usage under the MODIS dataset in Europe. **Top**: MODIS classification. **Bottom**: Suitability for green ammonia production

Appendix D

Supply chain inputs

Table D.1 Inputs by case for ammonia cost estimation

Component	Units	2022	MOD-AMB*	HIGH-AMB	O&M Fraction
Electrolyser	Million USD/Installed MW	0.979	0.203	0.1526	0.03
HB+ASU	Million USD/Installed MW	7.444	7.444	7.444	0.02
Battery Interface	Million USD/Installed MW	0.241	0.056	0.045	0.035
Fuel Cell	Million USD/Installed MW	1.065	0.221	0.166	0.03
Solar PV - Fixed	Million USD/Installed MW	0.857	0.24	0.184	0.02
Solar PV - Single Axis Tracking	Million USD/Installed MW	0.907	0.254	0.199	0.02
Wind	Million USD/Installed MW	1.435	0.90604	0.825	0.02
Battery Storage	Million USD/Installed MWh	0.331	0.076	0.0627	0.035
Compressed Gas Hydrogen Storage	Million USD/Installed t	0.5	0.5	0.5	0.02

* MOD-AMB case used for input costs for 2050 in Chapter 4.

Table D.2 Inputs for ammonia transport cost estimation

Parameter	Unit	Value
Ship speed	knots	18 [14]
Ship insurance cost	USD/day	2600 [14]
Brokerage factor	% of charter cost	2 [14]
Usable capacity of ship tank	%	94 [14]
Ship type	-	Panamax
DWT	t	82618 (from AIS database)
Charter fee	USD/day	97096 [14]
Berthing Fee	USD/day	150000 [14]
Fuel consumption	t NH3/day	75 [15]
Pipeline transport cost	USD/levelised t/100	2.56 [16]
Ammonia storage cost	USD/stored t	439 [17]

Appendix References

[1] International Renewable Energy Agency. *Renewable Power Generation Costs in 2019*. Abu Dhabi: International Renewable Energy Agency, 2019. ISBN: 978-92-9260-244-4. URL: https://irena.org/-/media/Files/IRENA/Agency/Publication/2020/Jun/IRENA_Power_Generation_Costs_2019.pdf.

[2] R. Nayak-Luke and R. Bañares-Alcántara. "Techno-economic viability of islanded green ammonia as a carbon-free energy vector and as a substitute for conventional production". In: *Energy & Environmental Science* 13.9 (2020), pp. 2957–2966. ISSN: 1754-5692. DOI: 10.1039/d0ee01707h. URL: https://dx.doi.org/10.1039/D0EE01707H.

[3] Z. Cesaro et al. "Ammonia to power: Forecasting the levelized cost of electricity from green ammonia in large-scale power plants". In: *Applied Energy* 282 (2021), p. 116009. ISSN: 0306-2619. DOI: 10.1016/j.apenergy.2020.116009. URL: https://dx.doi.org/10.1016/j.apenergy.2020.116009.

[4] G. Parkinson. *Tesla big battery adds new capacity and services on march to 100pct renewables grid*. Web Page. 2019. URL: https://reneweconomy.com.au/tesla-big-battery-adds-new-capacity-and-services-on-march-to-100pct-renewables-grid-55121/.

[5] Paul Graham et al. *GenCost 2021-22*. Report. 2022. URL: https://www.csiro.au/-/media/News-releases/2022/GenCost-2022/GenCost2021-22Final_20220708.pdf.

[6] TasNetworks. *Prescribed Transmission Services Prices for 2021-22*. Web Page. 2021. URL: https://www.tasnetworks.com.au/config/getattachment/64d81498-67a5-4ae1-a1c1-dab70ae96d7e/2021-22-prescribed-transmission-services-prices.pdf.

[7] T.S. Brinsmead, J. Hayward, and P. Graham. *Australian Electricity Market Analysis report to 2020 and 2030*. Web Page. 2014. URL: https://arena.gov.au/assets/2017/02/CSIRO-Electricity-market-analysis-for-IGEG.pdf.

[8] M. Pirolli. *Sustainable Energy Handbook*. Web Page. 2021. URL: https://europa.eu/capacity4dev/public-energy/wiki/sustainable-energy-handbook.

[9] K. Vaillancourt. *Electricity Transmission and Distribution*. Web Page. 2014. URL: https://iea-etsap.org/E-TechDS/PDF/E12_el-t&d_KV_Apr2014_GSOK.pdf.

[10] Australian Energy Market Operator. *Aggregated price and demand data*. Web Page. 2020. URL: https://aemo.com.au/energy-systems/electricity/national-electricity-market-nem/data-nem/aggregated-data.

[11] S.S. Beerbühl, M. Fröhling, and F. Schultmann. "Combined scheduling and capacity planning of electricity-based ammonia production to integrate renewable energies". In: *European Journal of Operational Research* 241.3 (2015), pp. 851–862. ISSN: 0377-2217. DOI: 10.1016/j.ejor.2014.08.039. URL: https://dx.doi.org/10.1016/j.ejor.2014.08.039.

[12] Mahdi Fasihi et al. "Global potential of green ammonia based on hybrid PV-wind power plants". In: *Applied Energy* 294 (2021), p. 116170. ISSN: 0306-2619. DOI: https://doi.org/10.1016/j.apenergy.2020.116170. URL: https://www.sciencedirect.com/science/article/pii/S0306261920315750.

[13] Nicholas Salmon and René Bañares-Alcántara. "Green ammonia as a spatial energy vector: a review". In: *Sustainable Energy Fuels* 5 (11 2021), pp. 2814–2839. DOI: 10.1039/D1SE00345C. URL: http://dx.doi.org/10.1039/D1SE00345C.

[14] H Rogers. *The LNG shipping forecast: costs rebounding, outlook uncertain*. Web Page. 2018. URL: https://www.oxfordenergy.org/wpcms/wp-content/uploads/2018/02/The-LNG-Shipping-Forecast-costs-rebounding-outlook-uncertain-Insight-27.pdf.

[15] N. Ash and T. Scarbrough. *Sailing on Solar: Could green ammonia decarbonise international shipping?* London: Environmental Defense Fund, 2019, pp. 56–57.

[16] Nicholas Salmon, René Bañares-Alcántara, and Richard Nayak-Luke. "Optimization of green ammonia distribution systems for intercontinental energy transport". In: *iScience* 24.8 (2021), p. 102903. ISSN: 2589-0042. DOI: https://doi.org/10.1016/j.isci.2021.102903. URL: https://www.sciencedirect.com/science/article/pii/S2589004221008713.

[17] W.C. Leighty and J.H Holbrook. "Alternatives to Electricity for Transmission, Firming Storage, and Supply Integration for Diverse, Stranded, Renewable Energy Resources: Gaseous Hydrogen and Anhydrous Ammonia Fuels via Underground Pipelines". In: *WHEC 2012 Conference Proceedings – 19th World Hydrogen Energy Conference*. Vol. 29. Toronto: JPdL International, 2012, pp. 332–346. ISBN: 18766102. DOI: 10.1016/j.egypro.2012.09.040.